



University of HUDDERSFIELD

University of Huddersfield Repository

Ali, Jafar

Modelling of thermal plume discharge into shallow and still water

Original Citation

Ali, Jafar (2011) Modelling of thermal plume discharge into shallow and still water. Doctoral thesis, University of Huddersfield.

This version is available at <http://eprints.hud.ac.uk/id/eprint/11118/>

The University Repository is a digital collection of the research output of the University, available on Open Access. Copyright and Moral Rights for the items on this site are retained by the individual author and/or other copyright owners. Users may access full items free of charge; copies of full text items generally can be reproduced, displayed or performed and given to third parties in any format or medium for personal research or study, educational or not-for-profit purposes without prior permission or charge, provided:

- The authors, title and full bibliographic details is credited in any copy;
- A hyperlink and/or URL is included for the original metadata page; and
- The content is not changed in any way.

For more information, including our policy and submission procedure, please contact the Repository Team at: E.mailbox@hud.ac.uk.

<http://eprints.hud.ac.uk/>

**MODELLING OF THERMAL PLUME
DISCHARGE INTO SHALLOW AND STILL
WATER**

**BY
JAFAR ALI**

University of Huddersfield
School of Computing and Engineering
Department of Engineering and Technology

A Thesis submitted to the University of Huddersfield
in partial fulfilment of the requirements for
the degree of Doctor of Philosophy

The University of Huddersfield in collaboration with the
British Waterways

February 2011

Abstract

The concerns of global warming are guiding most industries and commercial properties towards addressing their energy usage. In large buildings where air conditioning is required, there is often a need for “chillers” to control the temperature of the building. This process is not environmentally friendly and expensive in terms of energy used and maintenance issues. The alternative is to cool buildings using natural resources such as induced wind drafts and water extraction from rivers and canal. The latter has not been used with optimum effectiveness because the prediction procedures are not sufficiently developed to satisfy environmental legislation. The mathematical approaches are unrealistic and extremely conservative in their analysis and this causes many valid proposals to be rejected.

This research is aimed at addressing that situation. It will provide a valid interactive 3-dimensional analysis procedure that will better evaluate the potential of using any British Waterways canal or similar water source for cooling purposes.

After water has been used for cooling it is returned to the canal in a heated state as a thermal plume. It is the boundaries of the plume that must be predicted with reasonable accuracy so that environmental legislation is not infringed and livestock is not jeopardised. It is equally important to ensure the analysis is not over sensitive so as to result in rejection of valid proposals. Earlier work studied heat distribution but did not consider the thermal discharge into still and shallow water, as in a British Waterways canal. The studies below investigate several canal sites to evaluate a variety of situations where the discharge plume differs. Criteria including discharge direction, volume of water, temperature differences, speed of discharge and depth of discharge pipe all play a part in the formation of the plume. As such it is possible to develop an understanding of how the thermal plume merges into the still water and how the heat is diffused into the general body of water. In conjunction with site measurements a laboratory experimental scale model tank was built to replicate the real canal site. This allowed data to be varied and measured more readily. Two different types of discharge have been the subject of this research- the first being when the discharge pipe is located at the surface of the receiving water, the second being when it is submerged deeply below the surface. In all cases the temperature and velocity are measured at various points and at a variety of depths to provide a three dimensional plot across the mixing zone. In addition to the mathematical analysis, thermal imaging was used to predict the heat diffusion profiles on the surface of the receiving water in both the canal site and the model tank. CFD software is also used to evaluate the distribution of temperature and velocity within the mixing zone. The mathematical analysis produced an equation to predict the heat diffusion profile in surface discharge. And a number of equations were produced to model the plume path line in submerged discharge- relating to temperature and velocity dilution along and across the path lines. The relative effects of the bed and free surface proximity appeared significantly in the equations. A 3-dimensional model of the size of the plume is presented to demonstrate the results.

The procedure followed in this study will enable the Environment Agency personnel to assess the waste heat utilization with greater thoroughness and within a shorter period.

Acknowledgement

I would like to express my deepest gratitude and sincerest appreciate to my supervisor, Professor John D Fieldhouse for his invaluable guidance, encouragement, enthusiasm and support during the progress of this project.

I owe special thanks to God and my family.

Contents

Abstract	2
Acknowledgement	3
Contents	4
List of Tables	9
List of Figures	10
List of Symbols	17
List of Appendices	19
1. Introduction	20
1.1 Introduction	20
1.2 The Nature of the Problem	21
1.3 Canal Sustainable Cooling Solution	22
1.4 Environmental Consideration	22
1.5 Policy and Regulations	23
1.6 BW 1Dimensional ISIS Model	24
1.7 Research Questions	25
1.7.1 Hydraulic flow	25
1.7.2 Thermodynamic problem	26
1.8 Aims of the Research	26
1.9 Objective of the Research	27
1.10 Thesis Outline	27
1.11 Methods and Contribution	28
2. Literature Review	28
2.1 Introduction	28
2.2 Thermal Discharge	29
2.2.1 Buoyant Jet	29
2.2.2 Pure Plume	29

2.3 Types of Discharge	30
2.3.1 Submerged Discharge	30
2.3.2 Surface Discharge	31
2.4 Previous Studies	32
2.4.1 General Reviews	32
2.4.2 Review of Theoretical Analysis	34
2.4.3 Review of Computational Work	36
2.4.4 Review of Experimental Work	37
2.4.5 Relevant Studies	40
2.5 Mixing in Turbulent Flows	41
2.6 Thermal Discharge Simulation	42
3. Case study	43
3.1 Preliminary Case Study	43
3.1.1 Introduction	43
3.1.2 Sites Location	43
3.1.3 System Description:	47
3.1.4 Building Management System	49
3.1.5 Site Details	49
3.1.6 Canal	54
3.1.7 Initial thermal images	54
3.1.8 Measurements Procedure	55
3.1.9 Temperature Measurement	56
3.1.10 Flow Measurement	60
3.1.11 Depth Measurements	62
3.2 Refine Case Study	63
3.2. 1 Introduction	63
3.2.2 Central Services Building CSB - Surface Discharge	64

3.2.3 BBC Mailbox site	70
3.2.4 Canalside West	77
3.2.5 Lockside	78
3.2.6 Kirklees College Site	80
3.2.7 Enviroenergy Nottingham	80
4. Laboratory Experiment	82
4.1 Introduction	82
4.2 Objective of Experiments	82
4.3 Thermal Modelling	83
4.4 Experimental Setup and Apparatus	86
4.4.1 Model Tank	86
4.4.2 Water Supply	88
4.4.3 Experimental Method	90
4.5 Data Collection Procedure	91
4.5.1 Temperature measurements	91
4.5.2 Velocity measurements	95
4.5.3 Thermal Images	96
4.5.4 Dyed water discharge	97
4.5.5 Size Measurements	99
5. Thermograph	101
5.1 Introduction	101
5.2 Surface Discharge Thermal Images	102
5.3 Submerged Discharge Thermal Images	104
5.4 Model Tank Thermal Images	109
6. CFD Simulation	112
6.1 Introduction	112
6.2 Computational Analysis	112

6.2.1 Surface Discharge – CSB Site	113
6.2.2 Submerged discharge – Mailbox Site	118
7. Theoretical Analysis	123
7.1 Introduction	123
7.2 Surface Discharge Mathematical Model	123
7.3 Turbulent Diffusivity D	127
7.4 Submerged Discharge Mathematical Model	129
7.4.1 Plume Path Line	130
7.4.2 Plume Half Width	132
7.4.3 Temperature along Plume Path Line	133
7.4.5 Temperature across the path line	136
7.4.6 Velocity across the path line	138
7.5 3-Dimensional Model of Submerged Discharge	139
8. Results and Discussion	140
8.1 Introduction	140
8.2 Surface Discharge	140
8.2.1 Temperature dilution along the centreline of the plume	141
8.2.2 Temperature dilution across the centreline of plume	148
8.2.3 Temperature distribution on a plane on the centreline of plume	154
8.3 Submerged Discharge	157
8.3.1 Plume Path Line	158
8.3.2 Temperature along Plume Path Line	159
8.3.3 Velocity along Plume Path Line	161
8.3.4 Temperature across Plume Path Line	162
8.3.5 Velocity across Plume Path Line	166
8.3.6 Model Validation - Comparison of the Models against Canal Measured Data	170
8.3.7 Size of Plume – 3D Representation	177

9. Summary and Conclusions	185
9.1 Overview	185
9.2 Summary	186
9.3 Concluding Remarks	187
9.4 Future Work	191
10. References and Bibliography	191
Appendices	196

List of Tables

Table No.	Description	Page No.
4.1	Experimental trials parameters	94
8.1	Lateral turbulent diffusivity D_y	145
8.2	The five experimental runs reported in the current study	158

List of Figures

Figure No.	Description	Page No.
Chapter 1		
1.1	British Waterways Canal	22
Chapter 2		
2.1	Submerged discharge	31
2.2	Surface discharge	32
Chapter 3		
3.1	Central Services Building	44
3.2	Embankment – CSB	45
3.3	Canalside West – Outlet	45
3.4	Canalside West – Inlet	46
3.5	Lockside Building	46
3.6	Inlet/Outlet- Lockside	47
3.7	Cooling system schematic diagram	48
3.8	Exploded view of heat exchanger- ‘Coulson Vol.3, p 549’	48
3.9	Heat exchanger plate	49
3.10	Inlet screen – CSB	50
3.11a	CSB Discharge outlet	51
3.11b	CSB Discharge outlet	51
3.12	Normal View of CSW Outlet	52
3.13	Outlet-during dewatering of canal	52
3.14	Protective posts and mesh screen – Lockside	53
3.15	Thermal and digital image of Discharge plume	55
3.16	CSB- Temperature distribution along centre line of discharge	57
3.17	Temperature distributions along centreline of discharge	58
3.18	Lockside discharge	59
3.19	Plume temperature – Lockside	60

3.20	Velocity along centreline of plume – CSB	61
3.21	Velocity along the centreline of plume – Canalside West	62
3.22	Velocity along the centreline of plume – Lockside	63
3.23	Inlet pumps – CSB pump house	65
3.24	Discharge plume –CSB	66
3.25	Turbulent discharge – CSB	66
3.26a	Graduated pole caring flow meter and thermocouples	67
3.26b	Grids at CSB site	68
3.27	Measured temperature along the centreline of plume – CSB	69
3.28	Measured velocity along the centreline of plume – CSB	69
3.29	Canal depth at the mixing zone – CSB	70
3.30	Thermal plume	71
3.31	BBC Mail Box cooling water discharge to Birmingham Canal	71
3.32	Temperature and flow measurements for the canal bed at grid 2m distance from embankment	73
3.33	Plume moves to surface of canal, near embankment close to discharge point	73
3.34	Measured temperature along the centreline of plume – Mailbox	74
3.35	Measured velocity along the centreline of plume – Mailbox	75
3.36	Canal depth within the mixing zone – Mailbox	76
3.37	Thermal and digital image for a deeply submerged discharge	76
3.38	Measured temperature along the path line of plume – Canalside West	77
3.39	Measured velocity along the path line of plume – Canalside West	78
3.40	Measured temperature along the path line of plume – Lockside	79
3.41	Measured velocity along the path line of plume – Lockside	79
3.42	Plume path line – Enviroenergy Nottingham	81
3.43	Temperature along the path line - Enviroenergy Nottingham	81
3.44	Velocity along the path line of plume - Enviroenergy Nottingham	82
 Chapter 4		
4.1a	Experimental model tank	86
4.1b	Schematic diagram of experimental setup	87

4.2	Hot and cold water valves controlling cistern temperature	88
4.3	Movable discharge pipe	89
4.4	Discharge pipe flow control valves	89
4.5	By – pass	90
4.6	Thermocouples digital meter	92
4.7a	Photograph of data acquisition setup	93
4.7b	Schematic of data acquisition setup	93
4.8	Photograph of the schematic camcorders setup	96
4.9	Thermal and digital image of model tank	97
4.10	Submerged dyed plume discharge into model tank – plan view	98
4.11	Submerged dyed plume discharge into model tank – side view	98
4.12	Dyed water discharged into surface of model tank – side view	99
4.13	Plan view of the plume with dimensions	100
4.14	Side view of the plume with dimensions	100

Chapter 5

5.1	Thermal Camera connected to a PC	101
5.2a	Thermal image of Discharge plume	102
5.2b	Discharge plume	103
5.3	Thermal and digital image of plume from downstream	103
5.4	Typical photographic image of a discharge pipe and its corresponding thermal image	104
5.5	Thermal and digital image for a deeply submerged discharge	105
5.6	Mixing zone surface in submerged discharge	106
5.7a	Thermal image of Canalside West	107
5.7b	Canalside West	108
5.8a	Thermal image – Lockside	108
5.8b	Digital image – Lockside	109
5.9	Thermal and digital image of model tank	110
5.10	Heat diffusion on surface of tank (submerged discharge)	111

5.11	Thermal Camera show temperature profile along the line on the centreline of plume	111
------	---	-----

Chapter 6

6.1	Heat diffusion on a plane at the centreline of the discharge pipe	114
6.2	Heat diffusion on a plane on the surface of canal	114
6.3	Heat diffusion on a plane 0.6m below the surface of canal	115
6.4	Temperature dilution along the centreline of plume (0.075m) below surface	116
6.5	Velocity along the centreline of plume (0.075m) below surface	116
6.6	Heat diffusion on a plane normal to the centreline of plume (cross section)	117
6.7	Velocity distribution on a plane normal to the centreline of plume (cross section)	117
6.8	Heat diffusion on a plane at the centreline of the discharge pipe	118
6.9	Heat diffusion on a plane on the surface of canal	119
6.10	Heat diffusion on a plane on the canal bed	119
6.11	Centreline of plume at surface, bed and discharge layer and centreline temperature profile	120
6.12	Centreline of plume at surface, bed and discharge layer and centreline velocity profile	121
6.13	Heat diffusion on a plane normal to the centreline of plume (cross section)	122
6.14	Velocity distribution on a plane normal to the centreline of plume (cross section)	122

Chapter 7

7.1	Surface discharge flow configuration	124
7.2	Show (surface layer) grids points where the temperature and velocity been measured at CSB site	128
7.3	Schematic of the created blocks from the grids at the mixing zone	128
7.4	3-D model of the size of the thermal plume, Run 6 of the experiments	139

Chapter 8

8.1	Measured temperature along the centreline of plume (field trial)	141
8.2	Measured temperature along the centreline of plume (model tank)	142

8.3	Thermal Camera results	148
8.4	Temperature along the centreline of plume predicted by FLUENT	144
8.5	Centreline temperature decay (mathematical equation)	146
8.6	Comparison of the theories and experiments results of centreline temperature	147
8.7	Comparison of the theories and experiments results of centreline temperature	147
8.8	The structure of the heated surface discharge	148
8.9	Temperature across the centreline of plume for the mathematical model and field trial at $x = 0.5\text{m}$	149
8.10	Temperature across the centreline of plume for the mathematical model and field trial at $x = 1\text{m}$	150
8.11	Temperature across the centreline of plume for the mathematical model and field trial at $x = 1.5\text{m}$	150
8.12	Temperature across the centreline of plume for the mathematical model and field trial at $x = 2\text{m}$	151
8.13	Temperature across the centreline of plume for the mathematical model and field trial at $x = 2.5\text{m}$	151
8.14	Temperature across the centreline of plume for the mathematical model and field trial at $x = 3\text{m}$	152
8.15	Temperature across the centreline of plume for the mathematical model and field trial at $x = 3.5\text{m}$	152
8.16	Temperature across the centreline of plume for the mathematical model and field trial at $x = 4\text{m}$	153
8.17	Temperature across the centreline of plume for the mathematical model and field trial at $x = 4.5\text{m}$	153
8.18	Temperature across the centreline of plume for the mathematical model and field trial at $x = 5\text{m}$	154
8.19a	Heat diffusion on a plane at the discharge layer for $p = 0.018\text{m}$	155
8.19b	Heat diffusion on a plane at the discharge layer (field trial measured data)	155
8.20	Heat diffusion on a plane at the discharge layer for $p = 0.052\text{m}$	156
8.21	Heat diffusion on a plane at the discharge layer for $p = 0.0044\text{m}$	157
8.22	Theoretical plume path line and comparison with experimental data	159
8.23	Theoretical temperature along plume path line and comparison with experimental data	161
8.24	Theoretical temperature decay along plume path line and comparison with experimental (dimensionless) data	162
8.25	Theoretical velocity along plume path line and comparison with experimental data	162

8.26	Theoretical temperature across plume path line and comparison with experimental data. Run 4, F _d 14.39	163
8.27	Theoretical temperature across plume path line and comparison with experimental data. Run 6, F _d 41.48	164
8.28	Theoretical temperature across plume path line and comparison with experimental data. Run 18, F _d 38.59	164
8.29	Theoretical temperature across plume path line and comparison with experimental data. Run 20, F _d 31.51	165
8.30	Theoretical temperature across plume path line and comparison with experimental data. Run 23, F _d 16.29	165
8.31	Theoretical temperature across plume path line and comparison with experimental data. 20cm from the outfall for five different experiments	166
8.32	Theoretical velocity across plume path line and comparison with experimental data. Run 4, F _d 14.39	167
8.33	Theoretical velocity across plume path line and comparison with experimental data. Run 6, F _d 41.48	167
8.34	Theoretical velocity across plume path line and comparison with experimental data. Run 18, F _d 38.59	168
8.35	Theoretical velocity across plume path line and comparison with experimental data. Run 20, F _d 31.51	168
8.36	Theoretical velocity across plume path line and comparison with experimental data. Run 23, F _d 16.29	169
8.37	Theoretical velocity across plume path line and comparison with experimental data. 10cm from the outfall for five different experiments	169
8.38	Theoretical temperature and velocity along plume path line and comparison with canal measured data (Canalside West)	171
8.39	Theoretical temperature and velocity across plume path line and comparison with canal measured data (Canalside West)	172
8.40	Theoretical temperature and velocity along plume path line and comparison with canal measured data (Lockside)	173
8.41	Theoretical temperature and velocity across plume path line and comparison with canal measured data (Lockside)	174
8.42	Theoretical temperature along and across plume path line and comparison with canal measured data (Mailbox)	176
8.43	Theoretical velocity along and across plume path line and comparison with canal measured data (Mailbox)	177
8.44	Size of thermal plume for experimental run 4, F _d 14.39	178
8.45	Size of thermal plume for experimental run 6, F _d 41.48	179
8.46	Size of thermal plume for experimental run 18, F _d 38.59	179

8.47	Size of thermal plume for experimental run 20, Fd31.51	180
8.48	Size of thermal plume for experimental run 23, Fd16.29	180
8.49	Plan and sectional view of thermal plume below the surface at Canalside West site	182
8.50	Plan and sectional view of thermal plume below the surface at Lockside site	183
8.51	Plan, sectional and isometric view of thermal plume below the surface at Mailbox site	184
 Chapter 9		
9.1	Flow pattern regimes	189

List of Symbols

The following symbols are used in this report; note that the unit of length in the laboratory is in cm

D	Diffusion Coefficient, m/s ²
σ^2	Variance, m ²
t	Time, s
u, v, w	Velocity fluctuating value in x, y and z direction, m/s
U, V, W	Velocity mean value in x, y and z direction, m/s
ρ	Density, kg/m ³
ρ_a	Ambient density, kg/m ³
ρ_0	Discharge water density, kg/m ³
D_x, D_y, D_z	Turbulent diffusivity in x, y and z Direction respectively, m/s ²
F_d	Densimetric Froude number
U_r	Velocity ratio
ν	Kinematic Viscosity, m ² /s
μ	Dynamic Viscosity, Pa.s
A, B, A1, B1	Constants
A2, B2, a, α	Constants
M	Total Heat Diffusion
erf	Error function
g	Gravity, m/s ²
g_r	Gravity Ratio
D_0	Discharge pipe diameter, m
z_0	Discharge pipe depth from bed, m
H	Receiving water depth, m
U_0	Discharge velocity, m/s
g'	Buoyancy, m/s ²
Q	Flow rate, m ³ /s
B_0	Buoyancy flux, kgm ² /s ²
M_0	Momentum flux, m ⁴ /s ²
LM	Length scale, m
Re	Reynolds number
x	Longitudinal axis (along the plume), m
y	Lateral axis (across the plume), m
z	Vertical axis (depth wise), m
L	Maximum (x); plume length, m
T	Temperature mean value, °C
\hat{T}	Temperature fluctuating value, °C
T_0	Discharge temperature, °C
T_a	Ambient receiving water temperature, °C
ΔT	Temperature difference, °C

Subscripts

o	Discharge value
m	Model tank
p	Canal value (prototype)
r	Ratio
x	Spatial direction
y	Spatial direction
z	Spatial direction

List of Appendices

Description	Page No.
Appendix 1: Measurements Procedure	196
Appendix 2: Equipment Used	207
Appendix 3: Preliminary Field Measured Data (Temperature, Velocity and Depth)	211
Appendix 4: Refine Field Measured Data (Temperature, Velocity and Depth)	216
Appendix 5: Kirklees College Case Study	225
Appendix 6: Enviroenergy Nottingham Case Study	238
Appendix 7: 3-D Model MATLAB Code	253
Appendix 8: Experimental and Predicted Plume Path Line Data	255
Appendix 9: Experimental and Predicted Temperatures along and Across Plume Path Line	256
Appendix 10: Experimental and Predicted Velocity along and Across Plume Path Line	259
Appendix 11: Canal sites and predicted path line data	262

1. Introduction

1.1 Introduction

The disposal of heated water from power plants and cooling systems into a natural water environment is a major environmental problem. Water is normally drawn from natural or artificial sources into the cooling system heat exchanger, the cooling water increases in temperature within the system and it is ultimately discharged back into the lakes, rivers or canals. This results in a rise in the bulk temperature of the surrounding water. This type of cooling system is economically low cost since water is the most inexpensive fluid available, and is also environmentally friendly in terms of heat disposal. However if the thermal discharge affects negatively on the surrounding ambient fluid then the process is called thermal pollution. The main effect of the increased in ambient water temperature is the reduction of the dissolved oxygen which puts aquatic life at risk. The increase in temperature also affects the balance of natural and biological processes in the water.

There is a large number of studies of this type regarding water mixing and heated water discharge into cooler water. But the majority of them are based on assumptions - some use experimental model tanks but do not validate with real field trials whereas others only make use of mathematical models and again do not validate with field trials.

In this research a study of heated water discharge into still and shallow water is described using a comprehensive technique. A thermal camera is used to measure the heat diffusion profile on the surface of the receiving water using a number of British Waterways canal sites. The sites are then replicated in a laboratory environment using a scale model tank. The combined results are then used to develop a two dimensional mathematical model of heat diffusion in surface discharge. This is carried out using variable values of turbulent diffusivity. As for submerged discharges, the plume path line, temperature and velocity along and across the path line have been identified. Additionally, MATLAB software is used to develop the model towards a three dimensional representation showing the size of the plume throughout the canal. The study also used CFD software in the analysis of both types of discharge, surface and submerged.

Presently, the University of Huddersfield has three sites licensed to extract water for cooling purposes. All these sites have comprehensive records and all show that the process is safe for aquatic life. However, British Waterways' one dimensional mathematical model suggests they will not be safe and if the model is over-conservative in its prediction then British Waterways

may reject licensing applications that are in reality safe. It is this situation that demands a more realistic prediction tool be developed; a tool that is readily understood, adequate for the level of applications and easily manipulated to represent the varied situations that are likely to be experienced. This research is limited to the study of heated water discharge into a body of still and shallow receiving water.

1.2 The Nature of the Problem

The current architectural trend is to build large complexes and manage them centrally. Numerous commercial organisations occupy small spaces in large office blocks where computing facilities are common – all generating heat. To control overall building temperatures it is a necessity to include a cooling system in the building plans at the outset. Traditional air conditioning makes use of chillers to cool the system but if the building is located in close proximity to a British Waterways canal then an environmentally friendly alternative may be available. British Waterways currently have a number of sites around the country where canal water is used for cooling systems thus eliminating the need for chillers. This is an area of business which British Waterways wish to expand for both environmental and commercial reasons. Their current evaluation process is over-conservative and leads to many applications being rejected. As such they wish to re-evaluate their assessment method.

Whilst British Waterways are responsible for the evaluation of applications for abstraction licences, local Environment Agencies are responsible for policing of water abstraction and water quality in accordance with The Surface Waters (Fishlife) (Classification) Regulations 1997. These regulations provide classification and guidance for inspection, sampling and analysis of pollutants in inland freshwaters with the intention of protecting and improving the environment of aquatic life.

New applications for proposed abstraction and discharge licenses are assessed and authorised by BW and are regularly monitored by the local Environment Agency for compliance with the license and other appropriate environmental regulations. Therefore BW wish to undertake a series of investigations to gain a more thorough understanding of the effects of the mixing of the discharged water and the effect of heat transfer to allow sufficiently robust assessment of applications and consequent energy savings. It is intended to produce an optimal design for the discharge pipe in order to satisfy the environment agency regulations and derive a mathematical model to predict the heat diffusion profile within the canal.

1.3 Canal Sustainable Cooling Solution

British Waterways protects 2200 miles of canal across UK which can be used in water cooling systems, see Figure 1.1.

BW estimates an additional 1000 businesses on canal sites could use canal water for cooling purposes. According to British Waterways official web site this will result in a saving of £100 million on annual energy bills and a reduction of carbon dioxide emissions by 1 million tonnes each year. This value is equivalent to 400,000 family sized cars being taken off the roads. British Waterways benefit from the income of canal water sales which they reinvest in canal maintenance. All the figures used in this clause plus the comments are derived from British Waterways' official website.



Figure 1.1: British Waterways Canal

1.4 Environmental Consideration

Water is usually withdrawn from the canal into the heat exchanger of the cooling systems and returned to it after use; the returned water has a temperature greater than the ambient temperature of the canal which will cause a rise in canal temperature particularly in the region close to the outfall.

As discussed, water temperature influences levels of oxygen and nutrients which in turn influence aquatic life. To provide an example of the environmental impact of thermal fluctuations, a reduction of the optimum temperature by 5°C can reduce the growth rate of catfish by 50%, and a localised rise in canal temperature can influence the movement pattern of fish as they flee 'hot zones' (Hoar, 2005).

Although, the water temperature is an important positive influence in aqua physiology, distribution and lifestyle, the increase of temperature above a certain degree (28°C in BW canal) becomes a hazard to aquatic life. The dissolved oxygen and the solubility rate of oxygen will reduce when the canal ambient temperature exceeds 28°C, until life is no longer sustainable. According to the Environment Agency if the concentration of oxygen falls below 7mg/l for more than 50% of the time outside the mixing zone, then fish are at risk. For salmonid waters the concentration should not fall below 9mg/l. Additionally, the changes in the bulk temperature of the canal disrupt the chemical and biological balance of the canal, thus reducing the quality of the water. This demonstrates the importance of temperature control.

1.5 Policy and Regulations

As discussed, the Environment Agency is responsible for policing of water abstraction and water quality in accordance with The Surface Waters (Fishlife) (Classification) Regulations 1997. These regulations provide the framework for inspection, sampling and analysis of pollutants for inland freshwaters. The key points applicable to cooling water abstraction to prevent the loss of aquatic life and de-oxygenation of the water are (Environment, 1997):-

- For cyprinid (non-salmonid) waters the temperature downstream of the point of discharge should not be raised by more than 3 degrees Celsius on the edge of the mixing zone.
- The temperature downstream of the point of discharge, at the edge of the mixing zone must not exceed 10°C during the breeding season for species which require cold water for breeding.
- The maximum temperature shall never exceed 28 degrees Celsius for cyprinid waters.

Note:

These figures are further restricted for salmonid waters.

From an environmental perspective, schemes are acceptable to BW provided that (Environment, 1997):-

- The temperature of the receiving water outside the mixing zone should not be raised by more than 3°C and should never exceed 28°C.
- These temperatures are reduced to 1.5°C and 21.5°C respectively for salmonoid waters.
- The mixing zone is the area around the outfall outside of which the temperature standards do not apply. Guidance from the Environment Agency or Scottish Environment Protection Agency (SEPA) defines the size of the mixing zone.

The mixing zone, as a general rule, depends upon the ability of fish to move away from any unfavourable conditions around the outfall. It should not cross the full width of canal at the water surface and must leave at least one meter from the opposing bank to allow free movement of fish. Restrictions are also applied to the water velocity which must not exceed the standards for navigation provided in “The Code of Practice for Works Affecting British Waterways”.

1.6 BW 1Dimensional ISIS Model

During the visit to the BW Research Centre they explained their background studies carried out to date and demonstrated the use of ISIS software and their simplified version using an Excel spreadsheet. They provided the required introduction and background to the investigation.

Evaluation for abstraction was carried out by BW using ‘ISIS’ software which is considered to be the water industry standard software for evaluation of hydraulic flow and water quality. However this software is designed to model open channels in rivers and estuaries where high flow rates and high differential water levels are normally experienced. These are not normal canal conditions where flow close to zero and variations in water levels are relatively small. It is reported by BW that this has led to inconsistencies against the results obtained using the software and the results obtained from monitoring of certain existing installations. ISIS does not consider the local effect of the plume assuming the discharge to be fully mixed along the length and breadth of the canal. The Software is two parts ISIS Flow and ISIS Quality:

ISIS Flow:

ISIS Flow is used to model the hydrodynamics of a loop or branched network which includes a variety of hydraulic structures, locks, sluice gates, bridges etc and the results stored for further analysis using ISIS Quality

ISIS Quality:

ISIS Quality is a separate program modules used to model water quality in open channels using the hydrodynamic data provided from the ISIS Flow analysis to model the concentrations of water pollutants using finite difference approximation to Fick's Law for the advection-diffusion equation.

Every lock through the canal network is numbered for identification purposes and the distance between the locks is divided into lengths known as 'chainage'. The canal can then be surveyed for dredging purposes and the cross section at each chainage recorded. This data allows an approximation of the volume of water and surface area between locks to be calculated.

The published literature for the ISIS software gives a good starting point for any investigation. If flow occurs in an open channel, the calculations can be split into two areas:

- Hydraulic flow
- Heat transfer

The application of ISIS software firstly considers the hydrodynamic model for flow in open channels. Data capture is regulated over 20sec time intervals throughout a 168hour period to ensure balanced conditions are achieved. Readings are then taken on flow in open channels. Fick's law and the advection-diffusion equation are then applied to refine the theories used in the software. The results were therefore appropriate for use in canal applications- producing simplified Excel spreadsheets which required the input of basic data.

1.7 Research Questions

1.7.1 Hydraulic flow

What is the size of the discharge plume/mixing zone?

What determines the size of the mixing zone?

What is the effect of the discharge flow rate into canal?

What are realistic values for the discharge turbulent diffusivity?

What is the effect of the canal depth on the size of the plume and velocity profile?

What is the effect of the discharge pipe depth, free surface and canal bed on the plume and the velocity profile?

How does the relative proximity of the inlet/outlet configuration affect flow and recirculation?

How does the discharge velocity effect plume size and thermal diffusion?

How are plume flow characteristics effected by magnitude of heat load?

What is the effect of pipe diameter on the flow velocity and plume temperature dispersal?

What determines the plume path line?

1.7.2 Thermodynamic problem

How is temperature distributed in 3D through discharge plume?

What is the effect of ambient temperature variations?

How does the relative position of the inlet/outlet configuration and flow/recirculation affect temperature?

Does the temperature gradient across the plume and length of the plume relative to the width of the canal ensure that fish can bypass the plume?

What are the effects of the discharge pipe depth, the free surface and the canal bed on the temperature profiles?

1.8 Aims of the Research

- Produce a viable, uncomplicated and accessible model that may be used to evaluate all British Waterway's standard systems and satisfy Environment Agency regulations.
- Address varied discharges of any heated water discharge into a shallow and still water environment.

1.9 Objective of the Research

The following are the main objective of this study:

- Develop a number of equations to predict the thermal plume profile in shallow and still water
- Investigate two types of thermal discharge; surface and submerged.
- Carry out a detailed investigation into the behaviour of the thermal discharge into the canal and the subsequent rise in water temperature.
- To investigate the interaction of the discharge plume and heat transfer within the canal.
- Investigate dissipation and determine the thermal mixing area and size of the plume.
- Investigate further the existing licenses for abstract / discharged canal water (used in the operation of cooling systems) at a number of British Waterways canal sites experimentally and theoretically to demonstrate the compliance of the sites to the requirements of the Environment Agency.
- Model the thermal plume experimentally, computationally and theoretically.
- Validate the predicted data against the laboratory experimental data and actual canal site data

1.10 Thesis Outline

This chapter provides an introduction to the subject. The following chapter will review the major analytical, computational and experimental works on thermal discharge currently available. In Chapter 3, the preliminary and refined case studies are discussed and the experimental works on the real canal site are presented. Chapter 4 discusses the laboratory experimental work and the canal site simulation with the environmental scale model tank. Chapter 5 describes the use of thermal imaging in the study and presents thermal images of the thermal plume on the canal site and the model tank. Computational of Fluid Dynamics software is applied in Chapter 6 to predict the behaviour of the thermal plume. Chapter 7 describes the theoretical analysis and all derived equations which predict the behaviour of the thermal plume. The results obtained from the previous chapters are compared, discussed and presented in Chapter 8. In Chapter 9 the concluding remarks of the study are presented. The last two chapters 10 and 11 contain references and appendices respectively.

1.11 Methods and Contribution

The current thermal discharge models cannot be applied on BW's canals, because, as will be explained in the following chapter, they are mainly applicable to shallow flowing rivers or deep stagnant lakes.

This research will produce a model to predict the behaviour of the thermal plume in British Waterways canals and will aim to fill this gap. The models developed in this research apply all three types of thermal plume analysis; theoretical, computational and experimental. The work started with experiments on canal sites and data collection within the mixing zone. Temperatures were measured by thermocouples at grid points and various depths. Turbine flow meters were used to measure velocity at each point. In addition air temperature and wind speed are measured. Thermal imaging was used to see the heat diffusion on the surface of the canal and was compared to digital camera images. A laboratory experimental model tank was built to simulate the canal site and FLUENT software was used to model the flow and temperature. A number of equations were derived to predict the temperature and velocity profile and present a 3D model of the thermal plume.

2. Literature Review

2.1 Introduction

Initial background research was undertaken via internet searches for technical papers and previous experimental work carried out in this area plus textbook reading of appropriate technical subjects. The searches revealed a number of interesting articles which are referenced. They appear to be mainly concerned with the modelling dispersal of pollutants from effluent discharge and/or management of discharge into large rivers, lakes and estuaries and modelling the effects of tidal mixing.

In contrast, the requirement of BW is to determine surface and submerged temperature distribution and make an assessment of discharged heat load into canal. Discharge of warm water into a shallow canal occurs with little or no flow and hence mixing only occurs due to the turbulent discharge within a localised area and the remaining heat dissipation occurs by natural convection. No forced mixing occurs outside the localised area of the plume other than dispersal due to prevailing wind conditions.

2.2 Thermal Discharge

Typically, a thermal discharge source is a cooling system or power plant. This research is mainly focused on the heated water discharge from cooling system heat exchangers through a pipe into a body of shallow and still receiving water. The flow is turbulent and its driving forces are buoyancy and momentum. There is a discontinuity of temperature and velocity as the thermal discharge merges with the receiving water. The heated water discharged generates a strong shearing with the still receiving water. The shear force moves the ambient still water around the edges of the thermal discharge, whilst the still receiving water acts to reduce the speed of the discharge at the boundary. This process takes place within the mixing zone as the thermal discharge moves downstream. Distribution takes place in two directions, inward towards the centreline of the thermal discharge thus reducing the velocity and outward towards the still receiving water to entrain more ambient water into the mixing zone. Momentum is therefore being transferred continuously from the thermal discharge to the outer region causing the stationary and slow moving water to accelerate and the inner high velocity region to decelerate as it loses momentum (Demissie, 1980). The combination of the shear force generated at the boundary and turbulent mixing modifies the velocity profiles (Chadwick, 2004). The thermal discharge could be a jet or plume, and these two words are sometimes used interchangeably. The following are the correct definitions of the buoyant jet and pure plume.

2.2.1 Buoyant Jet

A buoyant jet or forced plume is a flow of water with low density discharged with high initial velocity through an orifice into a receiving water of higher density. The thermal discharge in this case has high kinetic energy and momentum. The buoyant jet flow is fully turbulent whenever its efflux Reynolds number, based on efflux velocity, orifice dimension and fluid kinematic viscosity is sufficiently large (Jirka, 2004).

2.2.2 Pure Plume

The thermal discharge called pure plume occurs when low density water discharges with a low initial velocity through an orifice into higher density of receiving water. In this research the thermal discharge studied is a pure plume.

Jets and plumes are classified to four different regions as follows:

1. Core region: a small region around the discharge outfall in which the temperature and velocity are very high and remain nominally constant.
2. Entrainment region: in this region the centreline velocity and temperature are decreased significantly, the lateral spread is much greater than vertical spread.
3. Stable region: in which the vertical entrainment is reduced or ended, the plume depth (thickness) is very small as the heated water spreads on the surface, the temperature remains relatively constant and velocity drops sharply.
4. Heat loss region: the end of the plume or the discharge may no longer be considered as a plume. The lateral spread is very large and provides a large surface of convective heat transfer. In this region temperature reduces to reach ambient water temperature.

2.3 Types of Discharge

Thermal discharge can be classified according to the location of the discharge pipe, the discharge pipe dimensions and cross section, the number of diffusers and so on. The main two types of thermal discharge into shallow and still receiving water based on locations are submerged and surface discharge.

2.3.1 Submerged Discharge

The structure design of the discharge pipe is varied from one site to another, because there are different types of structure. In this section the submerged discharge is described. The discharge pipe locates below the free surface of the canal with a certain depth see Figure 2.1. This type of thermal discharge is complex because the discharge pipe is submerged below the free surface of the receiving water and the thermal plume cannot be observed. In thermal submerged discharge the plume will be influenced by the free surface and the canal bed. It is deflected towards the free surface with increasing distance downstream because of the lack of entrainment in the region between the centreline of the plume and the canal surface. The deflection reduces as the depth of the discharge pipe increases. This is due to the increase of entrainment in the area above the centreline of the plume. Entraining ambient water into the plume region reduces the velocity of the plume in that region, so the velocity in the region

above the centreline of the plume has higher velocity than the lower region. Figure 2.1 illustrates the deflection of the plume in a shallow and deeply submerged discharge.

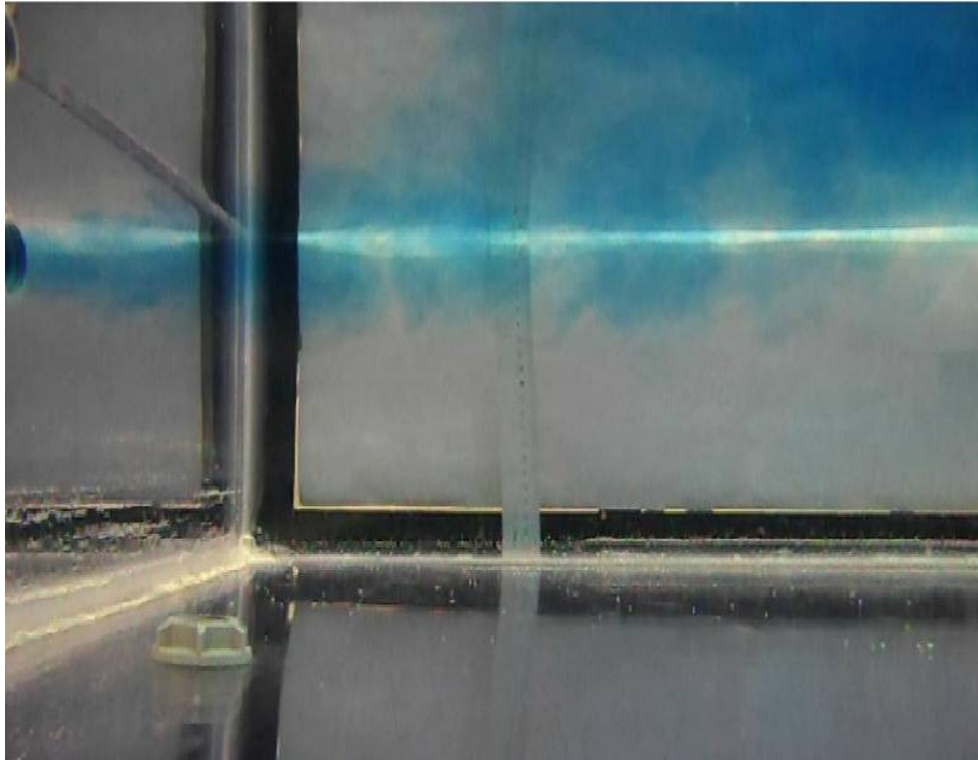


Figure 2.1: Submerged discharge

2.3.2 Surface Discharge

In surface discharge the discharge pipe is semi-submerged and the distance between the centreline of the plume and the free surface of the receiving water is equal to the radius of the discharge pipe. Surface discharge is preferred in some cases as the majority of heat transfer to the atmosphere is by evaporation and radiation. The receiving water is less affected by surface discharge as the heated plume remains on the surface, so only a small amount of heat distributes to the layer below the centreline of the plume. Therefore aquatic life can safely pass through the undisturbed space between the bed and plume. This type of discharge is easy to investigate as the discharge pipe is located on the surface and the thermal plume can be observed. In addition the vertical velocity and buoyancy effects are limited. The Central Services Building at the University of Huddersfield is given as an example of surface discharge as thermal plume of the flow clearly defined on the surface; this is illustrated in Figure 2.2.



Figure 2.2: Surface discharge

2.4 Previous Studies

As noted above, studies on thermal discharge are classified into three categories, theoretical analysis, computational analysis and experimental work. In the following sections past thermal discharge studies are explored beginning with general reviews followed by each category:

2.4.1 General Reviews

Much literature on thermal discharge studies is available but this review focuses on those studies which are most relevant to the theories of the current study.

Initial textbook reading investigated the mathematics of diffusion and fluid dynamics. The Mathematics of Diffusion (Crank, 1970) is a good mathematical textbook covering the standard basics of heat distribution by convection, conduction and radiation. The text outlined classical theories covering the heat advection diffusion equation, heat diffusion coefficients calculations, etc. The theories of Crank are most applicable to the surface discharge and non-buoyant jets. Cranks procedure is used in the current study to model the surface discharge.

Additional studies regarding fluid flow and heat transfer were also undertaken to underpin this research. Wastewater Engineering – collection, treatment, disposal (Metcalf & Eddy, 1972) discusses the fundamentals of fluid mechanics in open channels. It explores the work of Robert Manning in the nineteenth century and specifically Manning’s equation which is commonly used for flow calculations in open and closed channels. This equation provides typical values for the coefficient of roughness as applied to differing surfaces including “canals with rough stony beds [or] weeds on earth embankments”. The Manning’s equation and coefficients are used in the ISIS software model. Wastewater Engineering covers the basic fluid theory and flow in open channels and concentrates heavily on the environmental discharge, pollutants, bacteria and waste water treatment. The text discusses the effect of the temperature of wastewater and its impact on aquatic life, chemical reactions and reaction rates. It also describes the effect of effluent disposal by dilution and disposal into lakes and rivers and introduces the topic of mathematical modelling of plug flow in river mixing, estuary diffusion and the continuity equation for initial dilution of the discharge from a single or multi-port diffuser. However, the analysis of temperature dispersal through the plume and the extent of turbulent flow of the plume are not covered. The derived mathematical model, states that ‘it is assumed that waste is evenly distributed over the cross section of the river but this may be some distance from the discharge and that if the river is not extremely turbulent no mixing occurs along the axis of the river and the model should be regarded as plug flow’. For the BW canal, no flow occurs within the canal and therefore a steady state fully mixed approach has been assumed.

Thermal Effluent Disposal from Power Generation by (Zaric, 1978) is a valuable textbook in thermal discharge studies. It contains lectures presented at the international advanced course on Heat Disposal from Power Generation held August, 1976 in Dubrovnik, Yugoslavia. The aim of the book and its related course is to familiarise the participant with alternative methods of heat disposal as well as with the most recent techniques of engineering analysis and design necessary for their implementation and environmental evaluation (Zaric, 1978). The author presented each lecture in the course as a distinct chapter.

These three textbooks each take a different approach. One discusses the mathematics of diffusion, another the basics of fluid dynamics and waste water management, and the third compiles lectures presented a conference on heat disposal.

The available textbooks on thermal discharge, waste water management and turbulent flow are vast and all provide an excellent source of reference on the basics of thermal diffusion,

jet/plume properties, heat and mass transfer. The reader can consult the references and bibliography to appreciate this. In the following sections the literature review will focus on the technical papers published in this field. Because of the large number of publications it is intended to discuss only the work of the people who are mainly known in this field and the works that most closely relate to the current project.

2.4.2 Review of Theoretical Analysis

As was mentioned in the previous sections most available studies on thermal discharge describe incidences when the receiving water is deep and stagnant such as oceans and lakes or discharges into shallow and flowing water such as rivers. The location of the discharge pipe (submerged or on surface) also impacts on the study. The majority study surface discharge since this is easier to predict. In this study surface and submerged discharge are discussed with most focus on the latter. Taylor, (1921) studied diffusion in continuous and discontinuous motion ambient fluid. He developed a model to predict the molecular diffusion coefficient and states that the rate of heat transferred in x direction is determined by the rate of increase of the mean value of the square of the distance, parallel to the axis of x, which is moved through by a particle of fluid in time t , equation 2.1.

$$2D = \frac{d(\sigma_x^2)}{dt} \quad (2.1)$$

Where, σ_x^2 is the variance of a (longitudinal) spatial cross sectional average solute concentration profile. (Abramovich, 1963) cited the first attempt of computing the jet trajectory in cross flow by (Baturin and Shepelev) in 1934. They obtained the velocity along the centreline of the jet geometrically using velocity vector for the ambient and the jet. Subsequently Abramovich (1963) carried out same analysis used by (Baturin and Shepelev) to determine jet centreline velocity in cross flow using flow rate rather than area. Later attempts continued to determine the thermal discharge behaviour in cross flow. (Bowley and Sucec, 1969) produced a two-dimensional model to predict the jet trajectory in variable or uniform cross flow using conservation of mass. But this is not enough to model the plume trajectory without the momentum equations. (Launder and Samaraweera, 1979) developed a model to predict the spreading rate of jet in cross flow. (El-Baz, et.al, 1996) investigated the

development of surface jet in a current. They produced equations of shear flow for forward-marching finite volume. The relevant of the above papers gives a good point about the effects of the thermal discharge directions across or along the canal. However the discharge direction is less important in the current study as the ambient water is still.

Thermal discharge into deep still water has been studied widely by the researchers. In this type of thermal discharge the majority of studies focus on surface discharge where the discharge pipe is located at the surface of receiving water. (Patankar and Spalding, 1972) developed a procedure to solve the three dimensional parabolic equations. This work gave the researchers of thermal discharge a positive step to solve the equations of motions. Three Dimensional Heated Surface Jets by (Stolzenbach and Harleman, 1973) solved four governing equations in their model; continuity 2.2, longitudinal momentum 2.3, lateral momentum 2.4 and thermal energy 2.5 equations as follows:

$$\frac{\partial U}{\partial x} + \frac{\partial V}{\partial y} + \frac{\partial W}{\partial z} = 0 \quad (2.2)$$

$$\frac{\partial U^2}{\partial x} + \frac{\partial UV}{\partial y} + \frac{\partial UW}{\partial z} = \frac{1}{\rho} \frac{\partial \rho}{\partial T} g \int_{-\infty}^z \frac{\partial T}{\partial x} dz - \frac{\partial uv}{\partial y} - \frac{\partial uw}{\partial z} \quad (2.3)$$

$$\frac{\partial VU}{\partial x} + \frac{\partial V^2}{\partial y} + \frac{\partial VW}{\partial z} = \frac{1}{\rho} \frac{\partial \rho}{\partial T} g \int_{-\infty}^z \frac{\partial T}{\partial y} dz \quad (2.4)$$

$$\frac{\partial UT}{\partial x} + \frac{\partial VT}{\partial y} + \frac{\partial WT}{\partial z} = -\frac{\partial vT'}{\partial y} - \frac{\partial wT'}{\partial z} \quad (2.5)$$

It is assumed that the turbulent transfers in the x directions are neglected whilst lateral and longitudinal pressure gradients resulting from the temperature gradients are retained (the first term on the right hand side of the momentum equations). In the lateral momentum equation the pressure gradient is balanced by the mean convective terms that embody the lateral gravitational spreading, the Boussinesq assumption is also used in this work (Stolzenbach and Harleman, 1973). The authors used order of magnitude arguments to simplify and solve the elliptic equations. Although their model approved and satisfied the experimental analysis, the

assumptions of the lateral momentum equation neglected the turbulent transfer terms and therefore could produce unsatisfactory results. This model is restricted to the application of thermal surface jets into deep water.

(Launder and Spalding, 1974) solved the transport equations and governing equations numerically. They obtained the values of the two turbulent quantities, the turbulence kinetic energy k and turbulence energy dissipation rate ϵ . (Launder, et al, 1975) developed a method to determine the Reynolds stresses in turbulence model by solving the transport equations. (Launder, 1975) add gravitational effects and buoyancy to pressure correlation terms in the transport equations. This work combined with the proposal developed by (Launder, et al, 1975) and (Launder and Spalding, 1974) formed a comprehensive method to determine all the constants in the turbulence model. The studies of jets in stagnant ambient by (Launder, et. Al, 1975) predicted the shear stress and normal stress. From the above studies and their attempts to convert the elliptic equations to parabolic, it is understood that the thermal plume profiles have parabolic shapes.

2.4.3 Review of Computational Work

There is much available CFD software to model heat and fluid flow. ISIS is software developed by British Waterways senior engineers to model heat diffusion in the canal. An introduction on ISIS has been given in the previous chapter. CORMIX1 software includes interesting figures showing the discharge of a submerged vertical plume. This is primarily concerned with the geometry and dilution of effluent into deep water rather than the application to BW canal. It presents the effect of turbulent buoyant mixing in stagnant water and ambient density stratification of a continuously discharged effluent. (Pinheiro and Ortiz) investigated the use of CORMIX 1, PHOENICS and PLUMAC 2.2 in analysis of heated water discharged into still body of water. They proved that the results by using CORMIX 1 and PLUMC 2.2 have a good convergence and better adjustment than PHOENICS. FLUENT is one of the most popular CFD software used to model fluid flow and heat transfer. Neither of the CFD packages used models thermal plumes into still and shallow receiving water. The significance of reviewing these types of software is to make the reader familiar with some of the available software in this field. In the current study FLUENT software used to model the thermal plume into a British Waterways canal.

2.4.4 Review of Experimental Work

Numerous experimental studies are available on thermal discharge into deep still and shallow flowing ambient. Several of these studies are reviewed in this section starting with flowing ambient. The experimental technique used in the current study has been used by (Campbell, J. F. and Schetz, J. A., 1971 and 1972). They studied the behaviour of thermal jet discharge into waterways with current. They used dyed water in the experiments and installed two cameras on the side and top of the model tank to record the behaviour of the thermal plume and trajectories. (Cederwall and Brooks, 1971) investigated buoyant jets in still and flowing environments. Their model contains two main parameters the densimetric Froude Number and the ratio of discharge pipe diameter to the depth of receiving water. (Kannberg and Davis, 1974) investigated the behaviour of thermal jets deeply submerged in stagnant and co-moving water. They produced their model experimentally and primarily involved the densimetric Froude number without reference to the bed effects and the location of discharge pipe. Flow of Surface Buoyant Jet in Cross Flow by (Anwar, 1987) is the best paper carried out in eighties in terms of the experimental equipment employed. Its model tank was very long (50m). This paper predicted the profile for temperature and velocity at various layers through the depth of the model tank. It was found that the jet axis at all different depth is described by equation 2.6:

$$\frac{y}{h_j} = A \left(\frac{x}{h_j} \right)^n \quad (2.6)$$

Where x , y are distances, h_j is the cross section height of the discharge pipe (a rectangular discharge pipe), while A and n are constants. The three dimensional profiles produced in this study is not applicable to stagnant and shallow receiving water.

(Qi, et al, 2001) models turbulent jets in cross flow. Their study focused on the ratio of Reynolds number for the jet and the ambient as well as the momentum flux ratio. The above experimental studies gave good steps to undertake the laboratory work for the current project by conducting a model tank, using dyed heated plume and a dimensionless densimetric Froude number F_d in simulations. They also indicted to the F_d as a main affected parameter so it is taken in account for the new derived models.

The above studies revision described horizontal discharge. Turn now to studies where the discharge pipe is located on the bed at an angle relative to with the horizontal bed towards the surface. (Parr and Sayre, 1979) investigated multiple jets located at the bed of shallow flowing receiving water. The jet direction was not horizontal; the angle between the jets and the bed was 20° . They used most of the effected parameters to derive the model. (Seo, et al, 2001) studied the non horizontal submerged jets with angles into shallow receiving water with strong currents. The authors used four types of diffusers in their experiments; a co-flowing diffuser, tee diffuser, staged diffuser and alternating diffuser. They solved three governing equations; continuity and two momentums, the model may be biased without the energy equation. (Xin, 2000) investigated non horizontal multiple jets into shallow flowing receiving water. The study presented a numerical analysis of the jets behaviour using Hybrid Finite Analytical Method (HFAM). The obtained results were similar to (Parr and Sayre, 1979) model with a different method. The studies mentioned above can not be applied to the canal sites where the discharge pipe is horizontal.

Further studies on thermal discharge into cross flow are available when the discharge pipe is vertical toward the surface. In this case the discharge pipe will be located on the bed. (Ungate, et al. 1975) studied the vertical discharge in low Reynolds number. The model was significantly focusing on the Reynolds Number (Re), they concluded that the modelling of the turbulent jet is acceptable for $Re > 1500$. (Lee, 1980) investigated the behaviour of the plume discharged vertically into shallow water based on experimental data. The study used curve fitting techniques. (Yu-hung and Wen-xin, 2005) presented a numerical model of vertical discharge into shallow water. They solved the governing equations and presented their model as function of densimetric Froude number and the ratio of the discharge pipe diameter to the depth of receiving water. Regardless of the benefits which have been taken from the above papers such as the ways that producing the plume profiles, temperature and velocity ratios, and the papers presented to show the readers different types of discharge pipe structures.

There are many experimental studies on thermal discharge into deep and still water. The mathematical modelling of three dimensional heated surface jets by (McGuirk and Rodi, 1978) is the widest study in the late seventies in this field and centred on discharging heated water into stagnant and deep water. The paper solved the five governing equations: the continuity equation 2.7, two momentum equations 2.8 and 2.9 in x, y directions, thermal energy equation 2.10 and the equation of state 2.11. The authors made many assumptions to simplify the elliptic equations to parabolic and to simplify the momentum equations. They

state that because the flow extends much further in the longitudinal and lateral directions than in the vertical, gradients in the vertical direction are much larger than in the longitudinal and lateral. As a consequence, turbulent transport is important only in the vertical direction. Accordingly the turbulent momentum and heat fluxes in the longitudinal and lateral directions have been neglected (McGuirk and Rodi, 1978):

$$\frac{\partial U}{\partial x} + \frac{\partial V}{\partial y} + \frac{\partial W}{\partial z} = 0 \quad (2.7)$$

$$\frac{\partial U^2}{\partial x} + \frac{\partial UV}{\partial y} + \frac{\partial UW}{\partial z} = -\frac{\partial}{\partial x} \int_{-\infty}^z \Delta\rho \rho \cdot dz - \frac{\partial \overline{uw}}{\partial z} \quad (2.8)$$

$$\frac{\partial UV}{\partial x} + \frac{\partial V^2}{\partial y} + \frac{\partial VW}{\partial z} = -\frac{\partial}{\partial y} \int_{-\infty}^z \Delta\rho \rho \cdot dz - \frac{\partial \overline{vw}}{\partial z} \quad (2.9)$$

$$\frac{\partial UT}{\partial x} + \frac{\partial VT}{\partial y} + \frac{\partial WT}{\partial z} = -\frac{\partial \overline{wT}}{\partial z} \quad (2.10)$$

$$\rho = f(T) \quad (2.11)$$

These assumptions simplified analysis of the results obtained as they neglected the lateral and longitudinal turbulent transfers and heat fluxes. The five simplified equations contain seven unknowns, velocity in x, y, and z directions, temperature, two shear stresses and one heat flux. To set the number of governing equations equal to number of variables, two transport equations are used, these equations were modelled by (Launder, 1975, 1976) and (Launder, Reece and Rodi, 1975). Since the transport equations contained the turbulence parameters k – ε, two more equations were needed to solve them. The k – ε turbulence equations have been used to determine these two quantities. The finite difference method was used to solve the nine governing partial differential equations. Although this study included wide analysis, the model is limited to applications of warm water surface discharge into deep stagnant water. The study covered a number of previous works carried out in this field up to 1978 and commented on the lack of applications and experiments found in those works. The current research has got benefits from the ideas used in the above studies such as the effects of the parameters; density, gravity, and turbulence model on the plume behaviour.

(Horikawa, et al. 1979) investigated discharge of heated water in the surface zone using the diffusion coefficient; this was an encouragement to use the diffusion and turbulent diffusivity in the current research surface model. (Sarikaya, et al. 1995) produced a two-dimensional model of thermal discharge into the sea using oceanographic density. The study used exponential function and a computer program called THERMOD, no details have been given on the way that the program works. Development of a 3-D model for predicting warm water discharge diffusion by (Nakashiki, 1996) refers to the model tank testing of the turbulent mixing of warm water discharge jets from a multi-port outlet. The paper covers the introduction of the model tank testing techniques undertaken and its relevance to prediction of the flow of submerged discharge. It also suggests possible future work for multi-pipe discharge for use in modelling estuary and power station discharge. The paper indicates the use of Laser Doppler Velocimetry (LDP) to measure flow. It was interested idea to use the LDP for the velocity measurements in the current research, but could not because of lack of facilities in the laboratory.

2.4.5 Relevant Studies

In the previous clauses studies of thermal discharges have been discussed. These studies are classified into three categories: theoretical, computational and experimental. It can be said that none of them are applicable to the theory of the current project i.e thermal plume discharge into shallow and still receiving water. However the search on the previous studies and literature review revealed some work which is more relevant to the current study. The following describes studies on thermal discharge into shallow and still water. (Cederwall and Brooks, 1971) investigated buoyant jets into a stagnant environment. Their model primarily involved the densimetric Froude Number. The study did not consider the effects of the receiving water's bed. (Kannberg and Davis, 1974) studied deep submerged multiple buoyant jets into stagnant water based on the densimetric Froude Number and the discharge pipe diameter. Again the study did not indicate to the effects of the bed. The Horizontal Round Buoyant Jet in Shallow Water by (Rodney, et al. 1988) produced models of jet centreline paths and temperatures along that centreline. The literature review of this study covered the majority of works done in this field between 1972 and 1986, especially submerged discharge. The study considered all the affected parameters on thermal discharge, no discussion on the lateral profiles have been given. In general all these works are involved high discharge velocity jets and not plumes. Integral Model for Turbulent Buoyant Jets in Unbounded

Stratified Flows (Jirka, 2004) is the latest work studying thermal submerged discharge. Both types of discharge- plume and jet -are studied but the discharge plume into shallow and still water is not discussed deeply. This group of studies reviled with more information which have been used by the current project mainly the effects of the receiving water bed and depth, these were not been mentioned by the studies in the previous sections.

In general the studies in previous sections were investigating thermal water discharge into receiving water with theories similar to that in the current study which also discusses the same thing. The studies followed various methods to predict the heat diffusion and velocity profiles of the plume, so the conclusion of all the studies were the determination of temperature and velocity within the thermal discharge. But in every study there was at least one of the major conditions which was different. The following are some of the conditions which made the other studies not applicable to the canal and different with what has been done in this project:

Thermal discharge

- Some of them were investigating jets rather than plume
- Multi diffusers discharge pipe, whilst this thesis discuses single pipe
- Vertical pipe rather than horizontal
- Discharge pipe located inclined with the bed

Receiving water

- Deep and still such as seas, whilst BW canal is shallow
- Shallow and flowing such as rivers but canal water flow very close to zero

2.5 Mixing in Turbulent Flows

The study of turbulence flow is troublesome as it requires a complicated mathematical procedure and consideration of the flow's dynamic. (Sherwin and Horsley, 1996) state that when considering forced convection the definition of the convective heat transfer coefficient for any particular situation of the Reynolds analogy is based on two assumptions;

That the diffusion of momentum in a turbulent flow is equal to the thermal diffusion, that the thermal and temperature profiles of the flow are identical.

That turbulent behaviour exists throughout the whole flow, to the surface of a wall where the heat transfer exists.

The diffusion coefficients (Dx, Dy and Dz) appear in the heat advection diffusion equation 2.12. This is a summation of the molecular diffusion plus the turbulent diffusivity. These are the main factors in fluid mixing. All the relevant parameters in the equation 2.12 are a summation of the fluctuating value plus mean value.

$$\frac{\partial T}{\partial t} + U \frac{\partial T}{\partial x} + V \frac{\partial T}{\partial y} + W \frac{\partial T}{\partial z} = Dx \frac{\partial^2 T}{\partial x^2} + Dy \frac{\partial^2 T}{\partial y^2} + Dz \frac{\partial^2 T}{\partial z^2} \quad (2.12)$$

2.6 Thermal Discharge Simulation

The main requirement for a thermal discharge simulation is the equality of the densimetric Froude Number 2.13 for model (tank) and prototype (canal) and the equality of discharges temperature (Ungate, et al. 1975)

$$F_d = \frac{U}{\sqrt{\frac{\rho_a - \rho_0}{\rho_a} g D_0}} \quad (2.13)$$

Where (F_d) is the densimetric Froude Number, (U) is the discharge velocity, (ρ_a) is the canal water ambient density, (ρ_0) is the discharge water density, (g) is gravity and (D_0) is the discharge pipe diameter. There are parameters that cannot be kept equal for the model tank and canal. Such parameters include the discharge velocity, discharge pipe diameter, canal width and canal depth.

Where the discharge velocity into the canal is (U_p) and for the model (U_m), the velocity ratio for the model and prototype U_r , results in equation 2.14:

$$U_r = \sqrt{\left(\frac{\Delta\rho}{\rho}\right)_r g_r D_{0r}} \quad (2.14)$$

The density of water used in the model must equal the prototype (canal) water density with the same ambient temperature. Therefore Equation 2.14 will produce Equation 2.15:

$$U_r = \sqrt{D_{0r}} \quad (2.15)$$

$$\frac{U_p}{U_m} = \frac{\sqrt{D_{0p}}}{\sqrt{D_{0m}}} \quad (2.16)$$

For any thermal discharge simulation the reducing scale must be known to then obtain the discharge pipe diameter for the model (D_{0m}) and all the other dimensions from which to build the model tank. The discharge velocity (U_m) can be calculated from the Equation 2.16.

3. Case study

3.1 Preliminary Case Study

3.1.1 Introduction

For a number of years the University of Huddersfield has successfully utilised canal water as the primary source for its building cooling systems. The University now operates three independent sites, two located alongside the Huddersfield Narrow Canal and the third on the Huddersfield Broad Canal. All three sites vary in the capacity and configuration of the inlet and outlet. Historical data has been collected which may be used as a basis for the investigation. In this chapter investigations are carried out of all three sites. The positions of each site and the cooling systems are described. A survey was performed to collect data within the mixing zone. Grid points were graduated at different layers and then velocity and temperature measurements were placed in grids. In addition, thermography studies were carried out to predict the temperature distribution on the surface of the canal and defined the mixing zone.

3.1.2 Sites Location

2.1 Central Services Building – Huddersfield Broad Canal

The University library and main computing facilities are located within the Central Services Building (CSB) which lies at the upstream end of the Huddersfield Broad Canal. It is the largest of the three sites in terms of heat load and extraction capacity. The building is located

adjacent to the Huddersfield Basin between lock 1E of the Huddersfield Narrow Canal and lock 9 of the Huddersfield Broad canal see Figures 3.1 and 3.2.

2.2 Canal Side West – Huddersfield Narrow Canal

Site 2 lies at the rear of the Canal Side West (CSW) building between lock 1E and lock 2E. The discharge point into the canal is positioned upstream from lock 1E approximately 60m downstream of the road bridge at the west side of the building. The inlet and outlet are distinguishable by the galvanised steel cover plates which can be seen in Figures 3.3 and 3.4.

Outlet

2.3 Site 3: Lockside – Huddersfield Broad Canal

The Lockside building is immediately downstream of lock 1E of the Huddersfield Narrow Canal. Figures 3.5 and 3.6 show the area adjacent to the inlet/outlet, the routing of the pipes from within the building to the inlet and discharge point are not known.



Figure 3.1: Central Services Building



Figure 3.2: Embankment – CSB

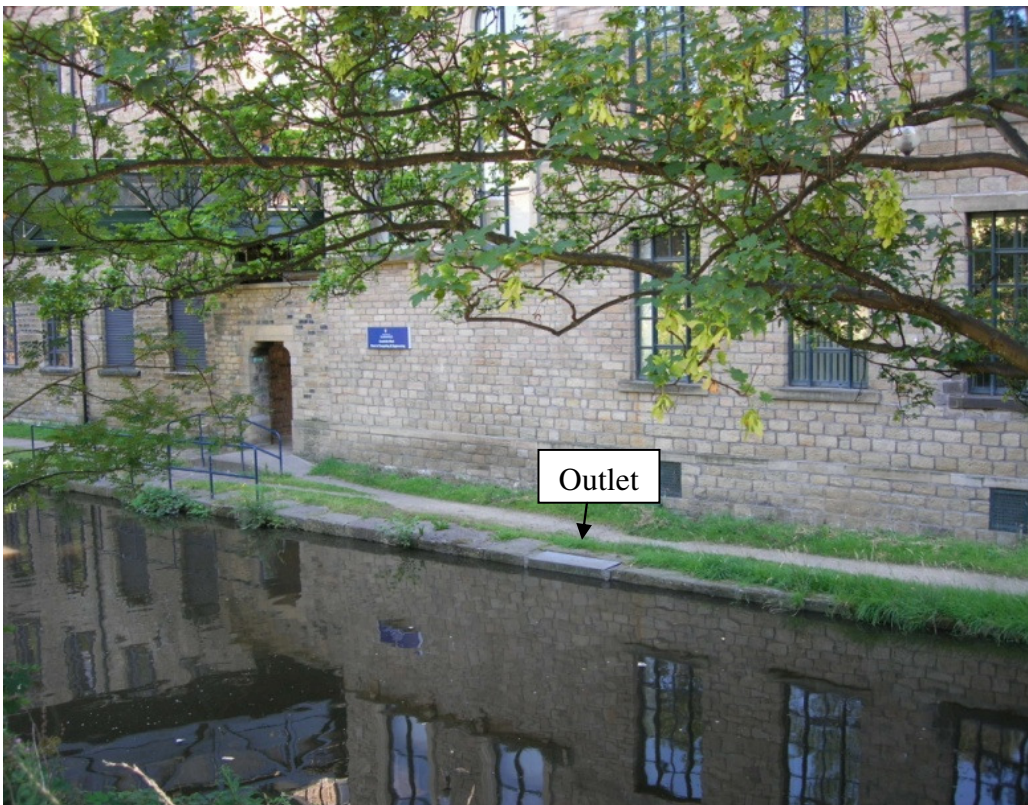


Figure 3.3: Canalside West – Outlet

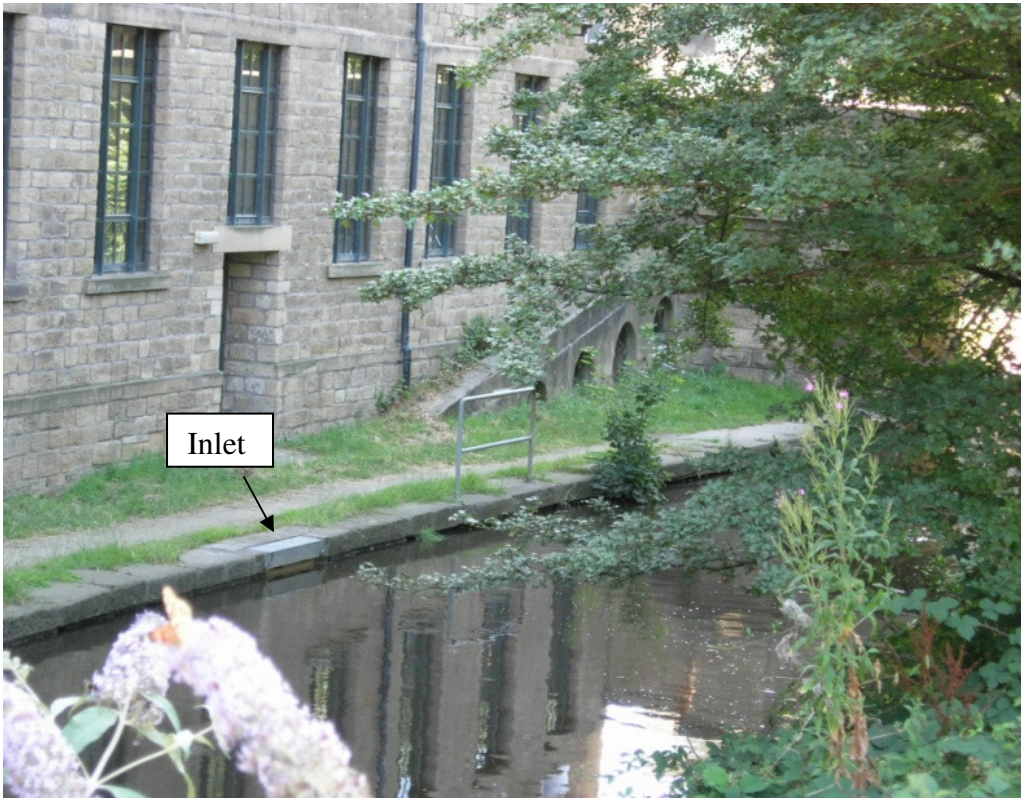


Figure 3.4: Canalside West – Inlet



Figure 3.5: Lockside Building



Figure 3.6: Inlet/Outlet- Lockside

3.1.3 System Description:

A typical schematic diagram of the chilled water plant for the building cooling system is shown in Figure 3.7. Cooling water is extracted directly from the canal, and is pumped around a bank of plate heat exchangers and then discharged back into the canal. The heat exchanger plates form alternative sections- with canal water in one section and condenser cooling water from the chillers in the next. This causes heat transfer from the refrigeration plant condensers into the cooler canal water. As the heat exchanger plates form a closed system, the water from the two sections is not mixed, the system is therefore classed as a ‘use once put-back system’ and no water is lost.

The principle of the plate heat exchangers used is shown in Figure 3.8 and a typical heat exchanger plate used for CSB can be seen Figure 3.9. As the inlet water is not filtered, silt and algae can (and does) enter into the cooling system, clogging the heat exchanger cooling plates. Periodic back-washing is carried out to clean the panels and ensure the efficient operation of the cooling system.

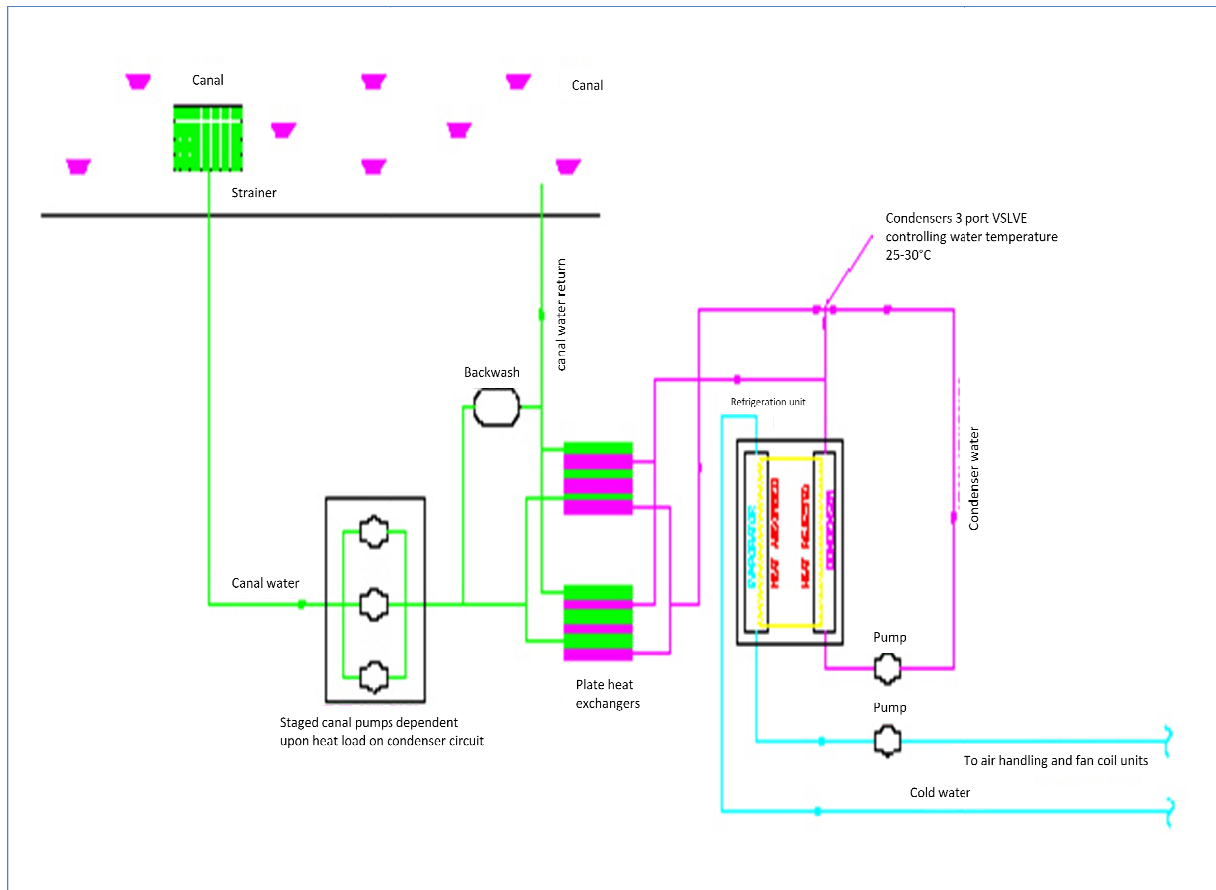


Figure 3.7: Cooling system schematic diagram

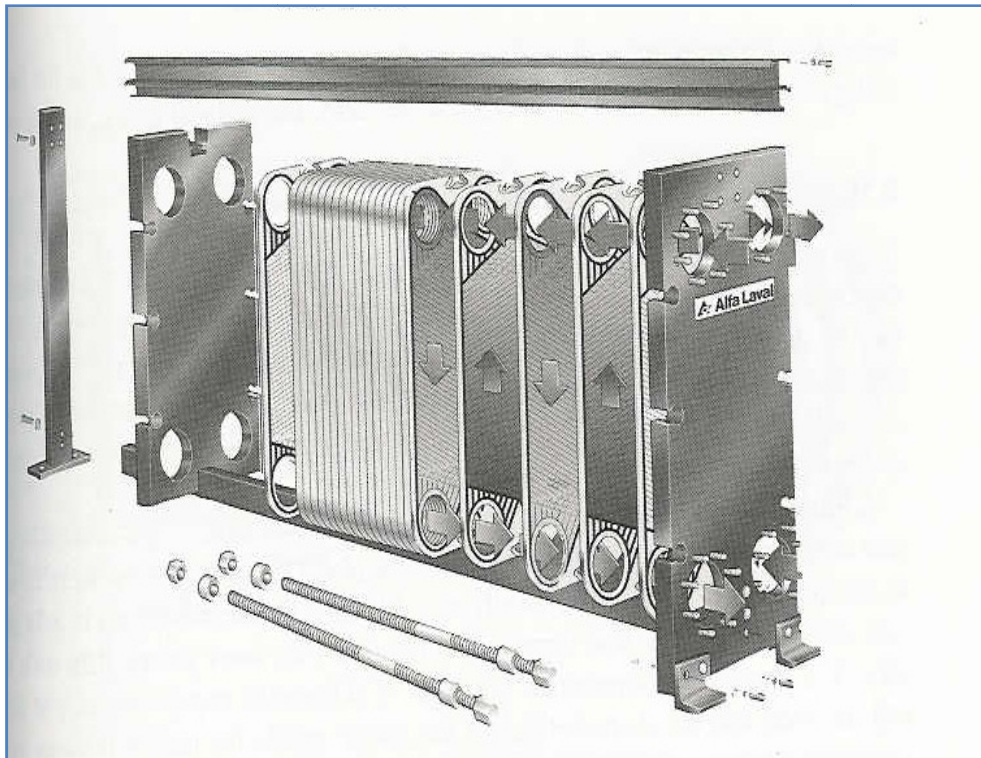


Figure 3.8: Exploded view of heat exchanger- 'Coulson Vol.3, p 549'



Figure 3.9: Heat exchanger plate

3.1.4 Building Management System

The building management system differs slightly for each cooling system but essentially CSB and CSW utilises a data logger to record the inlet and outlet water temperature and water flow rate every 15minutes. This is stored in the system's memory over a 10 day period

3.1.5 Site Details

5.1 Site Details - Central Services Building System

The inlet and outlet are positioned adjacent to each other beneath the foot bridge; both pipes are fitted with 90 degree elbows to extend the pipes downstream inline with the canal and adjacent to the embankment. The canal water is extracted via a 150mm diameter submerged

pipe, shown in Figure 3.10. A coarse mesh basket forms a screen over the inlet pipe to prevent fish being drawn into the inlet and prevent the ingress of coarse deleterious material.

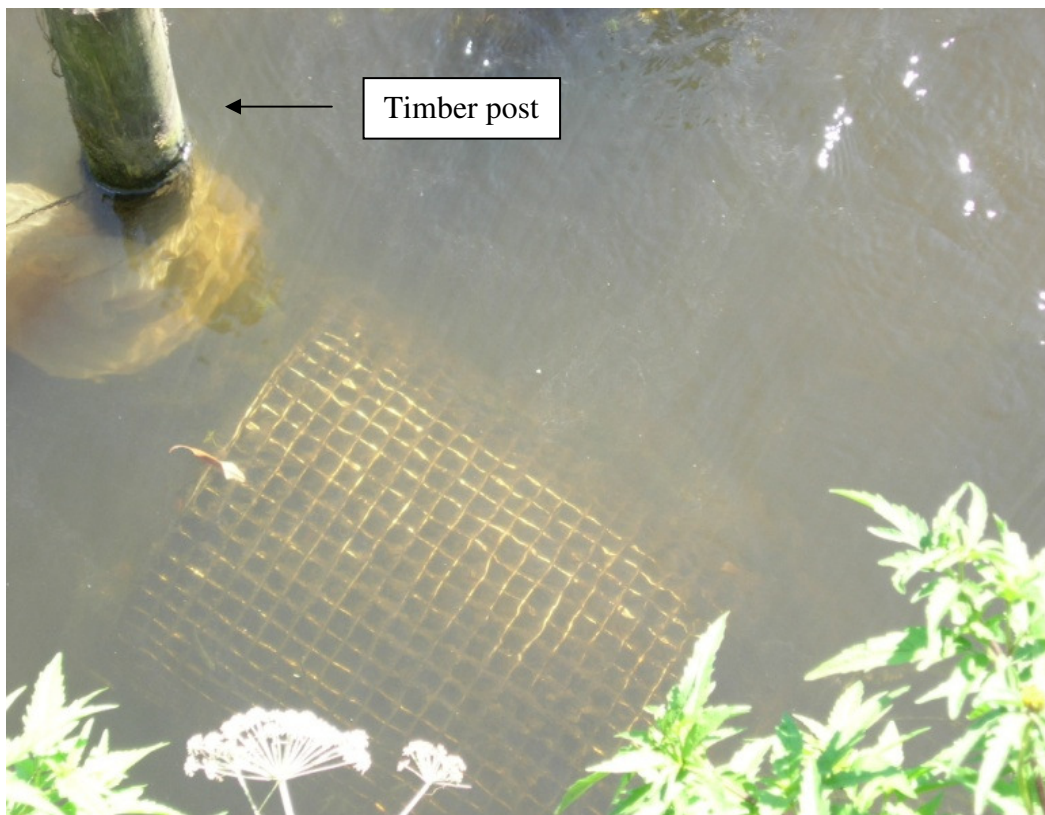


Figure 3.10 inlet screen - CSB

Over a period of time the 150mm outlet pipe has been damaged and fractured, reducing the length and placing the position of the discharge point upstream of the inlet. The discharge end of the pipe is now semi-submerged, resulting in the plume discharging across the surface of the canal. The concrete wall of the wharf forms the embankment. Timber posts are positioned to provide protection of the pipes from river traffic as shown in Figures 3.11a and 3.11b. The figures also indicate the extent of vegetation adjacent to the embankment in the area of the inlet and outlet discharge plume. The pump house and plant room are located within the adjacent buildings. The water inlet temperature is measured before the pipe junction for the three pumps and pressure gauges are installed in the delivery side of each pump in the pump room. The outlet temperature is measured in the plant room on the outlet side of the plate heat exchangers. The coordinate positions of the intake and outlet discharge were measured relative to the fixed datum at the base of the footbridge, the positions of the timber posts were also taken relative to the same datum which may allow for modelling of the heat diffusion.



Figure: 3.11a- CSB Discharge outlet

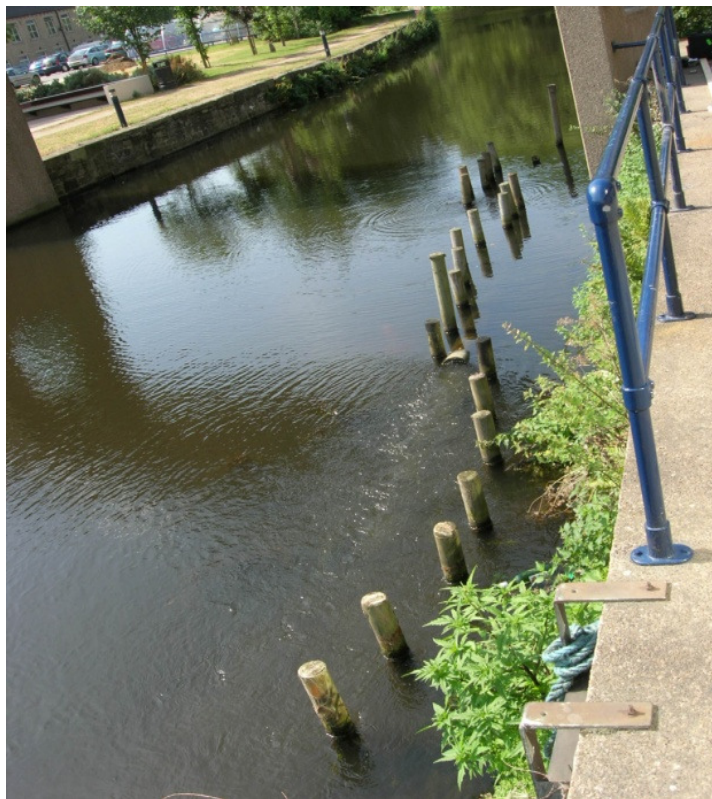


Figure 3.11b: CSB Discharge outlet

5.2 Site Details - Canalside West (Huddersfield Narrow Canal)

The inlet is positioned 40m upstream of the outlet discharge and both the inlet and outlet are directed across the canal perpendicular to the normal line of flow of the canal. Figure 3.12 shows the normal view seen of the CSW outlet.



Figure 3.12: Normal View of CSW Outlet



Figure 3.13: CSW outlet-during dewatering of canal

A coarse inlet and outlet screen is fitted to the buttresses shown in Figure 3.13. It is photographed following vandalism that caused partial dewatering of the canal. Following dewatering, it has been determined that the ends of the pipes are encased in a concrete buttresses and may stop some 300mm inside the buttress.

5.3 Site Details: Lockside (Huddersfield Broad Canal)

Due to building planning restrictions the configuration of the inlet and outlet differs from both sites 1 and 2. Both the inlet and outlet are oriented across the canal perpendicular to the flow of the canal as in site 2. However the inlet is positioned at the same elevation as the outlet but only 300mm on the upstream side of the outlet discharge at the same chainage below lock 1E.

Timber posts are used to provide protection against river traffic, (Figure 3.14), and a fine mesh cloth screen is positioned to keep away debris from around both the inlet and outlet.



Figure 3.14: Protective posts and mesh screen – Lockside

3.1.6 Canal

Usage

The canal forms part of the network which is used for growing narrow boating/leisure activities. Apart from peak holiday periods the canal appears generally to be little-used.

Flow

Little water flow has been experienced through these sections of the canal systems. Generally no flow is available over the weir at lock 1E, the water level being well below the weir level, any water flow is mainly due to lockages or vandalism.

No flow was evident other than that created by lock gate leakage and surface disturbance due to wind velocity (where the prevailing direction appears to be from the downstream direction, against the normal flow expected due to lockages).

Plume

Figure 3.15 show a very distinct velocity plume created by the semi-submerged discharge pipe causing turbulent flow and surface disruption. Whilst the surface velocity of the plume indicates a much larger area of surface disturbance, the edges of the plume are ill-defined and an acceptable temperature balance appears to be achieved before the full extent of the plume area is reached.

For this reason a surface area for the discharge plume of 5m long x 2m wide was selected to form the boundaries for the grid measurement.

3.1.7 Initial thermal images

Images were taken of the discharge at each of the three sites using a thermal image camera. This indicated the mixing area and temperature gradient within the discharge plume.

Figure 3.15 shows the comparison of the discharge plume at the Central Services Building (CSB) taken with a digital camera and the thermal image camera. The outlet pipe is semi-submerged and the mixing plume can be clearly seen on the canal surface. The figure shows the extent of the plume and the differing temperatures of the protective timber posts around the discharge pipe. The thermography studies are described in detail in Chapter 5.

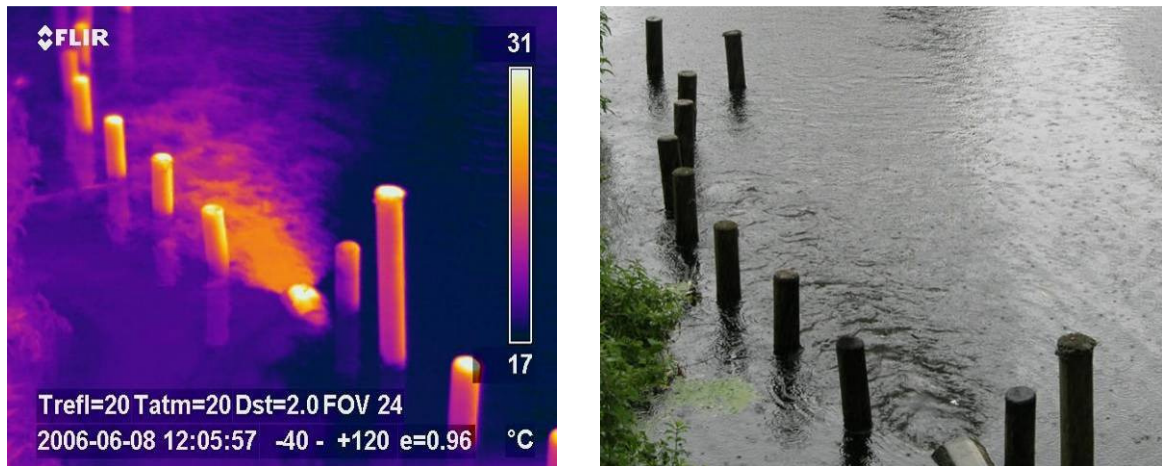


Figure 3.15: Thermal and digital image of Discharge plume

3.1.8 Measurements Procedure

The procedure for data collection was discussed and agreed with BW prior to the tests being undertaken using the sheets enclosed in Appendix 2.

Measurements were made along the embankment at a distance from the end of the outlet pipe to define the position of the discharge outlet and the relative positions of the grid. A timber lath was marked at appropriate lengths to give the distances from the centreline of the discharge pipe. This produced a two dimensional matrix along the length of the plume which could be readily reproduced- using the discharge pipe outlet position as the datum, which in turn was related back to the wharf/footbridge. A length of steel tubing was secured to the lath to which the thermocouple probe could be attached. This also acted as the depth measurement gauge by attaching a suitable measuring tape to produce a profile of the canal bed at the grid points.

Prior to temperature measurement, as agreed with BW in principle, the lock gate (1E) leakage rate was assessed from the areas of greatest discharge (i.e. from the centre and sides of the gates), by recording the time taken to fill a container of known volume. Photographs of the gate leakage and canal water level at the fixed weir were taken at the start and end of the trial.

Any flow over the bypass channel and fixed weir was measured. If no flow was observed, the height from the weir crest to the water level was recorded. An anemometer was used to record the wind speed and its direction, i.e. upstream or downstream.

Thermal images were taken at the start and end of the trial along with a number of digital photographs.

3.1.9 Temperature Measurement

Canal ambient water temperatures were recorded 15m upstream and downstream of the outlet discharge point. Ambient canal water and air temperatures were recorded with the use of 'k' type thermocouples and digital meter at the start and end of the trial.

The canal water temperature was then measured and recorded at the grid points at the depths agreed with BW, i.e. 50mm below the surface, at mid depth and 50mm above the bed. The details of equipment used for temperature measuring are contained in the Appendix 3.

CSB – Temperature

Initial temperature measurements were taken on particularly hot bright sunny days (+24°C ambient). When analysing the temperature matrix, it appears that the water temperature adjacent to the concrete wharf was being raised due to solar heat gain from the wharf. This caused anomalies in the results.

Appendix 3 contains the temperatures obtained at the grid points at various depths, i.e. 50mm below the surface, mid-depth and above the bed. Due to debris and aquatic growth it was not always possible to take the readings at 50mm above the canal bed. The tables (measured temperatures) indicate the temperature on the embankment side appears slightly higher than those in a similar position on the opposing side of the plume. This may be attributable to a heat gain from the embankment and the effect of the embankment, timber posts and plant growth disrupting free flow and thereby restricting dispersal of the plume.

The measurements taken at the surface layer indicate the maximum core temperature of the plume is contained within an area 400mm wide by 1m long equally displaced about the centreline of the discharge pipe. This core is not evident at the mid-depth indicating the turbulent flow possibly occurs close to the diameter of the discharge pipe. There is a less disruptive temperature distribution than the embankment side because the temperature distribution on the plume from the centreline of discharge in towards the centre of the canal is undisturbed and not effected by the aquatic growth, debris and timber posts (in contrast to the embankment side).

Figure 3.16 shows the temperature distribution at the various depths from the discharge pipe along the centre line of the plume. It can be seen that the temperature drops from 24°C at the discharge point to 19°C within a distance of 2m. Within a distance of 4m from the discharge point the surface, mid and bed temperatures have attained a common value at 18°C.

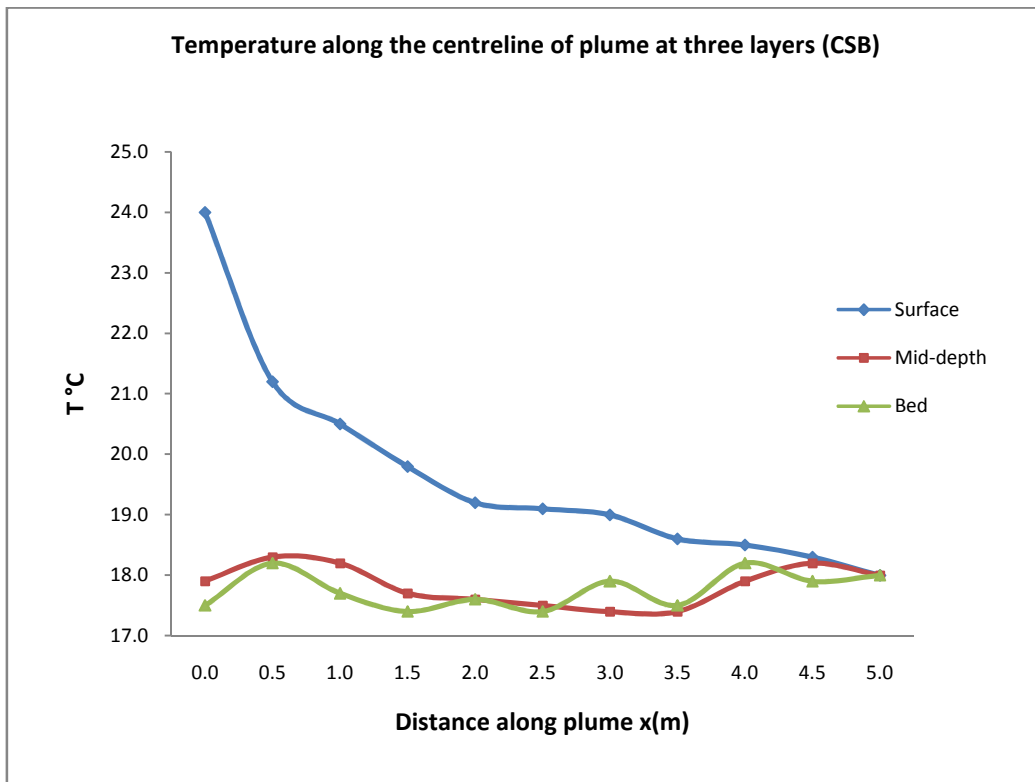


Figure 3.16: CSB-Temperature distribution along centre line of discharge

The chart, Figure 3.16 indicates a maximum plume discharge temperature 50mm below the surface at 24°C obtained using the thermocouple. The thermocouple temperatures were recorded at 4:00pm. The temperature reduced with increasing distance downstream. In the mid and bed layers the temperature started with a smaller value as the plume did not reach those areas until a certain distance from the outfall. And then the temperature dropped again to a value closer to the ambient temperature of canal water. The fluctuating in temperature was due the turbulence.

Canalside West – Temperature

The prevailing wind direction is from the downstream direction but the potential for recirculation from the outlet back into the inlet is not considered as a potential problem due to the relative upstream distance of the inlet from the discharge point.

No civil drawings were available for the discharge at CWS, but it was observed that the discharge pipe is fully submerged and is thought to terminate within a recessed concrete buttress covered with a mesh grill and cover plate. The pipe terminates approximately 300mm

from the edge of the embankment. The design of the discharge culvert, mesh screen and submerged discharge allows dispersal of the discharge plume before it emerges onto the canal surface. The area of the plume on the surface is not distinctly visible as at CSB, but can be seen from the thermal camera image. This indicates the warm water discharge spread over the surface area, therefore an area of plume of 2.5m long x 2.0m wide was selected for the grid size for data measurement. Appendix 3 contains the temperature measured at three layers; surface, mid depth and the bed.

Due to the reduced heat load at CSW, the discharge area is much smaller than CSB; Figure 3.17 shows the temperature distribution along the centreline of discharge projecting 2.5m across the canal with a maximum temperature variation of only 1.0 °C throughout its depth. Sub-surface circulation appears to be taking place as the temperature mid-depth is higher than at the surface. Observation of the temperature distribution shown in Figure 3.17 indicates an even transition of temperature; however the surface temperature on the upstream side is slightly higher than downstream, this may be due to the prevailing wind in the upstream direction causing free convection through the depth of the canal. No evidence of aquatic growth was seen at CSW (unlike CSB). The maximum temperature range throughout the boundaries of the measured volume is in the order of 18.9 to 17.5 °C.

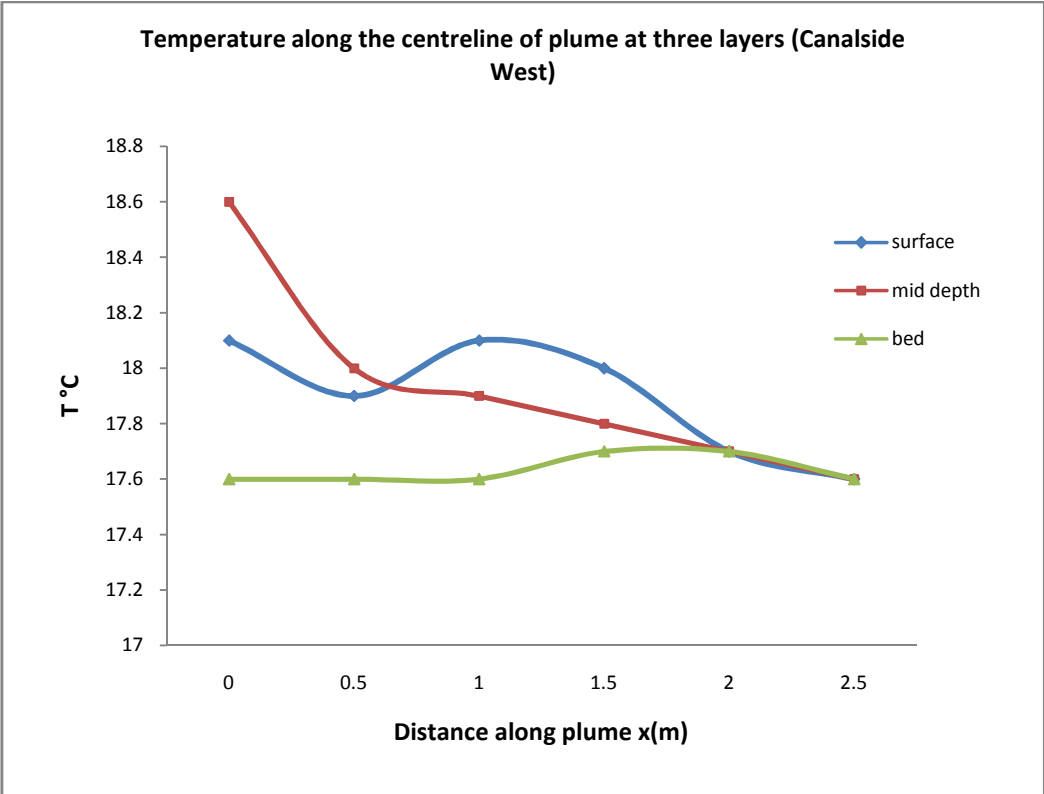


Figure 3.17: Temperature distributions along centreline of discharge

Lockside – Temperature

The discharge is directed through the timber posts and the mesh screen. The inlet is at the same elevation as the outlet and is only 300mm upstream of the discharge. Dependant upon flow rate, this installation has the greatest propensity to suffer from problems of recirculation of warm water discharge back into the inlet. This leads to a build-up of temperature.

As shown in Figure 3.18 the area of the discharge plume, shown as surface turbulence, is indistinct- being some 1m long x 1m wide -therefore with the aid of the thermal image camera the surface area for the study was assessed as 0.75m long x 1.0m wide.

As stated above, the intake and discharge are both fully submerged and are located alongside each other, protected by timber posts and mesh screen. This causes a disruption of the free flow of discharge which results in no clearly evident discharge plume. The thermocouple measured temperatures are shown in Appendix 3.

Figure 3.19 indicates a near constant temperature at mid-depth and at the canal bed, however the temperature peaks to 22.5°C at 0.5m from the point of discharge. This correlates with the surface thermal image. This is the point where the thermal plume reaches the surface as indicated in the thermal images.



Figure 3.18: Lockside discharge

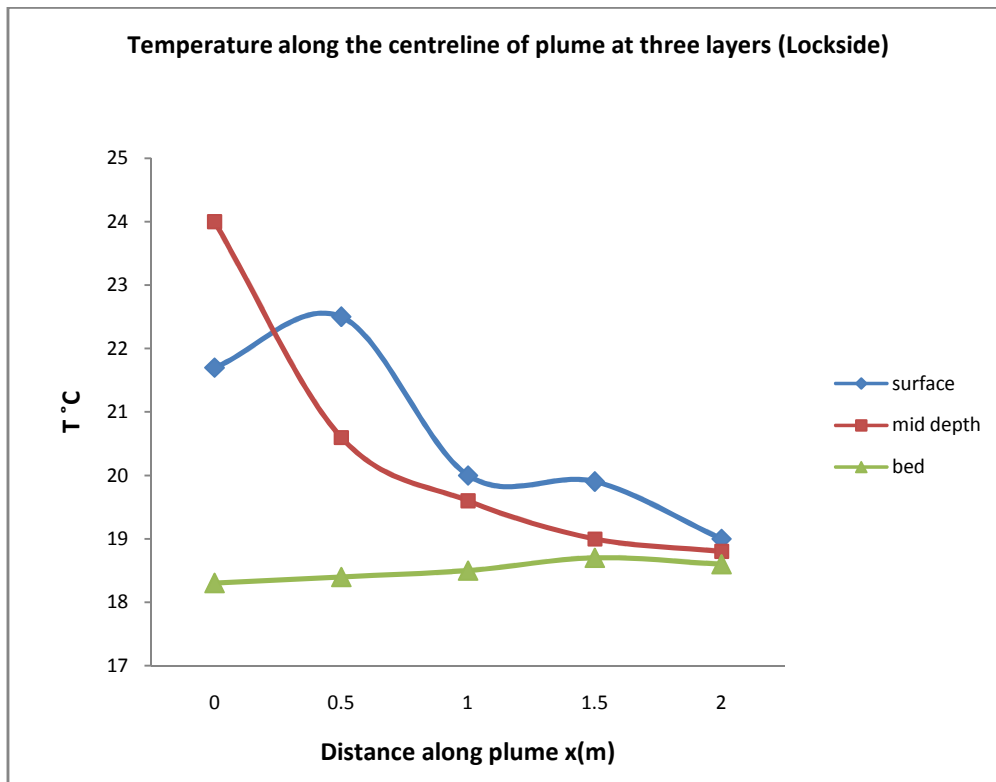


Figure 3.19: Plume temperature - Lockside

The ambient temperature was measured at 17.1°C up and downstream. The temperature at the bed is a near constant 18.5°C as shown in Appendix 3. Some recirculation may be taking place as a clear discharge flow cannot take place due to the mesh screen. A further measurement trial following the removal of the mesh screen and replacing it with a steel mesh screen may give an indication of possible recirculation.

3.1.10 Flow Measurement

To determine the velocity of flow through the discharge plume an investigation was made of the various types of flow meter available. Because the flow measurement required is in an open channel (rather than within a fixed installation in a pipeline), an in-line industrial type turbine flow meter is unsuitable. The velocity of the discharge flow was measured at the grid points using an impeller-type flow meter. Whilst no flow was observed, for reference, photographs were taken of the Goytre at CSB which joins the canal at the wharf just downstream at the opposing embankment of the CSB intake/discharge point. A similar

procedure was then undertaken to record the data for the Canal Side West and Lockside buildings. The equipment used for velocity measuring is detailed in Appendix 3.

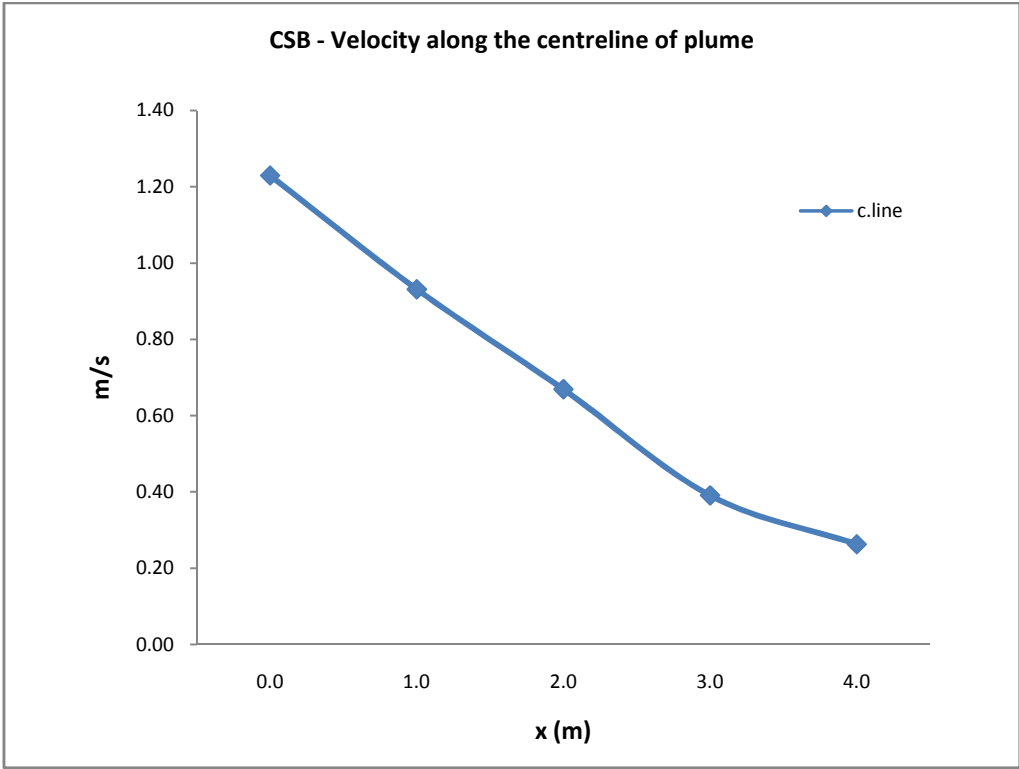


Figure 3.20: Velocity along centreline of plume measured 50mm below the surface – CSB

The velocity was measured at grid points at the surface of the CSB-site. Due to weeds and debris along the embankment it was difficult to measure the velocity at all the grids. The collected data is presented in Appendix 3. The maximum velocity measured at the discharge point is 1.23m/s. Figure 3.20 demonstrates the velocity along the centreline of the plume within a distance of 4m from the outfall.

The maximum flow for the Canalside West recorded at the outfall was 0.913m/s, degrading to 0.49m/s at the surface within 1m from the embankment. With the canal width of 10m, no problems were anticipated with temperature stratification causing distress to aquatic life. The measured velocities are presented in Appendix 3. Figure 3.21 shows the measured velocity along the centreline of plume at the surface of canal, therefore the maximum velocity appears is 0.49m/s. Whilst the discharge velocity 0.913m/s is not shown in the graph because the pipe located below the surface.

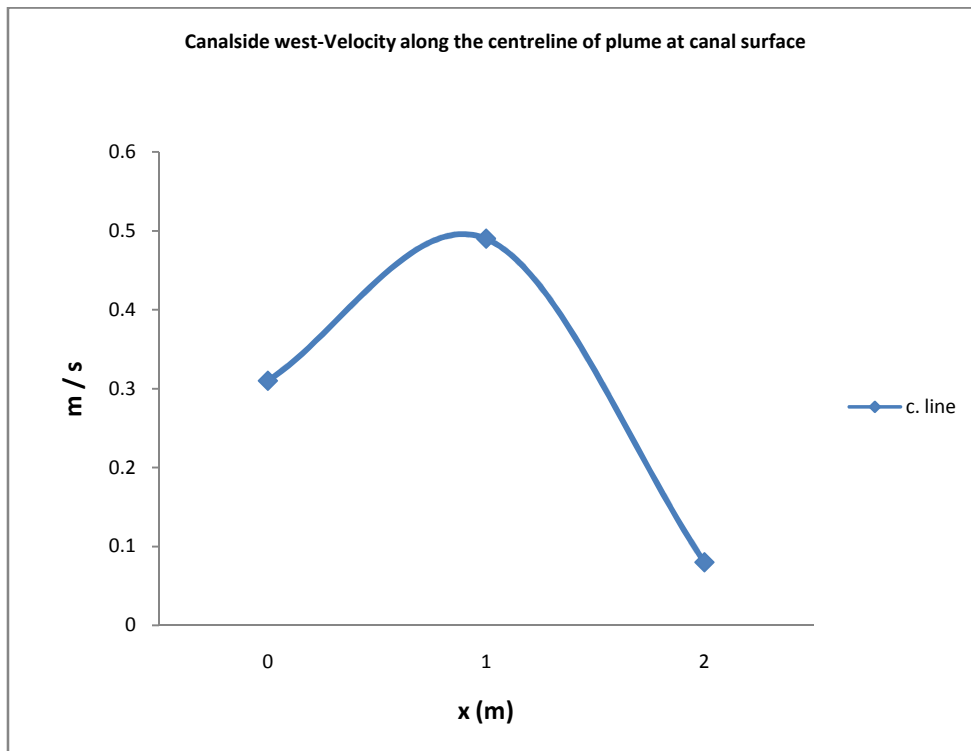


Figure 3.21: Velocity along the centreline of plume measured 50mm below the surface–
Canalside West

For the Lockside, a maximum velocity of 1.217m/s was recorded at the point of discharge, degrading to 0.31m/s at a distance of 2m from the discharge point at the canal surface. The measured velocities are presented in the Appendix 3 and the centreline measured velocity at the surface is described in Figure 3.22 with a maximum velocity 0.62m/s. Note that the discharge velocity 1.217m/s is not appeared because the Figure 3.22 shows the velocity profile on the surface of canal whilst the discharge pipe is located below the surface.

3.1.11 Depth Measurements

The graduated pole used to carry the measurement tools was used to measure the depth of canal at each grid point. The depths for all the sites are tabulated in Appendix 3.

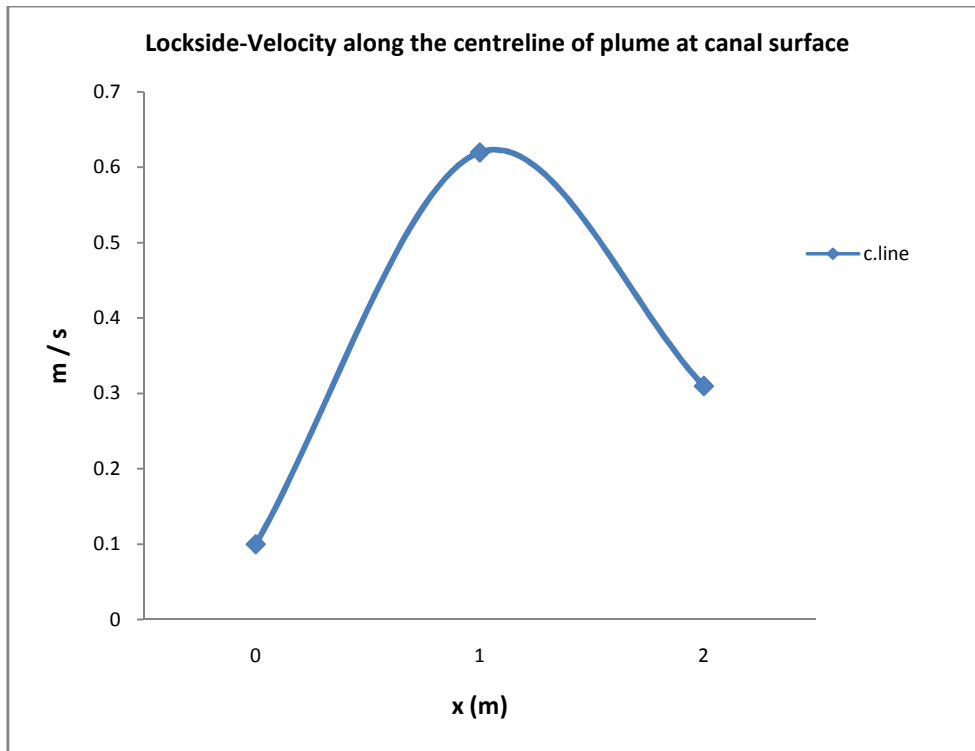


Figure 3.22: Velocity along the centreline of plume measured 50mm below the surface – Lockside

3.2 Refine Case Study

3.2.1 Introduction

To better refine the results due consideration was given to more practical investigations in order to obtain enhanced field trial data within different layers and along the plume core region. The survey carried out across all three sites at University of Huddersfield determined the plume size, velocity and temperature distribution across the plume and any evidence of recirculation. Additionally, investigation on additional British Waterways canal sites was carried out- BBC Mailbox on Birmingham canal, Kirklees College on Huddersfield canal and Enviroenergy on Nottingham canal. The sites are varied in the design of their discharge pipe structure. The CSB site (as mentioned in chapter one) is surface discharge and the other three sites are submerged discharge. The Central Services Building at the University of Huddersfield was selected as the primary site for refined investigations because the thermal plume of the flow occurs on the surface and is clearly defined. Canalside West, Lockside, BBC Mailbox, Kirklees College and Enviroenergy Nottingham were selected as submerged discharges for refined case study- the discharge pipes at these sites are submerged and located

a certain distance below the free surface of canal. The sites have licences from British Waterways to use the canal water as part of the building cooling system. As such the University and other sites are allowed to extract cold water from the canal and discharge warm water into it.

As discussed, by law the maximum temperature of canal ambient should not exceed 28°C, the reason being that the water begins to de-oxygenate and so the health of aquatic life is put at risk. As a result of such regulations, the University of Huddersfield, BBC Mailbox, Kirklees College and Enviroenergy must maintain a complete record of extraction volumes, inlet temperatures, discharge temperatures and surrounding environmental parameters.

3.2.2 Central Services Building CSB - Surface Discharge

The inlet pipe from the canal is split into three inside the pump house as shown in Figure 3.23. This allows the pumps to be switched automatically dependent upon demand from the air handling system. The inlet temperature is measured in the pump room on the single inlet pipe immediately before the branch for the pumps. Analogue pressure gauges are fitted in the discharge pipe for each pump (immediately after each pump).

The outlet water temperature is measured within the plant room on the outlet side of the plate heat exchangers. This is some considerable distance from the discharge point into the canal. The outlet pipe is lagged and travels within the plant room and adjacent building before going underground and connecting to the actual discharge pipe beneath the canal footbridge. A digital laser temperature reading was taken on the outlet gate valve in the pump room. However, due to the unknown temperature drop through both underground section and the submerged discharge pipe, these readings were disregarded. Furthermore, a pressure drop occurs through the plate heat exchangers (Figure 3.9), due to the unknown length of pipe and number of bends and elbows in the pipe before final discharge back into the canal. It is therefore considered that no pressure gauge readings can be used with a sufficient degree of accuracy.

The volumetric flow is recorded on a mechanical flow meter in the plant room. This provides the data readout for the water consumption figures supplied to BW. This reading was recorded over a known time period to determine the volumetric flow rate.



Figure 3.23: Inlet pumps – CSB pump house

Due to the fracturing of the discharge outlet pipe, the intake screen is now offset from the discharge outlet pipe and is semi-submerged. It is now positioned approximately 4.5m downstream from the outlet pipe discharge point, giving the appearance that the discharge plume may re-circulate the heated water into the intake. This may potentially lead to an unacceptable temperature build-up as is predicted by the ISIS software. However, the use of data logging equipment in the pump room and plant house indicates this is not happening and that the system does actually meet the specified requirements.

The embankment side of the discharge plume is affected by the following:-

Wooden stakes positioned to prevent damage to the pipe from narrow boats etc.

Debris and weeds proliferating close to the bank and at the intake screen,

Rubbish dumped into the canal which tends to collect within the weed growth, see Figure 3.24.

The flow in the plume is turbulent, (see Figure 3.25), which results in eddy currents and evidence of distortion of flow was apparent around the wooden stakes. This can be seen visually on the water surface and in the distortion of the temperature profile within the plume area. During the period of trials no flow was evident over weirs at lock 1E. Therefore theories

of flow in open channels were not considered to be relevant because the canal water is static, and the problem then resolves into surface discharge of warm water into a still body of water.



Figure 3.24: Discharge plume –CSB



Figure 3.25: Turbulent discharge – CSB

Data Collections:

To monitor the whole site, it was necessary to establish a reference grid over which the results of water flow and temperatures would be measured across, along and below the surface of the canal. The centreline of the outlet pipe and the end position of the pipe served as the zero position. A graduated pole was laid along the banking to give the linear reference points and a second pole was fixed at 90° to the banking to give the transverse reference positions. A third vertical pole was secured to the main pole to which the thermocouple probe and flow meter could be attached. This third pole was also graduated to indicate depth. The arrangement is shown in Figure 3.26a, and Figure 3.26b illustrates the grid points at the surface.

Ambient canal water temperatures were recorded 15m upstream and downstream of the outlet discharge point. Both the ambient canal water and air temperatures were recorded with the use of 'k'-type thermocouples at the start and end of the trial. The canal water temperature was then measured and recorded at grid points at various depths: the discharge layer, at mid depth and 50mm above the bed.



Figure 3.26a: Graduated pole carry flow meter and thermocouples

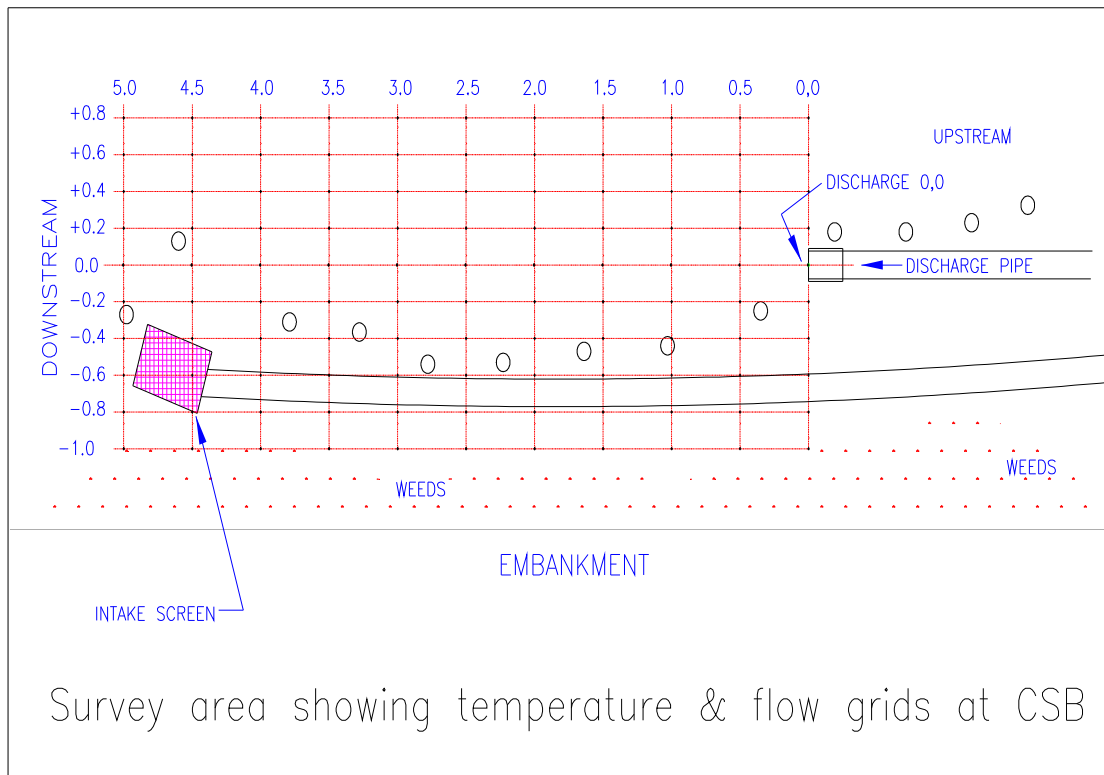


Figure 3.26b: Grids at CSB site

Figure 3.27 shows the measured temperatures along the centreline of plume. In the refined case study, temperature was measured by connecting thermocouples to an amplifier which received voltages from the thermocouples which were then sent to a computer through a data acquisition device (Labjack U12).

The techniques used to measure the velocity are similar to the techniques used in the preliminary case study. The velocity was measured at the discharge layer, not on the surface layer as in the preliminary case study. Figure 3.28 shows the measured velocity along the centreline of plume.

The depth of the canal at grid points was measured using the same procedure of measurements followed in the preliminary study. Figure 3.29 illustrates the depth of the canal at the mixing zone.

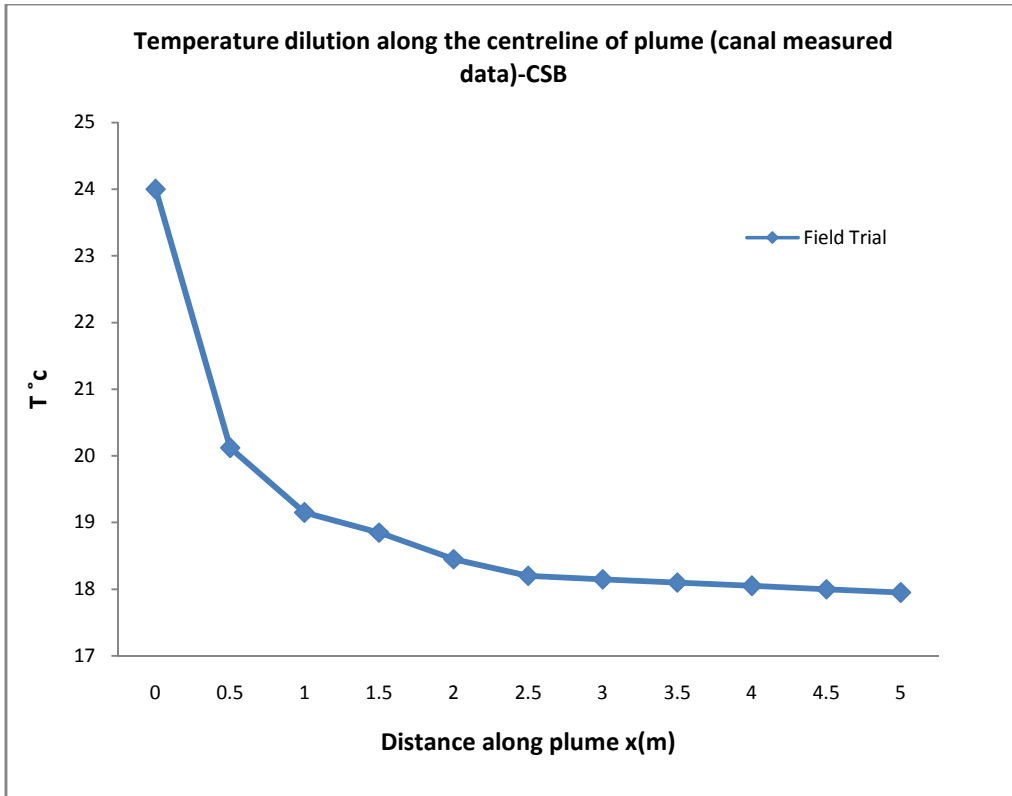


Figure 3.27: Measured temperature along the centreline of plume – CSB

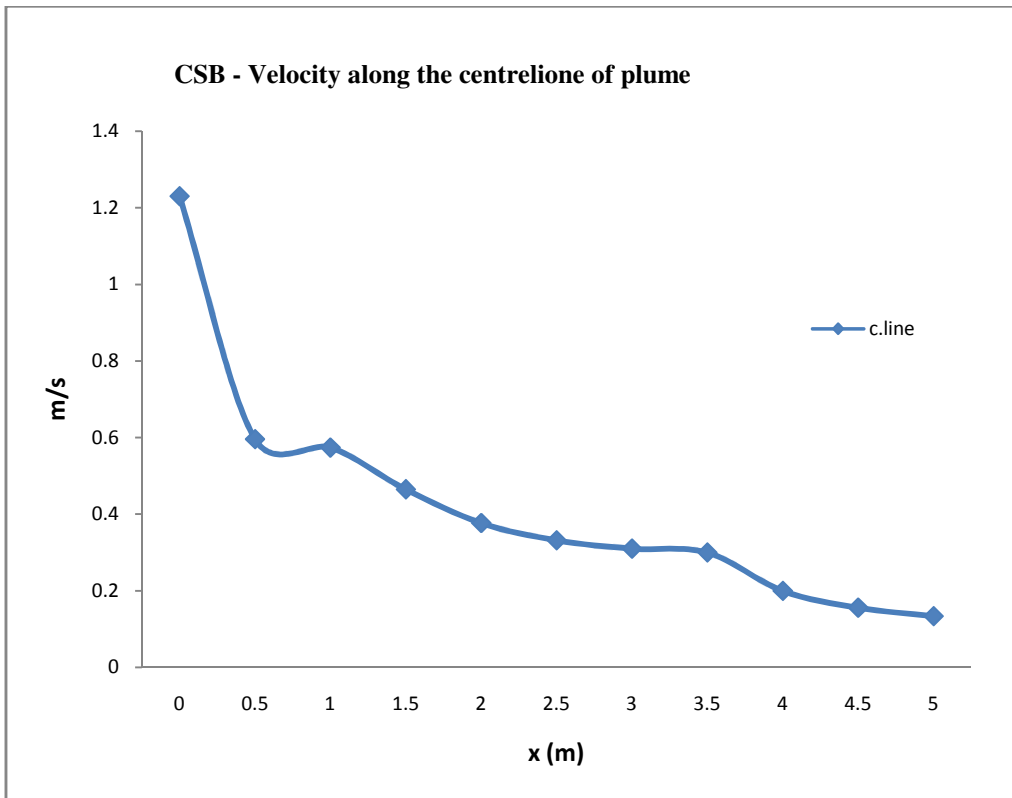


Figure 3.28: Measured velocity along the centreline of plume - CSB

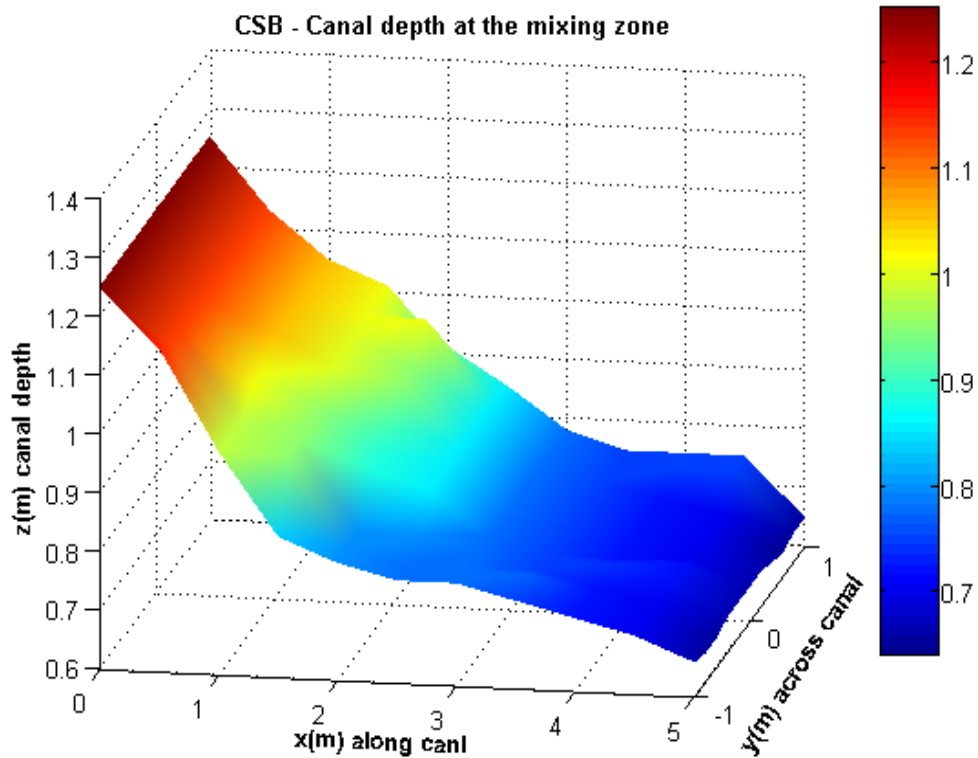


Figure 3.29: Canal depth at the mixing zone relation to canal surface– CSB

In the refine case study the data measurements were focused mainly on the core of plumes, i.e. the temperature and velocity along the centreline of plume. All the measured data is tabulated in the refine case study in Appendix 4. Thermal images are taken at the surface of plume and mixing zone, see Figure 3.30.

3.2.3 BBC Mailbox site

BBC Mail Box building lies at the upstream of the Birmingham Canal and is one of the largest British Waterways sites in terms of heat load (i.e. cooling water discharge into the canal) and extraction capacity. The discharge point into the canal is positioned approximately 100m downstream of the intake pipe, and is directed across the canal perpendicular to the normal line of flow of the canal (transversal discharge) via a 350mm diameter submerged pipe 400mm below the canal surface. Therefore the thermal discharge in this site is an example of submerged discharge into shallow and still receiving water. No evidence of aquatic growth was seen, see Figure 3.31.

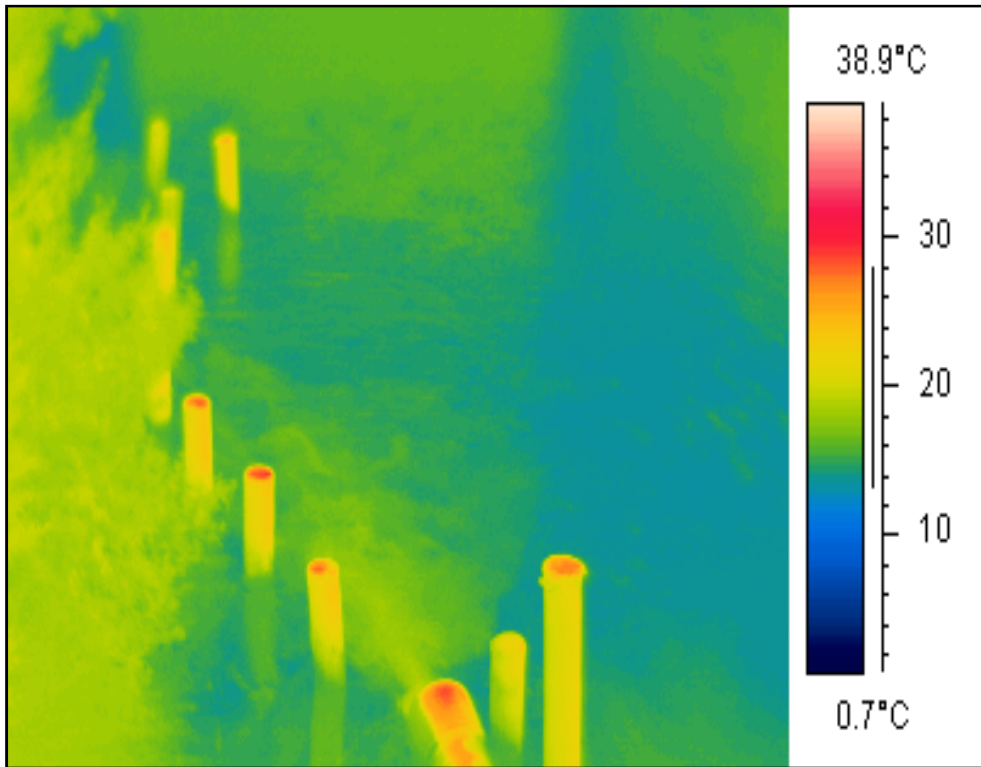


Figure 3.30: Thermal plume-CSB site



Figure 3.31: BBC Mail Box cooling water discharge to Birmingham Canal

The building management system utilises a data logger to record the discharge water temperature and water flow rate every six minutes which is stored in memory over a period of time.

The pump house and plant room are located within the building; the outlet temperature is measured in the plant room on the outlet side of the heat exchangers. The outlet pipe is lagged and travels within the plant room before going underground and connecting to the actual discharge pipe

As mentioned in chapter 1, the cooling water discharge into any British Waterways canal must comply with the requirements of Environment Agency:

For cyprinid (non-salmonid) waters the temperature downstream of the point of discharge should not be raised by more than 3°C on the edge of the mixing zone.

The temperature downstream of the point of discharge, at the edge of the mixing zone must not exceed 10°C during the breeding season for species which require cold water for breeding.

The maximum temperature must never exceed 28 degrees Celsius for cyprinid waters

Temperature Measurement

The tests being undertaken using the sheets are enclosed in Appendix 1. To define the position of the discharge outlet and the relative positions of the grid, measurements were made along the embankment at a distance from the end of the outlet pipe. A pole was marked at appropriate lengths to give the distances from the centreline of the discharge pipe. This produced a two-dimensional matrix along the length of the plume which could be readily reproduced using the discharge pipe outlet position as per the datum. Another pole was secured to the main pole at 90°, to which the thermocouple probe and flow meter could be attached. This also acted as a depth-measurement gauge by attaching a suitable measuring tape to produce a profile of the canal bed at the grid points. The temperature measurements were taken at the end of August, on particularly hot sunny days (+18°C ambient). There was one hour rain in the afternoon and the survey paused during the rain and then resumed. Thermal images were taken at the start and end of the survey along with a number of digital photographs. The canal ambient water temperature was recorded 20m upstream of the outlet discharge point plus the air temperature. Both temperatures were recorded with the use of 'k' type thermocouples and digital meter at the start and end of the trial. The canal water

temperature was then measured and recorded at the grid points (see Figure 3.32 and 3.33) at various levels: the surface, mid depth and approximately 50mm above the bed.

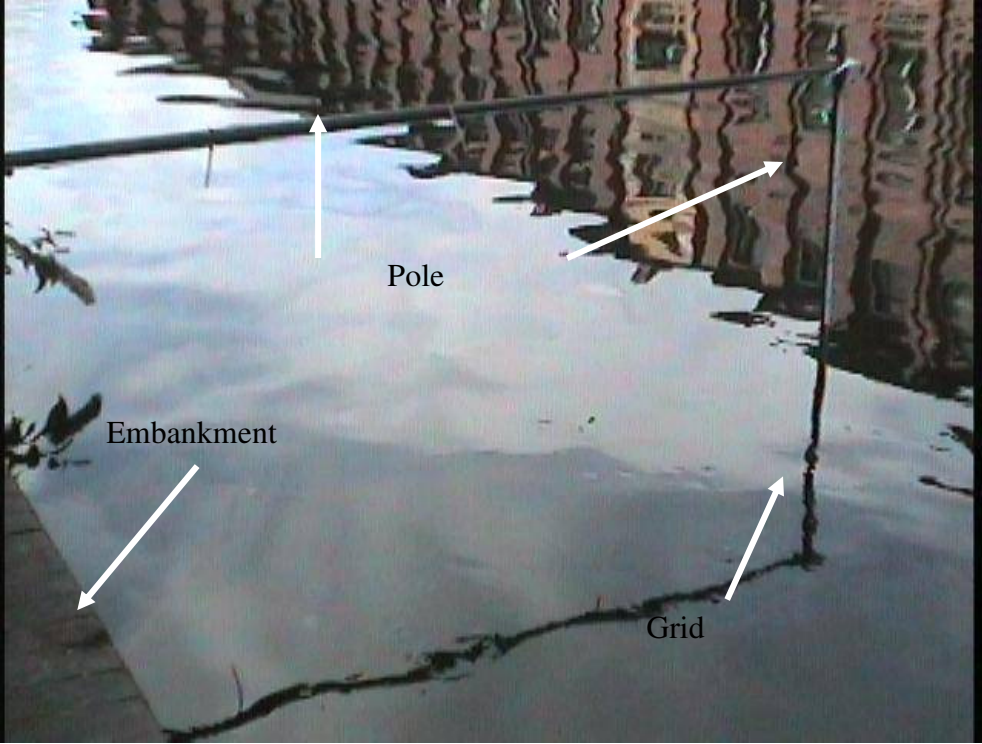


Figure 3.32: Temperature and flow measurements at a grid 2m distance from embankment.

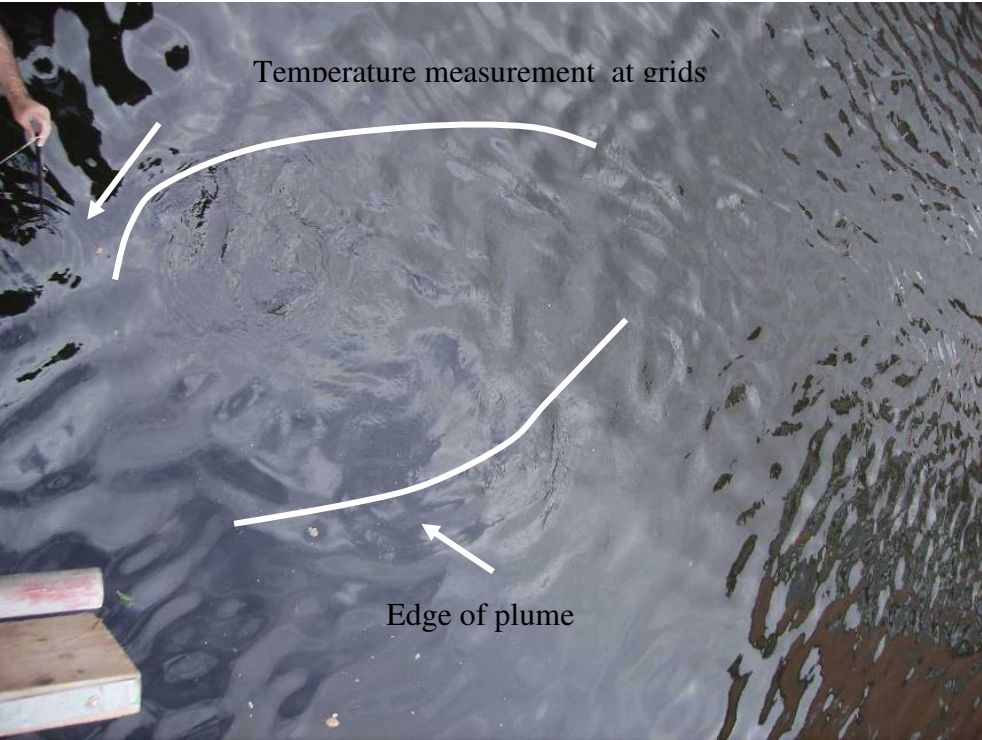


Figure 3.33: Plume moves to surface of canal, near embankment close to discharge point

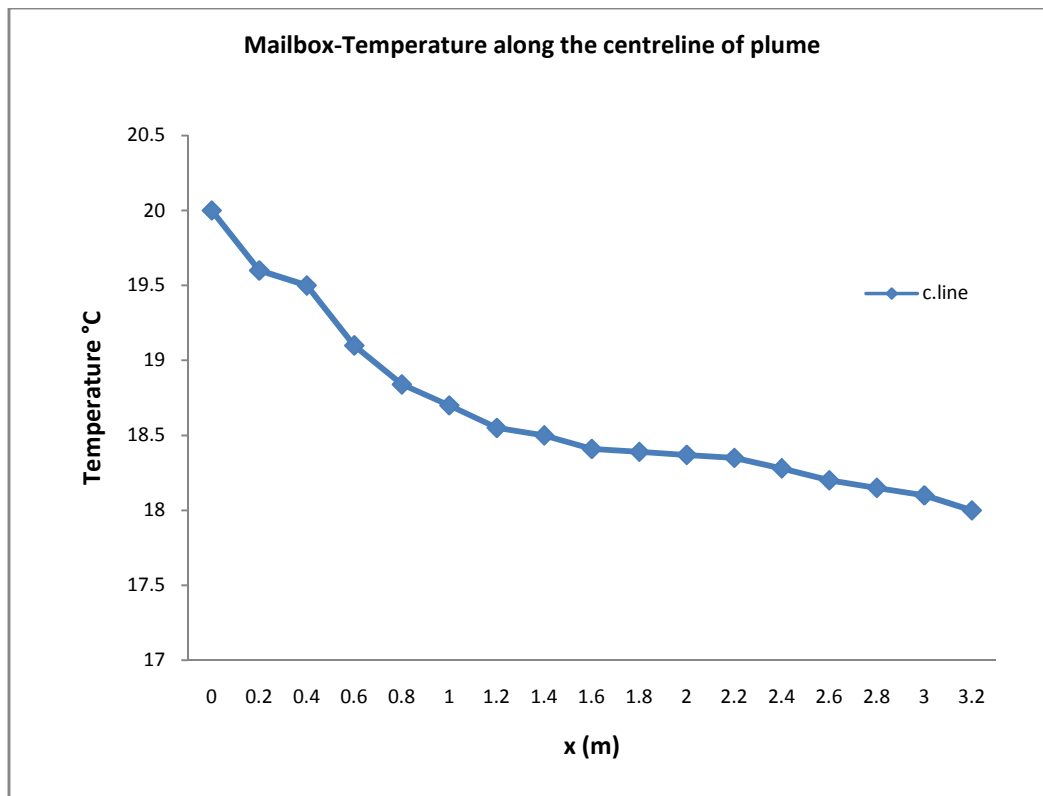


Figure 3.34: Measured temperature along the centreline of plume – Mailbox

Figure 3.34 shows the temperature measured along the centreline of plume. The maximum temperature recorded at the discharge point is 20°C

Since the discharge is spread over the surface area, a mixing zone area of 3m long (along plume) x 4m wide (2m upstream and 2m downstream from the discharge point) was selected for the grid size and data collections.

Flow

The velocity of the discharge flow was then measured at the grid points using an impeller flow meter. The measured velocities are tabulated in the refine case study in Appendix 4. The maximum velocity measured was 0.6m/s at the discharge point. Figure 3.35 shows the velocity along the centreline of plume. The mixing zone, as a general rule, must factor in the ability of fish to move away from any unfavourable conditions around the outfall and should not cross the full width of canal and leave at least one meter from the opposing bank to allow free movement of fish.

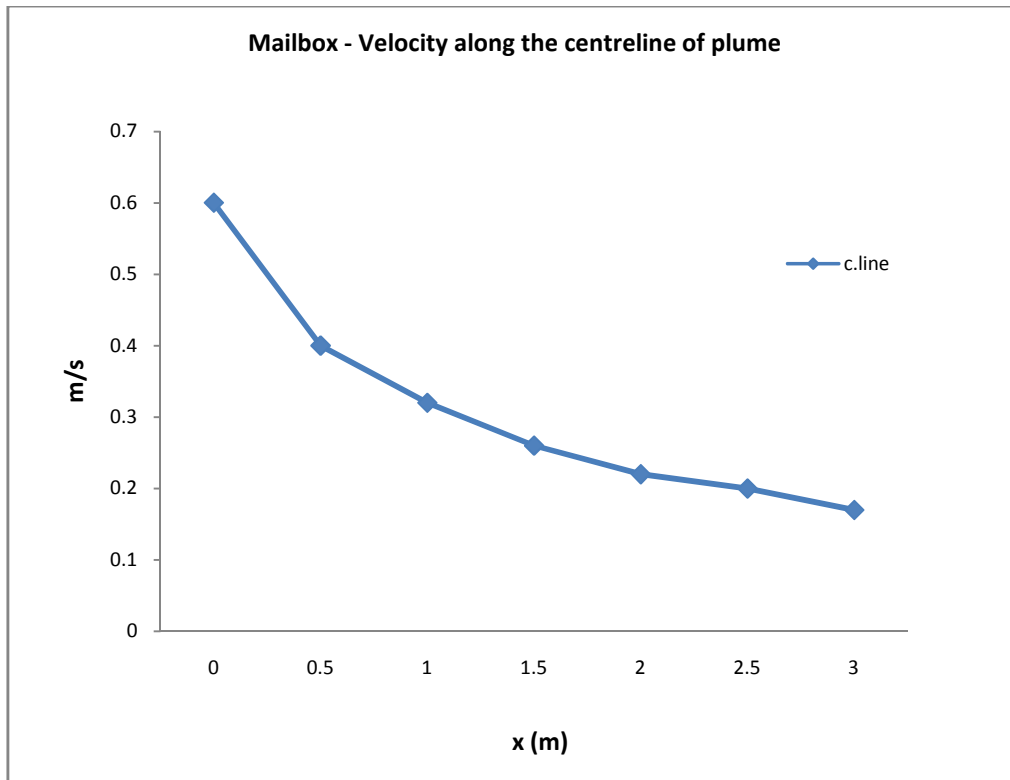


Figure 3.35: Measured velocity along the centreline of plume – Mailbox

The depth of canal was measured at each grid point and presented in a table in refine case study Appendix 4. The canal at this site is deeper than the University of Huddersfield sites; the discharge pipe is also twice the other three sites' discharge pipes. Figure 3.36 demonstrates the depth of canal within the mixing zone.

Thermal images were taken for the BBC Mailbox site, although the discharge pipe is deeply submerged. Figure 3.37a shows the mixing zone on the surface of the canal and edge of plume. The red colour is the reflection of the opposite buildings as it appears in the digital photo for the site see Figure 3.37b.

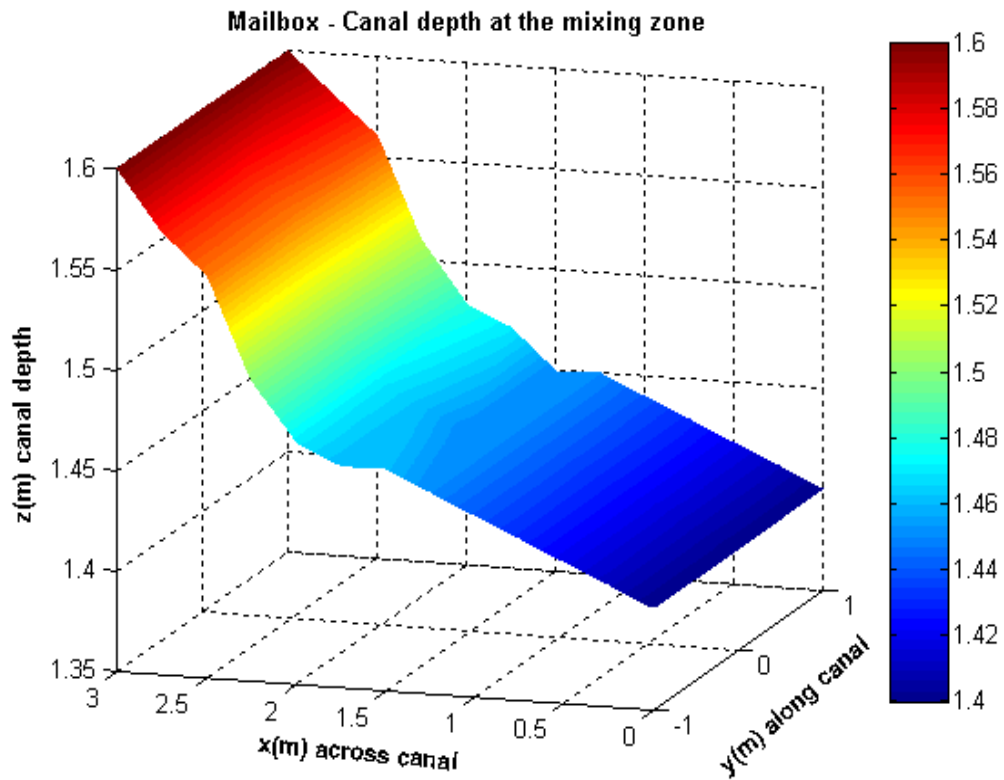


Figure 3.36: Canal depth within the mixing zone – Mailbox

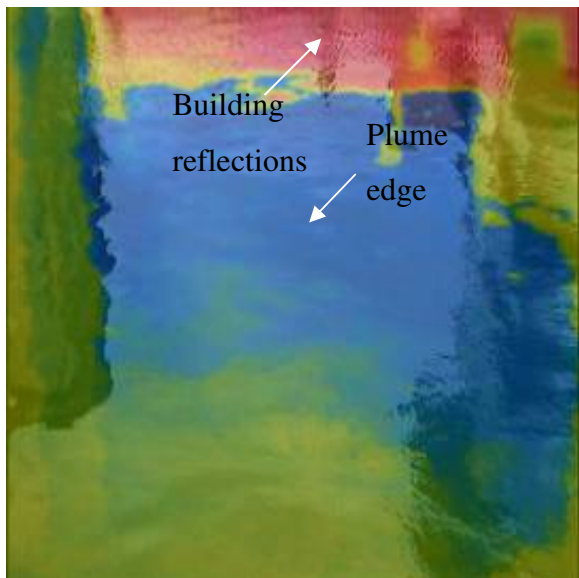


Figure 3.37a: Thermal image

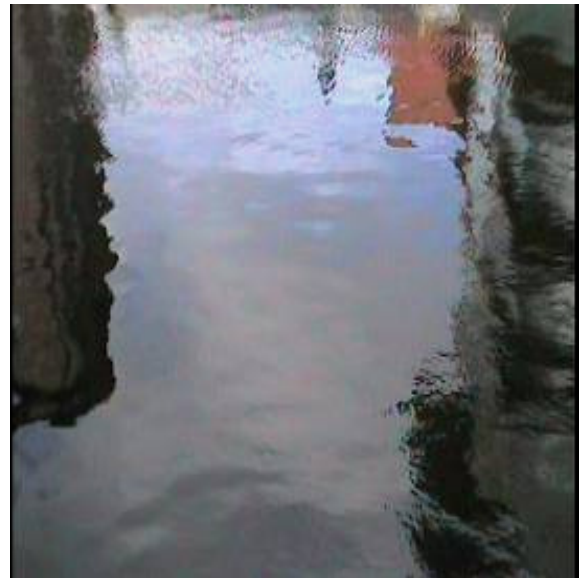


Figure 3.37b: Digital image

Figure 3.37: Thermal and digital image for a deeply submerged discharge

3.2.4 Canalside West

Canalside West uses submerged discharge and the direction of plume is transversal. The affected parameters are similar to the Mailbox site as both are the same kind of thermal discharge- submerged discharge into shallow and still receiving water. The procedures followed to carry out the survey at this site are similar to those followed at the Mailbox site. The collected data, temperature and velocity, along the centreline of plume are tabulated in the refine case study in Appendix 4. Figure 3.38 shows the measured temperature along the path line of plume. The plume path line is the centreline of plume, deflected to the free surface of canal due to buoyancy effects. In the CSB site, because the discharge is on the surface, the path line and the centreline of plume are same. For the BBC Mailbox site the data was collected only along the centreline of plume and not the path line, i.e. along a straight line and not the deflected path to the surface. Figure 3.39 shows the measured velocity along the path line of plume. The graphs in Figures 3.38 and 3.39 show the temperature along the path line of plume but as a function of the straight axis x. It is worthy to mention that the path line of the plume below the surface is predicted by an equation developed for this reason; this is described in detail in theoretical analysis in Chapter 7.

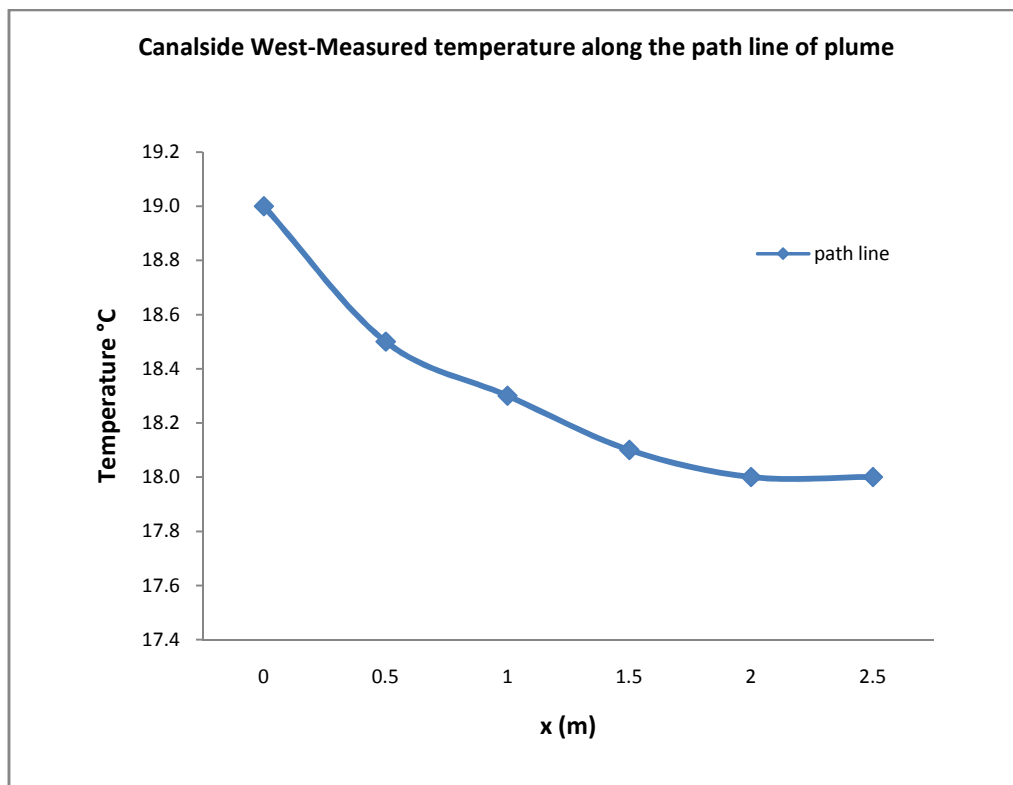


Figure 3.38: Measured temperature along the path line of plume – Canalside West

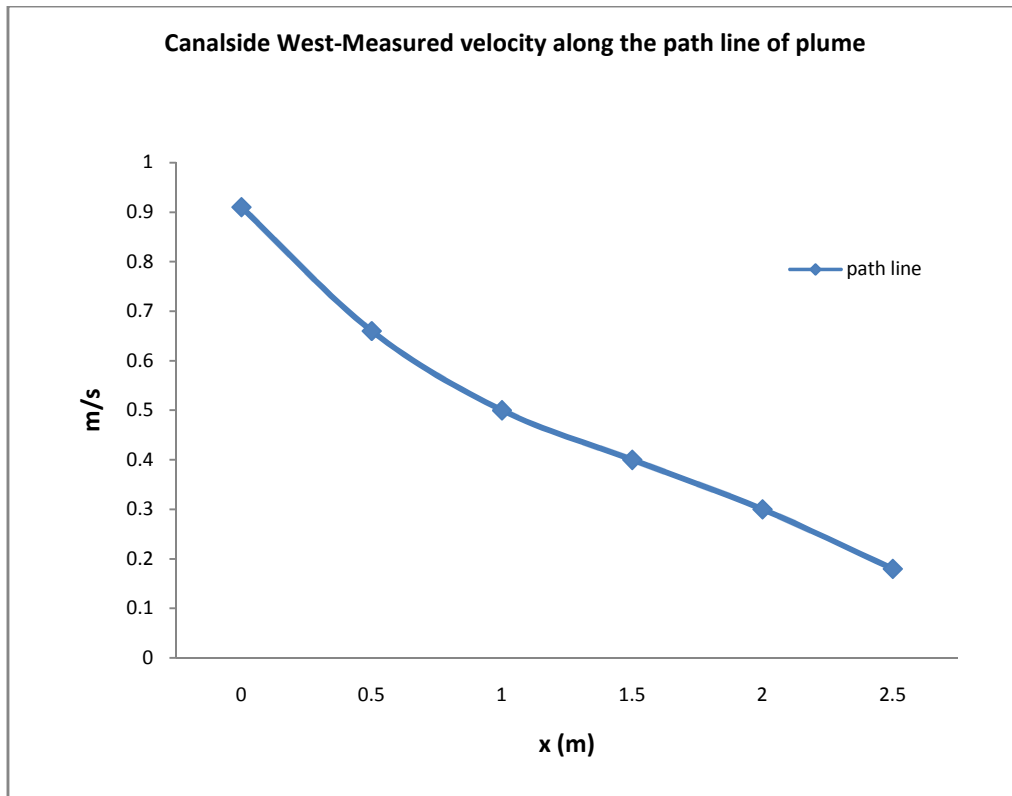


Figure 3.39: Measured velocity along the path line of plume – Canalside West

3.2.5 Lockside

Thermal discharge at the Lockside is submerged. As with the last two sites, the discharge pipe is located below the free surface of canal. The discharge pipe diameter is similar to the discharge pipe at the Canalside West and smaller than the Mailbox site. Temperature and velocity are measured following the same procedure as the other sites. Thermocouples were connected to the data acquisition device and then to a laptop to record the measured data. The obtained data is presented in a table in the refine case study in Appendix 4. The path line of the plume is predicted then the temperature and velocity along it are measured. The obtained data is presented in Figures 3.40 and 3.41. As mentioned earlier, to determine the surface area of the plume and mixing zone, a thermal camera is used in field trials at the sites.

In the refine case study, the temperature was measured by connecting the thermocouples to a computer via data acquisition device (Labjack 12) except the Mailbox site where digital meter is used.

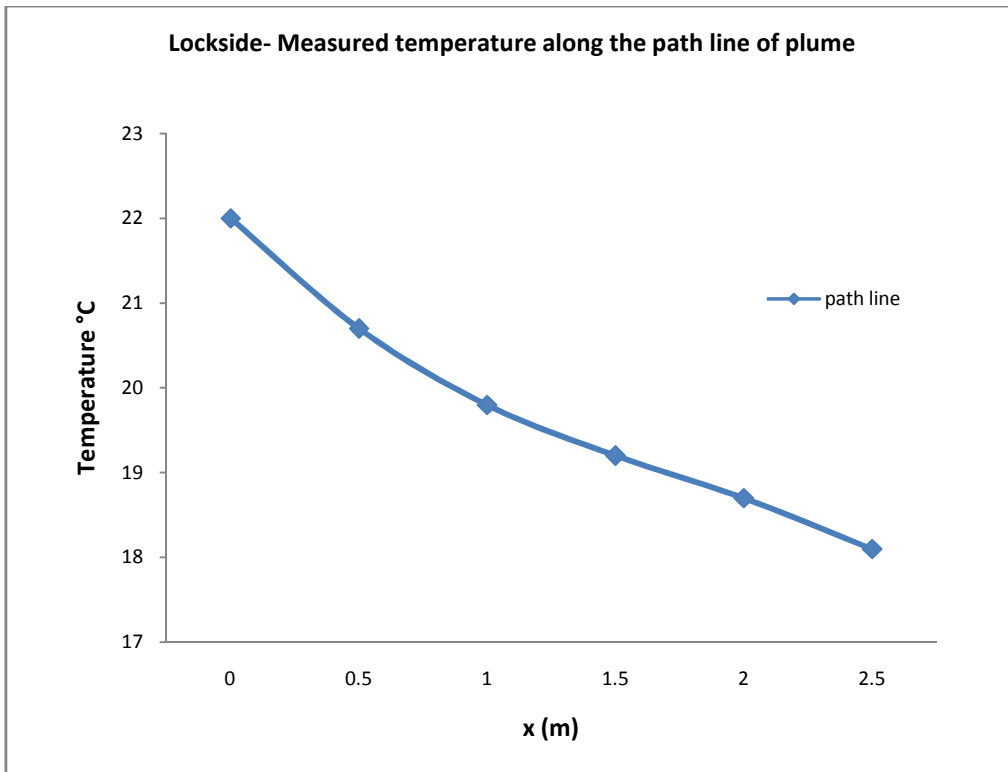


Figure 3.40: Measured temperature along the path line of plume – Lockside

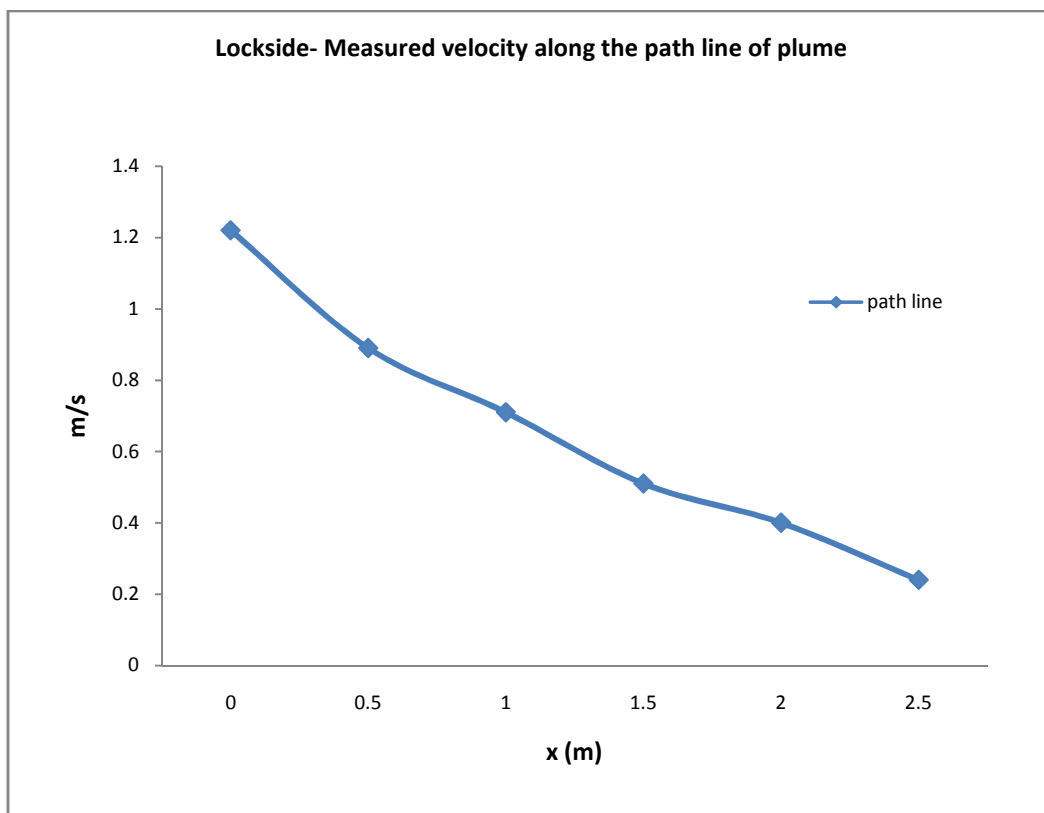


Figure 3.41: Measured velocity along the path line of plume – Lockside

3.2.6 Kirklees College Site

This case study was undertaken to determine the possibility of using a British Waterways canal water cooling system in a new building based on the Huddersfield Canal site by Kirklees College. It was found that the canal is able to absorb the rejected heat of 3470 kW within 3-4m distance from the outfall. The amount of heat discharged does not exceed the Environment Agency Regulation limit of 28°C, thus, there will be no risk on the aquatic life.

It is intended to present this case study as an appendix to reduce the size of the report. The case study is presented as a report since submitted to the Kirklees College, see Appendix 5. The site is not built yet; therefore only the theoretical predicted results have been presented.

3.2.7 Enviroenergy Nottingham

This case study carried out theoretically only and the experimental work fell outside the timeframe of the thesis.

The parameters used in this report are provided by the British Waterways; however in some cases, approximations are required. It is known that the discharge uses multi diffusers; three pipes with diameter 15in (0.381m) and a single pipe with diameter 6in (0.152m). The depth of canal at the margins is 0.5m and at the centre, 1m. The temperature difference is 5 °C and therefore it is assumed that the discharge temperature 25 °C and the canal ambient 20 °C.

Discharge velocity is not given. The maximum flow rate been measured is 1619 m³/hr (0.45m³/s). This value represents the total flow rate from the pipes (four discharge pipes). The following flow rates are obtained by assuming the discharge is proportional to the pipe areas, (i.e. the discharge velocity is the same) flow rate for the large pipes 0.1425m³/s and for the small pipe 0.02267m³/s. The discharge velocity will be 1.25m/s for both pipes.

The path line of plume from the centre of the discharge pipe to the free surface of canal is as illustrated in Figure 3.42. The temperature along the path line of plume should be as illustrated in Figure 3.43 and the velocity as in the Figure 3.44.

For the rest of the predicted results such as temperature and velocity across the path line and the size of plume see Appendix 6. This presents the preliminary report of Enviroenergy cooling water study in Nottingham canal.

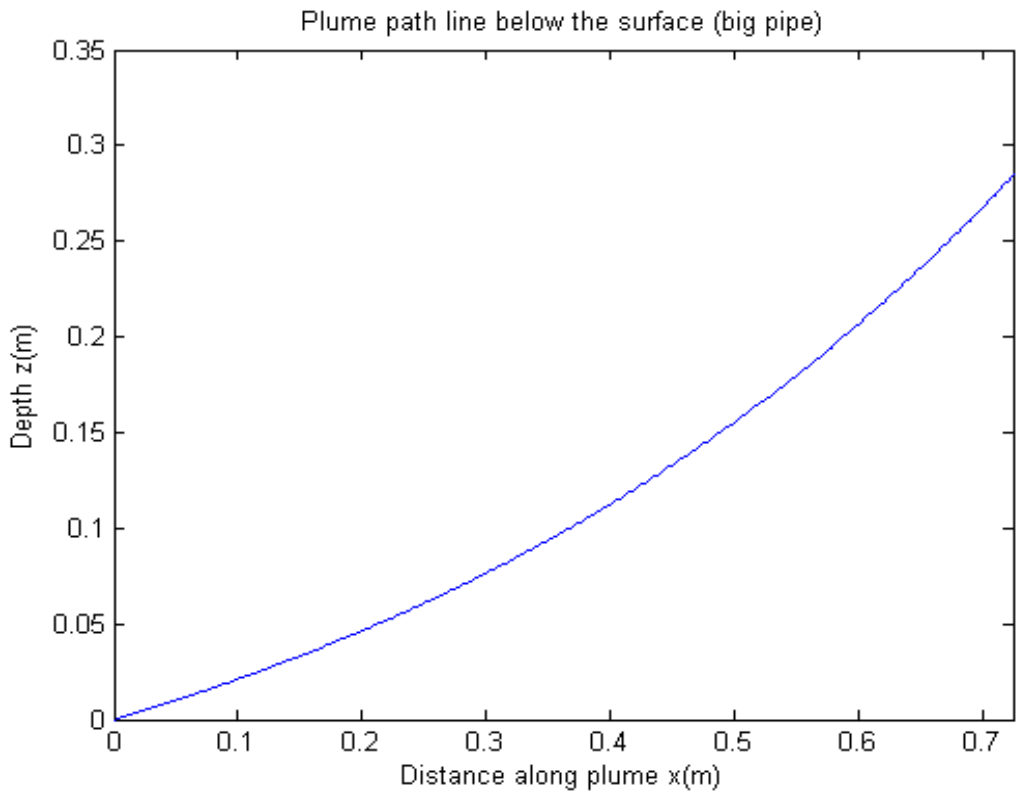


Figure 3.42: Plume path line – Enviroenergy Nottingham

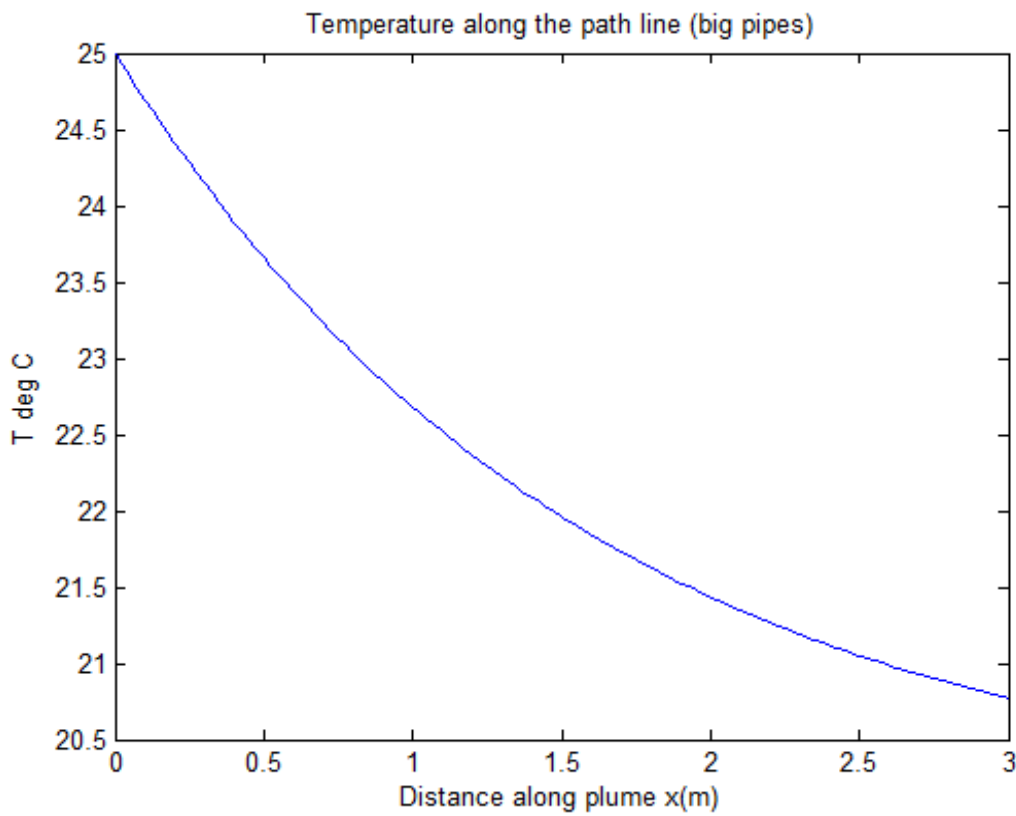


Figure 3.43: Temperature along the path line - Enviroenergy Nottingham

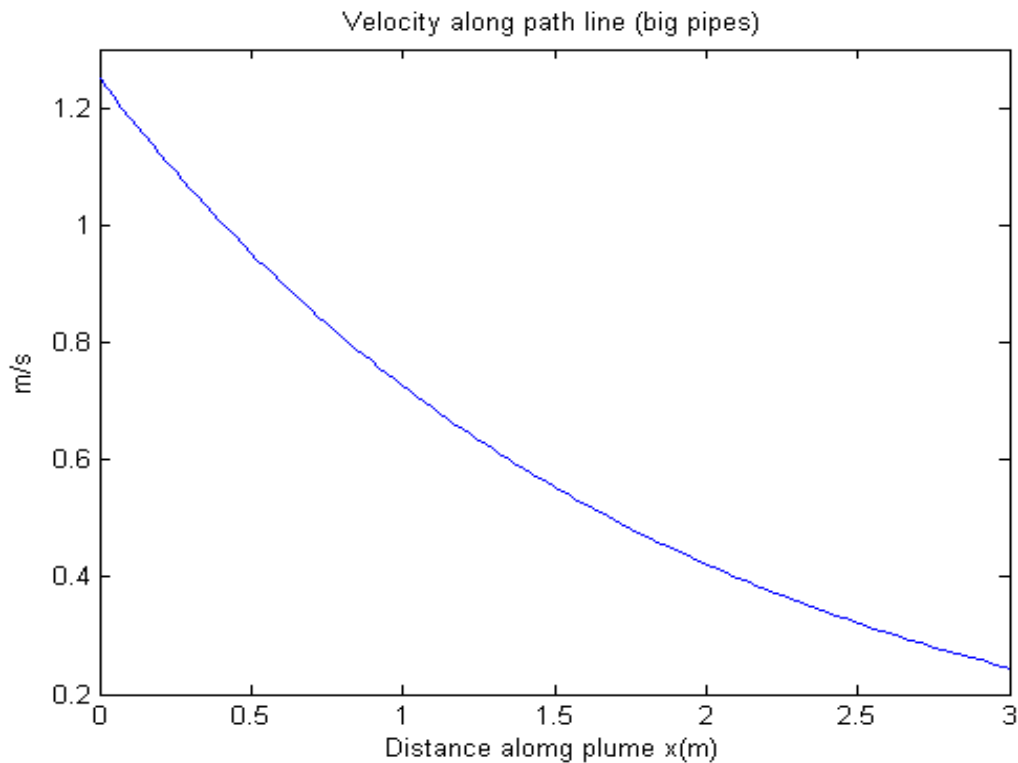


Figure 3.44: Velocity along the path line of plume - Enviroenergy Nottingham

4. Laboratory Experiment

4.1 Introduction

This chapter describes the experimental setup, the measurement tools and the used techniques. Surface and submerged thermal plumes discharged into shallow and still water were tested. In all trials dyed heated water was discharged into the receiving water tank. A thermal camera was used to measure the temperature on the surface as well as thermocouples, the latter connected to a data acquisition device or digital meter. Particles discharged with the heated water into the tank were used to measure the velocity within the plume. Two camcorders were installed at the top and the side of the tank to record the plume behaviour at each trial. The movie footages were converted to still images, then analysed.

4.2 Objective of Experiments

The objective of the experiments was to simulate the canal sites investigated in the case study chapter to obtain a consistent set of data in an environmental scale model tank. Tests were

performed under variable conditions such as velocities, temperature, pipe diameter and so on. The obtained data from the laboratory experiments with the onsite canal data were used to verify the theoretical model results. In addition the laboratory experimental data was used to develop a number of equations to predict the behaviour of thermal plume.

4.3 Thermal Modelling

The first step to simulate the thermal discharge is to determine the densimetric Froude Number. This dimensionless parameter will help to simulate canal in a laboratory scale model tank.

The densimetric Froude Number F_d , can be calculated from the Equation 2.14.

The discharge pipe diameter for the model tank must be known, at a scale to simulate the canal and build the tank. The canal parameters are known, and the remaining unknown is the discharge velocity (U_m) which can be calculated from the Equation 2.16.

Central Service Building site simulation (CSB): the discharge pipe diameter at CSB ($D_p = 0.15\text{m}$) and flow ($U_p = 1.23\text{m/s}$), canal's width and depth are 10m and 1m respectively. The dimensions reduced by 10 to build the model tank, so the discharge pipe diameter for the model will be ($D_m = 0.015\text{m}$) and the discharge velocity U_m calculates as below:

$$\frac{1.23}{U_m} = \frac{\sqrt{0.15}}{\sqrt{0.015}}$$

$$U_m = 0.39\text{m/s}$$

The discharge pipe diameter must be large enough to give a proper type of flow turbulent or laminar; the type of flow in any fluid can be determined by Reynolds number (Re). The discharge flow is laminar when $Re < 3000$ and its turbulent when $Re > 3000$ (Coulson, 2003). There is a transition region where $Re > 2300$ in very smooth, straight and uniform pipe, the value is slightly lower; $Re > 2000$ for pipes with usual degree of roughness of walls (Massey, 1989). In the case of the CSB site the Reynolds number (Re_p) is given by Equation 4.1:

$$\text{Re}_p = \frac{U_p \times D_{0p}}{\nu_p} \quad (4.1)$$

ν_p = kinematic viscosity

$$= \frac{\mu}{\rho}$$

μ = dynamic viscosity = 0.001028 at 24° C (Coulson, 2003)

$$\nu = \frac{0.001028}{1000} = 1.028 \times 10^{-6}$$

$$\begin{aligned} \text{Re}_p &= \frac{1.23 \times 0.15}{1.028 \times 10^{-6}} \\ &= 179474 \end{aligned}$$

The Reynolds number shows that the flow is turbulent at CSB site; also it can be seen by visual observation of the canal at CSB site. As the flow is turbulent for the prototype it must be turbulent for the model. To find out the flow type for the model denote the Reynolds number ratio (r) for model to prototype, Equation 4.2.

$$\text{Re}_r = \frac{\frac{U_p \times D_p}{\nu_p}}{\frac{U_m \times D_m}{\nu_m}} \quad (4.2)$$

$$\frac{U_p}{U_m} = U_r = D_r^{1/2} \quad (4.3)$$

$$\frac{D_p}{D_m} = D_r \quad (4.4)$$

Because the model tank and canal water have same temperature, therefore they have the same kinematic viscosity:

$$\frac{\nu_p}{\nu_m} = 1 \quad (4.5)$$

Therefore $Re_r = D_r^{3/2}$

This proves that the turbulence depends on the size of discharge pipe diameter:

$$\frac{Re_p}{Re_m} = \frac{D_p^{3/2}}{D_m^{3/2}} \quad (4.6)$$

$$\begin{aligned} Re_m &= \frac{179474 \times 0.015^{3/2}}{0.15^{3/2}} \\ &= 5675 \end{aligned}$$

If the Reynolds number is greater than 3000, it means the discharge flow of the model is turbulent. The Reynolds number for the model also can be calculated as follow

$$\begin{aligned} Re_m &= \frac{U_m \times D_m}{\nu_m} \quad (4.7) \\ &= \frac{0.39 \times 0.015}{1.028 \times 10^{-6}} \\ &= 5690 \end{aligned}$$

It is close to above value and shown that flow is turbulent.

Following the same procedure, to simulate BBC Mailbox site, discharge velocity for the model will be ($U_m = 0.19$ m/s) and the Reynolds Number ($Re = 6650$). The discharge velocity for the Canalside West model is ($U_m = 0.29$) and ($Re = 4227$). For the Lockside the discharge velocity for the model is ($U_m = 0.385$ m/s) and ($Re = 6034$). The Reynolds Numbers for all the models are greater than 3000, therefore the discharge flow in the model tank is turbulent.

4.4 Experimental Setup and Apparatus

4.4.1 Model Tank

The laboratory experiments were conducted using a tank, 2m long by 1m wide and 0.3m deep. It was constructed of transparent acrylic so as to allow visual observation of the thermal plume including photographs and videos of experiments. The tank was a 1/10th scale model to represent most anticipated situations that may exist in practice. Figure 4.1a shows the photograph of the experimental model tank. A schematic of the experimental setup is shown in Figure 4.1b. Note that the tank will be filled with water to the required level based on the depth of the simulated site. Discharge pipes were made from easy fit plastic so they could be changed easily to fit any desired diameter. The position of discharge and intake was based on their location on the simulated site. Intake water returned to a small tank where the temperature and flow were measured then extracted to drainage. The receiving water in the model tank was still and not moving as no current had been given. The entire experimental run was completed once the steady state was achieved and the temperature of plume was equal to the receiving water ambient temperature ($\Delta T = 0$). The time required to obtain the steady state condition depended on the discharge velocity and temperature, with longer times for higher discharge velocities and temperature.



Figure 4.1a: Experimental model tank

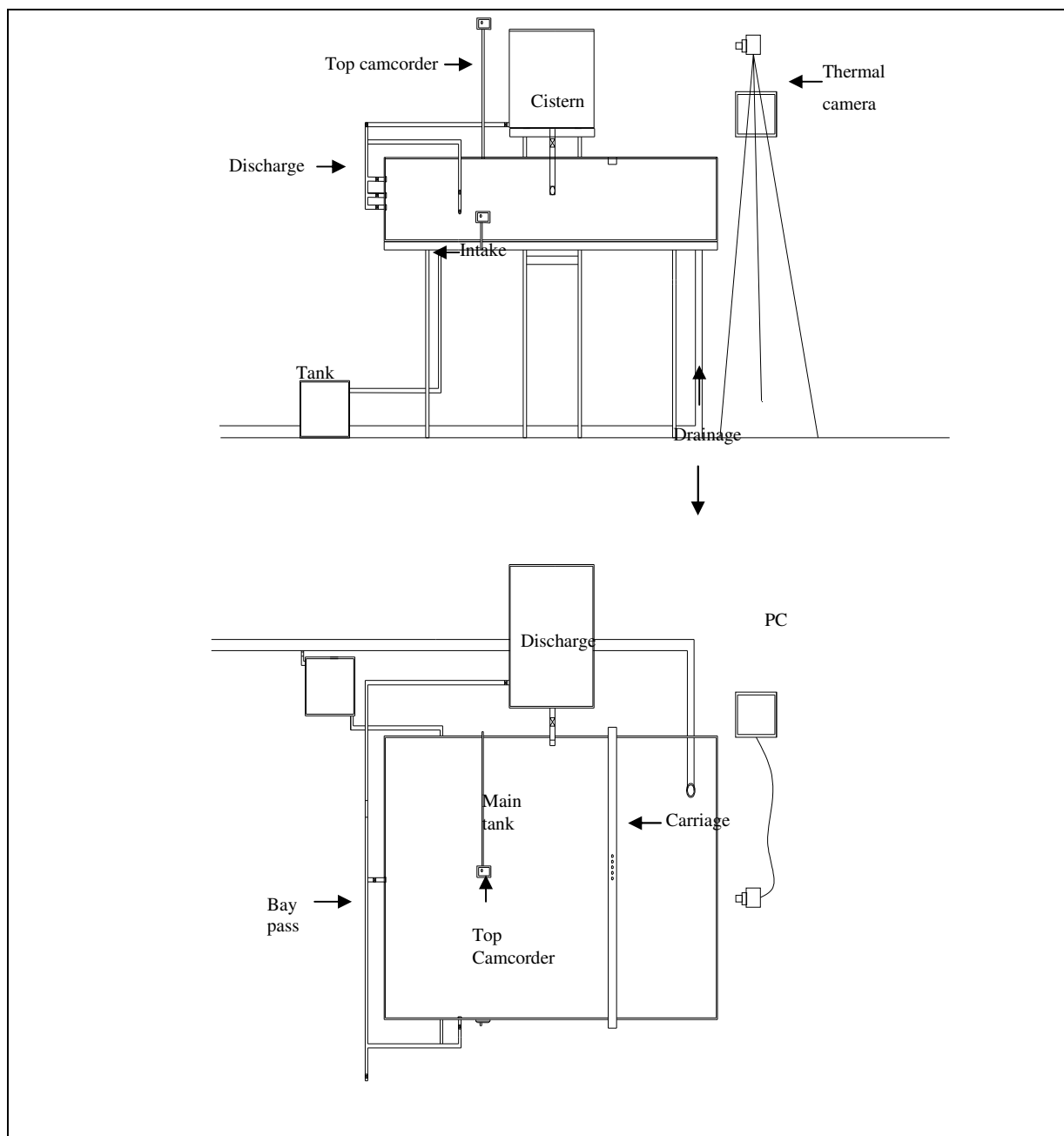


Figure 4.1b: Schematic diagram of experimental setup

The laboratory experiments were carried out in all seasons except summer when the temperature was highest; therefore the laboratory building temperature averaged 18°C. This temperature is equal to the average ambient temperature in summer when the thermal discharges are highly affected by the environment.

4.4.2 Water Supply

The discharge water was supplied from a constant head cistern installed next to the model tank. The cistern was connected to main hot and cold water pipes with flow control valves to maintain the required temperature, see Figure 4.2. The level of heated water is controlled by connecting the cistern to a number of pipes at different levels connected to the drainage. This kept the supplied water at a certain level which gave a required discharge velocity.

The heated water discarded into the model tank via discharge pipes. Two different discharge pipes were used: fixed and movable. The moveable plastic discharge nozzle was 0.032m diameter, used for simulation of canal sites with large discharge pipe diameters, Figure 4.3. The outlet of the plume discharge could be located at any side of the tank and at any desired depth. The main discharge pipe was fixed and distributed to five outlets at different sides and levels. Easy fit plastic pipes were used for the main discharge so the pipe diameter could be changed as required, whereas the majority of the tests were carried out with a discharge pipe diameter of 0.015m. Flow rate was controlled by two valves; one valve was located underneath the cistern, Figure 4.2 and another located just before the outlet next to the tank wall, see Figure 4.4. Always one of the valves was fully opened and the other only opened fully when a test was performed.



Figure 4.2: Hot and cold water valves controlling cistern temperature



Figure 4.3: Movable discharge pipe

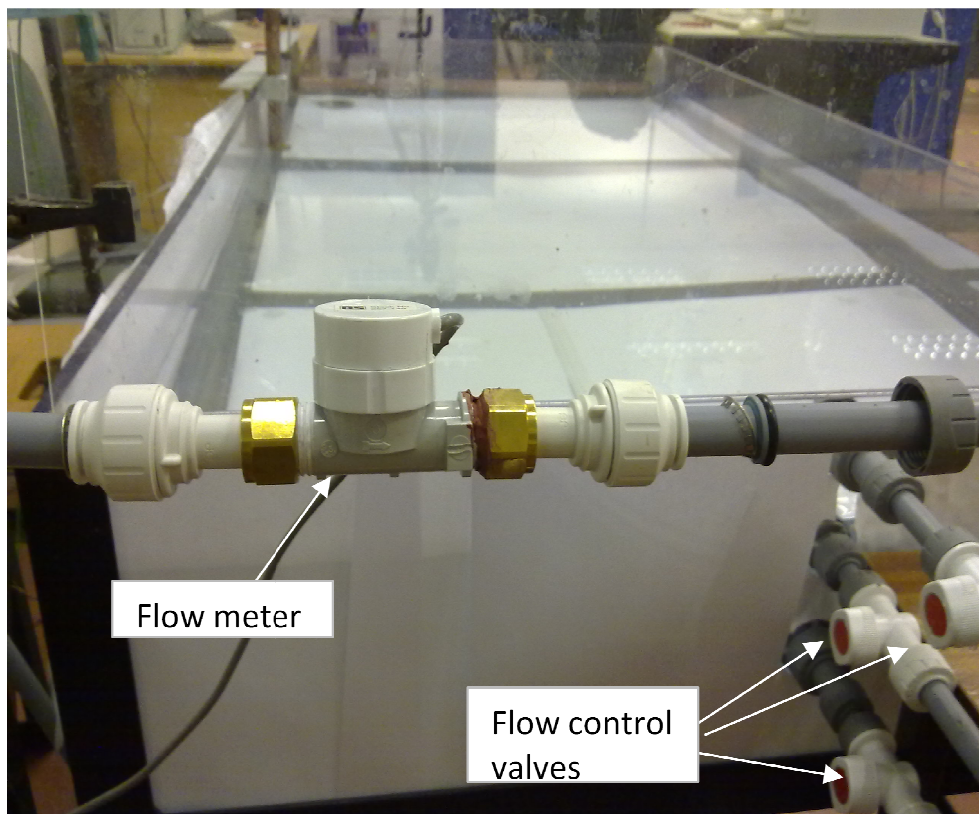


Figure 4.4: Discharge pipe flow control valves

A flow meter was installed on the discharge pipe to measure discharge velocity, Figure 4.4. A by-pass line was installed to allow preliminary adjustment of temperature and flow before water was discharged into the tank, Figure 4.5.

Intake pipes were located at the side of the tank at variable depths and provided with flow control valves. The intake pipe was operated only in the simulation of canal sites where the intake was influenced by the discharge i.e. when located within the mixing zone.



Figure 4.5: By - pass

4.4.3 Experimental Method

A set of experimental trials were carried out with different parameters for each trial. The parameters for 24 runs are scheduled in the Table 4.1. These parameters were influenced on the behaviour of the thermal plume in the receiving water. Densimetric Froude number F_d is not the only affected parameter investigated by many researchers in this field. There are other parameters which are affected on the diffusion of the thermal plume such as the depth of the discharge pipe and the depth of the receiving water. The parameters used in the current study were discharge pipe diameter D_0 , temperature difference between the discharge and the receiving water ΔT , discharge velocity U_0 and buoyancy \dot{g} . These parameters will involved in

determination of the densimetric Froude number F_d and the length scale L_M . Therefore F_d , L_M as well as the discharge pipe depth z_0 and the receiving water depth H are the main parameters effecting the plume behaviour. Also some parameters presented in the Table 4.1 are for information only and they will not be presented in the mathematical models with the current format. The Reynolds number Re show whether the flow is turbulent or laminar, however both types of flow were considered as the produced models will be applicable for both turbulent and laminar discharge. The values of the parameters for the experimental trials were selected based on the values of the sites on the canal. For example the minimum temperature difference found on the real canal sites was around 3°C and the maximum was around 8°C . Therefore the temperature differences used for the trials were a range between these two values (3°C , 4°C , 6°C , 7°C and 8°C). The minimum velocity for the canal site simulated was around 0.19m/s and the maximum was around 0.45m/s . The minimum densimetric Froude Number F_d recorded for the canal sites was 13.3 and the maximum value was 54.9. The densimetric Froude numbers used in the experimental trials were between these two. Similarly the values of the other parameters were selected. The worst scenario for the temperature were considered i.e. " $\Delta T = 8^\circ\text{C}$ " in several trials. To fulfil the experiments and to involve all the parameters, five temperatures are used for the discharge, three different velocities, two discharge pipe diameters and three different depths for the discharge pipe and the receiving water.

4.5 Data Collection Procedure

4.5.1 Temperature measurements

The receiving water ambient temperature in the model tank was defined as the initial basin temperature. The discharge water temperature was measured in the cistern and at the outfall. "k" type thermocouple sensors with high frequencies were used to measure temperatures. The diameter of the thermocouples was 0.1mm . Two methods were used to measure the temperature: one uses a digital meter to collect data and another using a computer. In method one, a rake of five thermocouples was used to measure the temperature within the mixing zone. The distance between each sensors depended upon the discharge water properties. Due to the low discharge velocities applied and to avoid any flow disturbance, the number of probes was limited to five and no more. In addition the probes could affect the direction of flow and the velocity. Thermocouples were connected to multi channels digital meter to read

the temperature for each sensor, Figure 4.6. The other method used to measure temperature is to use a single probe connected to a computer. The thermocouple in this method connected to an amplifier to increase the low receiving voltage is then connected to a data acquisition device (Labjack 12) and then to a computer. A program is installed on the computer to read the mean temperature of the thermocouple. Figures 4.7a, 4.7b show the photograph and schematic of the data acquisition setup.



Figure 4.6: Thermocouples digital meter

A thermal camera was used to measure the temperature on the surface of the mixing zone and to verify the thermocouples data. This will be discussed in detail in Chapter 5.

Five different temperatures for the discharge were used in the laboratory experiments; the temperature difference between the discharge and model tank ambient water were as follows; $\Delta T = 3^{\circ}\text{C}$, $\Delta T = 4^{\circ}\text{C}$, $\Delta T = 6^{\circ}\text{C}$, $\Delta T = 7^{\circ}\text{C}$ and $\Delta T = 8^{\circ}\text{C}$.



Figure 4.7a: Photograph of data acquisition setup

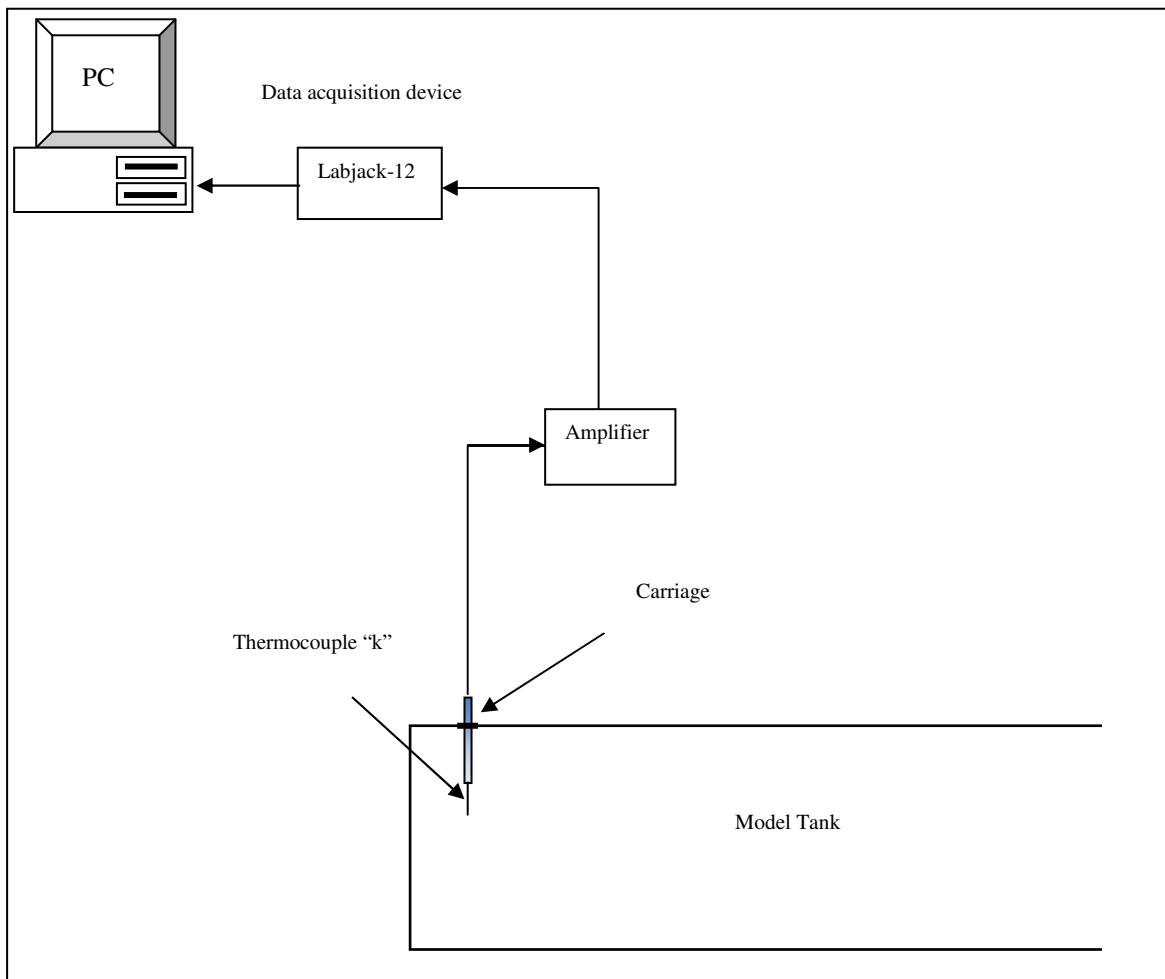


Figure 4.7b: Schematic of data acquisition setup

Run	D. diameter D _o (cm)	z _o (cm)	H (cm)	ΔT (°C)	U _o (cm/s)	Buoyancy g' (cm/s ²)	Q (cm ³ /s)	Buoyancy. flux B _o (kgm ² /s ²)	Momentum. Flux M _o (m ⁴ /s ²)	Length scale L _M (cm)	z _o / F _d	(H - z _o) / L _M	D _o F _d / (F _d - z _o)	Re	F _d
1	1.2	14.5	21.5	3	19	0.56	21.48	12.02	408.07	26.18	0.62554	0.26734	3.9737	2269.29	23.18
2	1.2	14.5	21.5	4	19	0.77	21.48	16.45	408.07	22.38	0.73232	0.31273	3.3943	2324.44	19.80
3	1.2	14.5	21.5	6	19	1.22	21.48	26.16	408.07	17.75	0.92239	0.39430	2.6949	2437.91	15.72
4	1.2	14.5	21.5	7	19	1.45	21.48	31.22	408.07	16.25	1.00764	0.43077	2.4669	2496.19	14.39
5	1.2	14.5	21.5	8	19	1.70	21.48	36.49	408.07	15.03	1.09023	0.46574	2.2800	2551.58	13.30
6	1.2	13.5	21.5	3	34	0.56	38.43	21.52	1306.74	46.86	0.32538	0.17072	6.2235	4060.84	41.49
7	1.2	14.5	21.5	4	34	0.77	38.43	29.44	1306.74	40.06	0.40891	0.17476	6.0789	4159.52	35.46
8	1.2	14.5	21.5	6	34	1.22	38.43	46.81	1306.74	31.77	0.51546	0.22035	4.8223	4362.58	28.13
9	1.2	14.5	21.5	7	34	1.45	38.43	55.86	1306.74	29.08	0.56311	0.24073	4.4143	4466.86	25.75
10	1.2	13.5	21.5	8	34	1.70	38.43	65.30	1306.74	26.90	0.56723	0.29739	3.5700	4565.98	23.80
11	1.2	14.5	21.5	3	45	0.56	50.87	28.48	2289.06	62.02	0.26412	0.11287	9.4114	5374.64	54.90
12	1.2	14.5	21.5	4	45	0.77	50.87	38.97	2289.06	53.01	0.30890	0.13204	8.0469	5505.24	46.94
13	1.2	14.5	21.5	6	45	1.22	50.87	61.95	2289.06	42.05	0.38947	0.16648	6.3823	5774.01	37.23
14	1.2	14.5	21.5	7	45	1.45	50.87	73.94	2289.06	38.49	0.42547	0.18188	5.8423	5912.02	34.08
15	1.2	14.5	21.5	8	45	1.70	50.87	86.43	2289.06	35.60	0.46032	0.19664	5.4000	6043.21	31.50
16	0.8	14.5	21.5	8	19	1.70	9.55	16.22	181.37	12.27	0.87879	0.57041	1.8857	1701.54	16.50
17	0.8	14.5	21.5	8	34	1.70	17.08	29.02	580.77	21.96	0.50000	0.31876	3.3143	3043.91	29.00
18	0.8	15.5	21.5	8	45	1.70	22.61	38.41	1017.36	29.06	0.40260	0.20646	5.1333	4028.81	38.50
19	1.2	7.7	14.7	8	19	1.70	21.48	36.51	408.07	15.03	0.57895	0.465866	2.2800	2551.58	13.30
20	1.2	7.7	16.7	8	45	1.70	50.87	86.48	2289.06	35.59	0.24444	0.25288	4.2000	6043.21	31.50
21	1.2	11	18	8	19	1.70	21.48	36.51	408.07	15.03	0.82707	0.465866	2.2800	2551.58	13.30
22	1.2	11	18	8	45	1.70	50.87	86.48	2289.06	35.59	0.34921	0.196699	5.4000	6043.21	31.50
23	0.8	11.5	18	8	19	1.70	9.55	16.23	181.37	12.27	0.69697	0.52974	2.0308	1701.54	16.50
24	0.8	7.7	14.7	8	45	1.70	22.61	38.43	1017.36	29.06	0.20000	0.240906	4.4000	4028.81	38.50

Table 4.1: Experimental trials parameters

4.5.2 Velocity measurements

As mentioned in the opening chapters, the current research investigates thermal plumes which have low initial velocity. The maximum discharge velocity studied is 1.23m/s at the CSB canal site and the laboratory simulation in the model tank is 0.4m/s. Another two discharge velocities are used in the laboratory experiments and those are; 0.19m/s and 0.34m/s. All three velocities used in the experiments are relatively small and easily disturbed. Therefore any measuring instrumentation which may disturb the flow of the plume was avoided, particularly those which required insertion of an object into plume and the mixing zone. Traditional instrumentation such as flow meters, pitot- tubes and films influenced the velocity of the plume, its direction and even the temperature gradients. For the same reasons a thermal camera and a maximum of five thermocouples probes were used to measure the temperature.

Flow visualisation technique has been used to measure the velocity of the thermal plume within the model tank. The technique filmed the flow without affecting the behaviour of the thermal plume. Two camcorders were installed on the top and the side of the tank to record the plume flow in the receiving water, Figures 4.8a and 4.8b illustrate the camcorders' schematic setup.



Figure 4.8a: Top camcorders

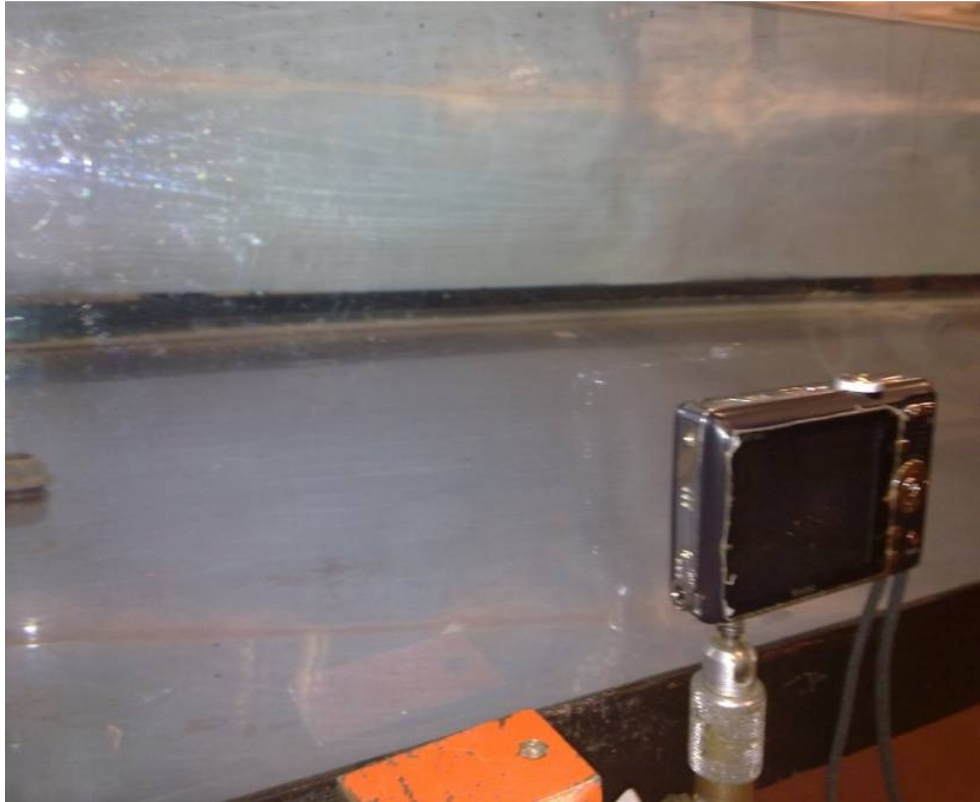


Figure 4.8b: Side camcorder

Figure 4.8: Photograph of the schematic camcorders setup

Small particles are inserted into the heated water then discharged into the tank. The camcorders were set up to start recording at the same time, one recording the plan view and the other the side view.

While the camcorders recorded the flow of plume, the motions of particles within the plume are captured. The speed of each camcorder is 27fps (frame per second), with 0.037s required to capture a frame. Adobe Premiere Pro 1.5 software was used to convert the movies to still images (frames). The distance that a particle moves within a frame dividing by 0.037sec gives a velocity at that point.

4.5.3 Thermal Images

In the laboratory experiment, thermal images (Figure 4.9a) give very clear heat diffusion profiles and show the plume on the surface of model tank (Figure 4.9b). The main advantage of the thermal camera's application in thermal plume study is its high accuracy without

disturbing the flow. The thermal image of temperature distribution is investigated in detail in Chapter 5.

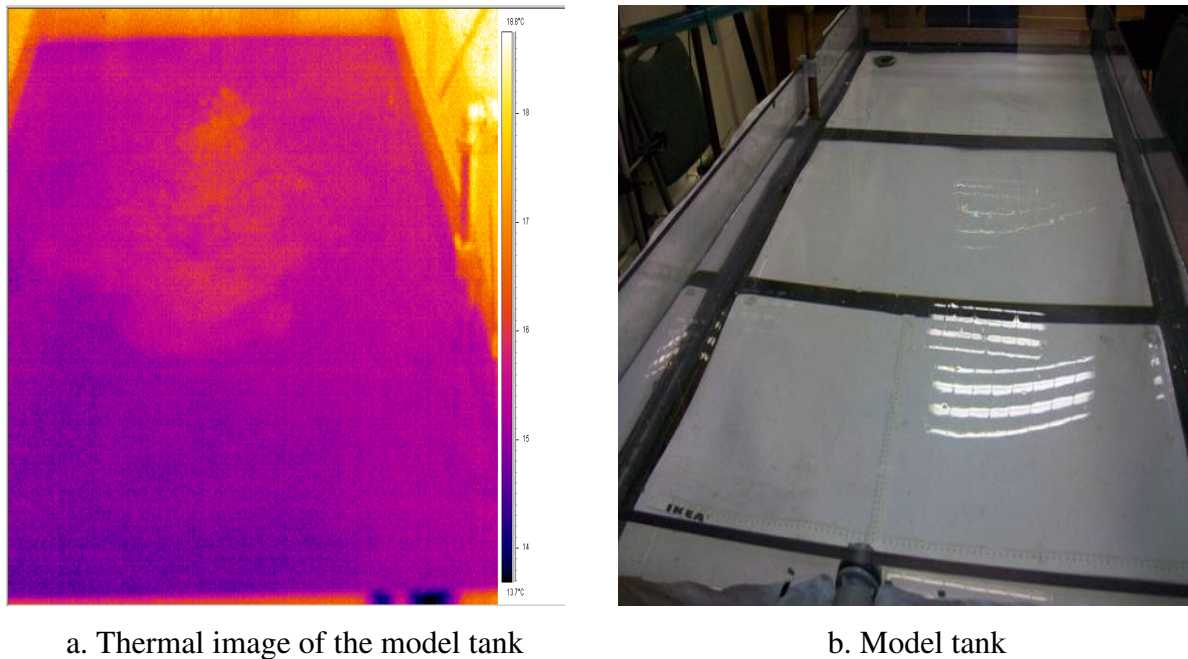


Figure 4.9: Thermal and digital image of model tank

4.5.4 Dyed water discharge

As mentioned above, the thermal camera is able to measure the temperature distribution on the surface of the mixing zone. Coloured water was discharged into the tank to demonstrate the behaviour of the thermal plume below the free surface and the vertical diffusion of the plume. Figure 4.10 shows a plan view of a submerged dyed plume discharged into the model tank. Figure 4.11 shows a side view of the submerged discharge into the model tank. It can be seen that the heated water in submerged discharge deflects to the surface as the hot water has less density than the ambient cold water. The effects of the density and the depth of the discharge pipe are the main parameters moving the plume to surface, and therefore the vertical diffusion towards the bed is very small.

Figure 4.12 illustrates the discharge of dyed heated water to the surface of the model tank. It is shown how the thermal plume remains on the surface and there is little diffusion towards the bed.

In addition to prediction of the mixing zone, the path line of the thermal plume below the surface is determined from the dyed plume.

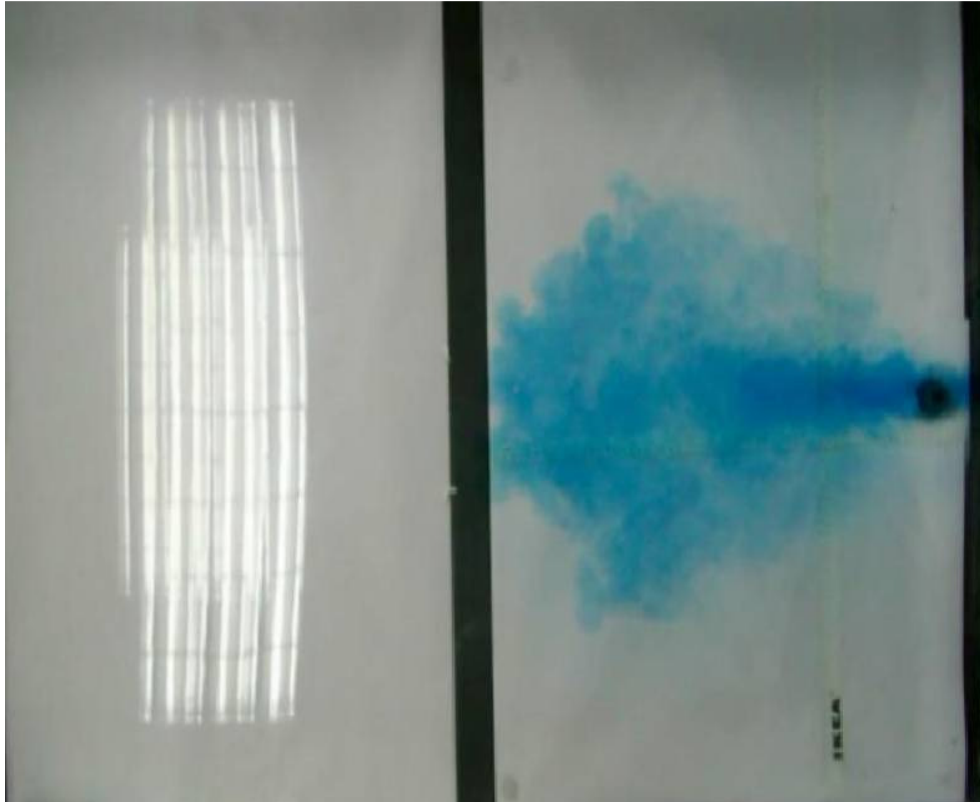


Figure 4.10: Submerged dyed plume discharge into model tank – plan view

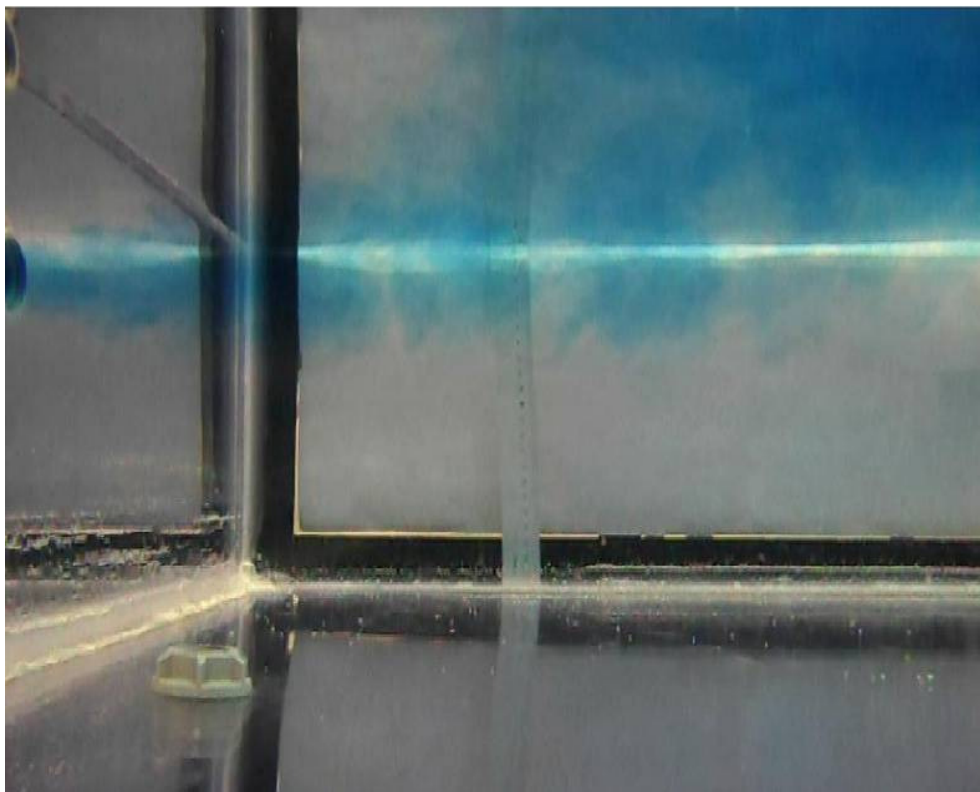


Figure 4.11: Submerged dyed plume discharge into model tank – side view

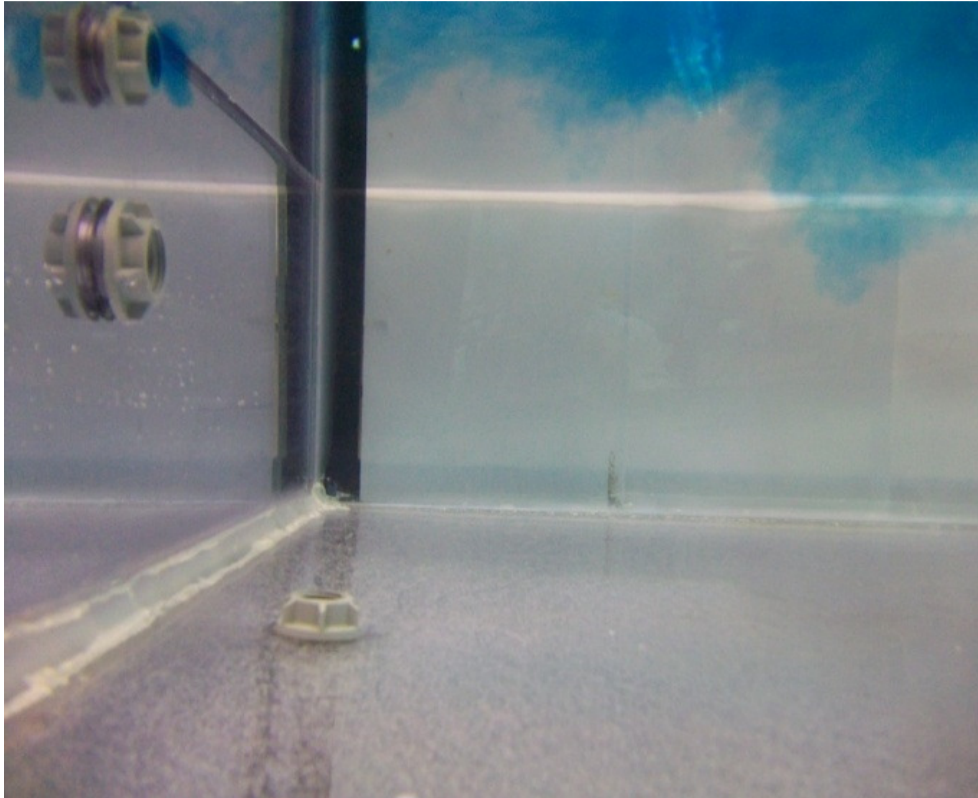


Figure 4.12: Dyed water discharged into surface of model tank – side view

4.5.5 Size Measurements

The size of the thermal plume in the receiving water is one of the problems that canal cooling water users may face. The Environment Agency regulations state that the plume size must not be too big so as to block the path of aquatics. The side views of the thermal plumes prove that the layers of the receiving water below the discharge centreline are not affected much by heated water, and as a result there will be a path for fish to pass.

The size of the thermal plume can be measured from dyed plumes. The size of plume is determined from the plan and side view of thermal discharge. The recorded images of the dyed plume are read by a computer programme- MATLAB -then scaled. Figure 4.13 shows the plan view of the thermal plume with dimensions, and then the width and the length of the plume can be measured. Figure 4.14 illustrates the side view of the thermal plume read and scaled by MATLAB. The vertical dimensions of the plume can be measured from this figure. The results of these measurements give the length, width and depth of the thermal plume from which the size of plume is calculated.

5. Thermograph

5.1 Introduction

One of the measurement methods used in this research was a thermograph technique using the Thermal Camera. Thermal cameras (Figure 5.1) show the diffusion of heat on the surface of a hot body. Human eyes are able to detect visible light but can see only a very small part of the electromagnetic spectrum. Infrared radiation from heat or thermal radiation (such as sunlight, fire, radiators etc.) lies between the visible and microwave range of the electromagnetic spectrum and it cannot be seen by our eyes. Thermal camera infrared thermography transforms an infrared image coming from a hot body into a radiometric coloured image which is representative of the thermal gradients across the body (Thermal Camera User Manual). The image may be observed on an LCD monitor and stored for future analysis and interrogation. The camera must be set to the right emissivity of the test material; emissivity is the capacity of a surface to emit heat at a given temperature. It is a relative quantity, and its value varies from (0 to 1) for water it is 0.96. To avoid unnecessary and unwanted reflections it is necessary to ensure the thermal camera is placed in a position relative to the test body without the effects of reflection - which is the most problematic issue facing the thermographer - especially with thermal water studies.

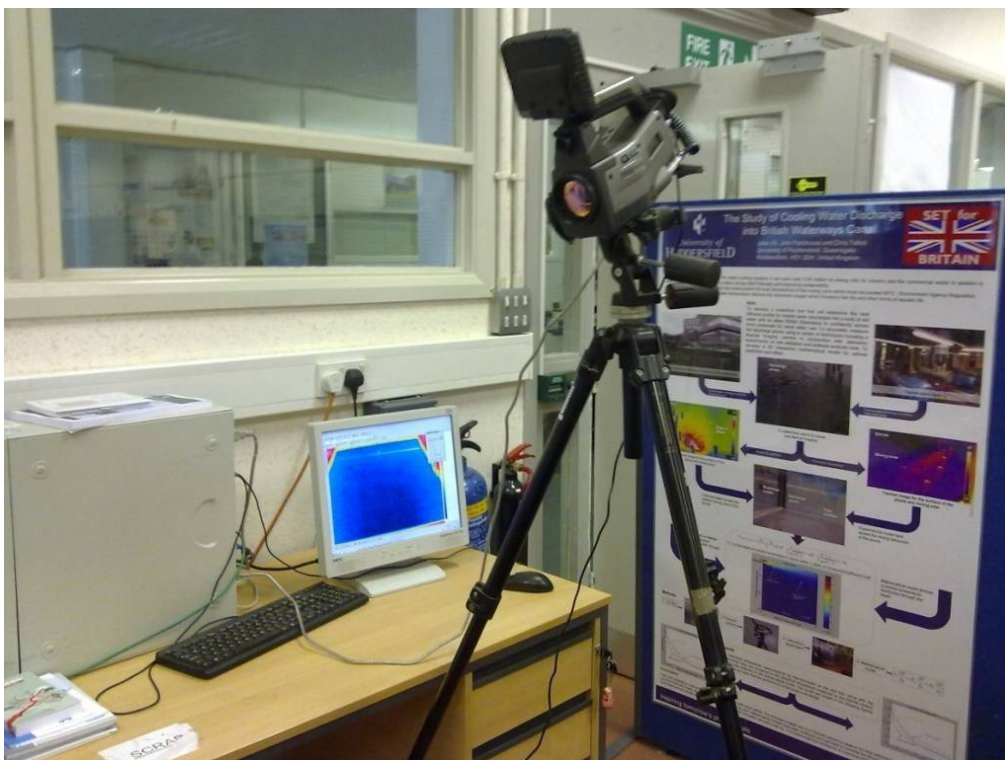


Figure 5.1: Thermal Camera connected to a PC

In this chapter a thermograph technique is described to measure the temperature distribution of the thermal plume discharge into receiving water. The thermal images provided for the surface of receiving water show clearly the mixing zone, shape of plume and edges of the plume. The process applied on both types of discharge studied submerged and surface discharge and observed the thermal discharge. In addition this was applied to the laboratory experimental model tank. In order to verify the accuracy of the thermocouples data, the centreline temperature decay was obtained from the thermal images and compared to temperature measured by the thermocouples. What is not evident from the thermal images is the three dimensional effect of the plume and how the temperature dissipates through the depth of the canal.

5.2 Surface Discharge Thermal Images

To indicate the mixing zone and temperature gradient within the discharge plume, images were taken of the discharge at the Central Services Building (CSB) site using a thermal camera. Figures: 5.2, 5.3 and 5.4 show the comparison of the discharge plume at the CSB site taken with the thermal image camera and a digital camera

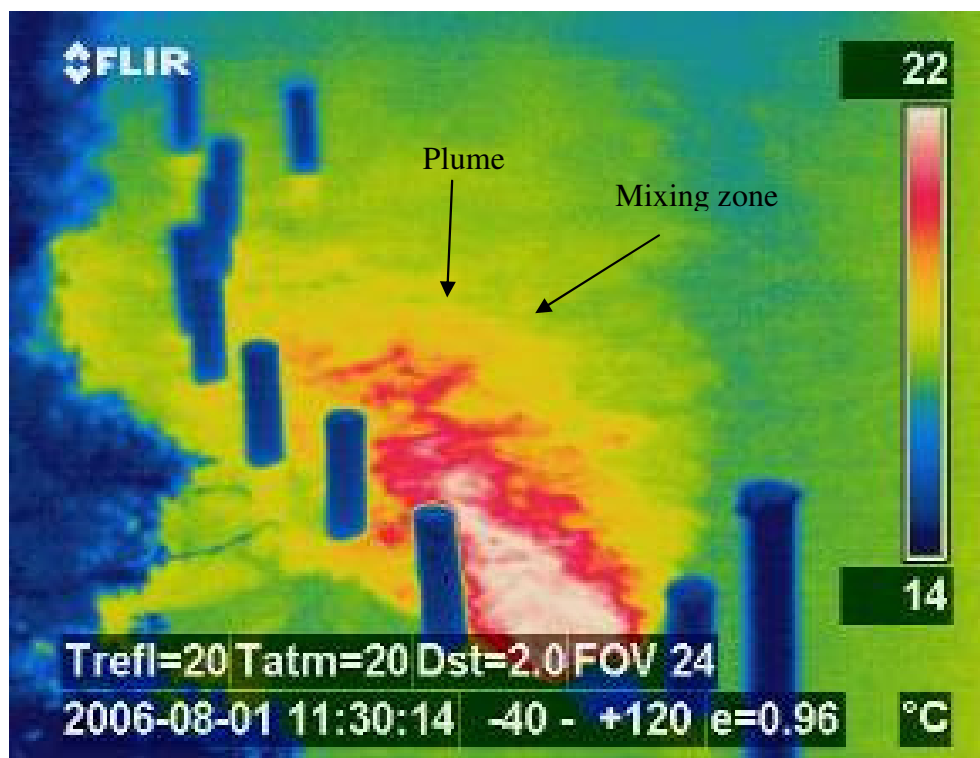


Figure 5.2a: Thermal image of Discharge plume

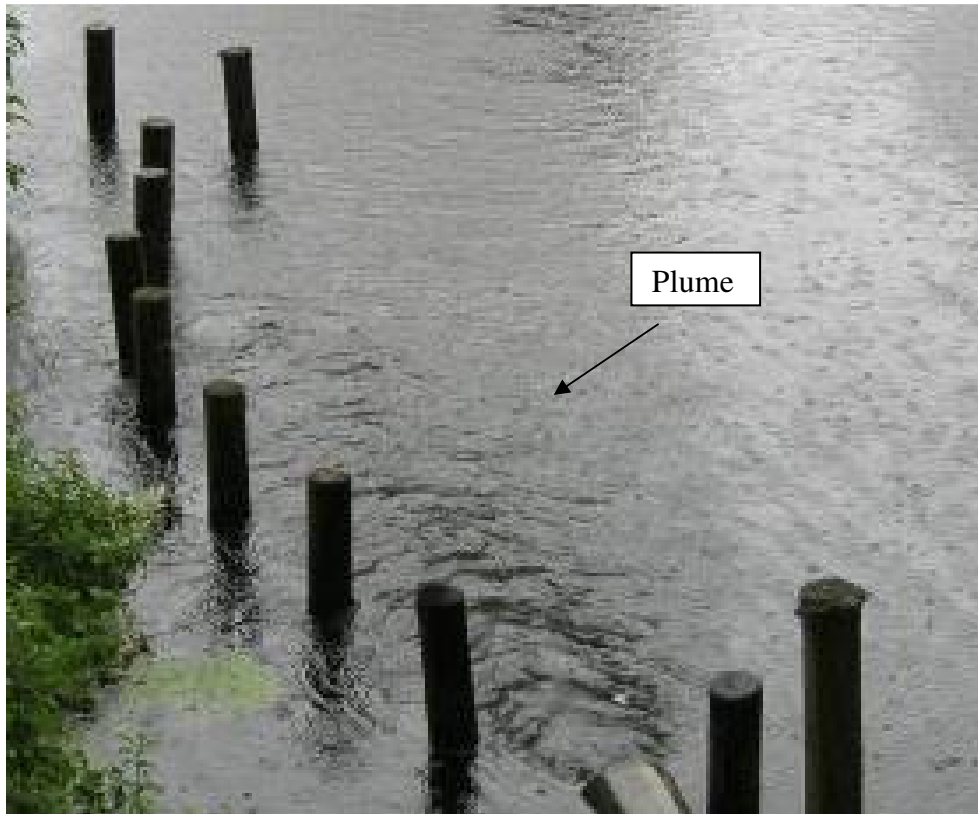


Figure 5.2b: Discharge plume

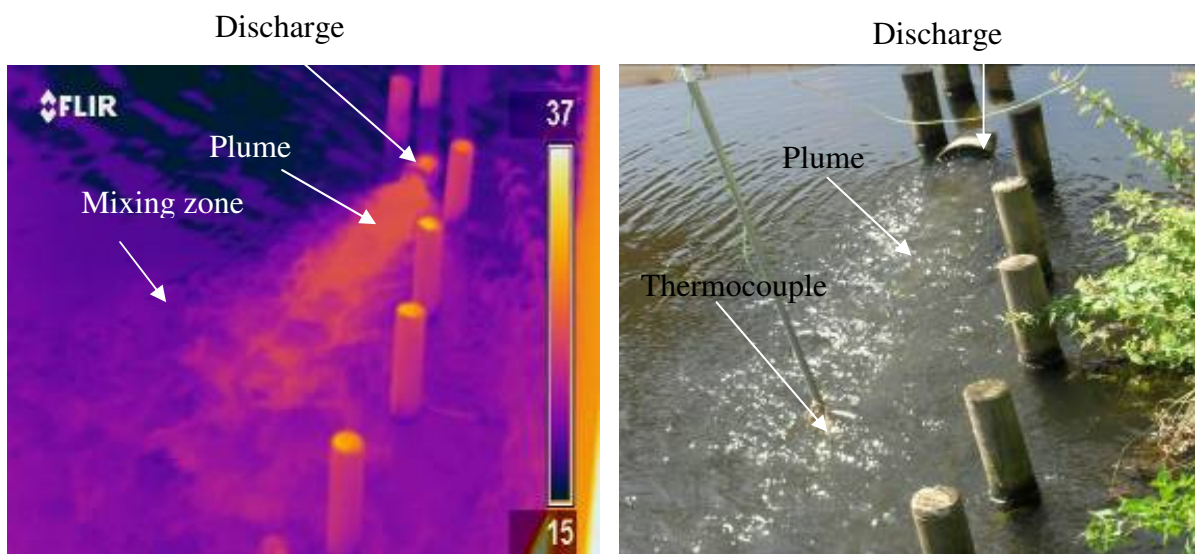
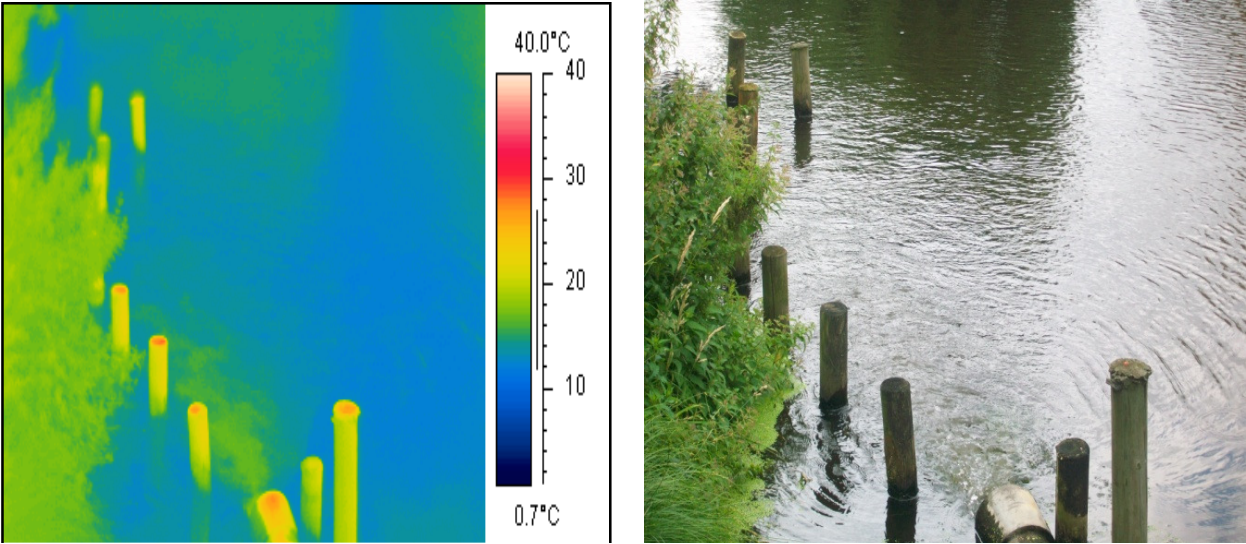


Figure 5.3: Thermal and digital image of plume from downstream

The outlet pipe is semi-submerged and the mixing plume can be seen clearly on the canal surface. Figure 5.2a shows the extent of the plume and the differing temperatures of the timber protective posts around the discharge pipe. The temperature at the outfall was around 22°C, and this dissipated quickly to around 20°C. It also showed the area required for the

plume to dissipate the remaining heat and attain the canal ambient temperature of 17°C. Figure 5.3a illustrates the images from downstream and the higher temperature of the upper section of the discharge pipe which projects above the canal surface. The variation of colour on the timber posts especially on the top of the posts is due to reflection.

Figure 5.4 shows the thermal image for CSB in different colours and the temperature at the discharge point is 20°C. The digital photographs illustrate the aquatic plant and weed growth adjacent to the embankment at the discharge pipe and intake screen. The thermal images illustrate the abrupt disruption of temperature dispersal of the plume in the same area. The figures also illustrate turbulent dispersal along the plume and the area of the plume temperature distribution. The temperature at any point within the plume and mixing zone can be measured from the thermal images.



Thermal image of plume
 Digital image showing plume
 Figure 5.4: Typical photographic image of a discharge pipe and its corresponding thermal image.

5.3 Submerged Discharge Thermal Images

Thermal images were taken for other British Waterways canal sites in which the discharge pipe is deeply submerged. The thermal camera is not able to measure the temperature of the plume below the surface. It takes recordings once the plume reaches the surface. The Mailbox site is a submerged discharge site and the Figures 5.5 and 5.6 illustrate the thermal images of the plume and mixing zone of the site. Figure 5.5a shows the end edge of the heated plume in the middle of Birmingham Canal. This is a good proof for the BBC Mailbox building management that their site does not block the aquatic path as it does not cross the canal and ends in the middle. The red colour and the two green solid colours to the left and the right of

the figure are the reflections of the opposite buildings as they appear in the digital photo for the site see Figure 5.5b. The blue colour is the canal ambient temperature.

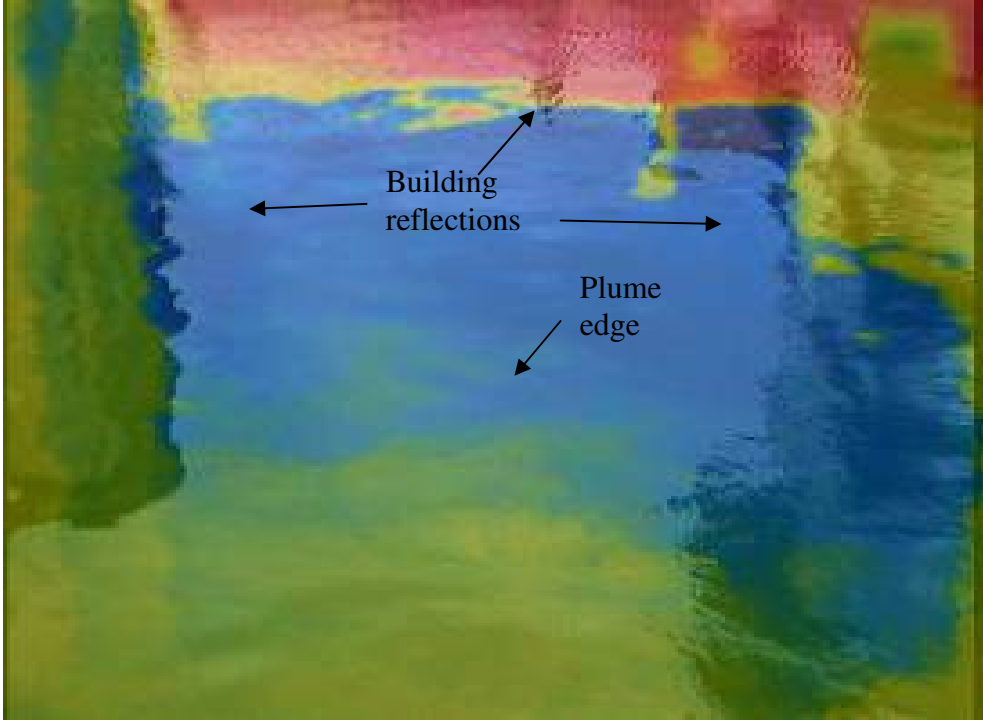


Figure 5.5a: Thermal image

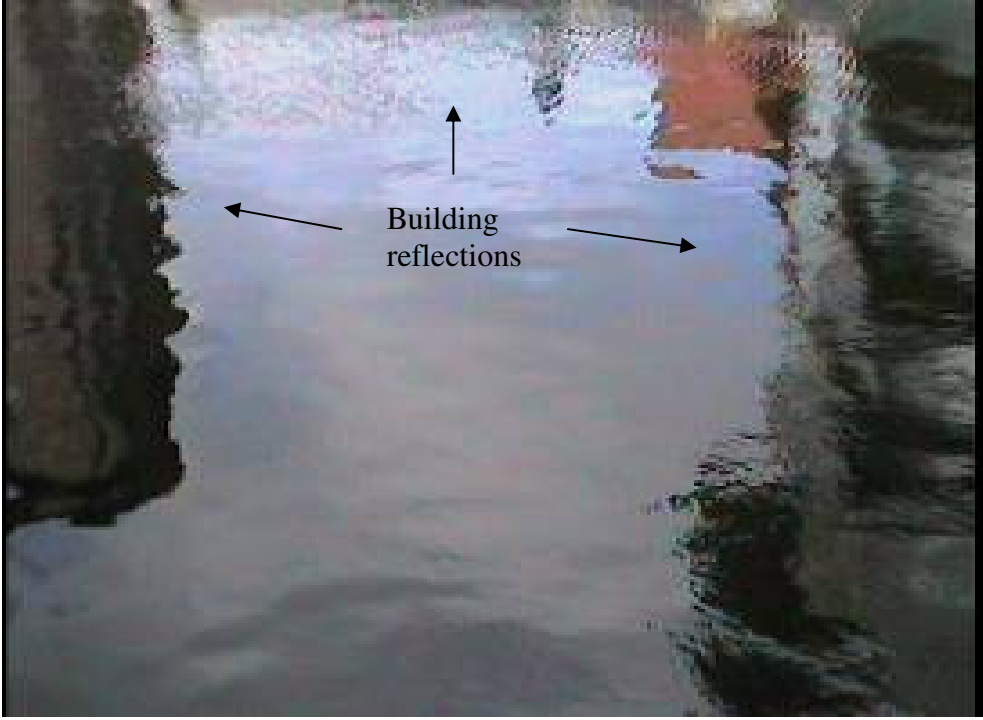


Figure 5.5b: Digital image

Figure 5.5: Thermal and digital image for a deeply submerged discharge

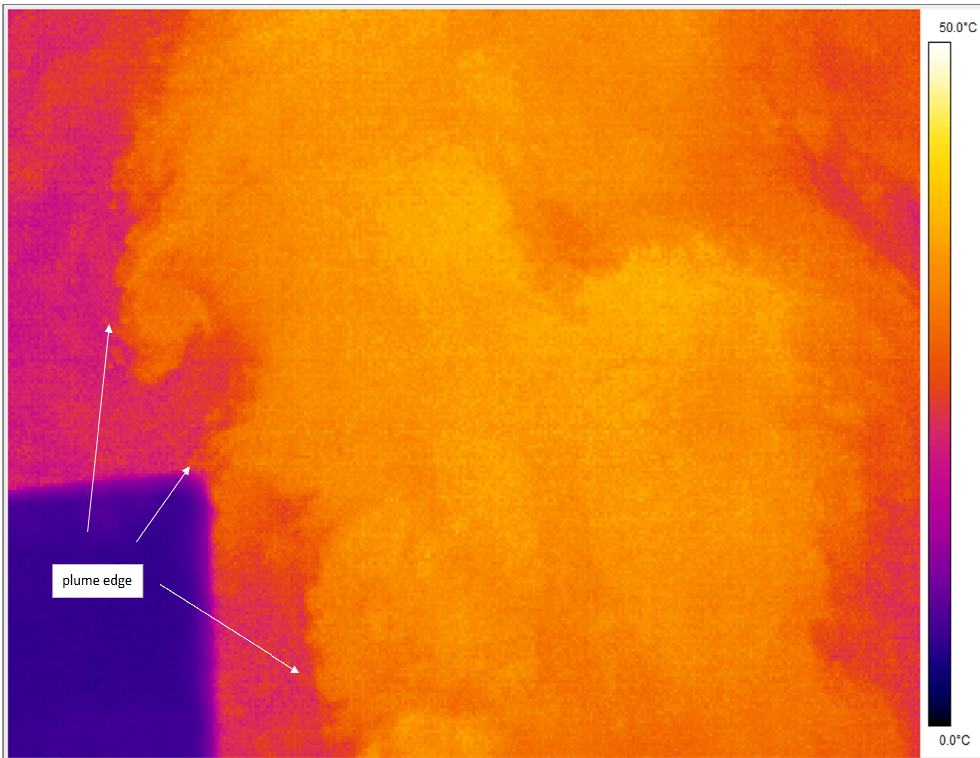


Figure 5.6a: Thermal image



Figure 5.6b: Digital image

Figure 5.6: Mixing zone surface in submerged discharge

Thermal image Figure 5.6a, shows the edge of the mixing zone which is difficult to observe by a normal digital camera except the area when the heated water reached the surface, Figure 5.6b. The temperature of the surface of the plume measured from the thermal image is about 18°C which equals to the thermocouple results.

Similar images were taken with the thermal image camera at Canalside West, see Figure 5.7. The outlet is fully submerged and the thermal image is indistinct and inconclusive, not giving the distinct image of the plume experienced at CSB. The relative differential temperature of discharge and canal ambient temperature is 1.5°C and the temperature was balanced when the flow reached the surface. Therefore the Canalside West site discarded a minimum heat load into canal and it was considered the best among the all sites studied in this project.

Similarly at Lockside the outlet is fully submerged as shown in the digital image, Figure 5.8b. The green region in the thermal image in Figure 5.8a is where the thermal plume reaches the surface. The temperature at the region is about 18°C then reduces to equal the ambient temperature of the canal. The higher temperatures indicated are the kerb stones on the canal embankment.

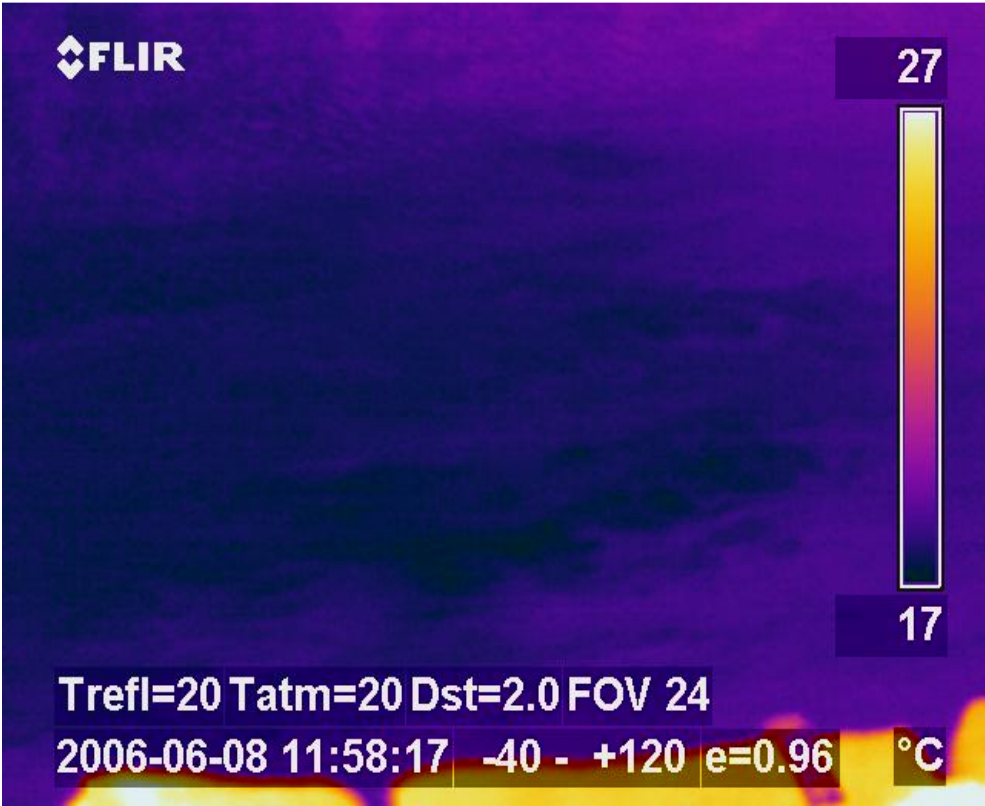


Figure 5.7a: Thermal image of Canalside West



Figure 5.7b: Canalside West

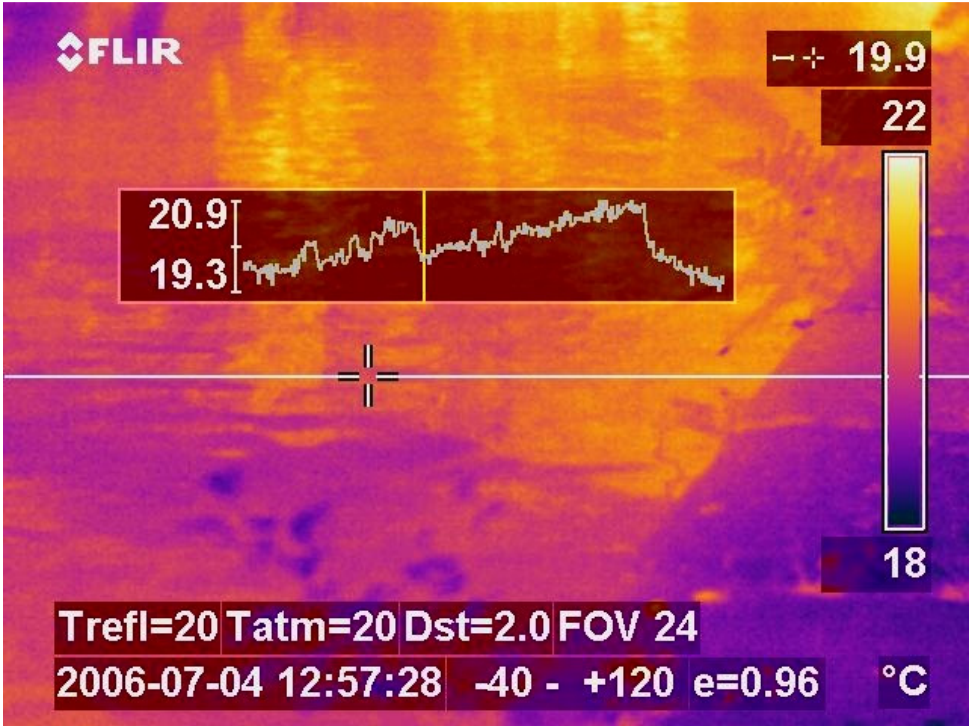


Figure 5.8a: Thermal image – Lockside



Figure 5.8b: Digital image – Lockside

5.4 Model Tank Thermal Images

As discussed in Chapter 4 the discharge velocities used in the laboratory experiment are small. The low flow discharge to the model tank is subjected to greater disturbance than the high flow discharge of the canal site. Therefore the use of the Thermal Camera in temperature measurements in the model tank is very important. The thermal images cannot predict the temperature of the plume in the layers below the surface but are still an important tool to use in the laboratory analysis. In the laboratory experimental trials performed (Table 4.1) the thermal camera plays a good role in temperature measurements as well as in the prediction of the surface area of the plume. Thermal image Figure 5.9a offers a very clear image of temperature distribution and the plume area on the surface of model tank. Figure 5.9b shows the experimental model tank.

Figure 5.10 shows the thermal image of the submerged discharge into the model tank and how the heat dissipates quicker than the surface discharge.

Figure 5.11 illustrates the screen of the Thermal Camera which shows an image of the model tank. The thermal Camera is able to measure the temperature of any point or along any line by producing a profile of temperature along that line. In the figure there is a line on the centre of

thermal plume on the surface of model tank. The temperature profile along that line is produced on the lower right hand side corner of the Figure 5.11.

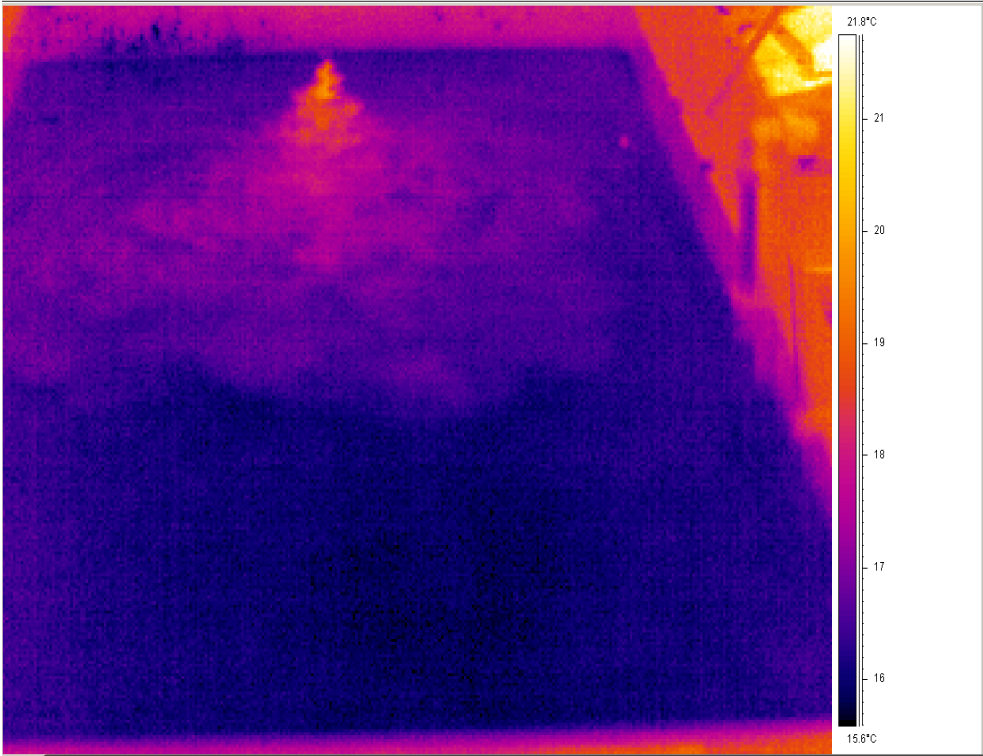


Figure 5.9a: Heat diffusion on surface of model tank (surface discharge)

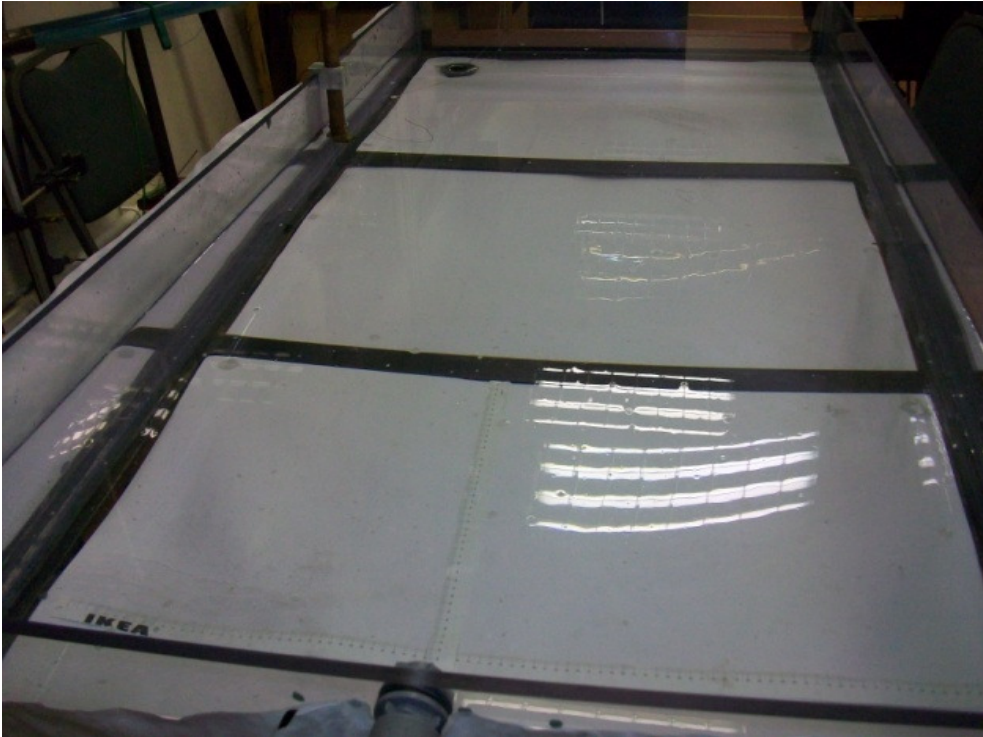


Figure 5.9b: Model tank

Figure 5.9: Thermal and digital image of model tank

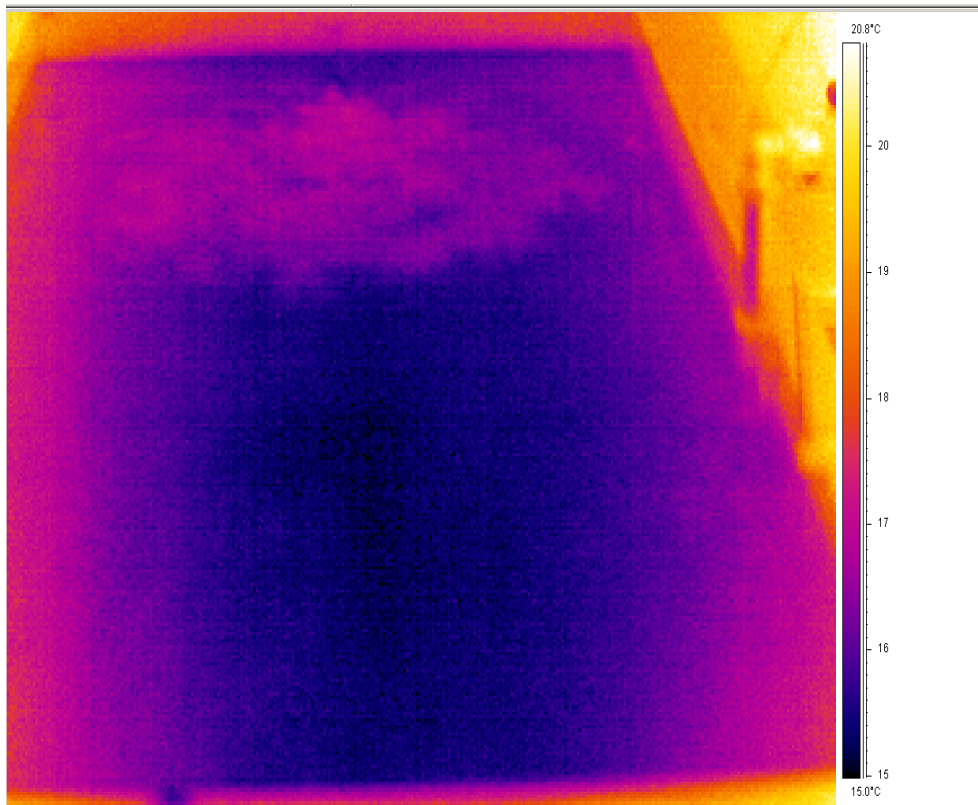


Figure 5.10: Heat diffusion on surface of tank (submerged discharge)

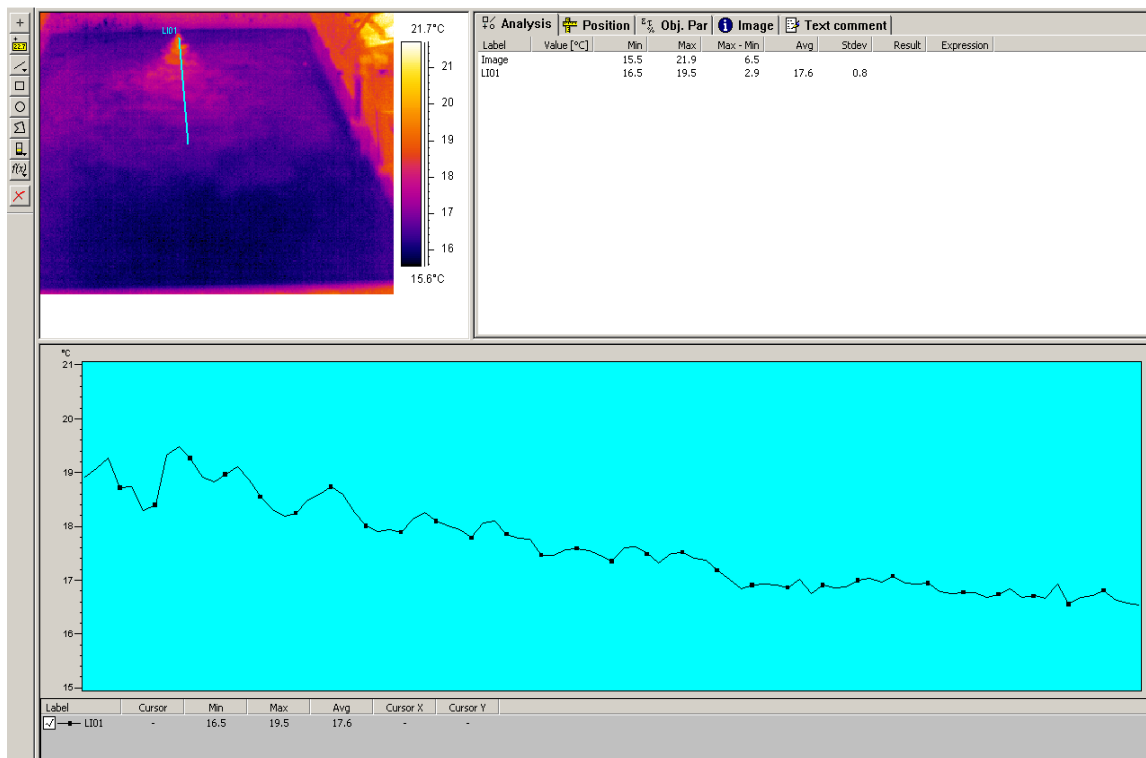


Figure 5.11: Thermal Camera show temperature profile along the line on the centerline of plume

Finally all the measured temperatures of the thermal images are compared with the thermocouples measurements and they will be presented in the Results and Discussion Chapter 9.

6. CFD Simulation

6.1 Introduction

The study of thermal plume discharge into shallow and still water experimentally were discussed in Chapters 3 and 4. In this Chapter the study will carry out modelling using one of the Computational of Fluid Dynamics CFD software packages, FLUENT. This is one of the most reliable CFD packages that are used worldwide for the analysis of fluid flow and heat transfer and used in this project to analyse the behaviour of the thermal plume. As an example of thermal discharge into the surface of the canal the analysis is initially performed on a CSB site. For the submerged thermal discharge the BBC Mailbox site is selected as an example.

6.2 Computational Analysis

FLUENT is a state of art computer program developed by the Fluent Incorporated Company to model heat transfer and fluid flow. It is also supplied as an educational software package and used by university students across the world. The basis of FLUENT is the solving of seven governing equations that are used in evaluating the thermal discharge and plume behaviour. The equations are; the continuity Equation (6.1), the momentum Equation in x direction (6.2), the momentum Equation in y direction (6.3), the momentum Equation in z direction (6.4), the thermal energy Equation (6.5), the state of water Equation (6.6) and the viscous shear stress Equation (6.7).

$$\frac{\partial U}{\partial x} + \frac{\partial V}{\partial y} + \frac{\partial W}{\partial z} = 0 \dots\dots (6.1)$$

$$\frac{\partial U^2}{\partial x} + \frac{\partial UV}{\partial y} + \frac{\partial UW}{\partial z} = -\frac{1}{\rho} \frac{\partial P}{\partial x} + \nu \left(\frac{\partial^2 U}{\partial x^2} + \frac{\partial^2 U}{\partial y^2} + \frac{\partial^2 U}{\partial z^2} \right) - \frac{\partial u^2}{\partial x} - \frac{\partial uv}{\partial y} - \frac{\partial uw}{\partial z} \dots\dots (6.2)$$

$$\frac{\partial VU}{\partial x} + \frac{\partial V^2}{\partial y} + \frac{\partial VW}{\partial z} = -\frac{1}{\rho} \frac{\partial P}{\partial y} + \nu \left(\frac{\partial^2 V}{\partial x^2} + \frac{\partial^2 V}{\partial y^2} + \frac{\partial^2 V}{\partial z^2} \right) - \frac{\partial vu}{\partial x} - \frac{\partial v^2}{\partial y} - \frac{\partial vw}{\partial z} \dots (6.3)$$

$$\frac{\partial WU}{\partial x} + \frac{\partial WV}{\partial y} + \frac{\partial W^2}{\partial z} = -\frac{1}{\rho} \frac{\partial P}{\partial z} - g + \nu \left(\frac{\partial^2 W}{\partial x^2} + \frac{\partial^2 W}{\partial y^2} + \frac{\partial^2 W}{\partial z^2} \right) - \frac{\partial wu}{\partial x} - \frac{\partial wv}{\partial y} - \frac{\partial w^2}{\partial z} \dots (6.4)$$

$$\frac{\partial UT}{\partial x} + \frac{\partial VT}{\partial y} + \frac{\partial WT}{\partial z} = k \left(\frac{\partial^2 T}{\partial x^2} + \frac{\partial^2 T}{\partial y^2} + \frac{\partial^2 T}{\partial z^2} \right) - \frac{\partial ut}{\partial x} - \frac{\partial vt}{\partial y} - \frac{\partial wt}{\partial z} + \Phi \dots (6.5)$$

$$\rho = f(T) \dots (6.6)$$

$$\zeta = \mu \frac{\partial u_x}{\partial y} \dots (6.7)$$

The software is used to solve all the governing equations in fluid flow and heat transfer. The solutions of the seven governing equations yields characteristics of the water flow such as: velocities in x, y, z directions (u, v, w), temperature T, density ρ, pressure P and viscosity μ. Every individual discharge type was modelled separately and the results for the centreline profiles, discharge layers profiles and flow path are presented within the following discussions.

6.2.1 Surface Discharge – CSB Site

The basic parameters used for modelling each site were; the discharge pipe diameter (0.15m) as located longitudinal on the surface of the canal, the discharge velocity (1.23m/s) and the discharge temperature (24°C). The canal ambient temperature used was (17°C). A section of the canal considered for the modelling was 20m in length (downstream), 10m width across the canal and 1.5m average depth. Three layers (planes) along the mixing zone were predetermined, in this case, a layer on the centreline of the discharge pipe, a layer on the surface of canal and a layer 0.6m below the surface. The three layers are all considered to be parallel to the centreline. Temperature diffusion at each layer was predicted using FLUENT with the results as presented in Figures 6.1, 6.2 and 6.3 each showing the plan view of the canal at the three different layers.

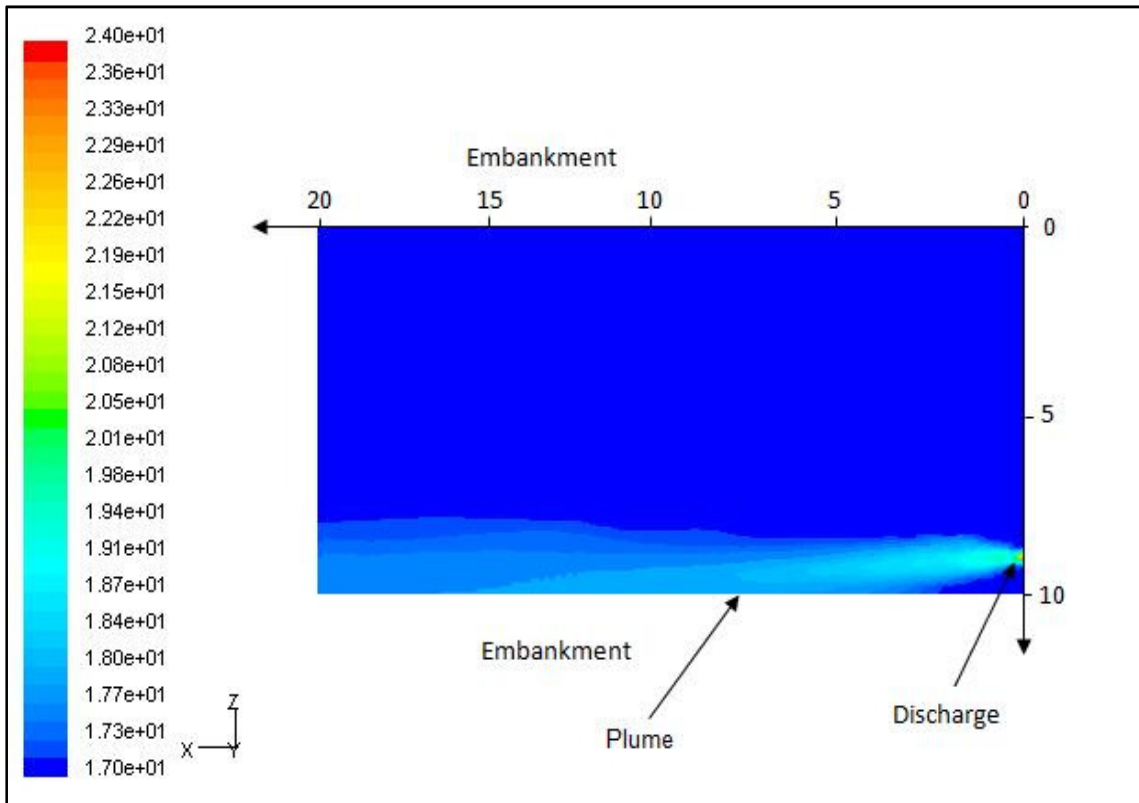


Figure 6.1: Heat diffusion on a plane at the centreline of the discharge pipe– CSB site

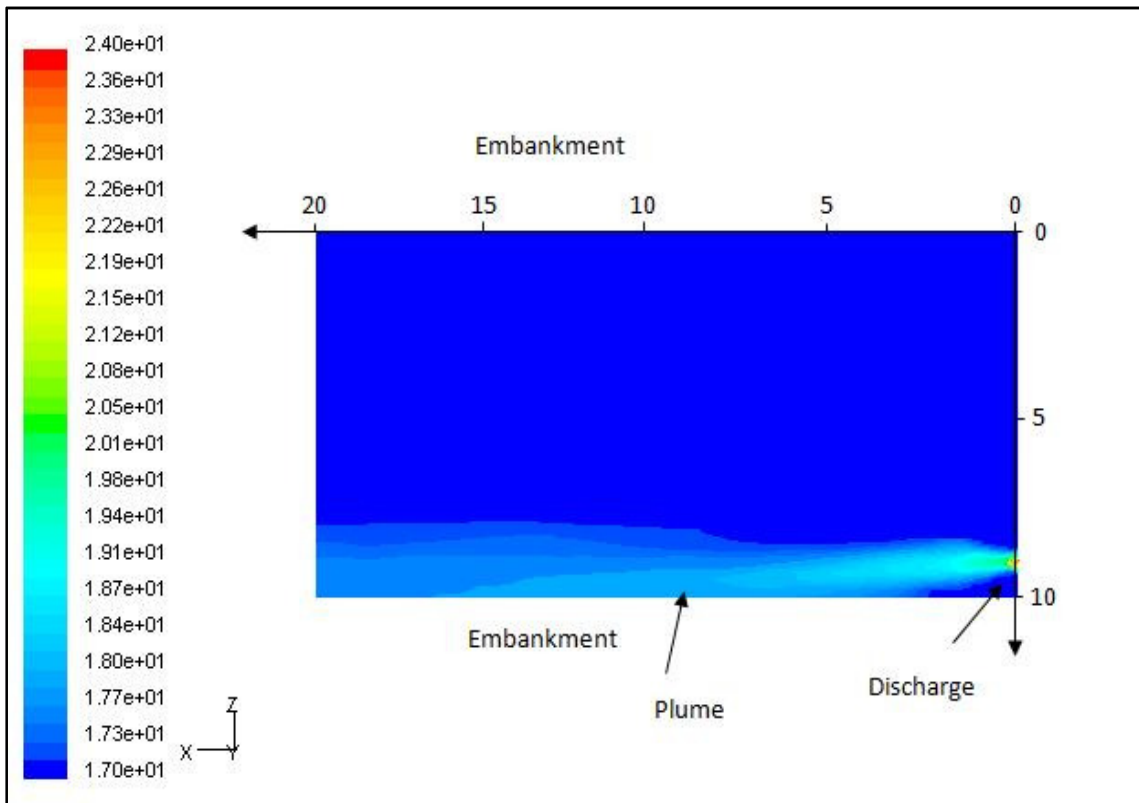


Figure 6.2: Heat diffusion on a plane on the surface of canal– CSB site

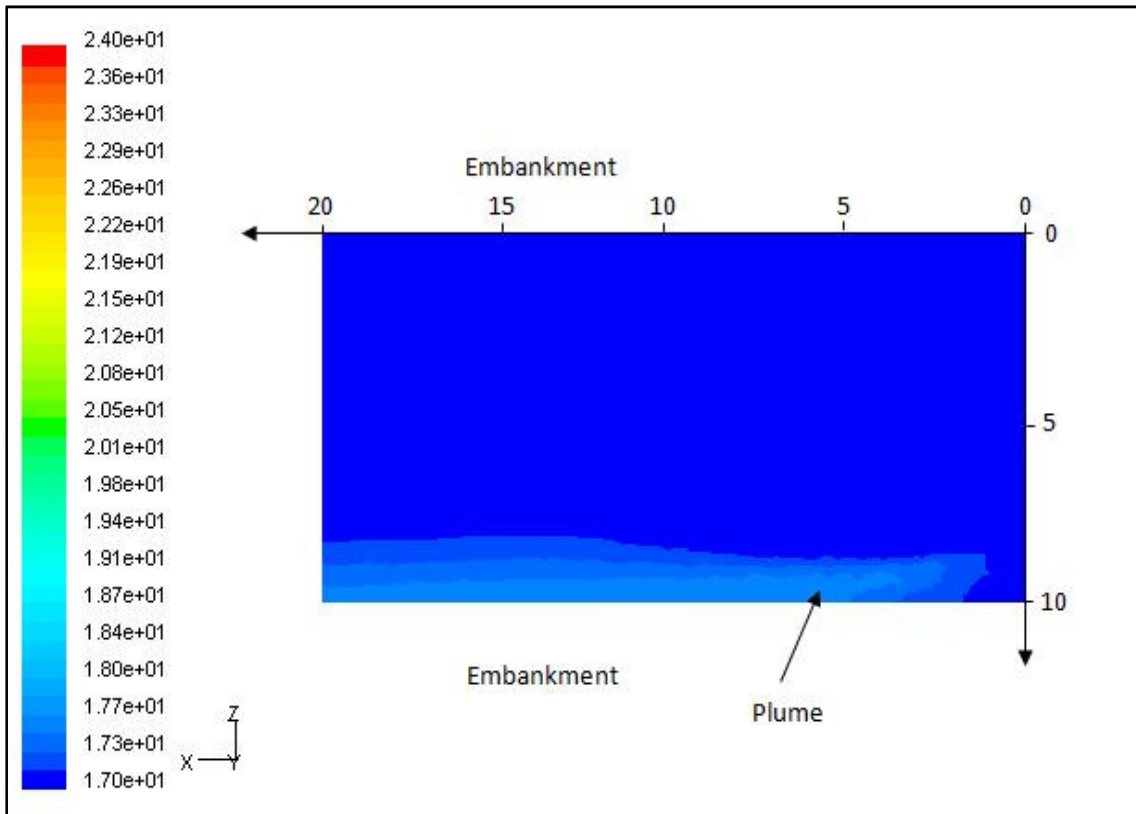


Figure 6.3: Heat diffusion on a plane 0.6m below the surface of canal- CSB site

The shape of the plume and the size of mixing zone obtained from the model are very clear in each figure with the edges of the plume being easily identified. The discharge pipe is shown on the right hand side where the temperature is at a maximum.

The temperature dilution and velocity profiles along the centreline of plume are as presented in Figures 6.4 and 6.5. These profiles show high temperatures and velocities in the area close to the discharge point. This area is the core region of the plume and as mentioned previously the temperatures and velocities are always the highest levels. The temperature and velocity distribution on a plane normal to the centreline of plume are determined and the results are as presented in the side views of the plume in Figures 6.6 and 6.7. The discharge in these figures is located on the top right hand side as indicated, where the temperature and velocity are maximum.

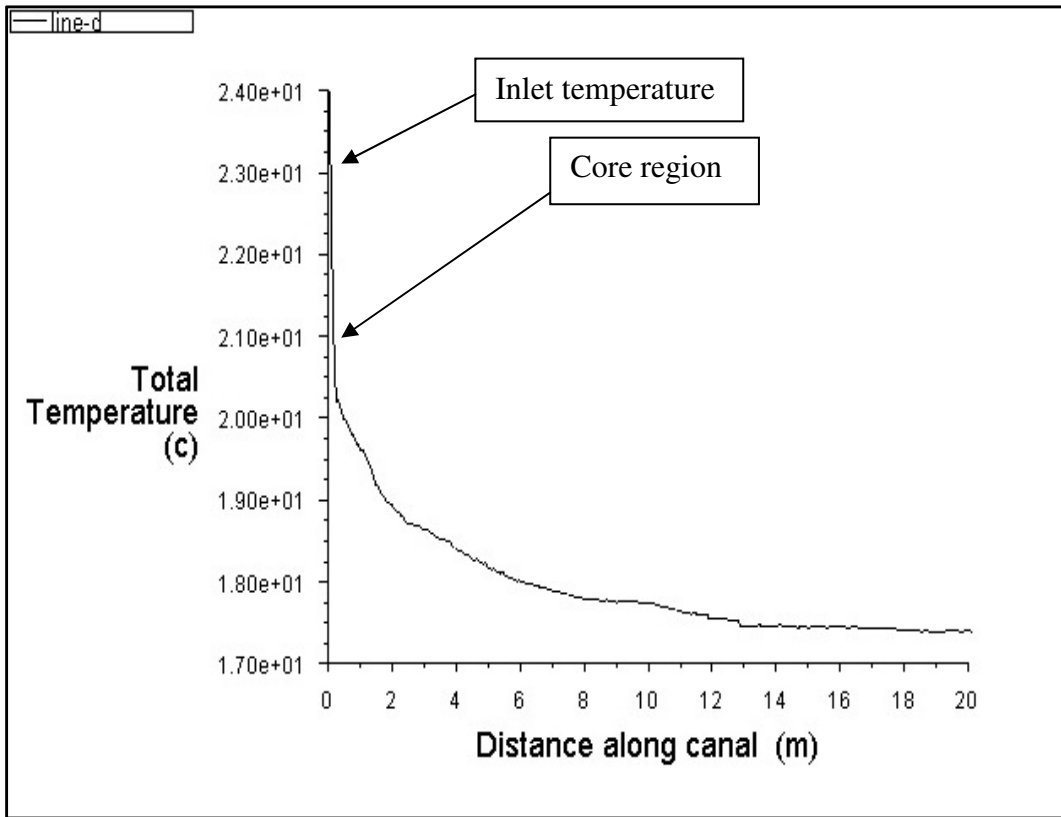


Figure 6.4: Temperature dilution along the centreline of plume (0.075m) below surface– CSB site

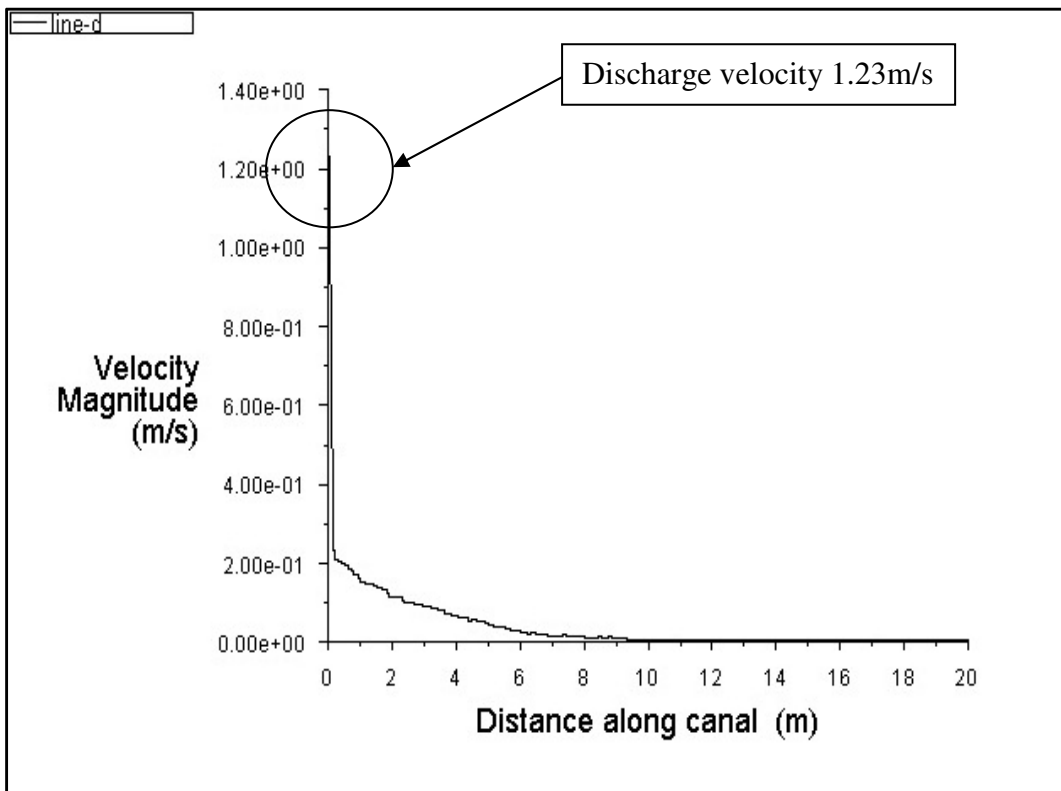


Figure 6.5: Velocity along the centreline of plume (0.075m) below surface – CSB site.

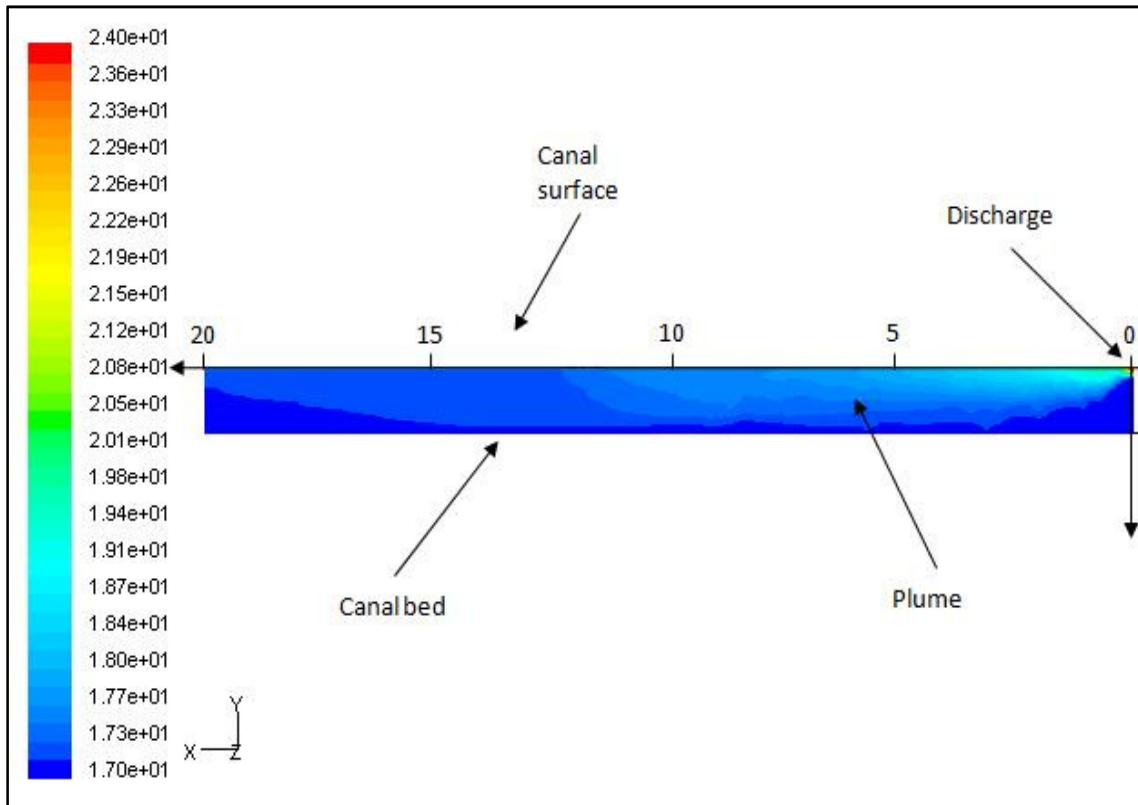


Figure 6.6: Heat diffusion on a plane normal to the centreline of plume (cross section)

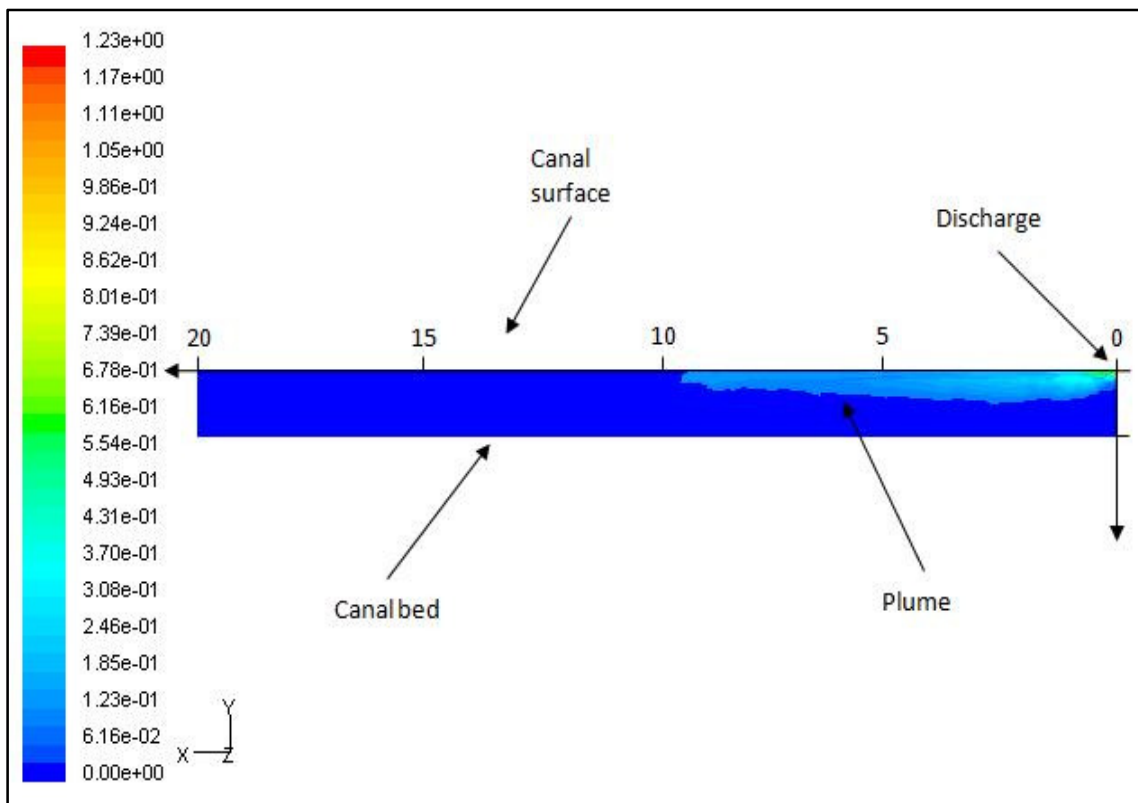


Figure 6.7: Velocity distribution on a plane normal to the centreline of plume (cross section)

6.2.2 Submerged discharge – Mailbox Site

The parameters used for modelling; the discharge pipe diameter (0.35m) positioned 0.475m below free surface of canal, the discharge velocity (0.6m/s) and the discharge temperature (20°C). The canal ambient temperature was considered to be 17°C. A section of canal considered for the modelling was 20m length (10m upstream and 10m downstream), 15m width across canal and 1.5m average depth. Three layers (plane) along the mixing zone were predetermined; in this case a layer on the centreline of the discharge pipe, a layer on the surface of canal and a layer on the bed. The three layers are all considered to be adjacent to the centreline. Temperature diffusion at each layer was predicted by using FLUENT with the results as demonstrated in Figures 6.8, 6.9 and 6.10 each showing the plan view of the canal at the three different layers. The shape of the plume and the size of mixing zone obtained from the model are very clear in each figure with the edges of the plume being easily identified. The edges of the plume can be recognized easily. The discharge pipe is shown on the left hand side where the temperature is at a maximum.

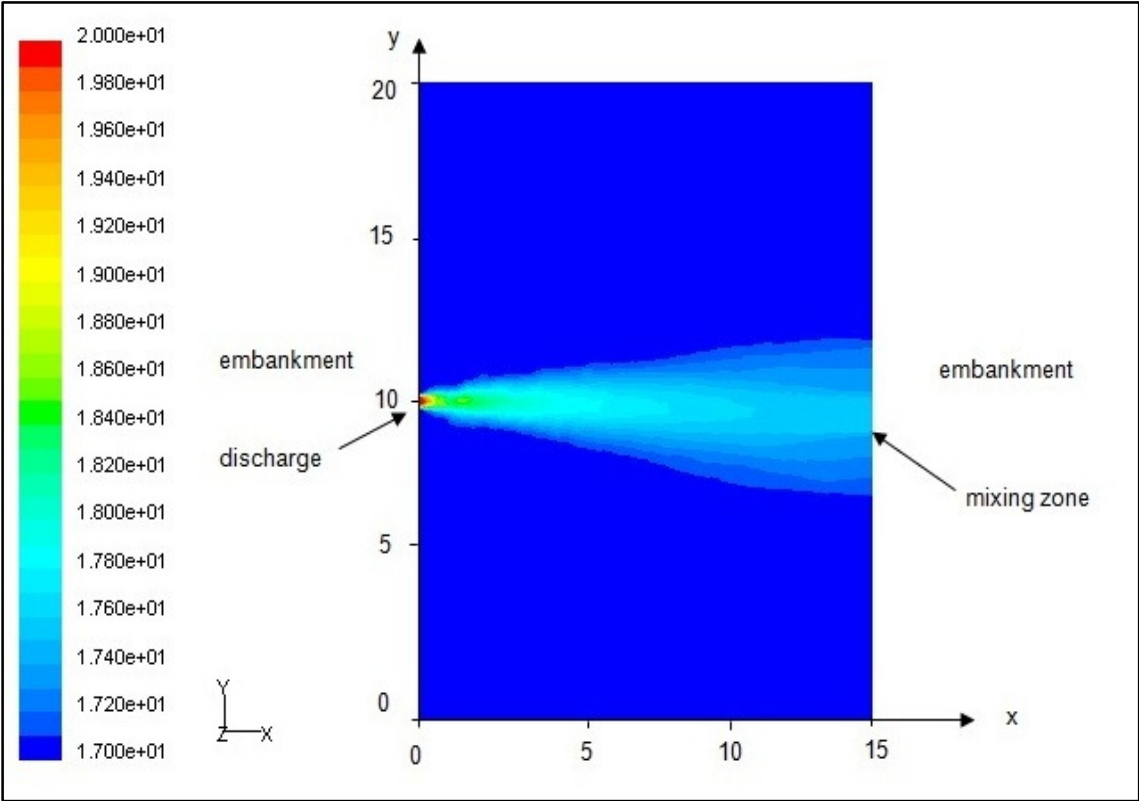


Figure 6.8: Heat diffusion on a plane at the centreline of the discharge pipe

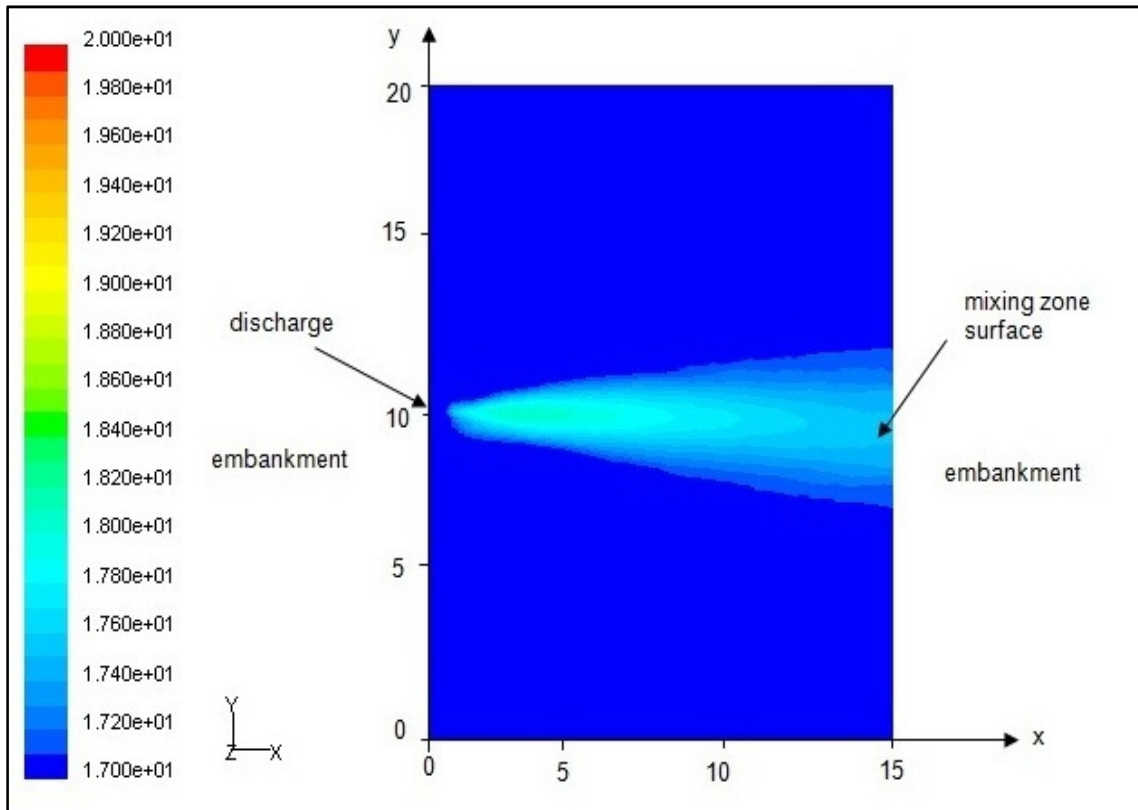


Figure 6.9: Heat diffusion on a plane on the surface of canal

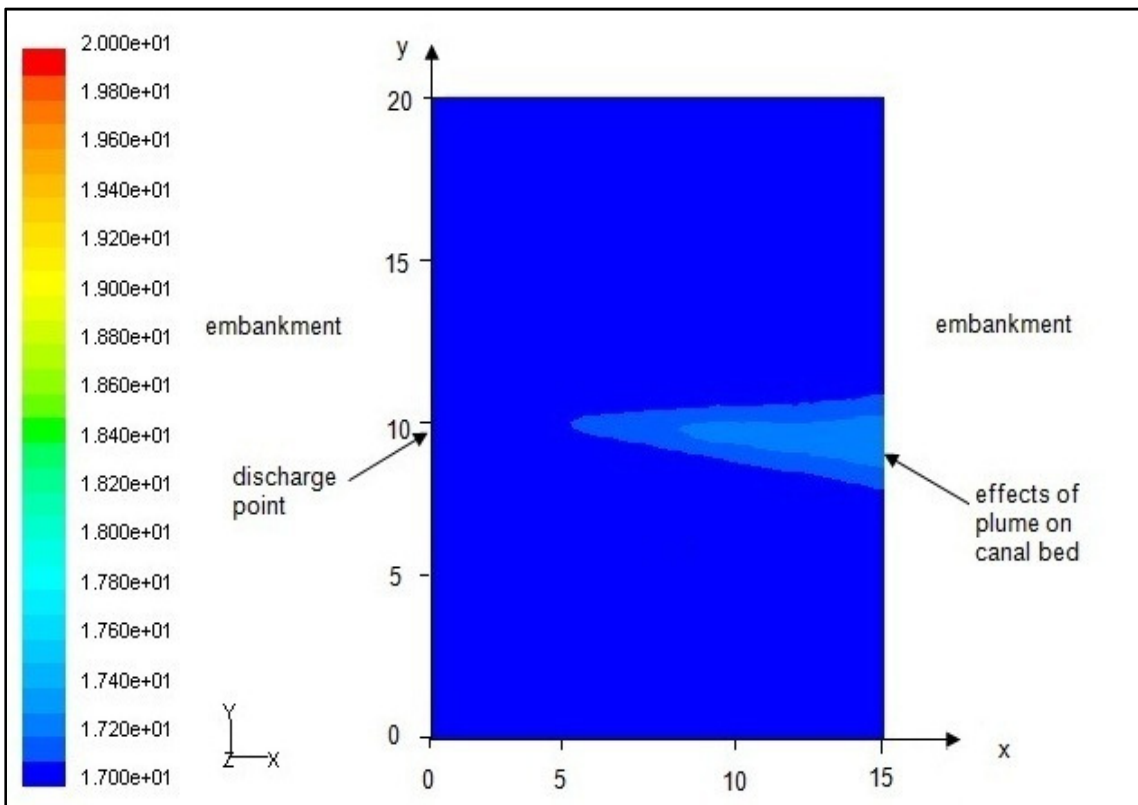


Figure 6.10: Heat diffusion on a plane on the canal bed.

The temperature dilutions for a range of layers along the centreline of the plume, as shown in Figures 6.11a, were determined and the results as presented in Figures 6.11b

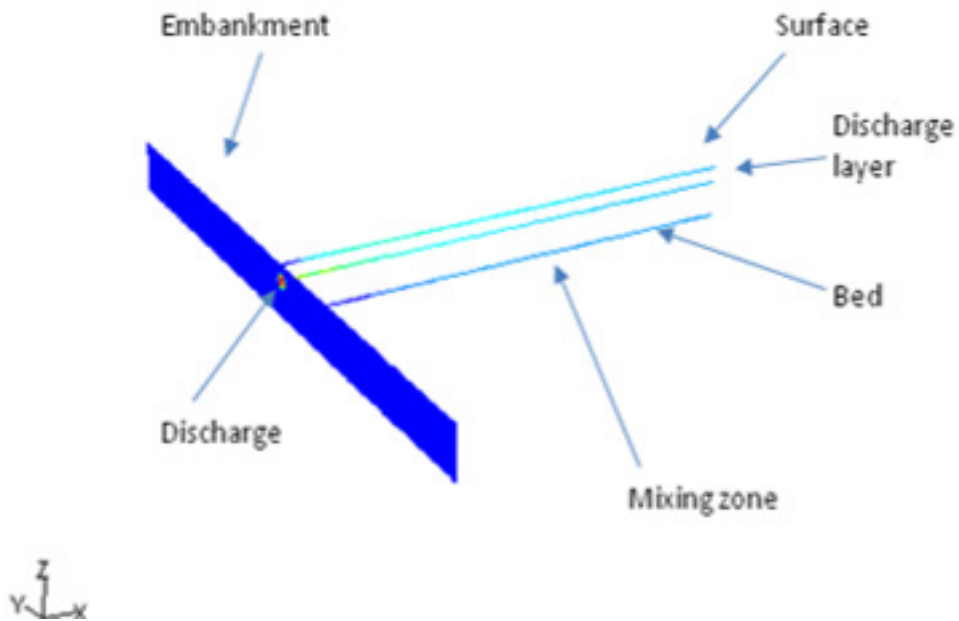


Figure 6.11a: Centreline of plume at three layers

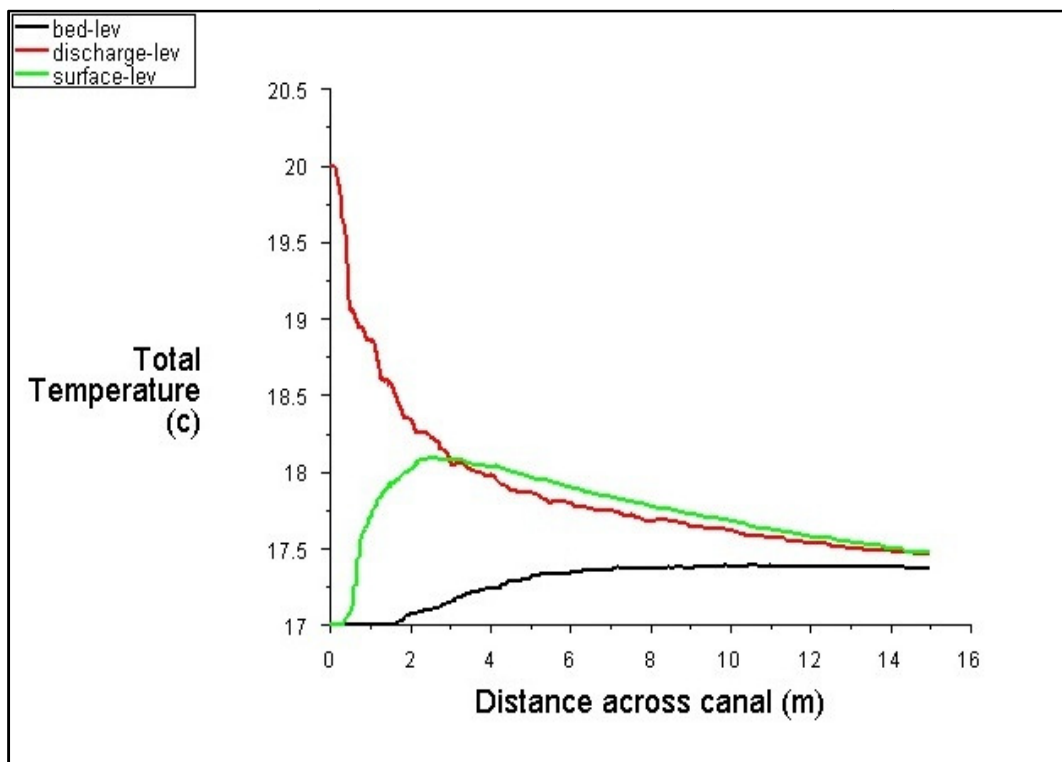


Figure 6.11b: Temperature along the centreline of plume at different layers

Figure 6.11: Centreline of plume at surface, bed and discharge layer and centreline temperature profile

Similarly the velocity profiles along a range of layers along the centreline of plume (Figure 6.12a) are shown in Figure 6.12b.

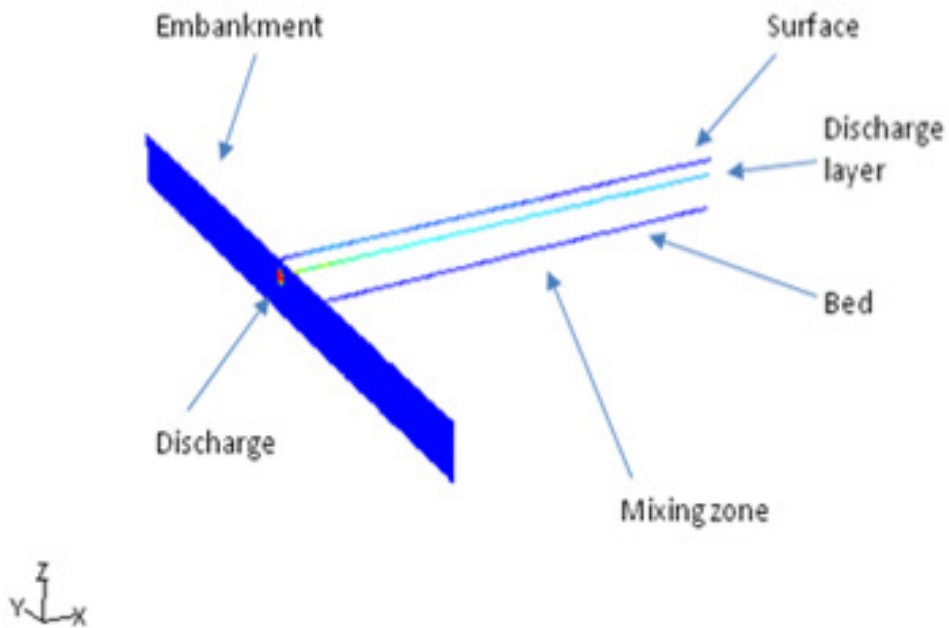


Figure 6.12a: Centreline of plume at three layers

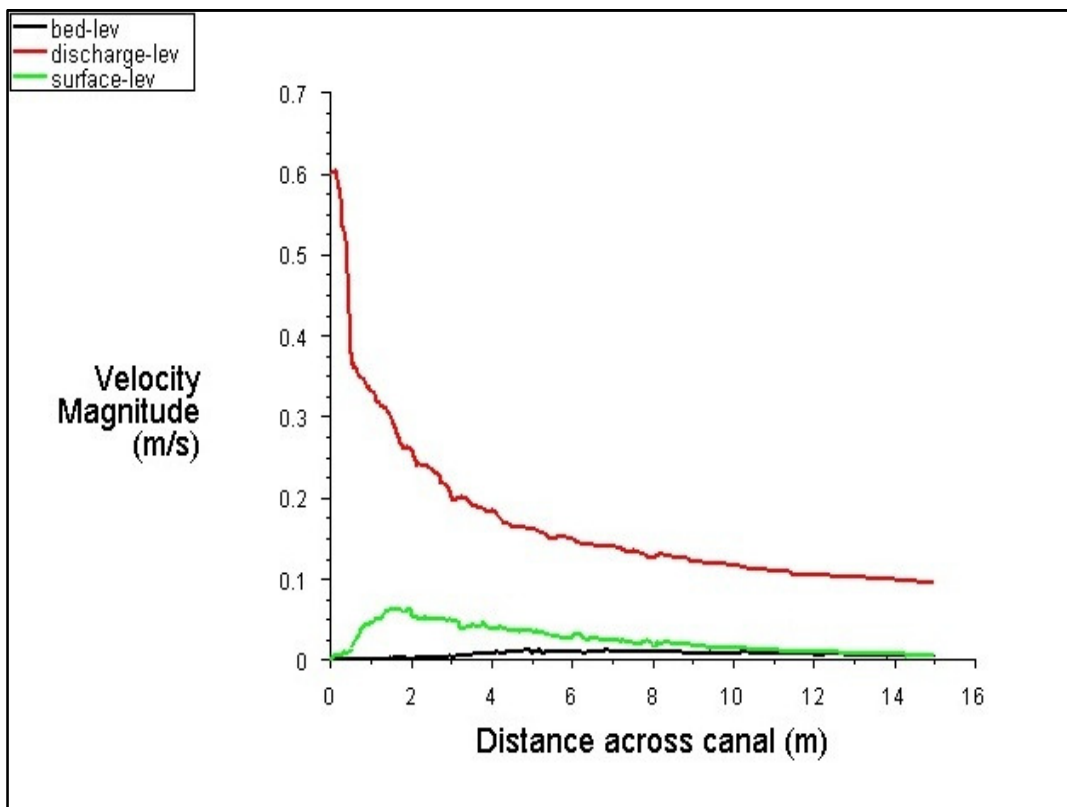


Figure 6.12b: Velocity along the centreline of plume at different layers.

Figure 6.12: Centreline of plume at surface, bed and discharge layer and centreline velocity profile

The temperature and velocity distribution on a plane normal to the centreline of plume are presented in Figures 6.13 and 6.14, the discharge is located on the right hand side.

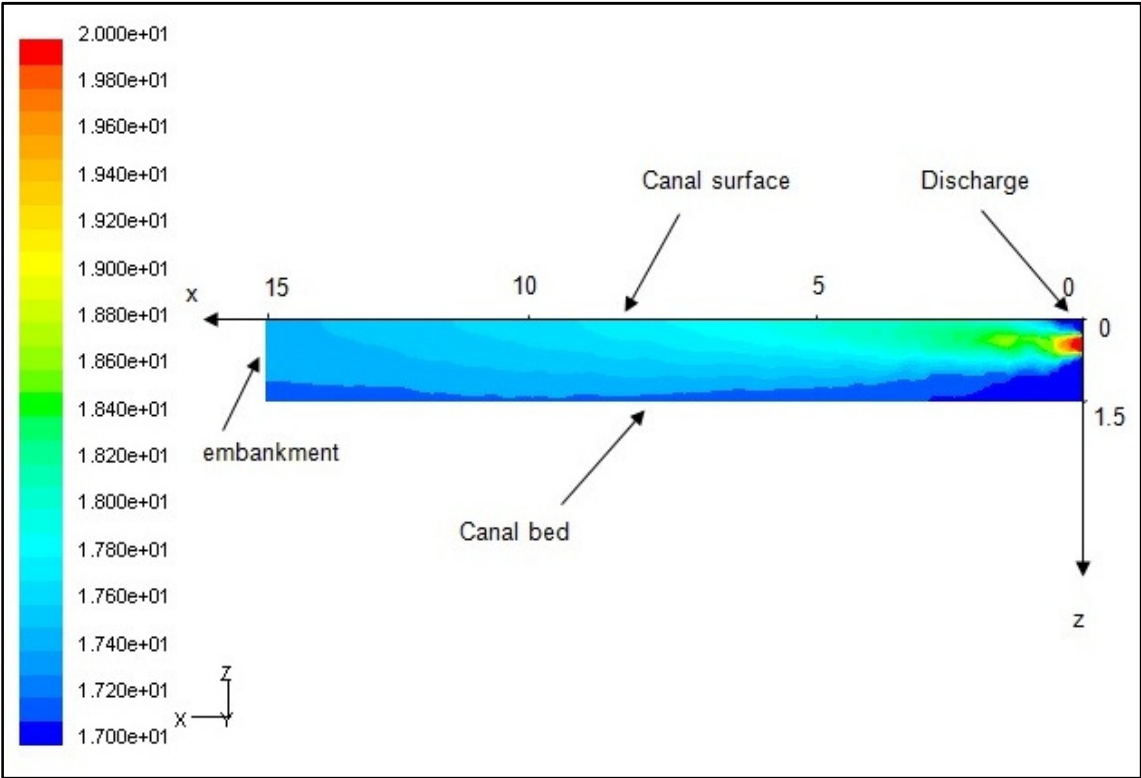


Figure 6.13: Heat diffusion on a plane normal to the centreline of plume (cross section)

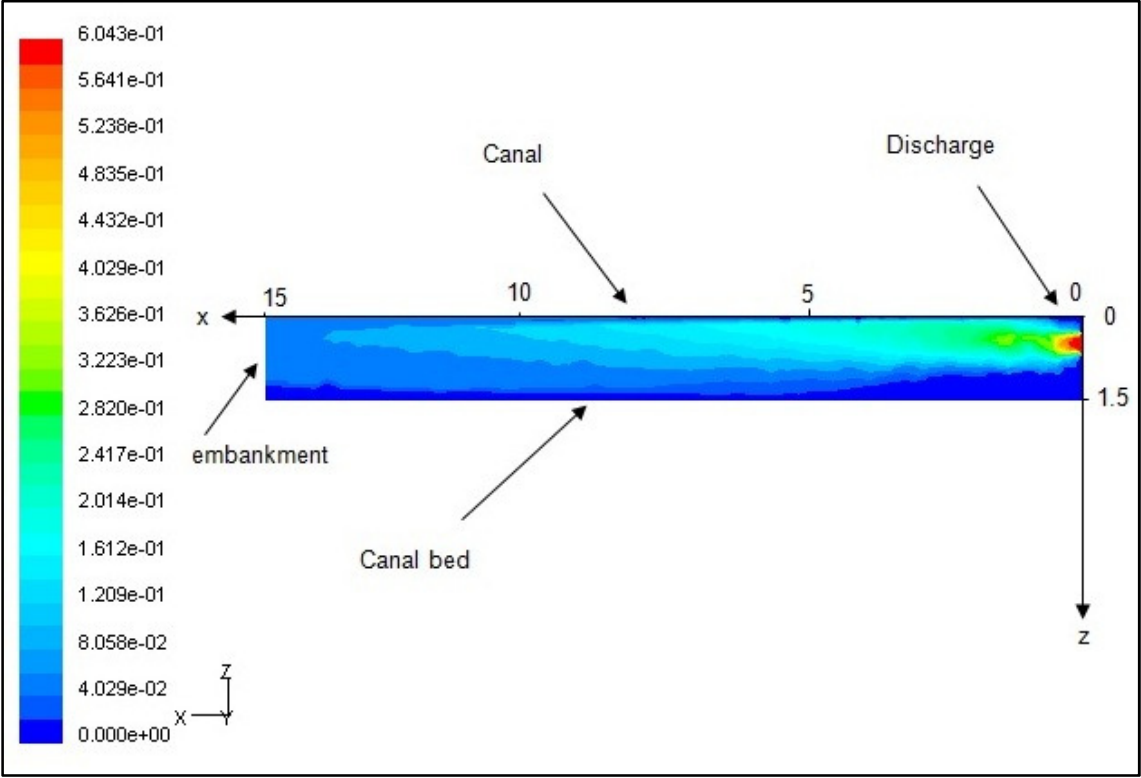


Figure 6.14: Velocity distribution on a plane normal to the centreline of plume (cross section)

7. Theoretical Analysis

7.1 Introduction

In the previous Chapter the experimental and computational studies are investigated. In this Chapter the theoretical analysis is discussed. Although the FLUENT software is able to model most of the fluid flows and heat transfer issues, its applications can be difficult and need a good mesh to obtain the most reliable results. This process needs a degree of expertise and it is this element of modelling that needs to be made more accessible to investigators who may be unfamiliar with FLUENT. The theoretical work in this Chapter is aimed to produce number of models which reduce the necessary technical expertise yet are equally reliable and specific as FLUENT in predicting the behaviour of thermal discharge into shallow and still receiving water. The models developed may be used by non technical investigators to evaluate the viability of discharging any heated water discharge into a still water environment. It is a necessity that good correlation between measured and predicted data should be achieved if the proposed modelling is to be accepted by the environment agencies. The analyses are carried out separately for surface and submerged discharge. Main part of the analyses is focused on the submerged discharge as this is the most common arrangement to be found in any discharge design proposal. A two dimensional equation has also been formulated to predict the heat diffusion profiles if a surface discharge design is subsequently encountered. Six equations have been derived. One predicts the plume path line in submerged discharge, another plume half width whilst the remaining four predict the temperature and velocities along and across the path line. The first two equations allow a three-dimensional model to be developed to predict the size of plume in submerged discharge.

The surface discharge model is derived from the advection diffusion equation whereas submerged discharge models are derived from the experimental measured data.

7.2 Surface Discharge Mathematical Model

This section is currently limited to the study of heated water surface discharge into the body of still receiving water. The work concentrates on the initial process – that of determining the heat diffusion profile and plume shape on the surface of the water. The domain in Figures 7.1 show the flow directions, the coordinates and the diffusion coefficient directions involved in the mathematical model. The main equation used is the advection diffusion as shown in

Equation 7.1. The left hand side of the equation represents flow and the right hand side represents the diffusions. To produce the model it is considered that the coefficient of heat diffusion is applied accordingly to suit the characteristics in the lateral and vertical directions – that is across the flow and depth-wise. The flow in the third direction, along the x axis, which is considered longitudinal downstream of the discharge, is velocity dependant. Steady state condition is considered to be when the temperature does not change with time and is further downstream beyond the plume.

$$\frac{\partial T}{\partial t} + U \frac{\partial T}{\partial x} + V \frac{\partial T}{\partial y} + W \frac{\partial T}{\partial z} = D_x \frac{\partial^2 T}{\partial x^2} + D_y \frac{\partial^2 T}{\partial y^2} + D_z \frac{\partial^2 T}{\partial z^2} \quad (7.1)$$

In equation (7.1) “T” is the mean temperature, “t” is time, U, V, W are mean velocity in x, y & z direction respectively and D_x, D_y, D_z are turbulent diffusivity in x, y & z direction respectively. In fact they are summations of turbulent diffusivity plus molecular diffusion coefficient. In this instance the turbulent diffusivity is much greater than the molecular diffusion value so this is neglected.

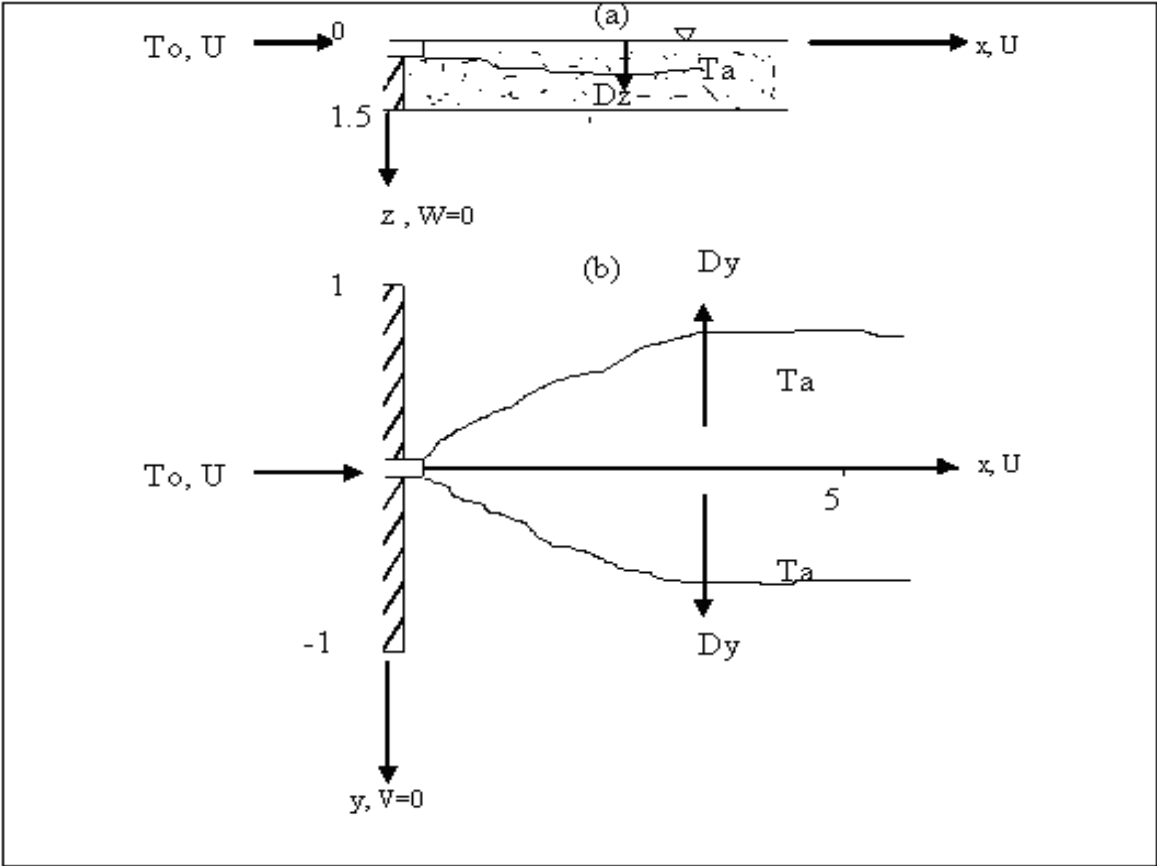


Figure 7.1: Surface discharge flow configuration, a. (sectional view), b. (plan view)

The flow steady state, since temperature does not change with time. The discharge pipe is horizontal on the surface of canal, so the lateral and vertical velocities V , W are very small and neglected. The advection term in “x” direction is much greater than the diffusivity D_x (Roberts and Webster, 2002) so it is neglected. Equation 7.1 is reduced to:

$$U \frac{\partial T}{\partial x} = D_y \frac{\partial^2 T}{\partial y^2} + D_z \frac{\partial^2 T}{\partial z^2} \quad (7.2)$$

In surface discharge the vertical diffusion D_z is small because the heated water remains on the surface as it has a smaller density than the receiving water and as has been observed from the thermal images, to produce a 2-dimensional heat diffusion model the D_z neglected. This yields Equation 7.2a:

$$U \frac{\partial T}{\partial x} = D_y \frac{\partial^2 T}{\partial y^2} \quad (7.2a)$$

Solution of the partial differential Equation 7.2a (Crank, 1970) gives:

$$T = \frac{A}{\sqrt{\frac{x}{U}}} e^{-\frac{y^2}{4D_y x/U}} \quad (7.3)$$

velocity $U = \frac{x}{t}$ sub to (7.3), yields :

$$T = \frac{A}{\sqrt{t}} e^{-\frac{y^2}{4D_y t}} \quad (7.4)$$

At the discharge point of the jet the boundary conditions are:

$$T = T_0 \quad \text{at } x=0 \quad -b < y < b$$

$$T = T_a \quad \text{at } x=0 \quad b < y < -b$$

T_0 , T_a is discharge and ambient temperature respectively.

If M is the total heat diffusion in canal with infinite length:

$$M = \int_{-\infty}^{\infty} Tdy \quad (7.5)$$

Sub equation 7.4 into Equation 7.5: is giving the spreading of an amount M of heat discharge at $x=0$

$$T = \frac{M}{2\sqrt{\pi Dt}} e^{-\frac{y^2}{4Dt}} \quad (7.6)$$

Take the error function (erf) for the Equation 7.6 (Crank, 1970), and add the ambient temperature, yields:

$$T(x, y) = \left(\frac{T_0 - T_a}{2}\right) \left(\operatorname{erf} \frac{b-y}{2\sqrt{p \cdot x}} + \operatorname{erf} \frac{b+y}{2\sqrt{p \cdot x}}\right) + T_a \quad (7.7)$$

“erf” is a standard mathematical function encountered in integrating the normal distribution (which is normalized form of the Gaussian Function) which is fitted with the plume half width, (erf) defined by:

$$\operatorname{erf}(x) = \frac{2}{\sqrt{\pi}} \int_0^x e^{-y^2} dy \quad (7.7a)$$

Equation 7.7 gives the heat diffusion on the surface of canal where “p” is a principal parameter equal to D_y/U .

The limitation of the Equations 7.7 is not applicable to the submerged discharge. The reason for that is that the effects of buoyancy are not considered in the main Equation of heat diffusion as in equation 7.1.

7.3 Turbulent Diffusivity D

In reality the turbulent diffusivity is variable from one location to another, even along the same plume. It varies in all directions as its value is influenced by many parameters such as flow, cross section of canal, shape of bed, concentration of discharge and ambient temperature. In fact its value is hard to predict and for that reason researchers undertaking thermal discharge studies tend to avoid the use of this value. Empirical data are used to determine the turbulent diffusivity at each grid point. The advection diffusion Equation 7.1 for heat and steady flow is used to evaluate the value of D in all directions x, y and z. These are obtained by substituting the mean value of the collected measured data (Temperature: T and velocity in x, y, z directions: U, V and W respectively) from the field trial on canal site. The value of D is a summation of thermal molecular diffusion and turbulent diffusivity. The latter is much greater than the first and for that reason the molecular diffusion can be neglected. The number of grids in the survey area on canal site is 11 x 11 at each layer, with grid steps 0.5m longitudinally and 0.2m laterally, see Figure 7.2.

The boundary layers grids (i.e. the top and bottom rows, left and right columns) are boundary conditions, the remaining grids are (9 x 9) at three planes 0.2m, 0.4m, 0.6m below the surface. These grids are connected to create 128 element bricks, 64 between upper and middle layer (four grids from each layer) and another 64 elements between middle layer and lower layer, see Figure 7.3. The turbulent diffusivity may then be determined for the centre point of each element.

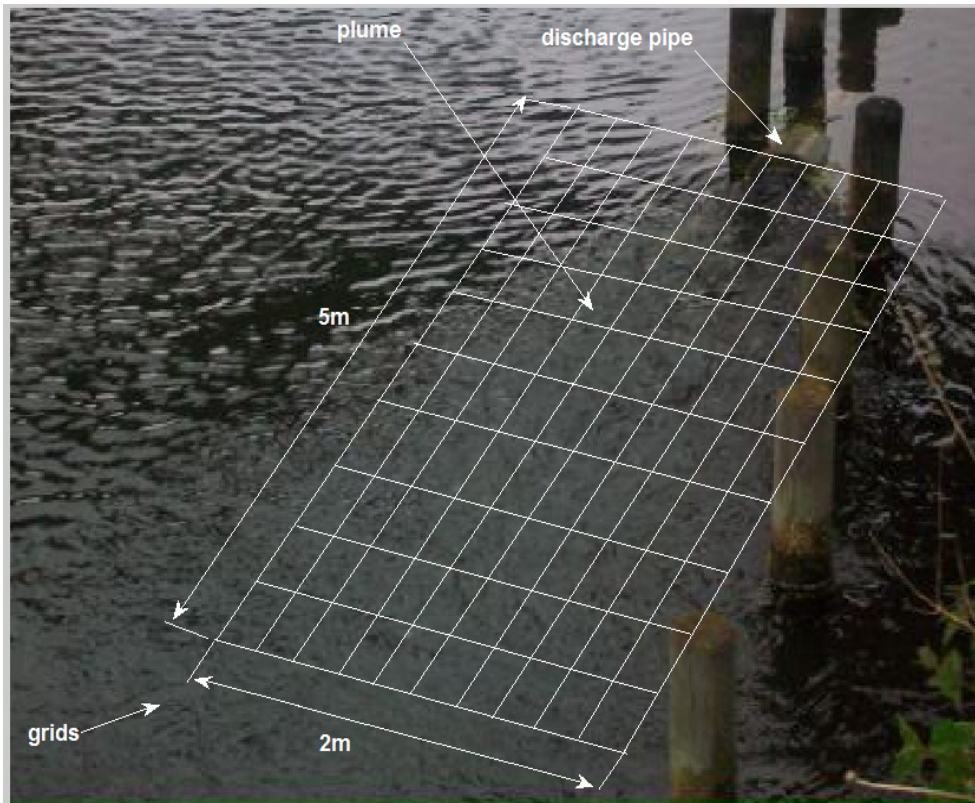


Figure 7.2: Show (surface layer) grids points where the temperature and velocity been measured at CSB site

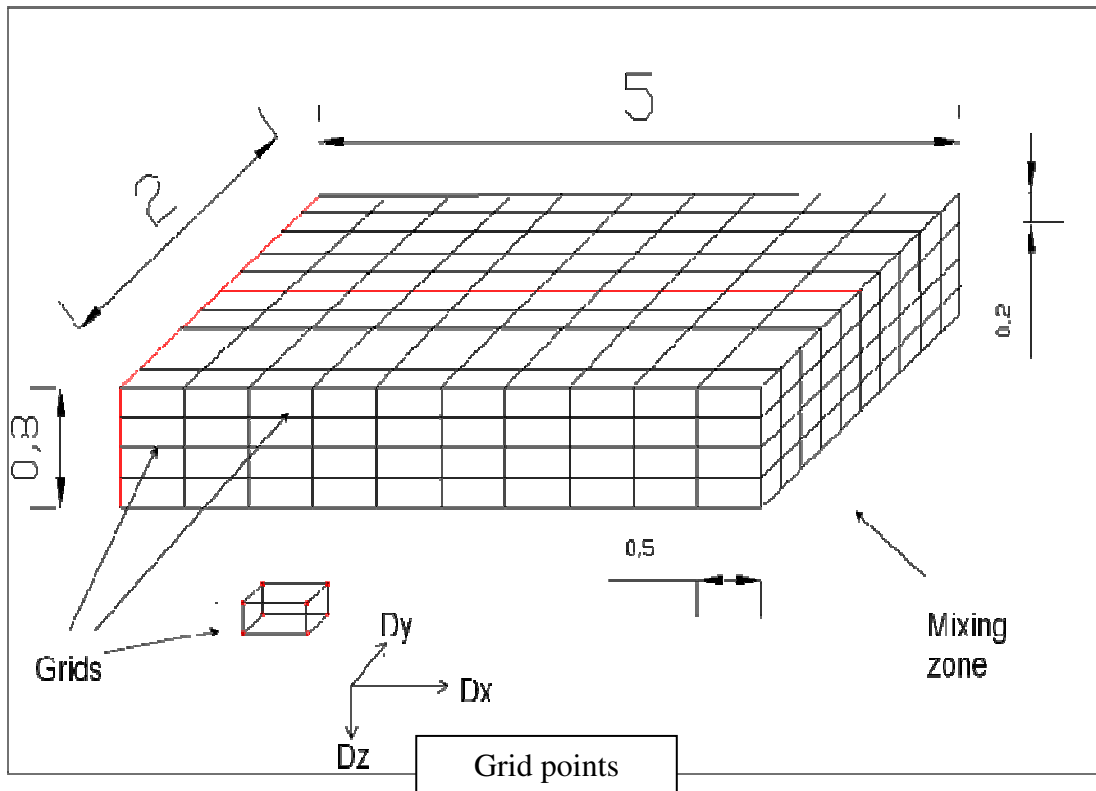


Figure 7.3: Schematic of the created blocks from the grids at the mixing zone

7.4 Submerged Discharge Mathematical Model

The theory related to the submerged thermal discharge is different to that of surface discharge in several ways. In the last section the theoretical analysis for surface discharge was investigated and an equation for heat diffusion presented. In submerged discharge the effects of buoyancy is much greater and the deflection of the plume towards the surface will occur. In addition the behaviour of the thermal plume below the free surface is the main issue of submerged discharge. Therefore six equations are derived from the empirical data to predict the behaviour of submerged plume. One equation is to determine the “core” path line of the plume moving to the surface of the receiving water, an additional equation for plume half width, and another equation is to predict the temperature profile along the path line. A fourth equation is used to predict the velocity profile along the path line and the last two equations are to determine the temperature and velocity profiles across the path lines. The 3D model produced needs MATLAB software for its effective application. From the equations it is found that the profiles of the thermal plume within the shallow and still water could be represented as function of:

$$\text{Plume profiles} = f(\Delta T, U_0, D_0, z_0, H) \quad (7.8a)$$

And dimensionless parameters:

$$\text{Plume profiles} = f\left(F_d, \frac{D_0}{H - z_0}, \frac{H - z_0}{L_M}\right) \quad (7.8b)$$

(Note that for all the produced equations these parameters may be abstracted, divided or multiplied with one to another to form the final model as in Equations 7.10b and 7.10c). Where F_d is a dimensionless densimetric Froude Number, ΔT is temperature difference between discharge and receiving water ambient temperature, U_0 is discharge velocity, L_M is the length scale, H is the depth of receiving water and z_0 is the depth of the discharge pipe (from centre of the pipe to the bed). The main parameter which is involved in all the equations is the Length Scale (L_M), according to (Jirka, 2004) and works done by others in this field; (L_M) is the best parameter for the length scale which makes the derived equations dimensionless:

$$L_M = \left(\frac{\pi}{4}\right)^{0.25} D_0 F_d \quad (7.9)$$

The procedures followed to derive the six equations are as follow:

1. Find the equation's best fit to the measured data. This may be of any form, typically exponential, polynomial, etc.
2. Apply the fitted equation to each experimental trial Run and a number of equations will be obtained.
3. Solve the obtained equations in step 2 simultaneously to determine the constants in the fitted equation for that specific Run.
4. Repeat the steps 2 and 3 for all the experimental Runs. Now the constants are known for all the Runs and vary from one Run to another
Find the relation of each constant with the effected parameters (Table, 4.1).
5. Determine the constants in the related equations, step 5 and then substitute the values in the equation in step1.

The following sections present the associated equations

7.4.1 Plume Path Line

In submerged discharge the outfall is located below free surface of the canal and the thermal plume moves to the water surface after a certain distance. The laboratory experimental measured data in Figure 8.22 show that the exponential Equation 7.10a gives a best fit to the plume trajectory to the surface. The exponential is a convenient and efficient equation for thermal plume analysis, gives the parabolic type of the fluid dynamics governing differential equations; continuity Equation 2.2, momentum Equations 2.3 and 2.4, energy Equation 2.5 and heat diffusion Equation 2.12, described in the literature review. These equations also used by FLUENT to model the fluids flow and heat transfer which have a parabolic shapes similar to the exponential equation.

$$z = a e^{\alpha x} \quad (7.10a)$$

Where, z is the vertical axis through the depth of the canal, x is the horizontal axis along the plume, “ a ” and “ α ” are constants. For every laboratory experimental Run the path line of the dyed heated plume is measured whilst it was deflecting to the surface. This means that at any

distance “ x ” along the plume the value of “ z ” was measured. Then, these measured values of “ z ” and “ x ” for each Run substituted to the Equation 7.10a, a number of equations obtained and solved simultaneously to determine the constants “ a ” and “ α ”. This procedure was repeated for all the experimental trials in Table 4.1. After the constants been determined for all the experimental trials it is found that they are varied from a Run to another because each Run has different parameters. Now to make the Equation 7.10a applicable to any thermal plume discharge, the constants’ relationship to the relevant parameters must be found. There was a linear relation between the constants “ a ”, “ α ” and the parameters $\frac{z_0}{F_d}$, $\frac{D_0 F_d}{H - z_0}$ respectively as follow:

$$a = A \frac{z_0}{F_d} + B \quad (7.10b)$$

$$\alpha = A1 \frac{D_0 F_d}{H - z_0} + B1 \quad (7.10c)$$

Where z_0 is the discharge pipe depth from the centre of the pipe to the bed, F_d is densimetric Froude number, D_0 discharge pipe diameter, H is the depth of the water in the tank (canal), A , B , $A1$ and $B1$ are constants. Solve the Equation 7.10b for all the Runs to determine the value of the constants “ A ” and “ B ”, similarly find the constants “ $A1$ ” and “ $B1$ ”. The following were found ($A = 0.1$, $B = 0$, $A1 = 1.4$ and $B1 = 0$), substitute them to the Equations 7.10b and 7.10c will result:

$$a = 0.1 \frac{z_0}{F_d}$$

$$\alpha = 1.4 \frac{D_0 F_d}{H - z_0}$$

Now substitute the “ a ” and “ α ” values to the Equation 7.10a to get the equation that models the path line of the plume, Equation 7.10. It is clear from the equation that the main dependant parameters involved in the path line trajectory is the densimetric Froude number, discharge pipe diameter and the depth of the discharge pipe.

$$z = \left\{ 0.1 \frac{z_0}{F_d} \exp \left(1.4 \frac{D_0 F_d}{(H - z_0) L_M} x \right) \right\} - 0.1 \frac{z_0}{F_d} \quad (7.10)$$

Note that the last term $0.1 \frac{z_0}{F_d}$ is a small value abstracted from the equation 7.10 to make $z = 0$ when $x = 0$, i.e. the plume path line started from the centre of the discharge pipe not above it. The length scale (L_M) is cancelling the effects of the length units (dimensionless); it is applied to all the derived equations. The plume path line graphs will be presented in the next chapter and the measured and the predicted data are tabulated in Appendix 8.

7.4.2 Plume Half Width

In the laboratory experimental trials dyed heated water was discharged into the model tank to see the behaviour of the plume and to measure the size of the plume. The lateral distances from the plume centreline to the edge of the plume (plume half width) were measured for every Run. From the dyed heated plume in Figure 4.13 can be said that the quadratic Equation 7.11a gives a best fit to the plume half width, therefore it is selected as a convenient and efficient equation for thermal plume half width. The polynomial quadratic Equation 7.11a gives the parabolic type similar to that given by the fluid dynamics governing differential equations; continuity, momentum, heat diffusion and energy equation in modelling the thermal plume profile.

$$y_h = a_0 + a_1x + a_2x^2 \quad (7.11a)$$

Where “ y_h ” is the lateral distance from the centreline to the edge of the plume (plume half width), “ a_0 ”, “ a_1 ”, “ a_2 ” are constants and “ x ” is distance along the thermal plume. For every experimental “Run” a number of “ y_h ” measured along the longitudinal axis “ x ” and then they substituted to Equation 7.11a, as a result a several equations obtained. These equations were solved to determine the constants “ a_0 ”, “ a_1 ”, “ a_2 ” for every Run. Because the parameters used in the experimental Runs were different in value as shown in Table 4.1 the constants were not same. This indicated to the effects of the parameters on the values of the constants. To generalize the Equation 7.11a to appropriate for any application of thermal plume discharge into shallow and still water, the relation of the constants with the effected parameters determined. It is found that the constant “ a_0 ” in every Run was equal to the radius of the discharge pipe in that Run, this is shown that the plume half width is equal to the discharge pipe radius when $x = 0$.

$$a_0 = \frac{D_0}{2} \quad (7.11b)$$

The constants “a1” and “a2” were relating linearly to the discharge pipe diameter and it's depth as follow:

$$a_1 = AD_0 + B \quad (7.11c)$$

$$a_2 = A1z_0 + B1 \quad (7.11d)$$

Substitute the discharge pipe diameter and the discharge pipe depth for each Run to the Equations 7.11c and 7.11d, two sets of equations will be obtained, a set of the constant “a1” equations and a set of constant “a2” equations. Solve each set of the equations simultaneously to find that (A = 15.5, B = 0, A1 = 0.1 and B1 = 0), substitute them to the Equations 7.11c and 7.11d yield:

$$a_1 = 15.5D_0$$

$$a_2 = 0.1z_0$$

Substitution of the above values to Equation 7.11a yields Equation 7.11 which determines the half width of the plume.

$$y_h = \frac{D_0}{2} + 15.5 \frac{D_0}{L_M} x - 0.1 \frac{z_0}{(L_M)^2} x^2 \quad (7.11)$$

7.4.3 Temperature along Plume Path Line

After the plume path line has been measured for all the experimental trials by using the dyed water, the temperature along that line measured. The measured temperatures “T” along the plume path line in Figure 8.23 shown that the exponential Equation 7.12a gives a best fit for the measured temperature ratio curve. The exponential is a convenient and efficient equation for thermal plume temperature decay. The exponential equation gives the parabolic shape for

the heat dilution similar to the energy Equation 2.5 and heat diffusion Equation 2.12 used in modelling temperature profile of the thermal plume.

$$\frac{T - T_a}{T_0 - T_a} = a e^{-\alpha x} \quad (7.12a)$$

Where T_a is the tank water ambient temperature, T_0 is the discharge temperature; “ a ” and “ α ” are constants. All the measured temperatures in a single experimental “Run” with their distance “ x ” from the outlet substitute to Equation 7.12a formed a number of equations. These equations solved simultaneously to determine the constants “ a ” and “ α ”. This method repeated to determine the constants values for all the trials tabulated in Table 4.1. The obtained constants were compared with the parameters in each Run it was found that the constant “ a ” is equal to one. Whilst the constant “ α ” was relating linearly with the position of the discharge pipe and length scale $\frac{H-z_0}{L_M}$ as follow:

$$\alpha = A \frac{H - z_0}{L_M} + B \quad (7.12b)$$

Substitute the value of α , H , z_0 and L_M for each Run to the above equation; solve the obtained equations from all the experimental Runs yields ($A = 3.2$ and $B = - 1.89$). Substitute the constant A and B to the Equation 7.12b results:

$$\alpha = 3.2 \frac{H - z_0}{L_M} - 1.89 \quad (7.12c)$$

The constants in Equation 7.12a replaced with the effected parameters resulted the T equation. The predicted value of T in this instant were not good fitted the measured temperature. Therefore the constant B changed for each Run to make the predicted value best fits the measured data. This repeated for each Run, now new values for B obtained and they were different for each Run. These values were relating linearly with the parameter F_d as follow:

$$B = A2F_d + B2 \quad (7.12d)$$

Where A_2 and B_2 are constants, their values determined by solving the B equation for all the Runs, it was found that ($A_2 = 0.06$, $B_2 = 0$). Substitute these values to Equation 7.12d gives:

$$B = -0.06F_d$$

Substitute the values of A and B to the equation 7.12b yields:

$$\alpha = 3.2 \frac{H - z_0}{L_M} - 0.06F_d \quad (7.12e)$$

Substitute the Equation 7.12e to Equation 7.12a to obtain the Equation 7.12 which determines the temperature along the path line of the plume.

$$T = \left((T_0 - T_a) \exp \left(\left(-3.2 \frac{H - z_0}{L_M} - 0.06F_d \right) \frac{x}{L_M} \right) \right) + T_a \quad (7.12)$$

7.4.4 Velocity along Plume Path Line

The measured velocities along the path line of the plume, Figure 8.25 shown that they are best fitted the exponential curve Equation 7.13a, and therefore it is selected to form the velocity equation. The exponential is a convenient and efficient equation for thermal plume velocity decay. The exponential equation has a parabolic shape similar to the fluid dynamics governing differential equations; continuity Equation 2.2 and momentum Equations 2.3 and 2.4 stated in the literature review.

The measured velocities for every experimental trial substituted to the Equation 7.13a along with their distances “ x ” from the discharge outlet. The constants “ a ” and “ α ” were known for all the Runs and they were varied from a Run to another depending on the effected parameters values.

$$U = a e^{-\alpha x} \quad (7.13a)$$

A comparison between the constants values and the parameters values undertaken to alternate the constants to effected parameters. It was obvious that the constant “ a ” equal to the

discharge velocity “ U_0 ”. Whilst the constant “ α ” was relating linearly with discharge pipe location, canal depth and the length scale $\frac{H-z_0}{L_M}$ as follow

$$a = U_0 \quad (7.13b)$$

$$\alpha = A \frac{H - z_0}{L_M} + B \quad (7.13c)$$

The values of the constants A and B were determined by solving the Equation 7.13c for all the Runs, ($A = 0.26$, $B = - 2.11$). The Equations 7.13b and 7.13c were substituted to Equation 7.13a, the predicted data was not good fitted the measured velocities. Therefore a procedure similar to that in the last section was carried out to determine the value of the constant B as a function of an effected parameter. It was found that ($B = - 0.066F_d$), and then the constants A and B were substituted to Equation 7.13c as follow:

$$\alpha = 0.26 \frac{H - z_0}{L_M} - 0.066F_d \quad (7.13d)$$

Finally the Equations 7.13b and 7.13d substituted to the Equation 7.13a result the Equation 7.13 which predicts the velocity along the plume path line.

$$U = U_0 \exp\left(\left(-0.26 \frac{H - z_0}{L_M} - 0.066F_d\right) \frac{x}{L_M}\right) \quad (7.13)$$

7.4.5 Temperature across the path line

The last two equations derived to predict the temperature and the velocity along the path line of the plume as function of the longitudinal axis “ x ”. Whilst the temperature and the velocity across the path line will be predicted as a function of the lateral axis “ y ”. As can be seen from Figures 8.26 – 8.30 the lateral measured temperatures have exponential shapes, so the

exponential Equation 7.14a selected to form the lateral temperature equation. The reason of using the exponential among the other functions as mentioned in the previous sections is given the parabolic type of the fluid dynamics governing differential equations described in the literature review.

$$T = a e^{-\alpha y^2} \quad (7.14a)$$

The measured temperatures for every Run substitute to the Equation 7.14a and the constants “ a ” and “ α ” determined. The constants values compared with the parameters values for all the Runs. It was found that the constant “ a ” is equal to the peak temperature “ T ” along a lateral axis “ y ”. This means that the constant “ a ” is equal to the path line “core” temperature where it is value is higher. Therefore the Equation 7.12 that predicts the path line “core” temperature replaced the constant “ a ” in the Equation 7.14a. The constant “ α ” was relating to the location of the discharge pipe as in Equation 7.14c.

$$a = \left((T_0 - T_a) \exp \left(\left(-3.2 \frac{H - z_0}{L_M} - 0.06 F_d \right) \frac{x}{L_M} \right) \right) + T_a \quad (7.14b)$$

$$\alpha = A \frac{H - z_0}{L_M} + B \quad (7.14c)$$

The values of “ α ”, H , z_0 and L_M in each Run were substituted to Equation 7.14c, a set of equations obtained, solved simultaneously to find the values of ($A = 5.5$ and $B = 0$).

Substitute the values of A and B to Equation 7.14c results:

$$\alpha = 5.5 \frac{H - z_0}{L_M} \quad (7.14d)$$

The equations 7.14b and 7.14d substituted to the Equation 7.14a gave the Equation 7.14 to determine the temperature profiles across the path line of the plume. To avoid the effects of the units of the length the lateral distance “ y ” divided by plume width “ $2y_h$ ”. Plume width “ $2y_h$ ” is better than the L_M (length scale) to make the lateral axis dimensionless because the plume width is the maximum lateral distance “ y_{\max} ” within the mixing zone.

$$T(x, y) = \left\{ (T_0 - T_a) \exp \left(\left(-3.2 \frac{H - z_0}{L_M} - 0.06F_d \right) \cdot \frac{x}{L_M} \right) \exp \left(- \left(5.5 \frac{H - z_0}{L_M} \right) \cdot \frac{y^2}{(2y_h)^2} \right) \right\} + T_a \quad (7.14)$$

7.4.6 Velocity across the path line

Similar procedures as in the previous section were followed to derive equation for the velocity across the path line. The exponential Equation 7.15a was best fitting the measured data curve. Based on the theory that the exponential equation is given the parabolic type of the fluid dynamics governing differential equations, the Equation 7.15a selected to model the lateral velocity profile.

$$U = a e^{-\alpha y^2} \quad (7.15a)$$

The constant “ a ” was equal to the velocity at the path line of the plume therefore it replaced by the Equation 7.13, whilst the constant “ α ” was relating to the parameters which formed the location of the discharge pipe, Equation 7.15c.

$$a = U_0 \exp \left(\left(-0.26 \frac{H - z_0}{L_M} - 0.066F_d \right) \frac{x}{L_M} \right) \quad (7.15b)$$

$$\alpha = 10.5 \frac{H - z_0}{L_M} \quad (7.15c)$$

Substitute Equations 7.15b and 7.15c to the Equation 7.15a results Equation 7.15 to predict the velocity profiles across the plume path line. The effected parameters are similar to those in the equation along the plume path line.

$$U(x, y) = U_0 \exp \left(\left(-0.26 \frac{H - z_0}{L_M} - 0.066F_d \right) \cdot \frac{x}{L_M} \right) \exp \left(- \left(10.5 \frac{H - z_0}{L_M} \right) \cdot \frac{y^2}{(2y_h)^2} \right) \quad (7.15)$$

In all the above cases the curves of best fit have obtained by using the various parameters from the laboratory experimental trials. The measured and predicted data are tabulated in Appendices 8, 9 and 10 and will be discussed in the results and discussion section.

In fact there are infinitely many choices of mathematical functions that will approximate the experimental data curve, the polynomial quadratic equation selected to model the plume half width. The others look exponential as shown in the presented graphs in results and discussion section, therefore the exponential approximation were used to model the plume path line, temperature and velocity which give something similar to the other functions.

7.5 3-Dimensional Model of Submerged Discharge

The 3-dimensional model of the size of the plume below the free surface of the canal has been derived and presented graphically in Figure 7.4. A number of equations have been used to produce this 3-D model, their formulation being achieved through a mathematical procedure as follows.

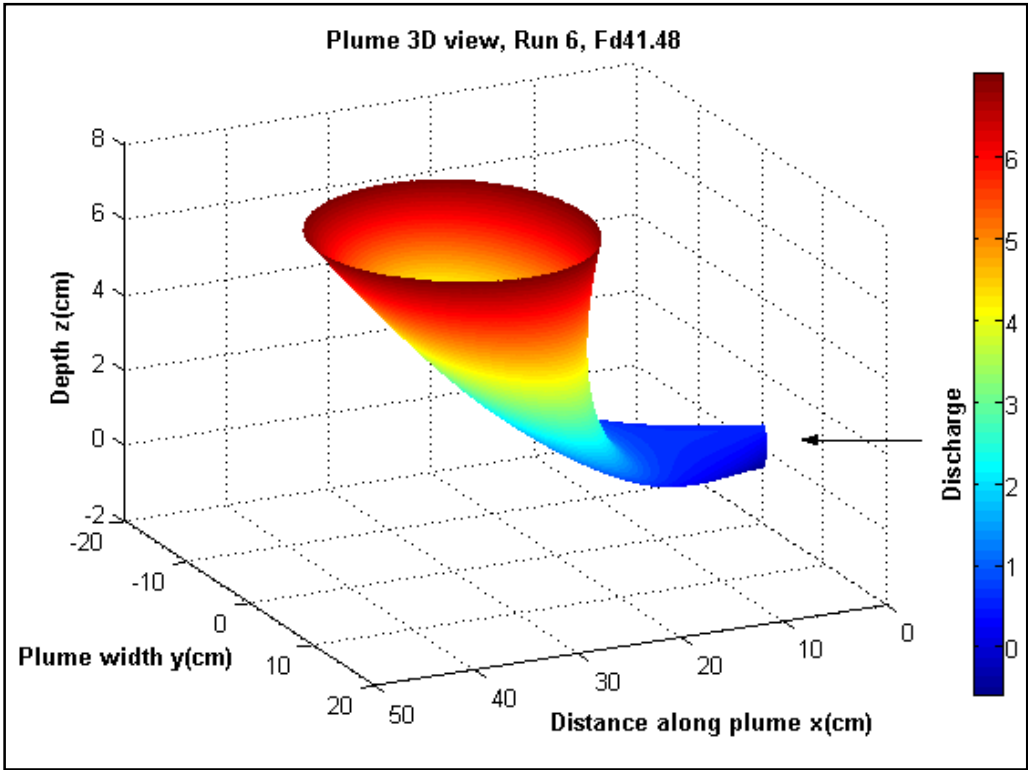


Figure 7.4: 3-D model of the size of the thermal plume, Run 6 of the experiments

The final model is formulated using the experimental data. The edges of the plume are determined from the flow of dyed water as shown in the digital images with mathematical equations derived to fit the edges. An equation is derived from the experimental data to predict the plume half width and another produced to determine the upper vertical edge of the plume. These two equations are combined with the equation of the thermal plume centre path line to form the 3-D model. Figure 7.4 shows the 3-D size of the thermal plume below the free surface of the receiving water. MATLAB software is needed to create the final 3-D model. Appendix 7 presents the MATLAB code of the 3-D model of the size of the plume.

8. Results and Discussion

8.1 Introduction

In this chapter the results from the experiments, thermal images, computational and mathematical analyses will be presented and discussed. For the surface discharge type of installation there was the possibility to gather data from on-site measurements. As such the temperature along and across the centreline of the plume as measured from the experiments are used for comparison with the theoretical predictions. Note that in case of surface discharge only temperature has been modelled. For the submerged discharge the temperature and velocity along and across the path line of the plume as measured using the laboratory experiments are presented and compared with the mathematical predictions. The predicted models for both types of discharge are validated against the canal site measured data. Surface thermal discharge and submerged thermal discharge are discussed separately starting with the surface discharge.

8.2 Surface Discharge

The Central Services Building CSB site at the University of Huddersfield is an example of a canal site in which the thermal plume discharges onto the surface of the water. Two case studies are performed on the canal site and the data for both studies are presented in Appendices 3 and 4. In the preliminary case study the temperatures are measured on a plane just above the centreline of the plume (at 50mm below the surface) while in the refined case study the temperatures are measured on a discharge layer 75mm below the surface. Since the theoretical model predicts the temperature on the centreline of plume the refined case study

has been used primarily in the investigations. In the following sections the temperature decay along and across the centreline of the plume for the experiments and the theoretical analysis will be presented and discussed.

8.2.1 Temperature dilution along the centreline of the plume

The centreline of the plume is a straight line from the centre of the discharge pipe along the plume length. It is the core of the plume within surface discharge profile where the discharge temperature is higher than any region within the mixing zone. Because of this the majority of the thermal plume studies are focused on the centreline of the plume.

The methodology followed in this research and investigated in the previous chapters started with a case study on the real canal site. The maximum temperature measured in the field trial was 24°C at the outlet of the discharge, and the velocity at the same point was 1.23m/s. The discharge pipe diameter was 0.15m located at the surface of canal as it is illustrated in Figure 3.11. The data collected from the initial survey has been presented and discussed in Chapter 3. From the data it was possible to plot the resulting temperature along the centreline of the plume as shown in Figure8.1.

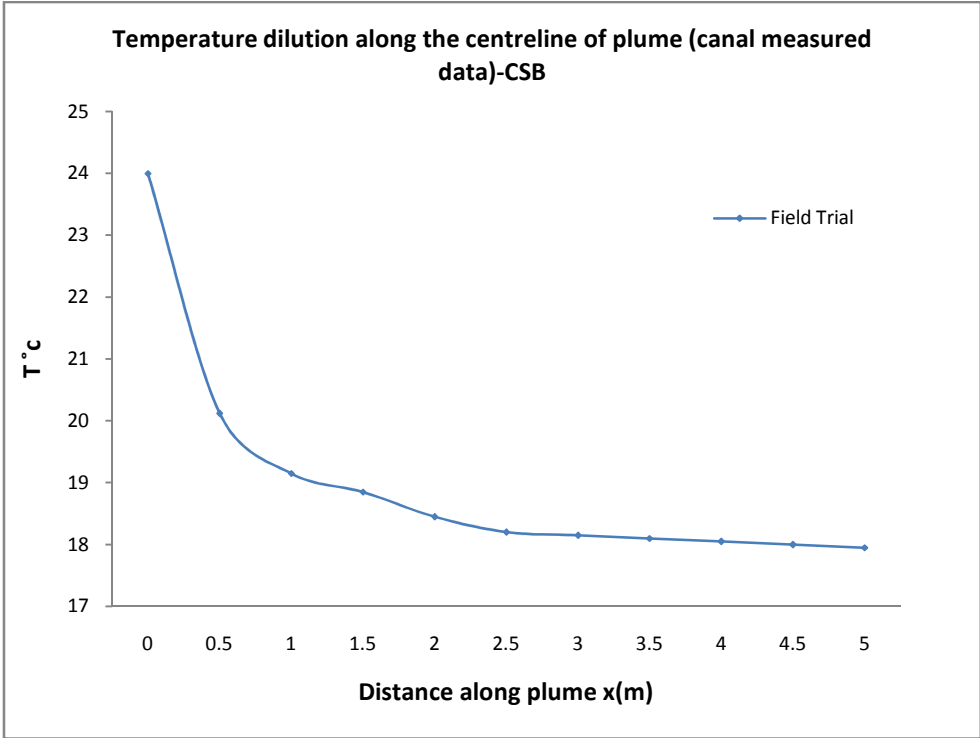


Figure 8.1: Measured temperature along the centreline of plume (field trial)

After the experiments on the canal site, laboratory experiments were carried out to study the plume more readily and controllably in a scale model tank. The model tank was designed and built to simulate the canal site using the dimensionless parameter densimetric Froude Number F_d . For convenience the size was selected to be 1/10 scale thus the discharge pipe diameter in the model tank became 0.015m. The discharge temperature must not change and the velocity was calculated to be 0.4m/s. For such an arrangement the temperature along the centreline of plume was measured and presented in Figure 8.2. Reference to Figure 8.1 shows the results to be very close.

The purpose designed tools and instruments as used in collecting the data is presented in Appendix 2. The Thermal Camera is one of the main pieces of equipment used in the current research to measure temperature distribution on both the surface of canal and model tank. The advantages of using thermal images are the very clearly defined surface area of the plume and mixing zone as well as the edges of the plume and its penetration across the surface of the water.

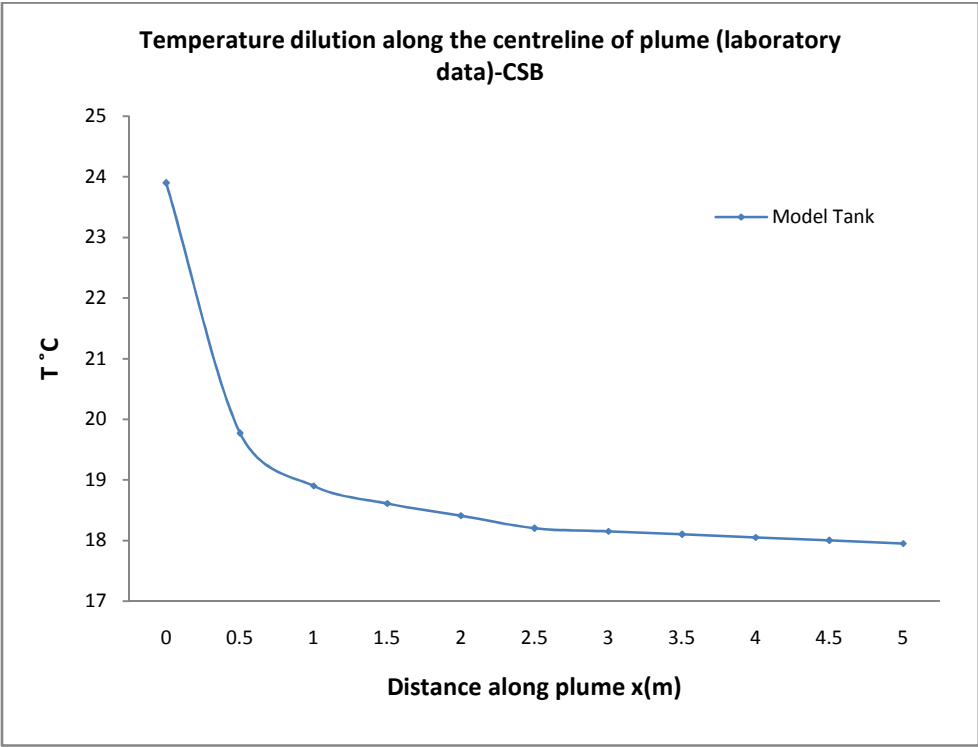


Figure 8.2: Measured temperature along the centreline of plume (model tank)

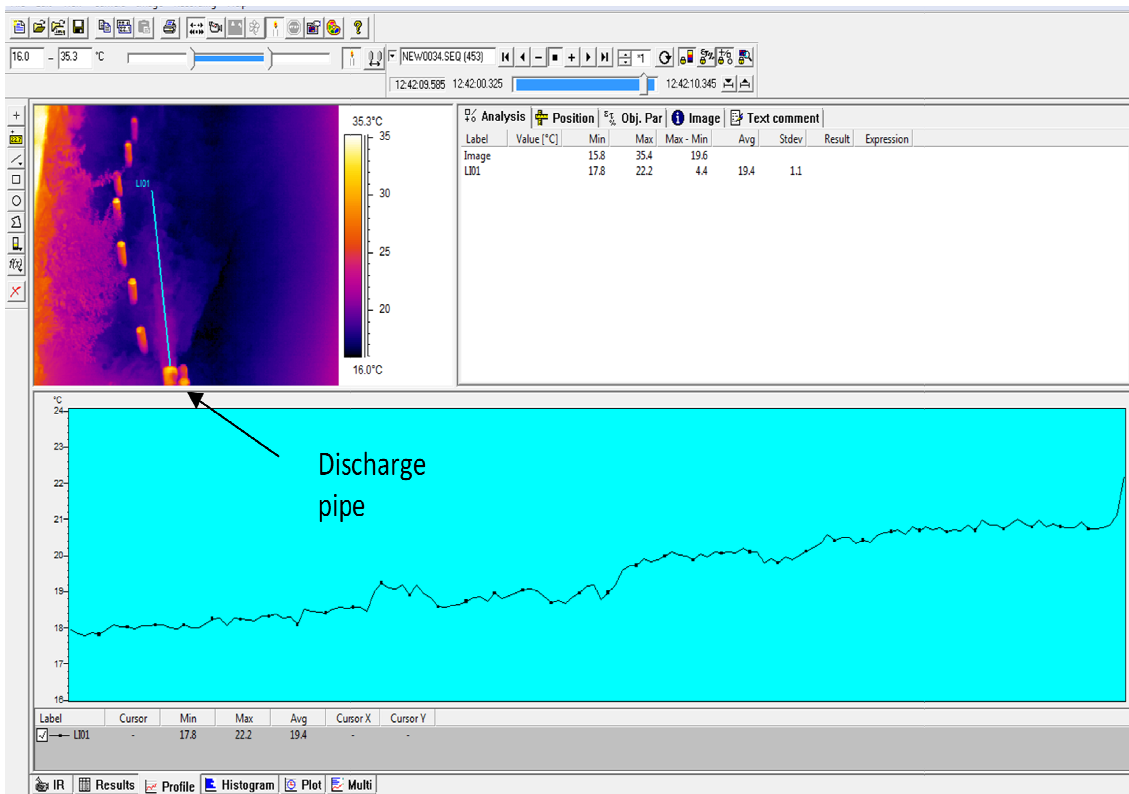


Figure 8.3: Thermal Camera results – CSB site

The disadvantage of the thermal camera is that it is not able to detect the temperature distribution below the surface, particularly with on-site testing. Attempts were made to create thin access windows within the tank walls so the thermal images could be recorded but this was not particularly successful. Figure 8.3 demonstrates the thermal camera results for the canal site. The lower half of the figure shows the temperature profile along the straight line on the centre of plume in the thermal image. The maximum temperature along the line 22.2°C and the minimum 17.8°C. The thermal image is for the free surface but in fact the maximum temperature of the plume is 24°C below the surface and is measured by thermocouples at the centre of the outfall. The results of the computational work by using the CFD package FLUENT gave a detail results for the plume behaviour and was presented earlier in Chapter 6. This investigated the Temperature and velocity distribution at different layers within the mixing zone, the temperature along the centreline of the plume along a length of 20m from the outfall being presented in Figure 8.4. The graph shows a highest temperature for the distance 0 to 0.2m along the plume, that distance being the core region of the plume. It is seen that the temperature then reduced to around 18 °C within 5m from the discharge point. This profile will be compared with the experimental measured data, and then both will be used to prove the validity of the derived model.

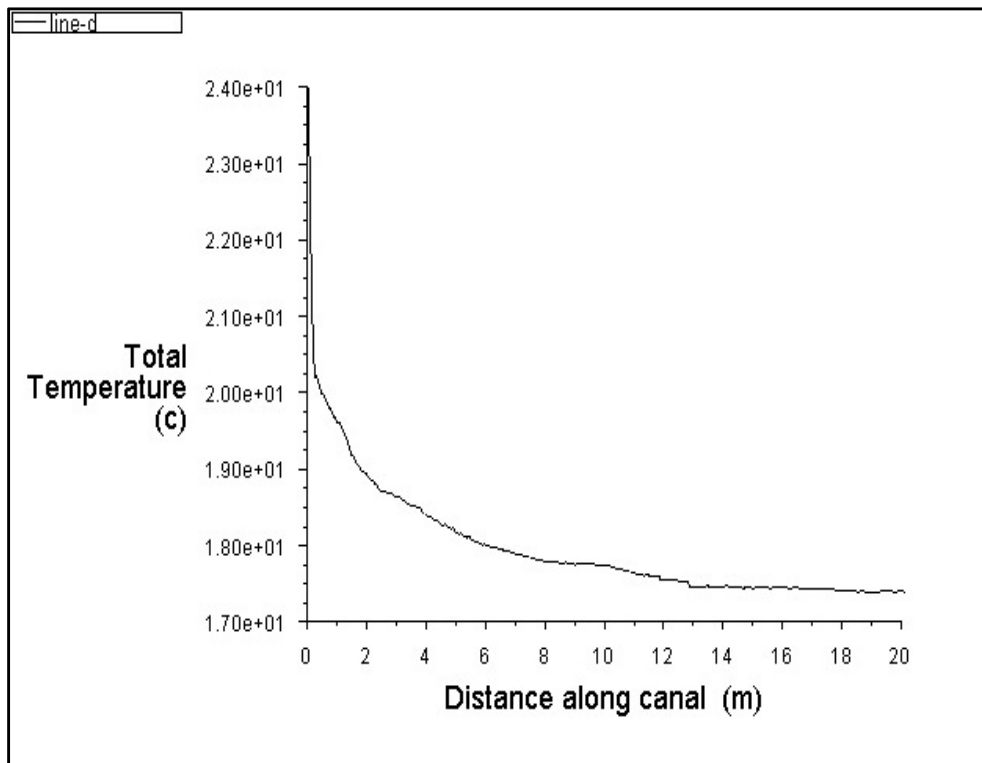


Figure 8.4: Temperature along the centreline of plume predicted by FLUENT – CSB site

FLUENT makes use of heat transfer and fluid flow equations to undertake a thermal study of the discharge and as such it requires little intervention to produce acceptable results. Although the results obtained from FLUENT are as presented in Chapter 6, the current research makes use of mathematical equations to predict the behaviour of thermal plume. The principal reason for this approach emanates from one of the objectives of the research in that it must be readily understood and not make use of software that requires significant expertise to create the differing models that may be encountered. FLUENT is an excellent package but it requires cost of software, its updating and specialist training to implement. In essence the aim of this research is to produce an interactive model that can be readily modified and run by non technical British Waterways personal.

The mathematical Equation 7.7 was derived from the heat diffusion Equation 7.1 and intended to determine the temperature distribution on the surface of mixing zone. The equation is not contained the effects of buoyancy even gravity so it is applicable only on the surface thermal plume when the discharge is located on the surface. The main parameter in the equation is “p” which is equal to the turbulent diffusivity divided by the discharge velocity. The turbulent diffusivity affected is the lateral diffusivity D_y across the plume.

Lateral turbulent diffusivity D_y for the CSB site is calculated from the method described in section 7.3 and some of the values are presented in Table 8.1.

Distance along plume x(m)	Turbulent Diffusivity $D_y \text{ m}^2 / \text{s}$	
	Distance across plume y(m)	
	0.1	-0.1
0.75	0.0373	0.0373
1.25	0.007	-0.017
1.75	0.0053	-0.0036
2.25	0.0026	0.0022
2.75	0.0973	0.0158
3.25	0.0505	0.0074
3.75	0.0246	0.0304
4.25	0.0366	0.0257
	Average	0.0224625

Table 8.1: Lateral turbulent diffusivity D_y

The results produce some negative values of turbulent diffusivity caused by the transfer of heat from a low heated element to a high heated element due to turbulent eddies. This negative turbulent diffusivity has been investigated theoretically by Avramenko and Basok, (2006) where they showed this negative diffusivity being as a result of the turbulent eddy flows. The average value of D_y is $0.02246 \text{ m}^2 / \text{s}$, therefore the value of “p” becomes 0.018m. To determine the temperature profile along the centreline of plume, the lateral distance “y” should be cancelled from Equation 7.7. The result will be as illustrate in Equation 8.1.

$$T(x) = (T_o - T_a)\left(\text{erf} \frac{b}{2\sqrt{p \cdot x}}\right) + T_a \tag{8.1}$$

Figure 8.5 show the temperature dilution along the centreline of the plume as predicted by Equation 8.1. It shows a dramatic loss in the temperature within a distance 1m from the discharge point and then the temperature remains steady at around 18°C after 2m from the discharge.

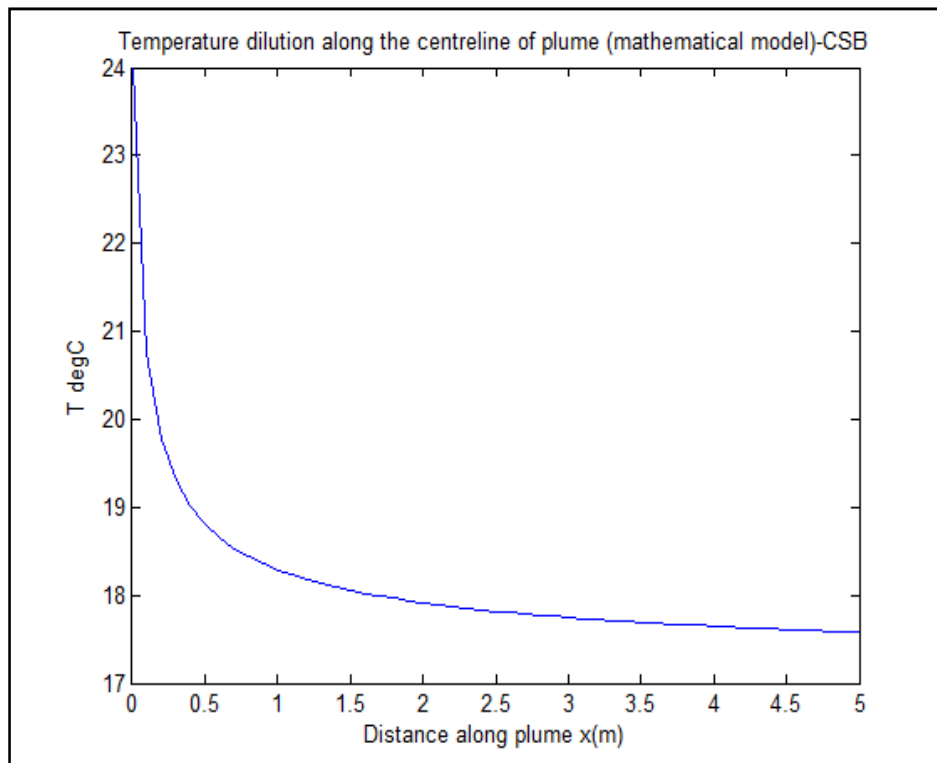


Figure 8.5: Centreline temperature decay (mathematical equation)

Finally it is necessary to undertake a comparison of the data obtained from the experiments and the theoretical results. The field trial and model tank temperature measured by thermocouples along with the temperature measured by the thermal camera are compared with the results of analyses by FLUENT and mathematical model, see Figures 8.6 and 8.7. Figure 8.7 shows the comparison of the dimensionless results, the temperature is divided by the discharge temperature and the distance along the plume is divided by the maximum value of x to give the dimensionless values. As predicted by (Stolzebach and Harleman, 1971) the surface thermal discharge is divided into four regions. These regions can be seen from the results demonstrated in Figure 8.8 – the core, the entrainment, the stable and the heat loss region.

1. Core region: in which the centreline temperature is remaining very high
2. Entrainment region: the centreline temperature decreased sharply
3. Stable region: the centreline temperature remains relatively constant
4. Heat loss region: where the heat loss will resume, then beyond this region the plume will lose its property and fully mixed with the receiving water. Figure 8.8 demonstrates the regions on the graph, except the heat loss region which may happen after 5m from the outfall.

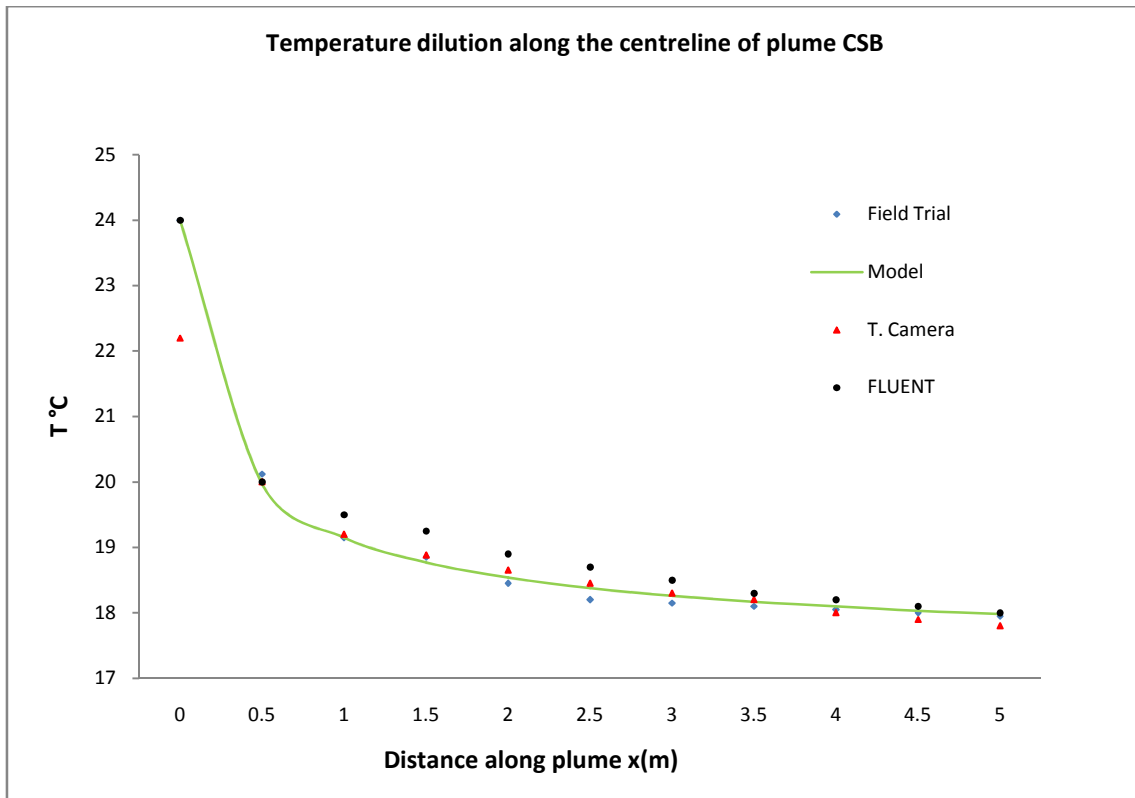


Figure 8.6: Comparison of the predicted centreline temperature against the experimental and FLUENT data

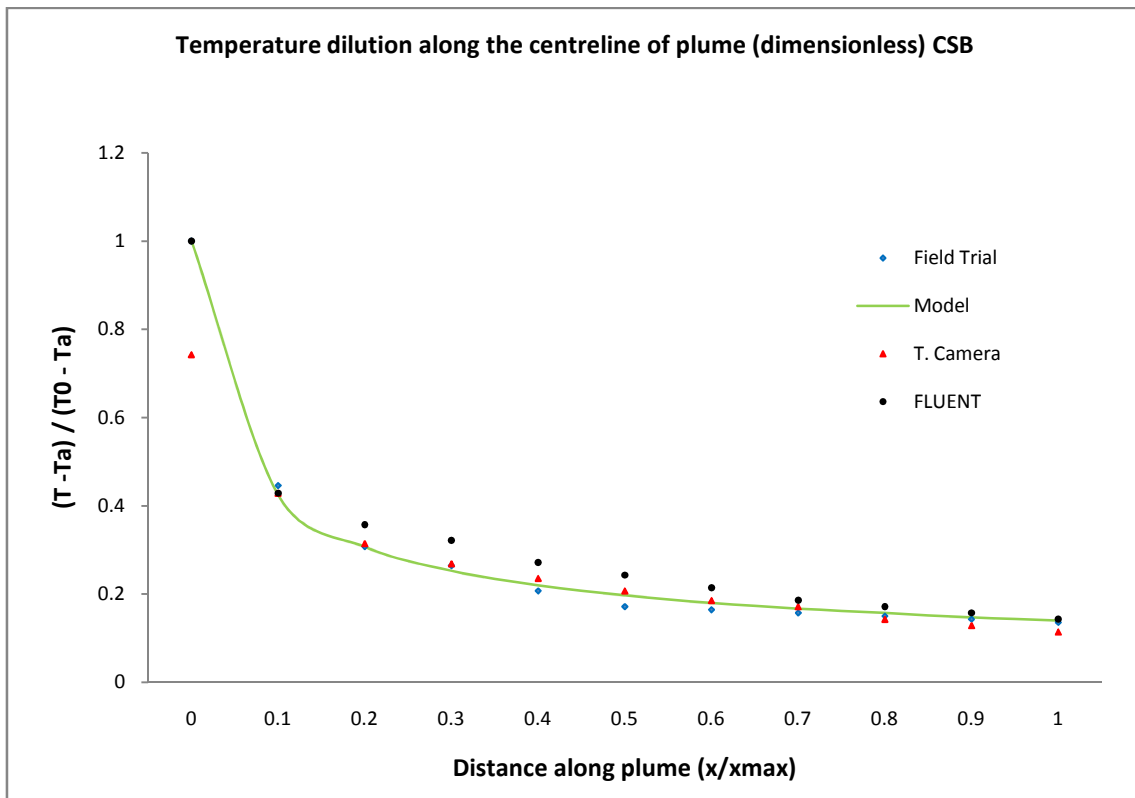


Figure 8.7: Comparison of the predicted centreline temperature against the experimental and FLUENT data (dimensionless)

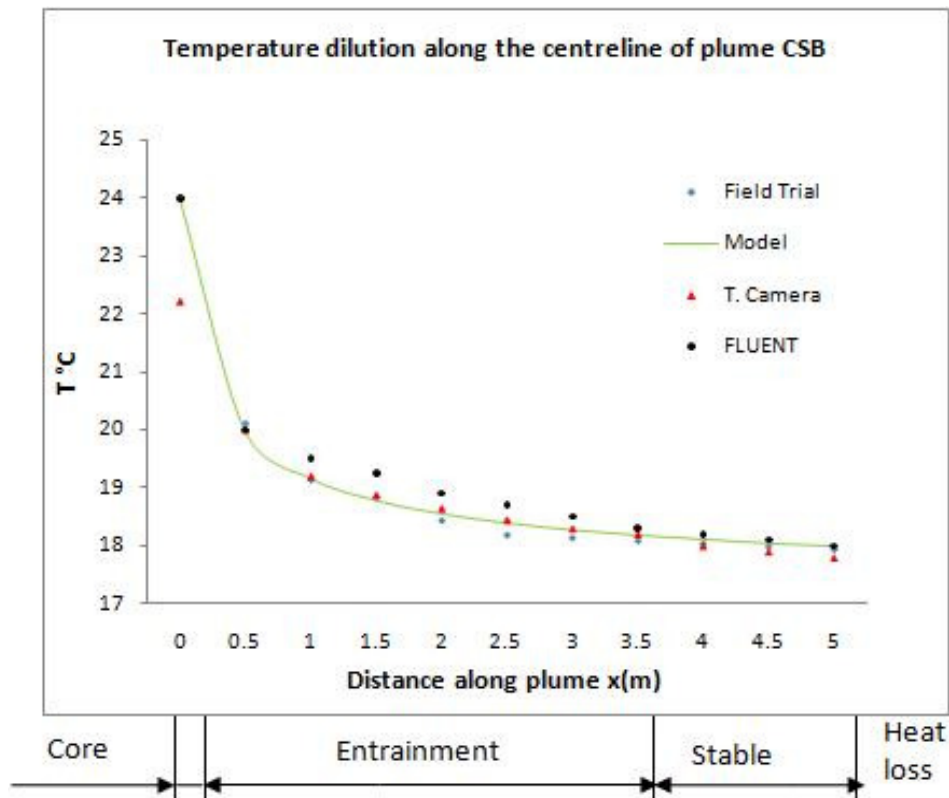


Figure 8.8: The structure of the heated surface discharge

The results of the various trials are shown in Figure 8.6 to validate the derived model against the other data. The solid line indicates the predicted model data whilst the symbols indicate the measured results. The trapezium indicates the field data temperature as measured by the thermocouples whereas the triangles indicate the field data measured by the thermal imaging camera and the round symbols present the FLUENT results. The derived model results are very close (96%) to the canal measured data. The FLUENT results also compare well to the measured canal data..

It must be noted that the thermal camera results show only the surface temperature of the discharge whereas the rest are calculations and measurements 75mm below the surface. Regardless there is a good match with all the results.

8.2.2 Temperature dilution across the centreline of plume

The temperature across the centreline of plume (y axis) will be presented in this section. The comparison is made between the mathematical results of Equation 7.7 and field trial measured data. The Lateral temperature distributions are determined at ten locations of (x) starting from

0.5m to 5m from the outfall on the centreline of plume (discharge layer). The results are then validated against the canal measured data with the comparisons shown in Figures 8.9 – 8.18. For each figure the symbols indicates to the canal measured data, while the solid line indicates to the mathematical results.

It can be seen from the figures that the general form of the graphs are similar, with the mathematical model predicting lower temperatures than measured in some cases. This is certainly the case with measurements less than 3metres from the outlet but not so with extended distances. In fact the higher measured temperature appeared in the region outside the plume, as in figure 8.9, where the width of the plume is around $y = \pm 40\text{cm}$. Any measured temperature beyond that point should be equal to the canal ambient temperature of 17°C as been modelled but because of the air ambient temperature the canal surface temperature indicates a slightly higher temperature of around 17.15°C . Similarly for the remaining profiles with the plume width equal to $y = \pm 1\text{m}$ and greater the predicted results are in a good fit with canal measured data, as shown in the figures 8.14 – 8.18.

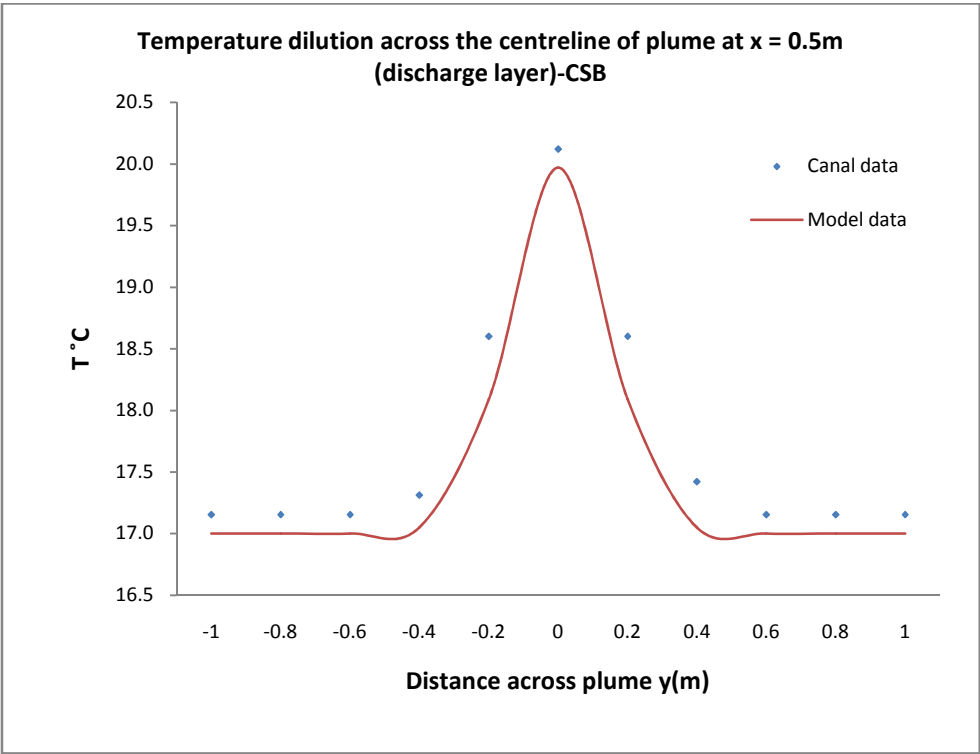


Figure 8.9: Temperature across the centreline of plume for the mathematical model and field trial at $x = 0.5\text{m}$

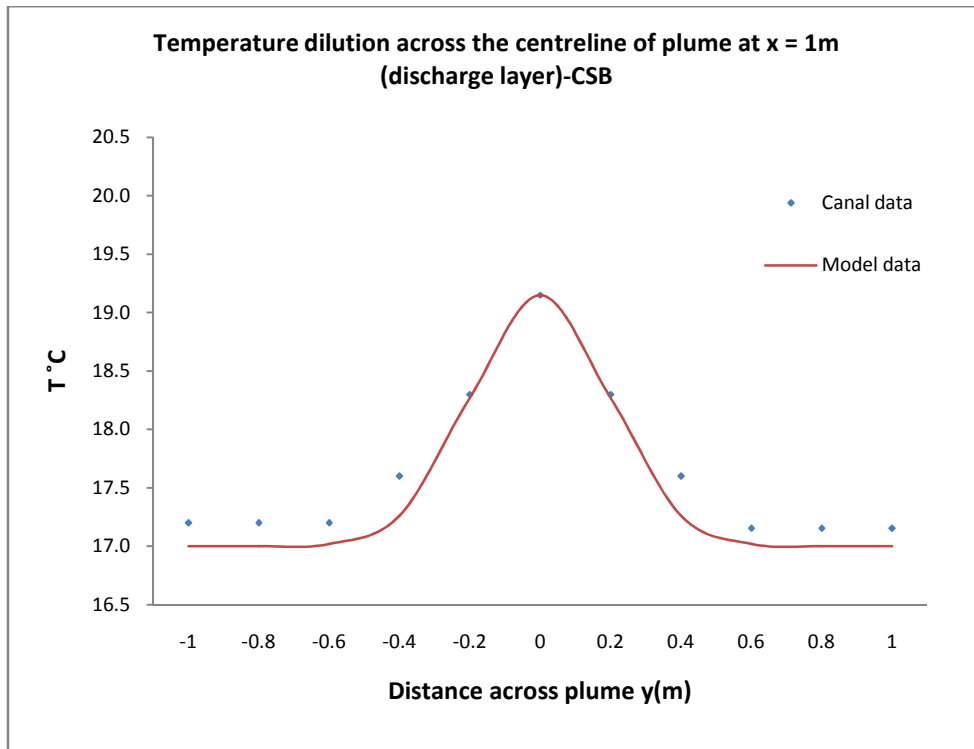


Figure 8.10: Temperature across the centreline of plume for the mathematical model and field trial at x = 1m

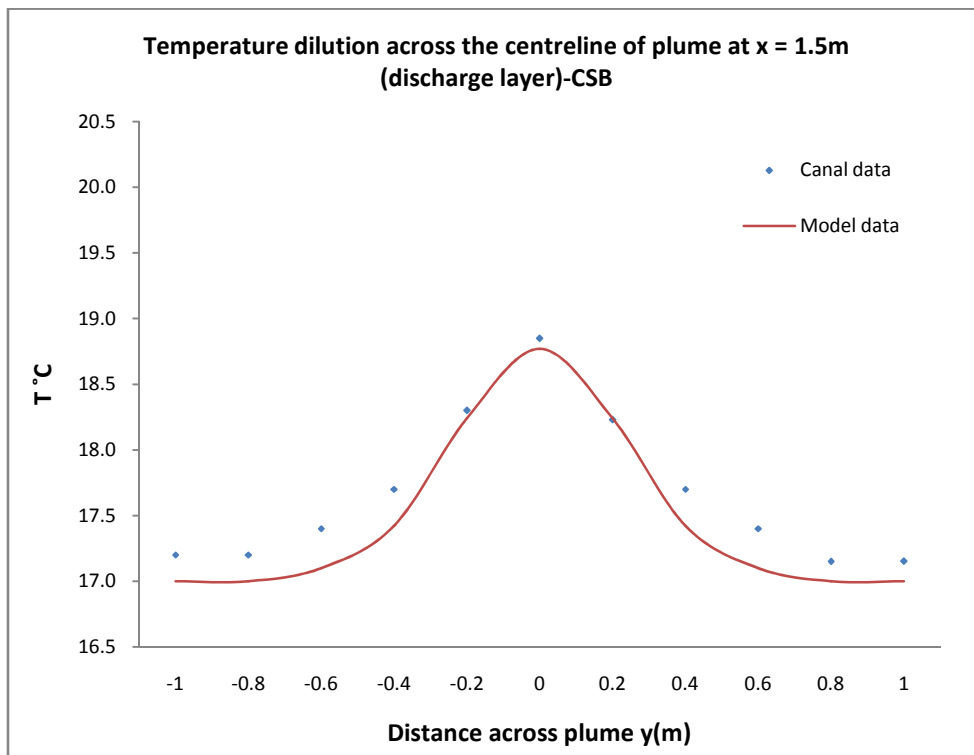


Figure 8.11: Temperature across the centreline of plume for the mathematical model and field trial at x = 1.5m

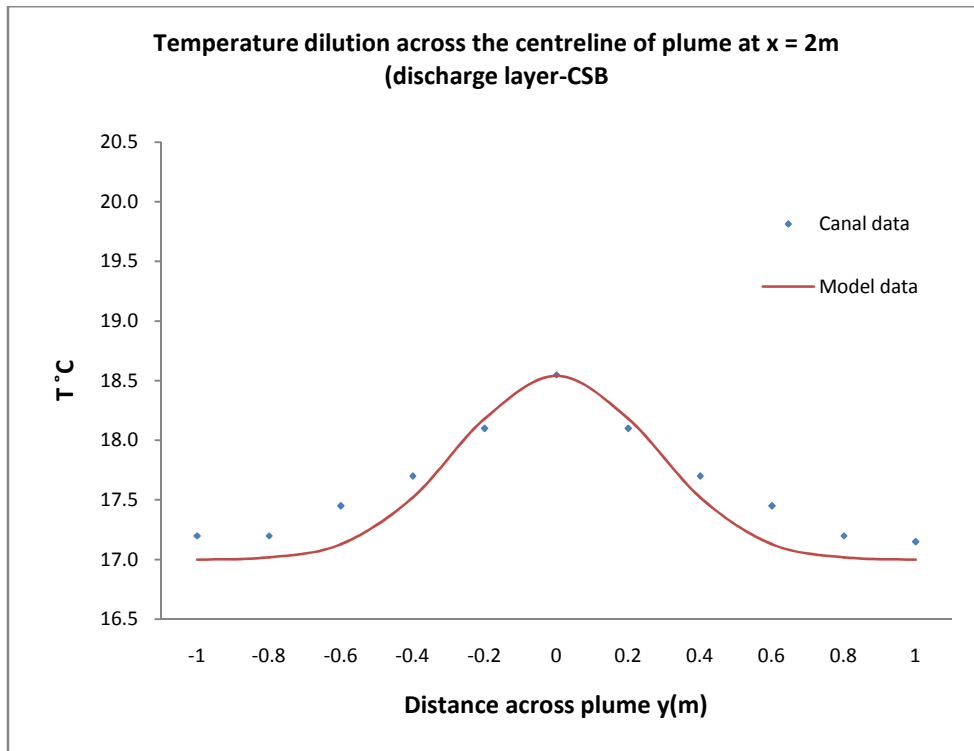


Figure 8.12: Temperature across the centreline of plume for the mathematical model and field trial at x = 2m

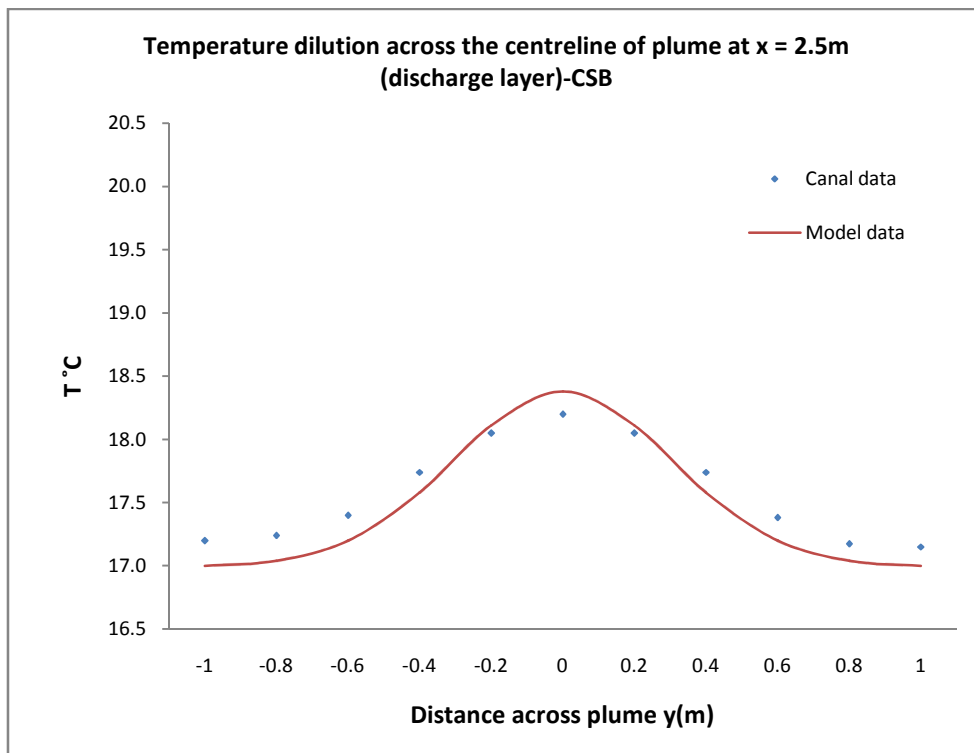


Figure 8.13: Temperature across the centreline of plume for the mathematical model and field trial at x = 2.5m

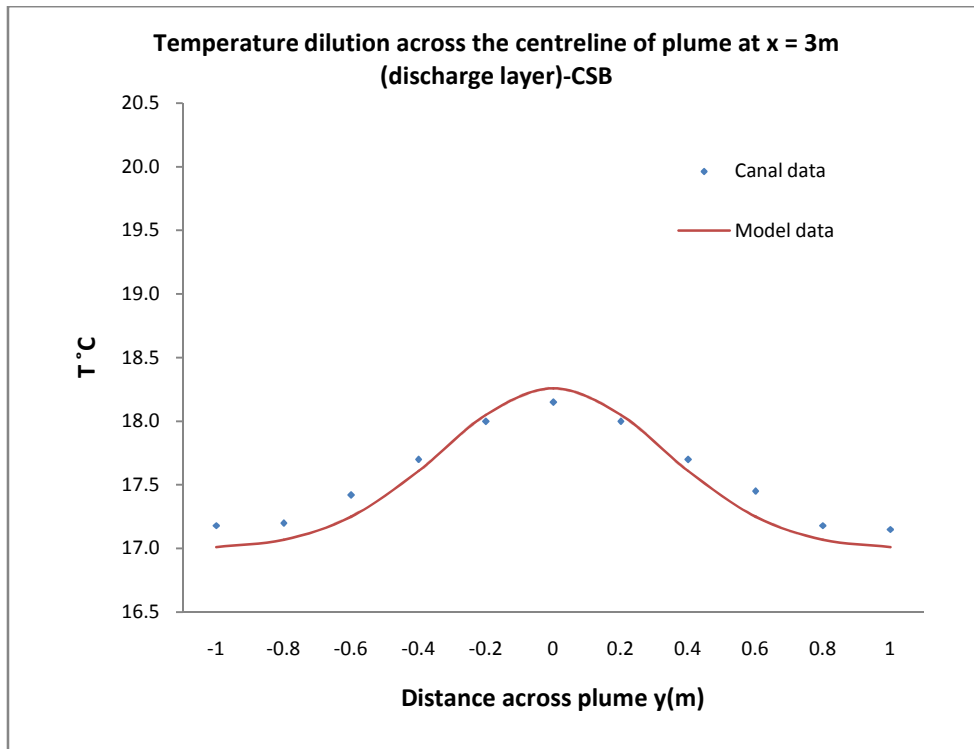


Figure 8.14: Temperature across the centreline of plume for the mathematical model and field trial at x = 3m

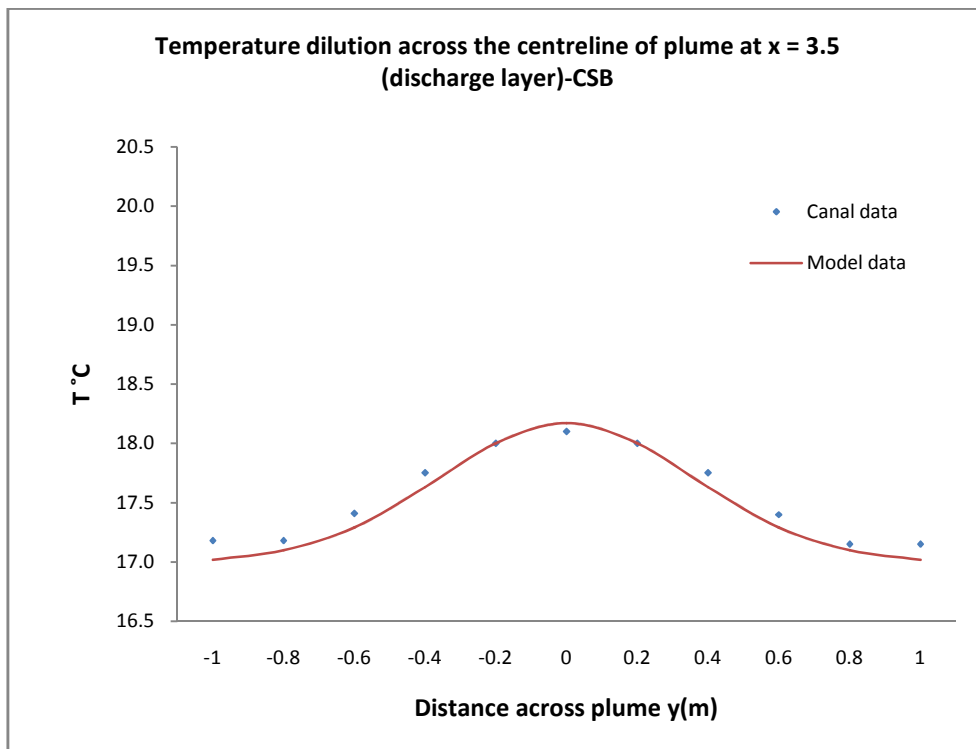


Figure 8.15: Temperature across the centreline of plume for the mathematical model and field trial at x = 3.5m

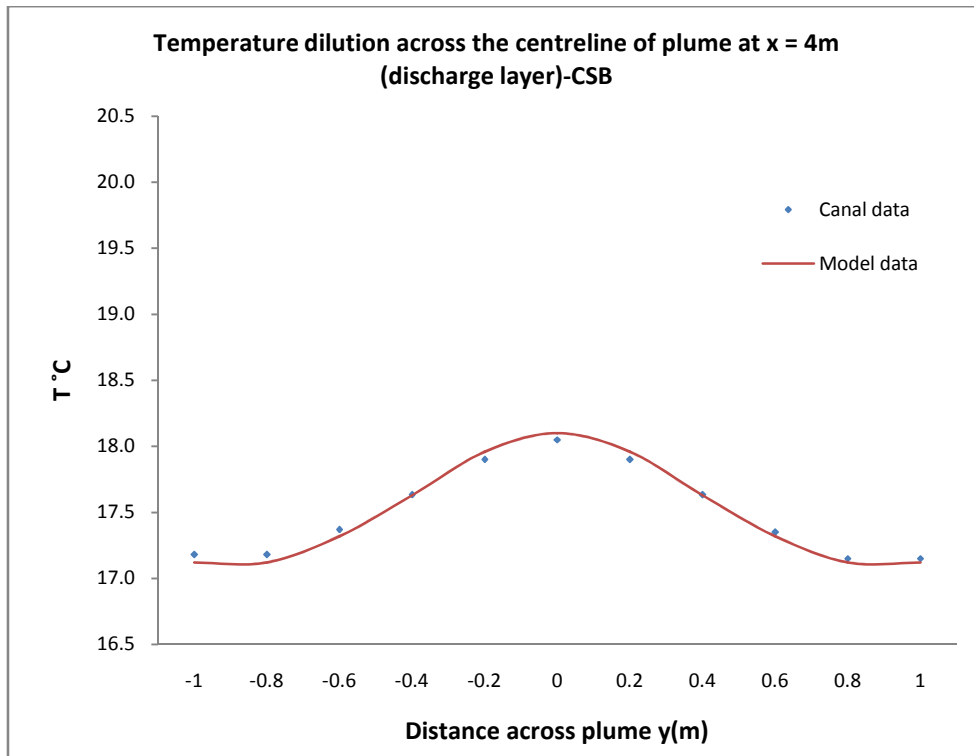


Figure 8.16: Temperature across the centreline of plume for the mathematical model and field trial at x = 4m

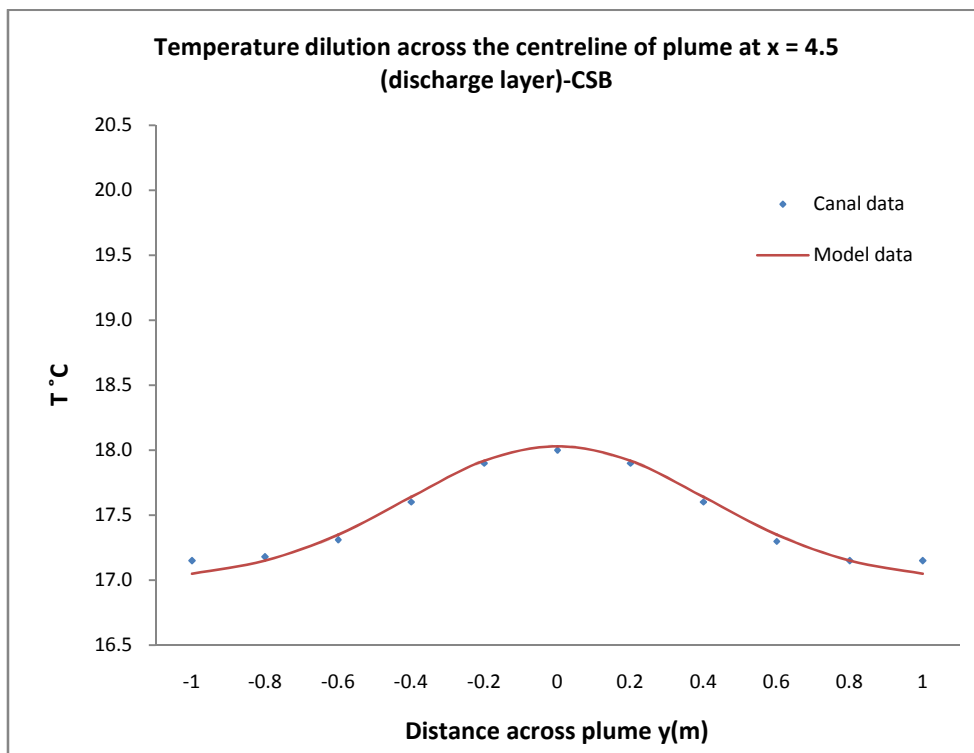


Figure 8.17: Temperature across the centreline of plume for the mathematical model and field trial at x = 4.5m

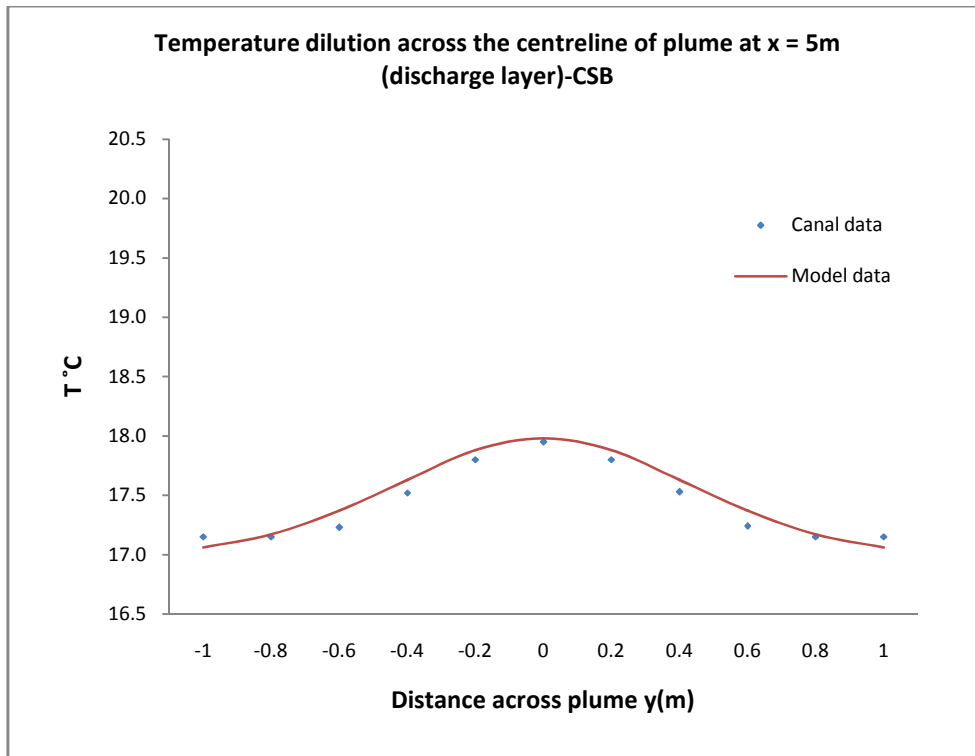


Figure 8.18: Temperature across the centreline of plume for the mathematical model and field trial at $x = 5\text{m}$

8.2.3 Temperature distribution on a plane on the centreline of plume

The two dimensional Equation 7.7 was derived for the case of surface thermal discharge to predict the temperature distribution on a plane on the centreline of plume. In the previous two sections temperature profiles are presented one dimensional along a single line. In this section heat diffusion profiles on a plane at the discharge layer will be presented.

By substituting all the parameters into Equation 7.7 the result will be the heat diffusion profile as illustrate in Figure 8.19a, while Figure 8.19b shows the heat diffusion measured from the field trial. The area around the discharge point in Figure 8.19b is bigger than that in Figure 8.19a. The reason is the number of measured data used to create the field trial image is small in relation to those used to create the mathematical model figure (dense data). The turbulent diffusivity is influenced by the width of the discharge plume so the bigger the value used for D results in a wider plume as shown in Figure 8.20 whereas Figure 8.21 shows the heat diffusion profiles for a smaller value of turbulent diffusivity D .

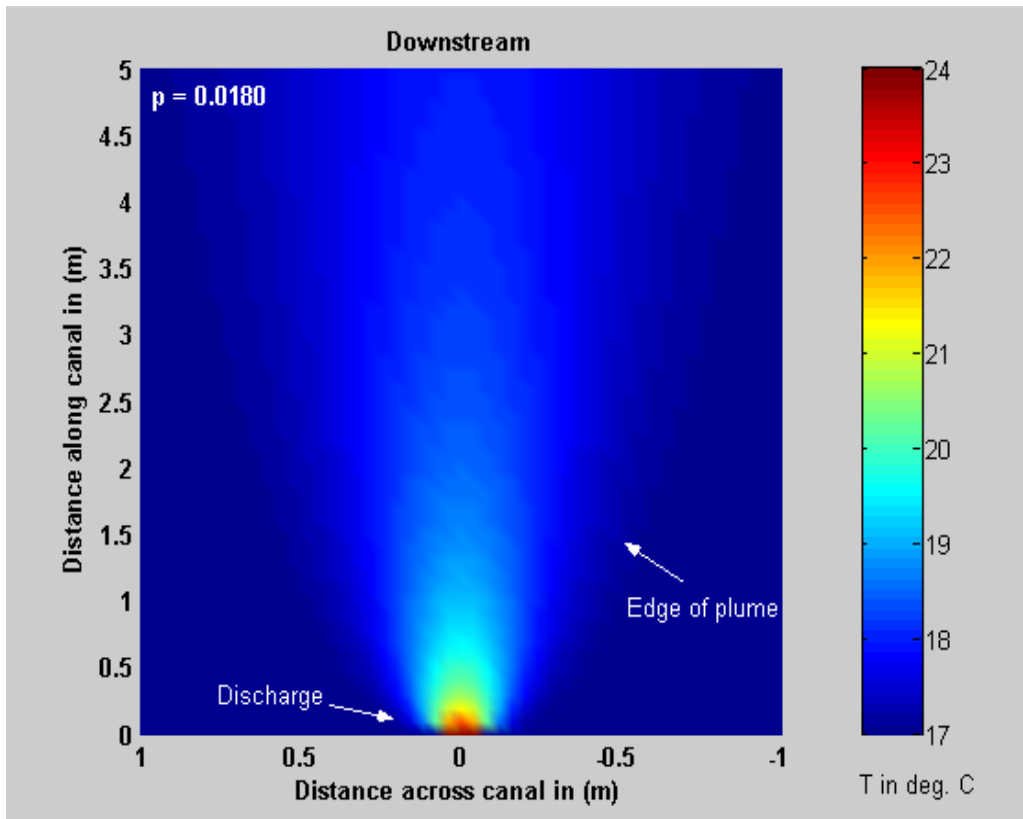


Figure 8.19a: Heat diffusion on a plane at the discharge layer for $p = 0.018\text{m}$ (mathematical model)

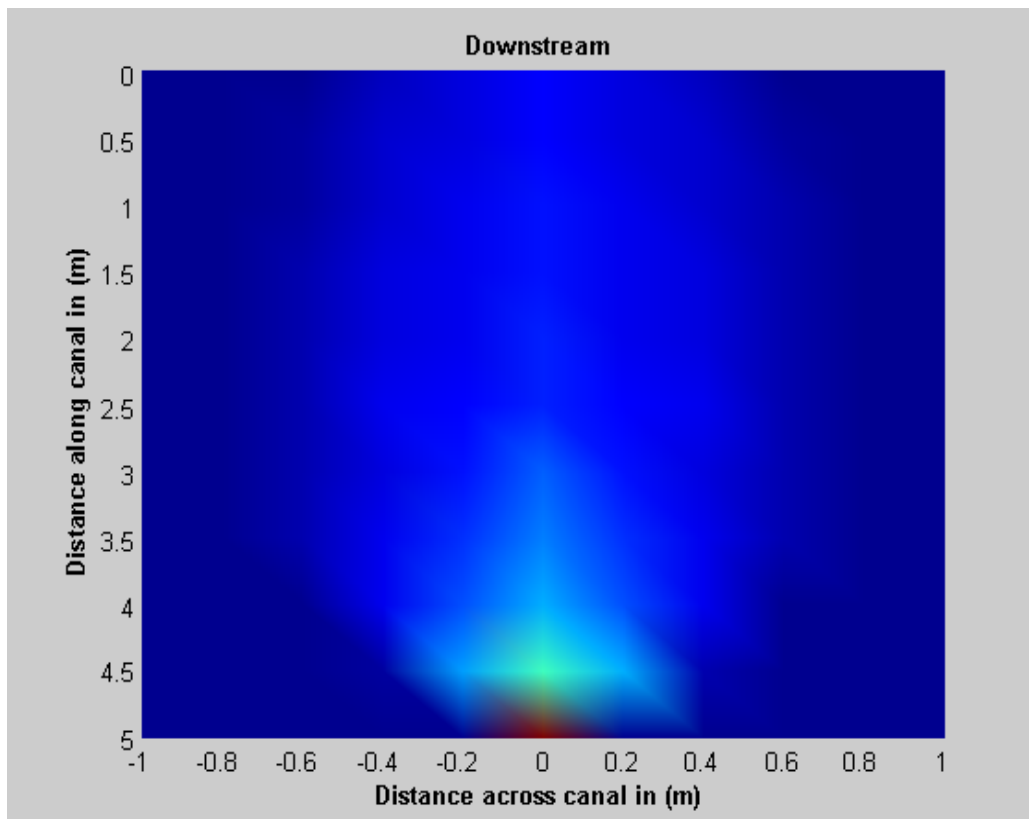


Figure 8.19b: Heat diffusion on a plane at the discharge layer (field trial measured data)

In Figure 8.20 the lateral turbulent diffusivity D_y is higher than that in Figure 8.19a, thus the discharge plume is wider, whilst the temperature along the centreline is lower. In addition the plume half width will be bigger. The increased in value of D_y parameter “ $p = D_y/U$ ” will increase as can be seen from that shown in Figure 8.19a “ p ” is 0.018m whilst in Figure 8.20 “ p ” is 0.052.

Figure 8.21 show a sharp, penetrating, shape of plume as the lateral turbulent diffusivity is small and the discharge heated water moves faster through the water. In addition the temperature dilution along the centreline of the plume is slower than the other two previous cases.

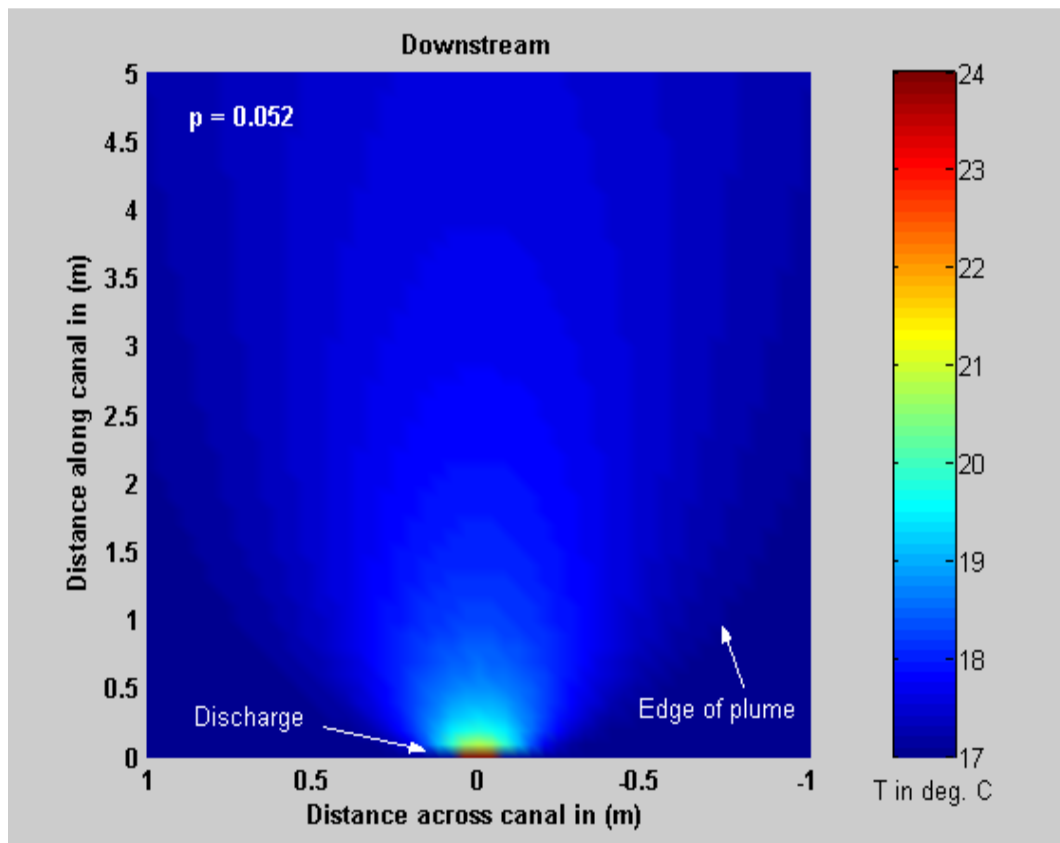


Figure 8.20: Heat diffusion on a plane at the discharge layer for $p = 0.052m$

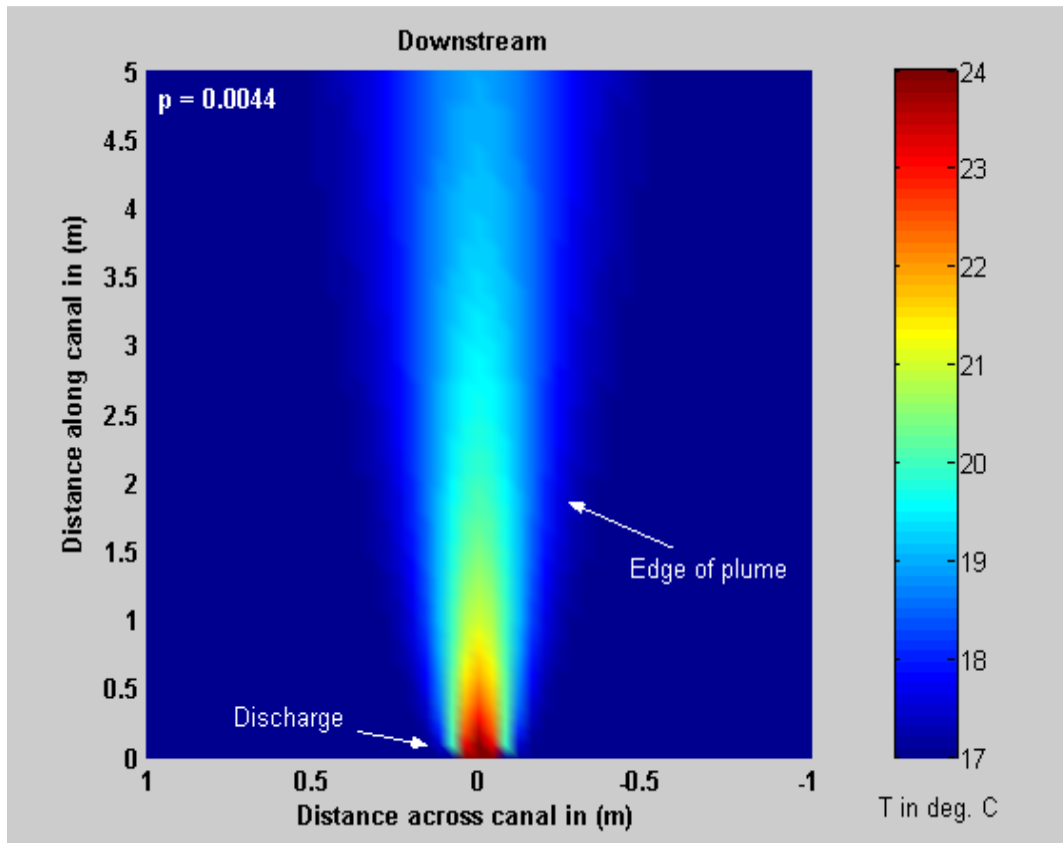


Figure 8.21: Heat diffusion on a plane at the discharge layer for $p = 0.0044\text{m}$

8.3 Submerged Discharge

In submerged discharge system the results and discussion are based on the mathematical models derived from the laboratory empirical data and the canal site studies. As the thermal images record only surface temperature profiles these will not form the focus of this section, neither will the FLUENT results. However the thermal images obtained on the canal site studies along with their digital images are presented and discussed in Chapter 5 whereas the FLUENT results are presented in detail within Chapter 6. As such the field trial experiments, laboratory experiments and the mathematical model are considered in depth. In the current study of submerged discharge the investigation will focus on behaviour of thermal plume below the free surface of canal. From the total of 24 experiments (see Table 4.1) carried out in the laboratory randomly five have been selected for presentation and to compare them against the mathematical results, Table 8.2. The five selected runs have different densimetric Froude Numbers of ($F_d14.39$, $F_d41.48$, $F_d38.59$, $F_d31.51$ and $F_d16.29$) for runs number (4, 6, 18, 20 and 23) respectively. With the graphs presented in this section the symbol denotes to the experimental measured data and the solid line graph denotes the predicted data.

Run	Pipe diameter D_o (cm)	z_o (cm)	H (cm)	$\Delta T = T_o - T_a$	U_o (cm/s)	Buoyancy g' (cm/s ²)	Q (cm ³ /s)	Buoyancy flux B_o (kgm ² /s ²)	Momentum Flux M_o (m ⁴ /s ²)	Length scale Lm (cm)	Re	Fd
4	1.2	14.5	21.5	7	19	1.45	21.48	31.22	408.07	16.25	2496.19	14.39
6	1.2	13.5	21.5	3	34	0.56	38.43	21.52	1306.74	46.86	4060.84	41.48
18	0.8	15.5	21.5	8	45	1.70	22.61	38.43	1017.36	29.06	4028.81	38.59
20	1.2	7.7	16.7	8	45	1.70	50.87	86.48	2289.06	35.59	6043.21	31.51
23	0.8	11.5	18	8	19	1.70	9.55	16.23	181.37	12.27	2551.58	16.29

Table 8.2: The five experimental runs reported in the current study

8.3.1 Plume Path Line

In surface discharge model the centreline of plume is a straight line located along the centre of discharge pipe just below the free surface of receiving water. In submerged discharge the centreline of the plume is located at a certain distance below the free surface of the receiving water and progressively rising to the surface dependant on the number of parameters. In general the entrainment section above the plume centreline will increase thus causing the plume to move to the surface. The centreline of the plume when it is moving to the surface is called the “path line”. The upward curve of the path line will be faster with reducing depth of discharge and to zero when the discharge pipe is located on the surface. This feature means the depth of the discharge pipe z_o becomes one of the main parameter influencing the plume path line, as shown in Equation 7.10b. This equation is derived from the experimental trails performed in laboratory, at each trial the path line of the plume is determined then the equation of the curve is formulated. Figure 8.22; demonstrate the theoretical results obtained from the Equation 7.10b compared with the experimental measured data. The figure explains the exact path of the centreline of the plume from the discharge pipe to the free surface of the receiving water. The measured experimental data of the path line and the obtained theoretical data are tabulated in Appendix 8. The smallest densimetric Froude Number of the experiments run moves to surface before the other runs as demonstrated in Figure 8.22, whilst the biggest densimetric Froude Number run is not the last one to move to the surface. The reason is the bed effect which delays the path line deflection towards the surface as the plume tends to remain attached to the bed. A slight difference can be seen between the laboratory experimental data and the predicted data but in general the results are agreeable.

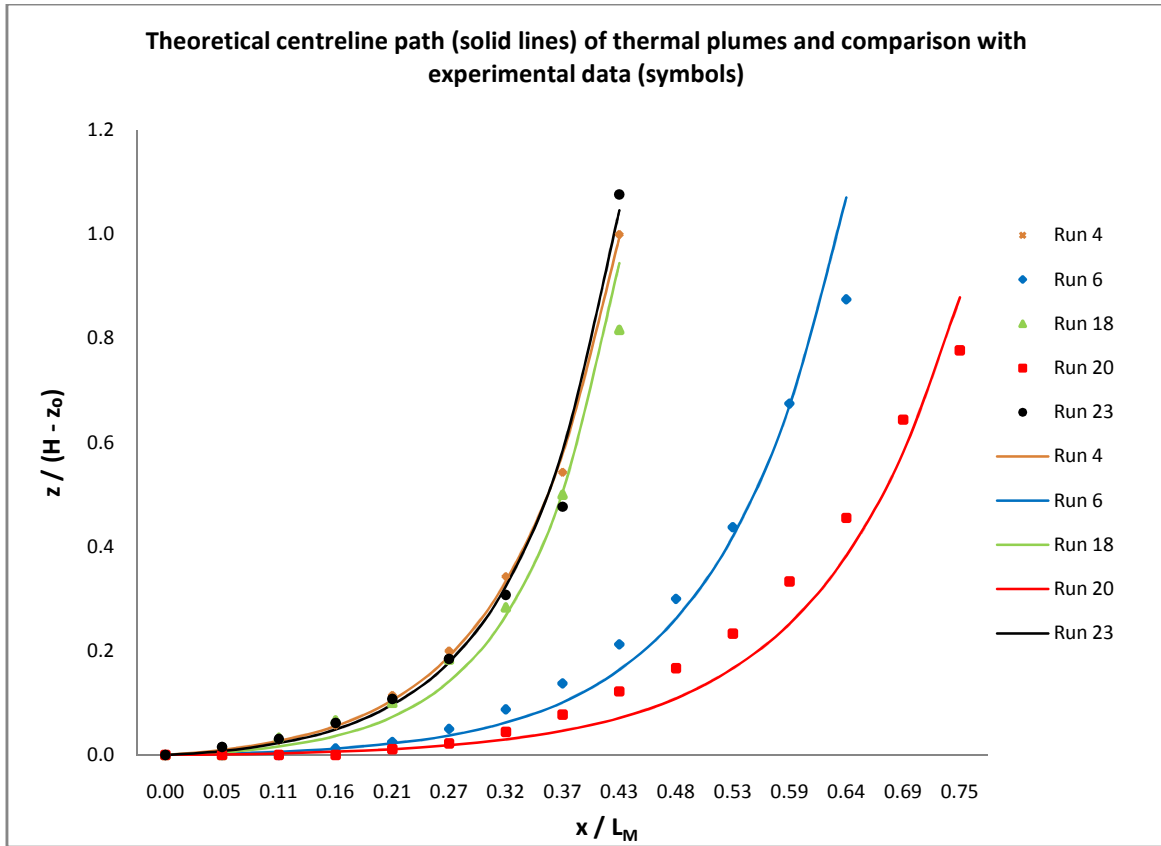


Figure 8.22: Theoretical plume path line and comparison with experimental data (x is divided by the biggest value of L_M for Run 6)

8.3.2 Temperature along Plume Path Line

In the previous section the thermal plume path line below the free surface of the receiving water has been discussed. In the following sections the path line profile will be discussed with reference to its temperature and velocity characteristics. Equation 7.12b has been formulated to predict the temperature along the path line of the thermal plume. The resulting temperature is along the path line curvature and as a function of the longitudinal axis x . Figure 8.23 shows temperature decay along the path line of the plumes as illustrated in Figure 8.22. Figure 8.24 illustrates the dimensionless value of temperature decay along the path lines in Figure 8.22. The dimensionless Figure 8.24 can be better understood if it is compared to the path lines in Figure 8.22. The experimental and theoretical temperatures along the plume path line are presented in the Appendix 9. The three experiment runs have the same discharge temperature of 25°C but the dilutions are different, see Figure 8.23. Run 20; see Table 8.2 has the highest temperature along its path line whereas its F_d is lower than that in run 18 and bigger than that in run 23. The reason is the depth of the discharge pipe in this run is smaller than the other

two runs; therefore the plume moves faster in a straight line and dissipates its temperature more slowly. Run 23 has a smaller discharge velocity so is moving more slowly through the receiving water and losing its temperature faster. Run 18 has the same discharge velocity as run 20 but it has got a smaller discharge pipe diameter and bigger depth which reduce the flow rate and thus the temperature.

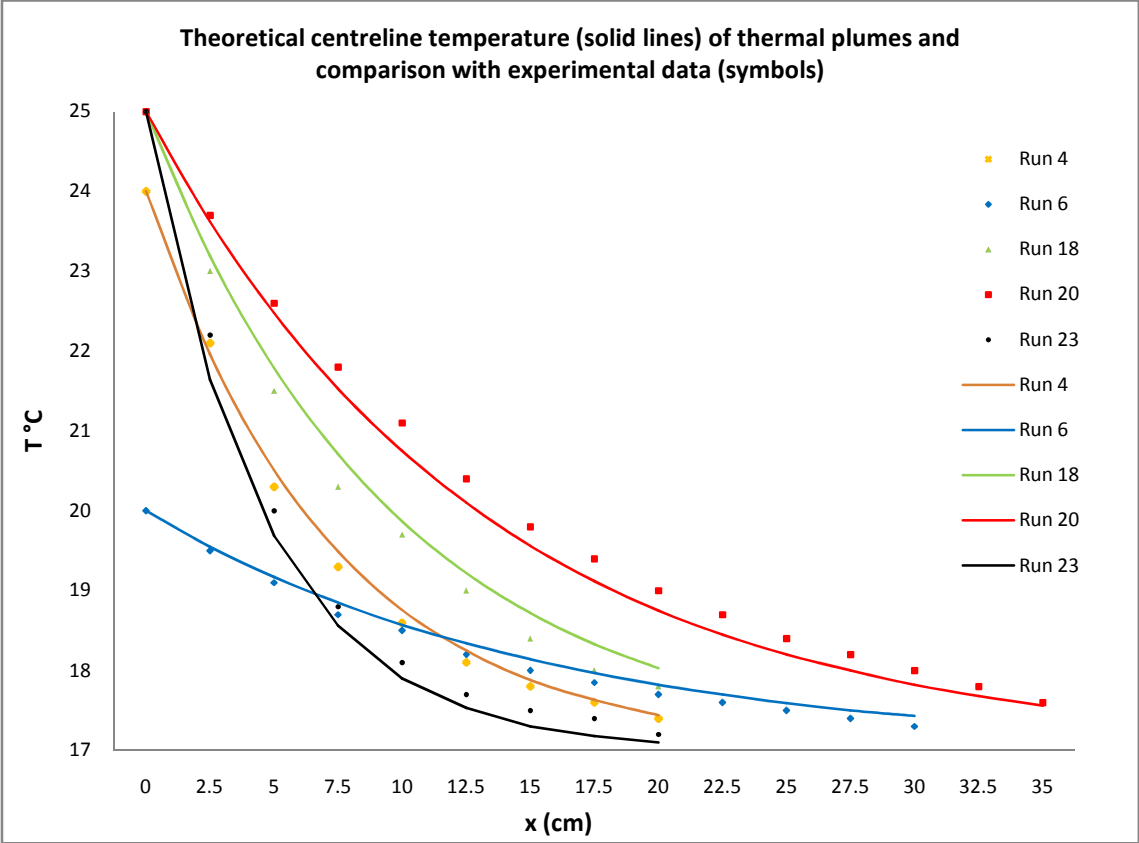


Figure 8.23: Theoretical temperature along plume path line and comparison with experimental data

Figure 8.24 show how fast the temperature reduced, so the fastest temperature decay is with run 23 (F_d 16.29) whilst the lowest temperature dissipation in run 20 (F_d 31.51).

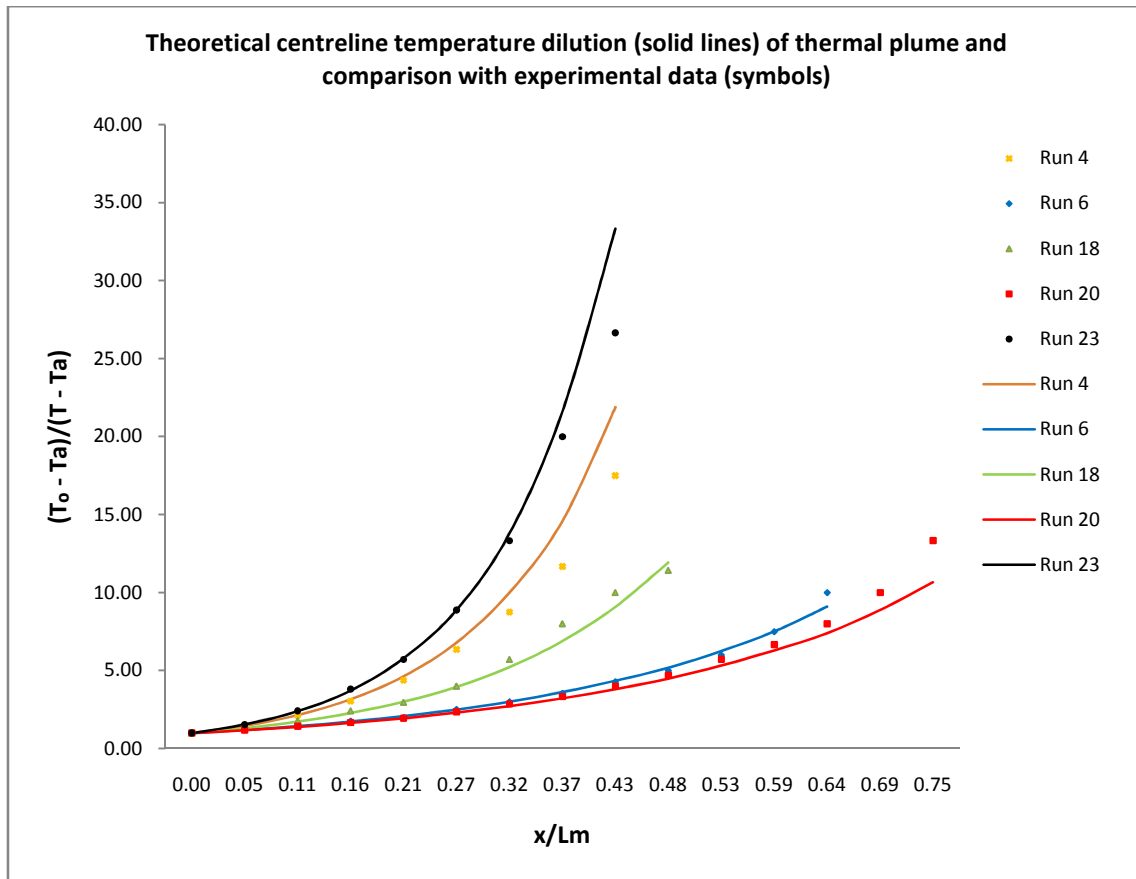


Figure 8.24: Theoretical temperature decay along plume path line and comparison with experimental data (x is divided by the biggest value of L_M for Run 6)

8.3.3 Velocity along Plume Path Line

Figure 8.25 shows the velocity profiles along the path line of the plume as determined by the Equation 7.13b and then compared with the data collected from the experiments. The full data related to these profiles is presented in the Appendix 10. The discharge velocity is the main parameter influencing the velocity profile of the thermal plume. In Figure 8.25 runs 4 ($F_d 14.39$) and 23 ($F_d 16.29$) have the same discharge velocity 19cm/s and different discharge depth and densimetric Froude Number. Therefore the path line velocity for run 23 is relatively higher than that in run 4. The runs 18 ($F_d 38.59$) and 20 ($F_d 31.51$) also have same velocity whilst run 20 has a velocity along the plume path line that is higher than the velocity in run 18. The reason is the discharge pipe depth for run 20 is smaller than that in run 18. In addition the bed has an effect on the thermal plume such that it moves in a straight line as it remains attached to the bed and only after a certain distance does it then move towards the surface.

This can be clearly seen from the graphs with run 20 extending a further distance than the others.

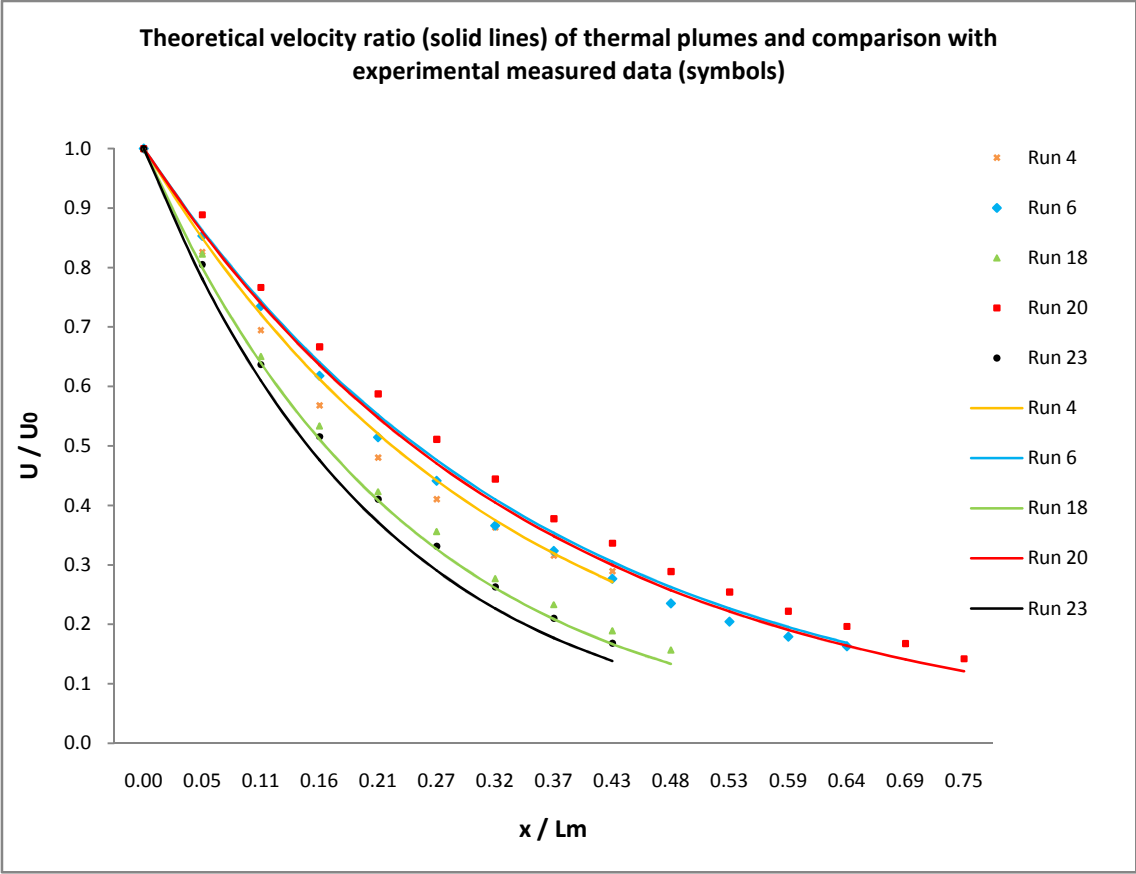


Figure 8.25: Theoretical velocity ratio along plume path line and comparison with experimental data (x is divided by the biggest value of L_M for Run 6)

The profiles presented in the last three sections are complicated as they are affected by more than one parameter. To improve understanding and clarity the following section considers each profile in turn and discusses the influence of the parameters as listed in Table 8.2.

8.3.4 Temperature across Plume Path Line

In the last two sections the temperature and velocity along the path line of the plume below the surface were discussed. In the current and the following section temperature and velocity across the path line will be discussed. The lateral plume distribution, or as it is called in some studies the distribution along the minor axis (y), has a Gaussian profile. Equation 7.14b has been derived to determine temperature distribution across the path line and aims to represent

the Gaussian profile. Figures 8.26 to 8.30 illustrate the temperature profiles across the thermal plume at four different distances ($x = 5\text{cm}, 10\text{cm}, 15\text{cm} \text{ \& } 20\text{cm}$) from the discharge point and for different runs with different parameters. The figures are a comparison of theoretical and experimental results. The experimental and theoretical data that formed the figures are presented in Appendix 9. It is clear from the figures that the predicted data are close to the laboratory measured data, however in some cases (runs) that the measured data are bigger than the predicted data and vice versa. The reason for that is the turbulent flow which causes fluctuation on the frequency of the thermocouple resulting in variation of the temperature. Note that the mean temperature is used during all the parts of the current research. Figure 8.31 shows the temperature profiles for all the five runs at a distance 20cm from the discharge point. It is shown from the figure that temperature for run 20 at $x = 20$ is higher than the others temperature, whereas the run 23 has the lowest although it has a high discharge temperature. That is because the latter has a low densimetric Froude Number.

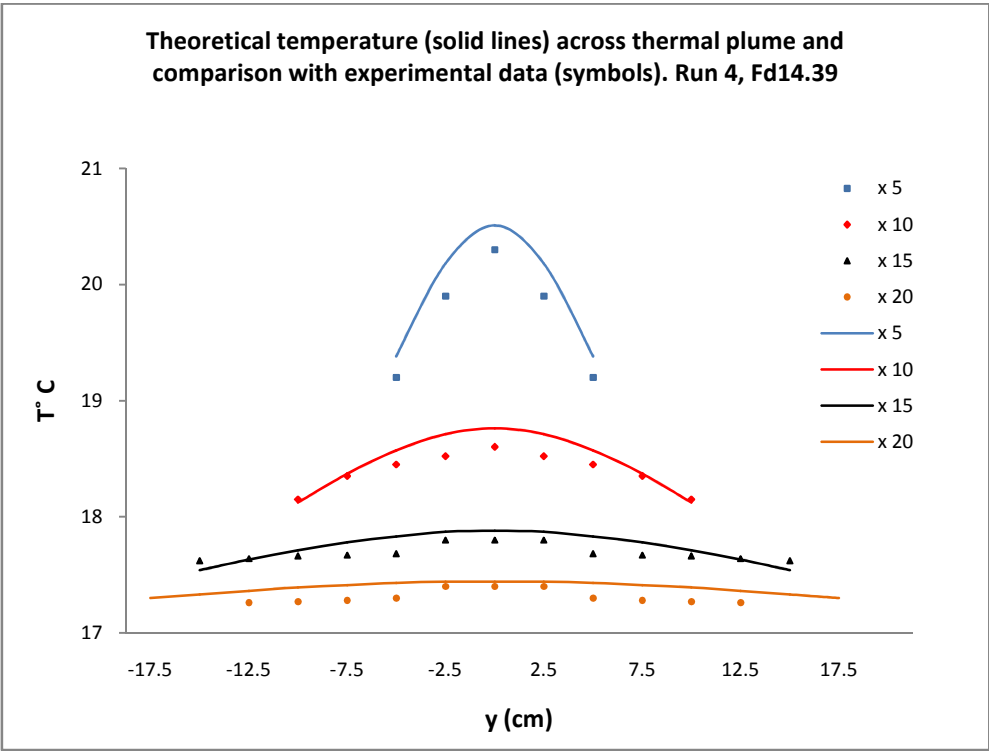


Figure 8.26: Theoretical temperature across plume path line and comparison with experimental data. Run 4, $F_d 14.39$

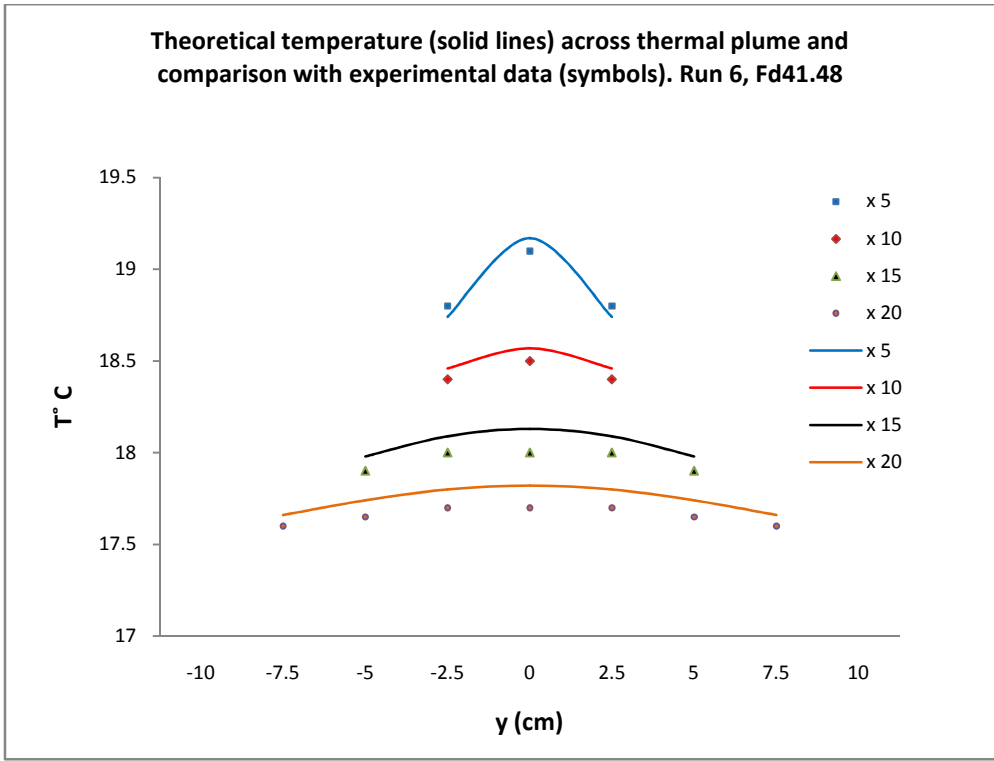


Figure 8.27: Theoretical temperature across plume path line and comparison with experimental data. Run 6, F_d 41.48

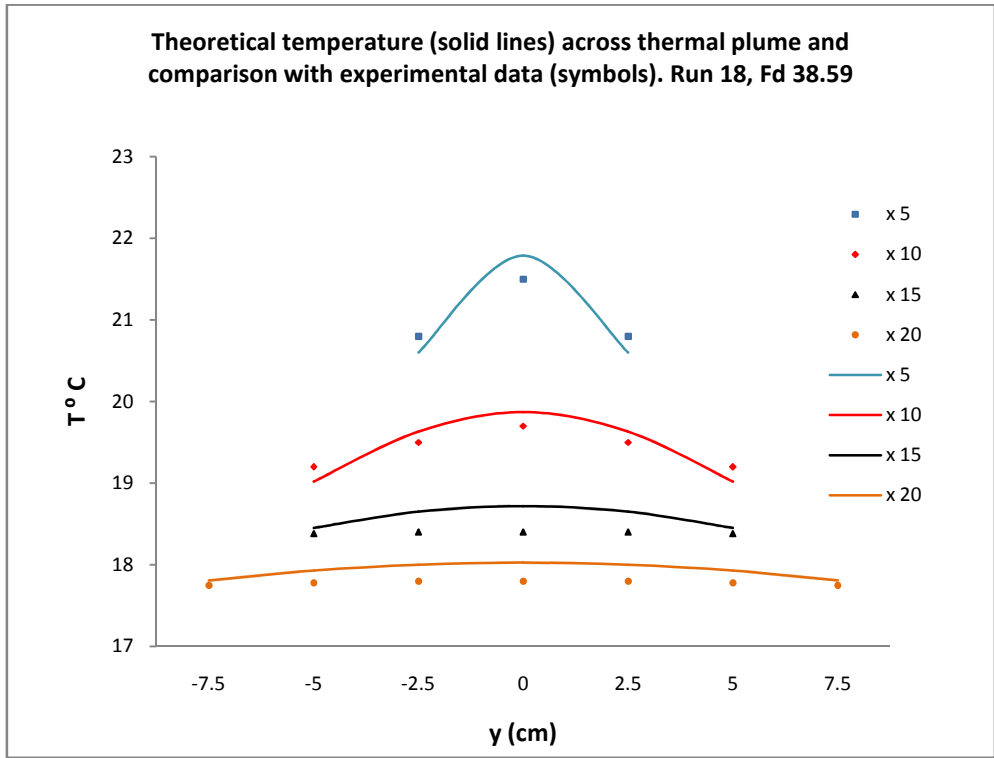


Figure 8.28: Theoretical temperature across plume path line and comparison with experimental data. Run 18, F_d 38.59

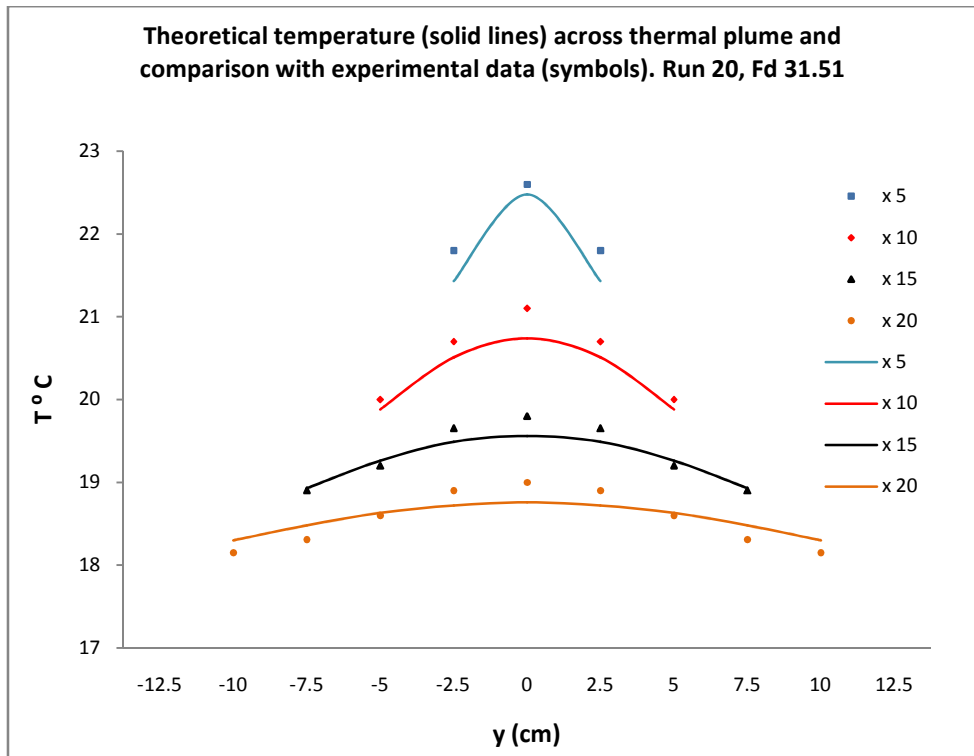


Figure 8.29: Theoretical temperature across plume path line and comparison with experimental data. Run 20, F_d 31.51

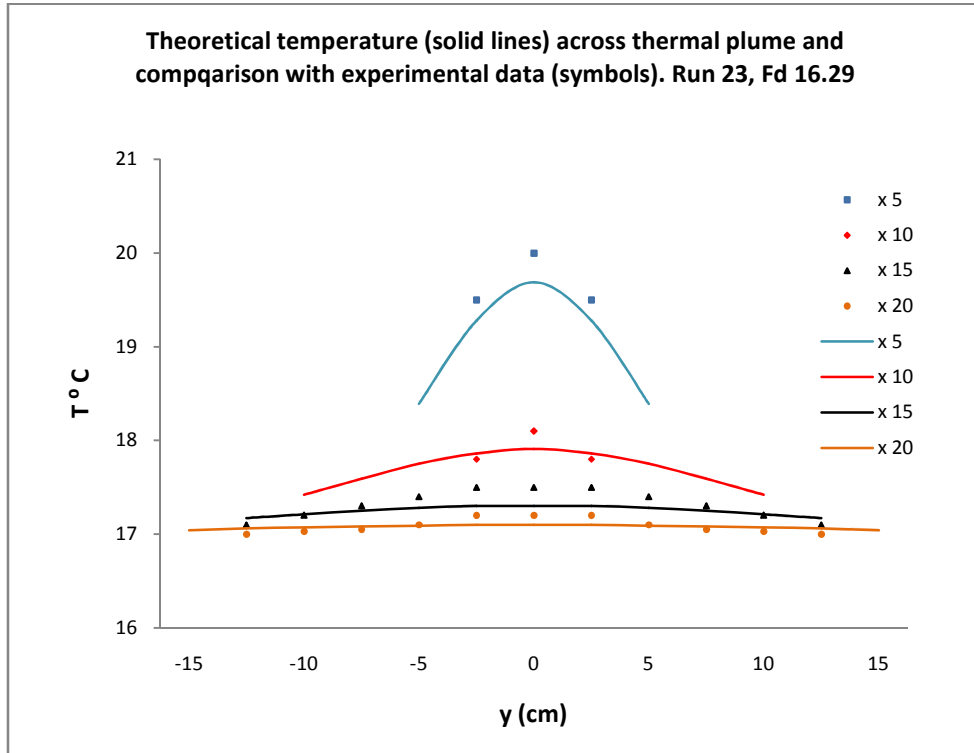


Figure 8.30: Theoretical temperature across plume path line and comparison with experimental data. Run 23, F_d 16.29

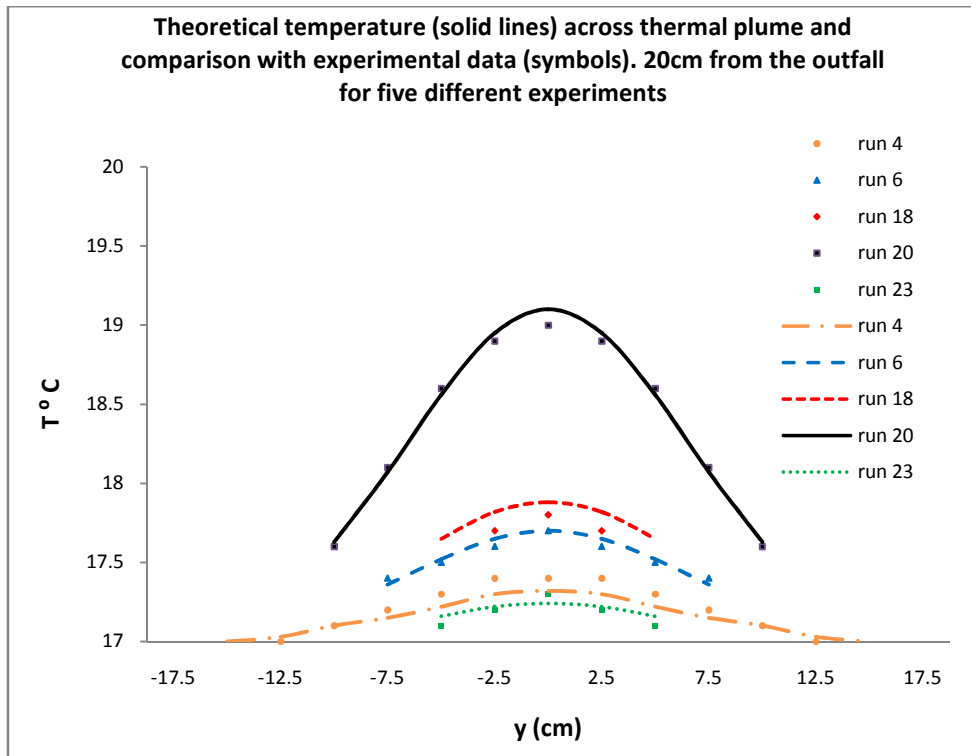


Figure 8.31: Theoretical temperature across plume path line and comparison with experimental data. 20cm from the outfall for five different experiments

8.3.5 Velocity across Plume Path Line

There is little doubt that the discharge velocity is the main parameter to influence the general path line velocity profile of the plume. The effect of the discharge velocity appears clearly in Figures 8.32 to 8.36. These figures demonstrate the velocity profiles across the thermal plume path line (plume width) for the theoretical model (Equation 7.15b) and their comparison with the experimental measured data. The figures show the velocity along the y axis for three different distances ($x = 5$, $x = 10$ and at the point when plume reaches the surface) along the path line of the plume. Appendix 10 contains tabulated velocities of the measured and theoretical data.

The comparisons of the experimental and predicted velocities in the following figures show a good fit. The peak value is on the centreline (path line) of the plume then this value reduced with expanding the plume laterally also with moving longitudinal downstream. Figure 8.34 present the results for the Run 18 at two position of x (5cm & 22.5cm) whilst at x(2.5cm) the results not presented because at this distance the plume is too narrow and not expanded laterally.

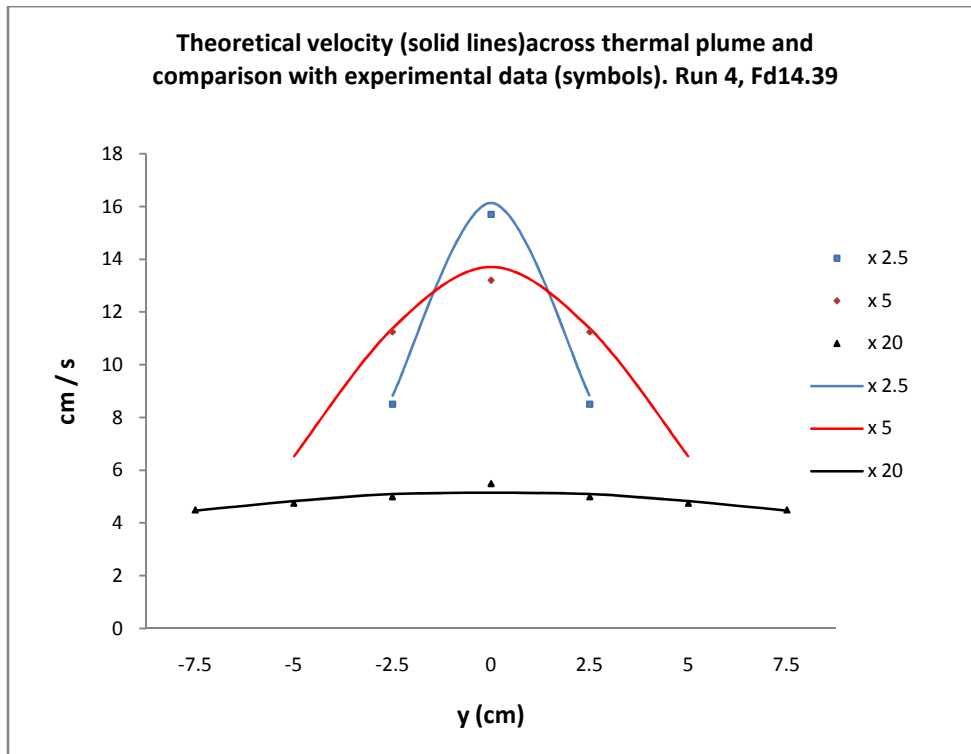


Figure 8.32: Theoretical velocity across plume path line and comparison with experimental data. Run 4, F_d 14.39

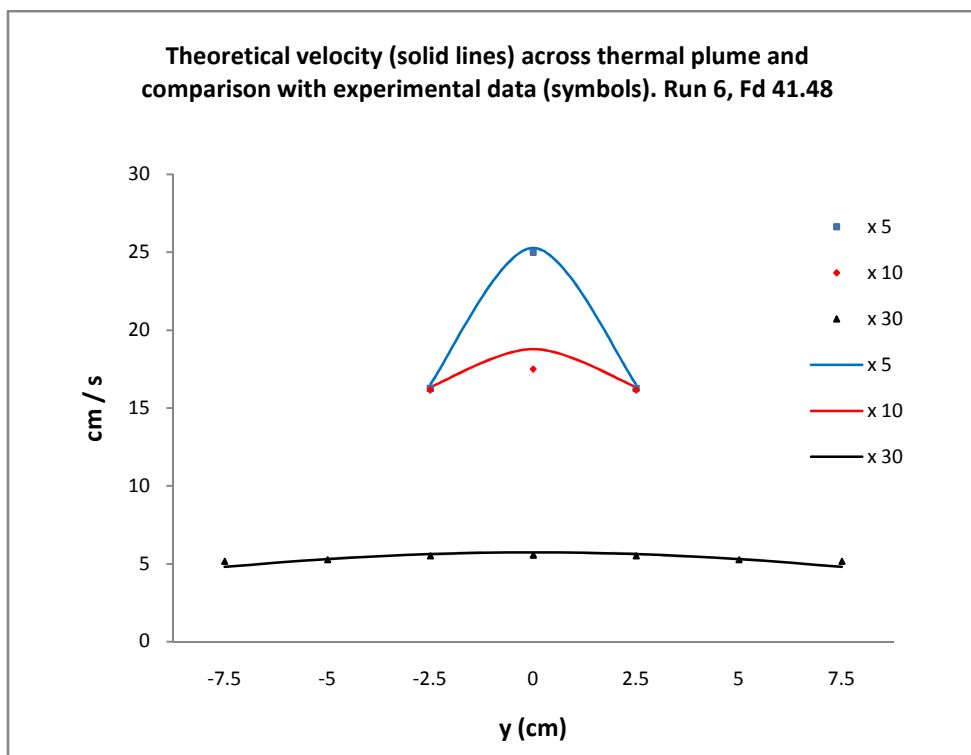


Figure 8.33: Theoretical velocity across plume path line and comparison with experimental data. Run 6, F_d 41.48

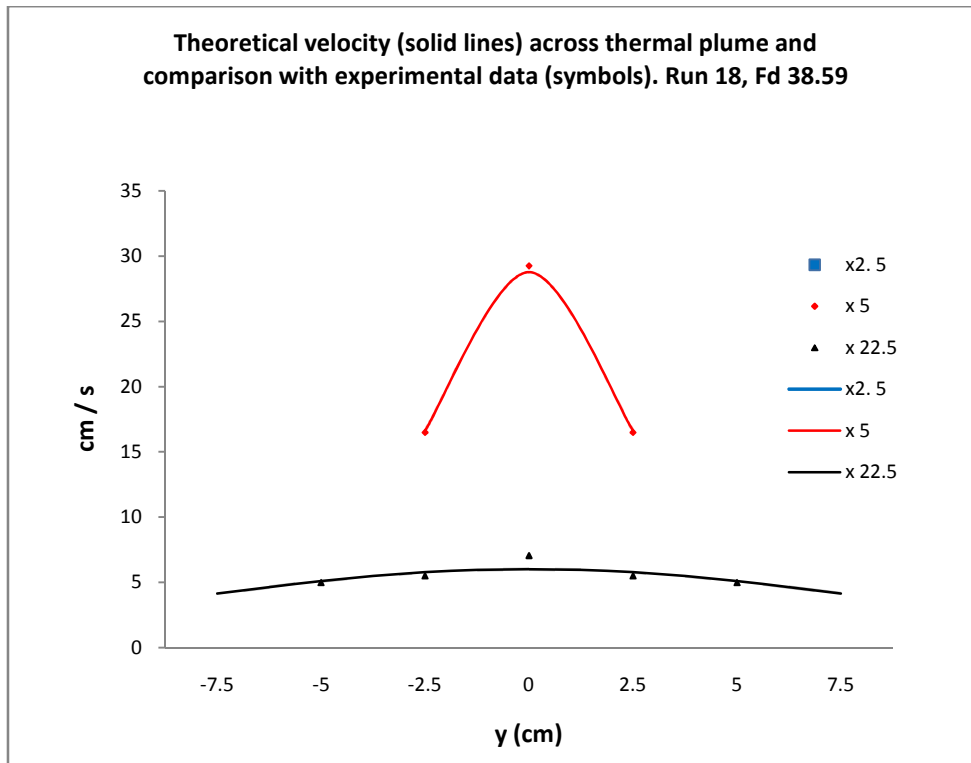


Figure 8.34: Theoretical velocity across plume path line and comparison with experimental data. Run 18, F_d 38.59

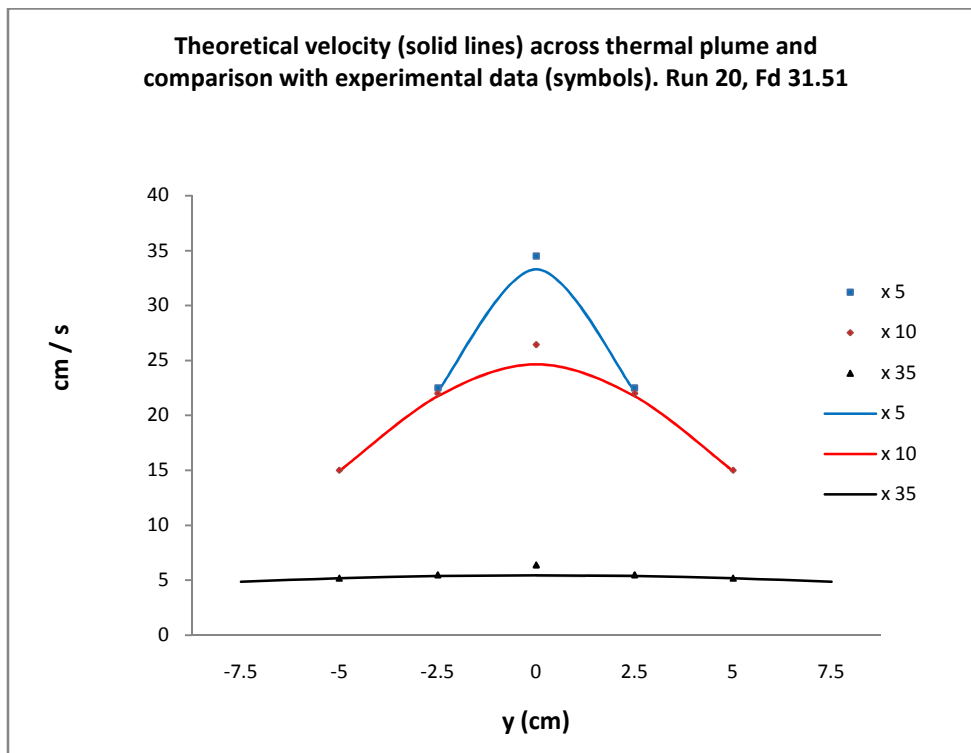


Figure 8.35: Theoretical velocity across plume path line and comparison with experimental data. Run 20, F_d 31.51

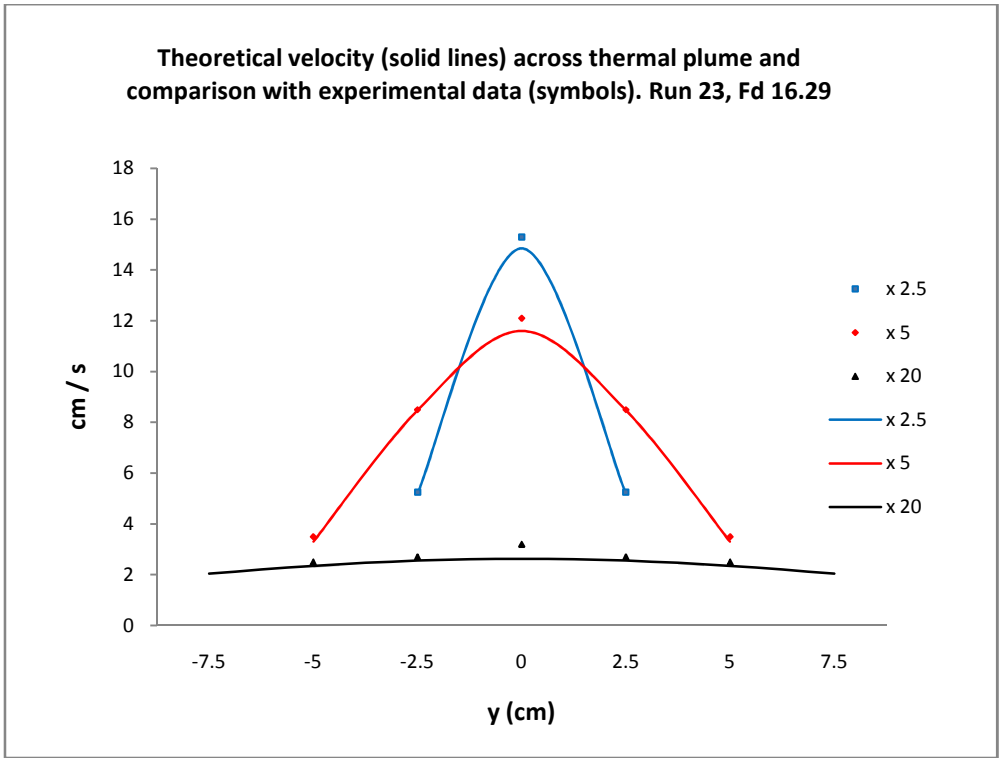


Figure 8.36: Theoretical velocity across plume path line and comparison with experimental data. Run 23, F_d 16.29

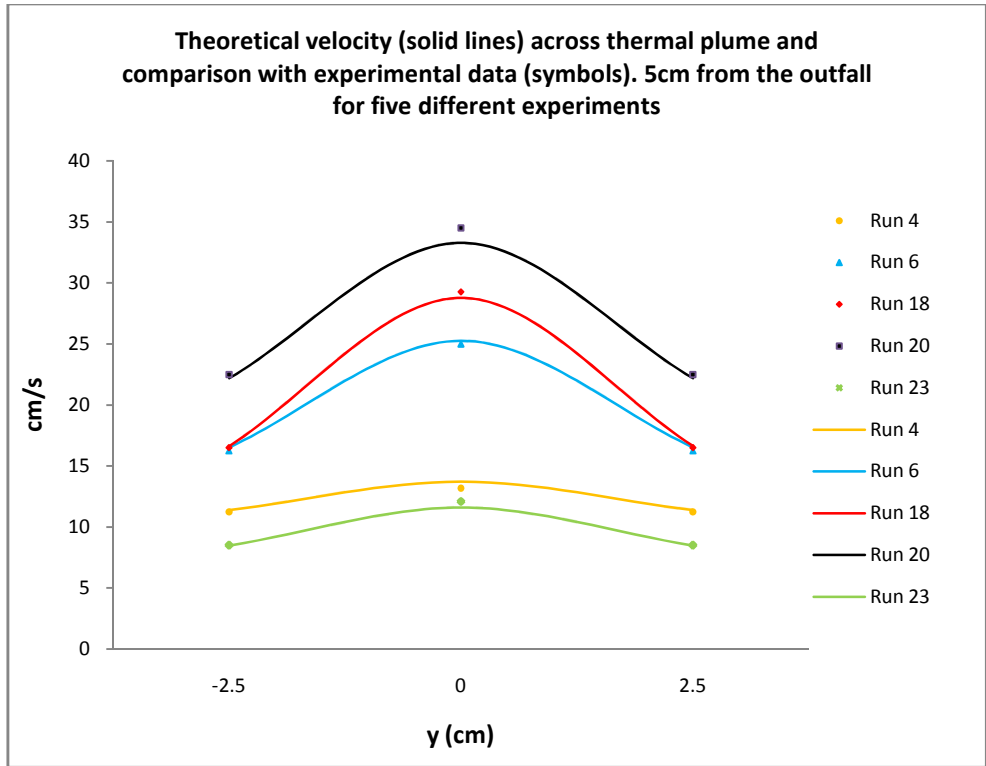


Figure 8.37: Theoretical velocity across plume path line and comparison with experimental data. 10cm from the outfall for five different experiments

Figure 8.37 demonstrates the lateral velocity distribution across the plume path line for the five experiments at distance $x = 10$ cm. The highest velocity profile shown from the figure is for run 20 (F_d 31.51) and the lowest profile for the run 4 (F_d 14.39). It worth mentioning that run 18 (F_d 38.59) has the same discharge velocity of run 20 and run 23 (F_d 16.29) has the same discharge velocity of run 4, whereas they have lower velocity profile. The high velocity profiles for the runs 20 and 23 are because their discharge pipes depths are small.

8.3.6 Model Validation - Comparison of the Models against Canal Measured Data

The following compares all the theoretical equations against the data collected from the British Waterways canal site tests. The surface discharge model investigated and tested against the Central Services Building CSB site is explained and discussed in Section 8.2 of Chapter 8. For the submerged discharge models discussed in the previous sections three different canal sites have been selected for comparison with the theoretical results – these been discussed earlier in Chapter 3. In all cases the canal site profiles along the plume path lines as present in the following figures are dimensionless. The x distance divided by the parameter length scale L_M , whereas the temperature and velocity are divided by their initial discharge values. The graphs shown in Figure 8.38 show the temperature and velocity profiles along the plume path line for the Canalside West for the experimental and theoretical studies whereas Figure 8.39 shows the profiles across the path line for a range of distances along the plume. The data in these figures is presented in Appendix 11. It is clear from the Figures 8.38 & 8.39 that the theoretical result represents the actual measured results very closely with 95% accuracy for the temperature and 90% for the velocity. The possible difference is because the turbulent flow which influence the reading of the thermocouple. In this instance the model is verified.

Figures 8.40 show the comparison of the theoretical results against experimental measured data at the Lockside canal site. The temperature and velocity along the path line of plume are presented in this figure and again there is a good similarity between the theoretical result and the actual –so validating the model again in this example. The temperature and velocity across the path line for this site are presented in Figure 8.41. The theoretical and the experimental obtained data along and across the plume path line for Lockside are available in Appendix 11.

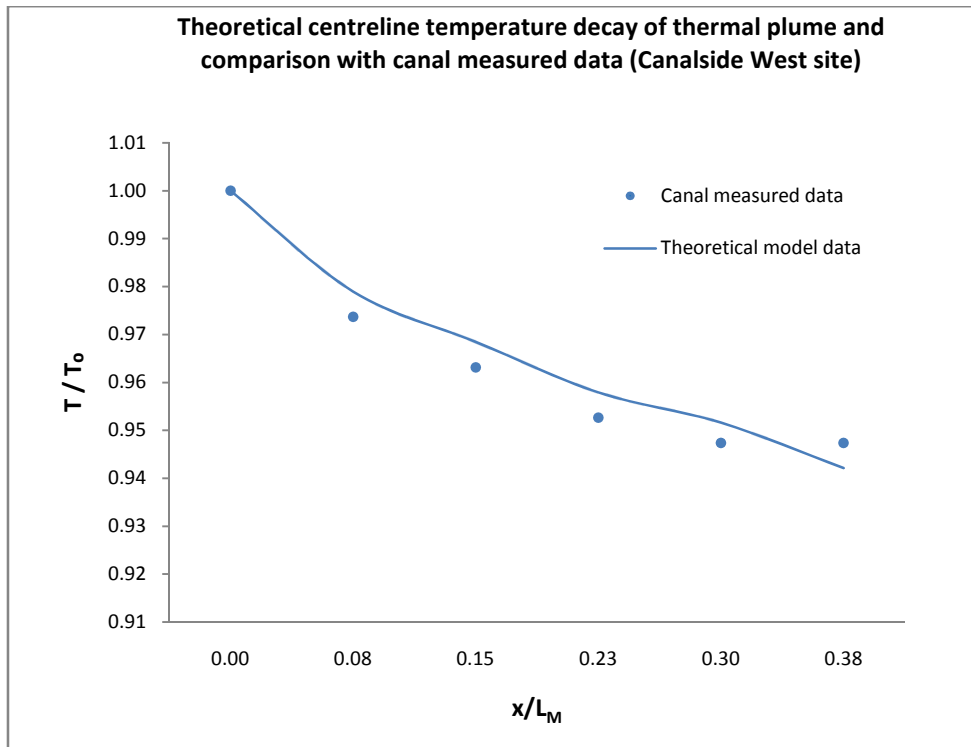


Figure 8.38a: Temperature along path line

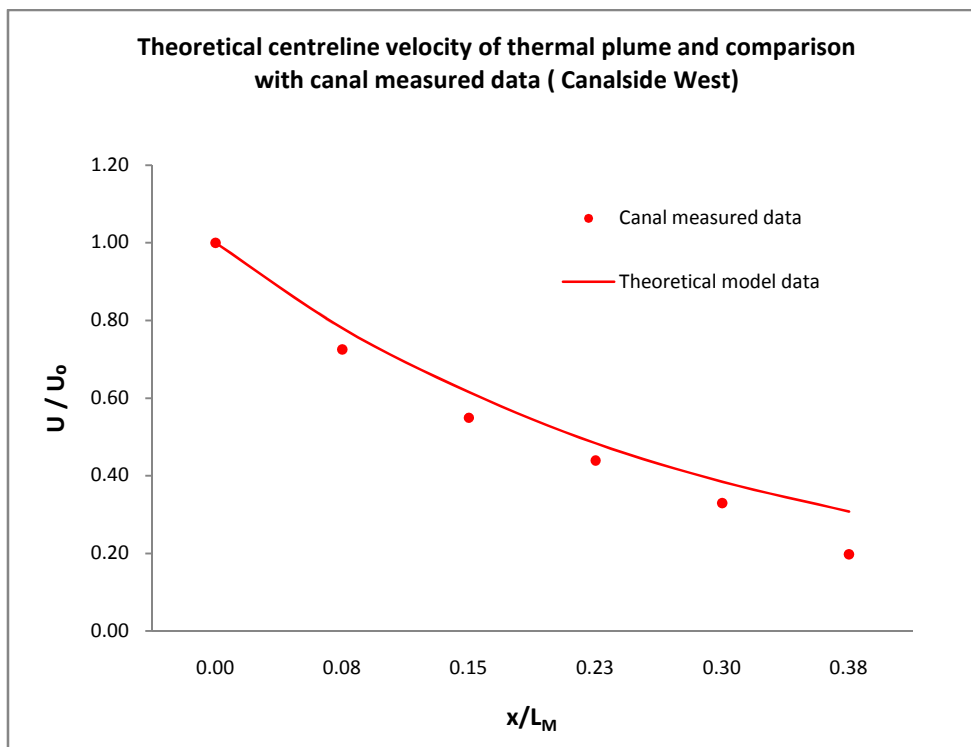


Figure 8.38b: Velocity along path line

Figure 8.38: Theoretical temperature and velocity along plume path line and comparison with canal measured data (Canalside West)

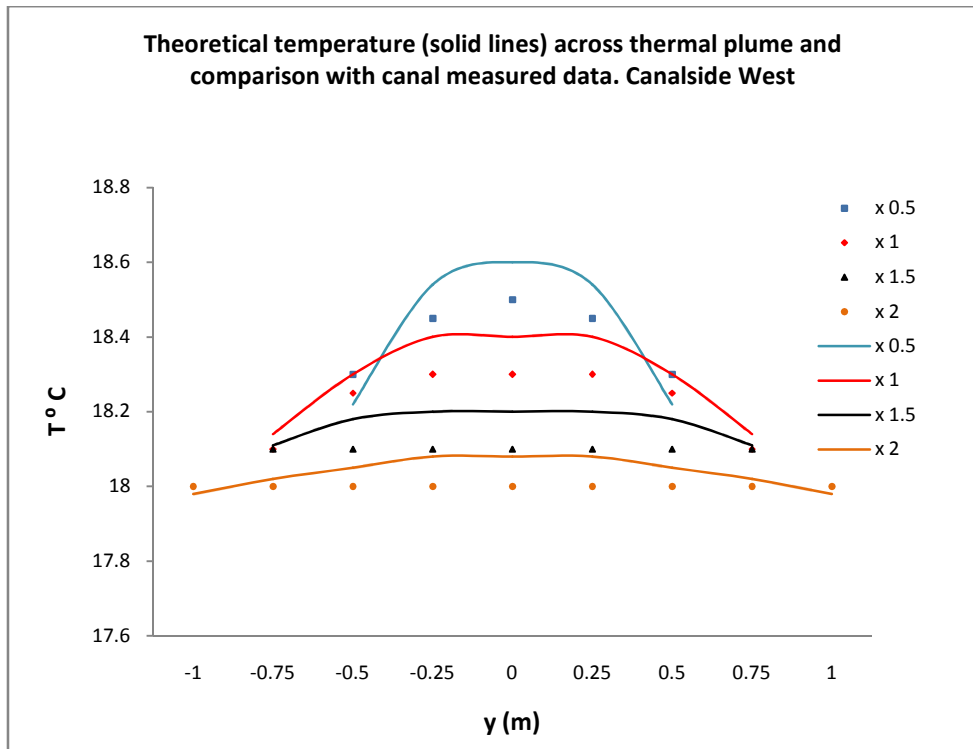


Figure 8.39a: Temperature across path line

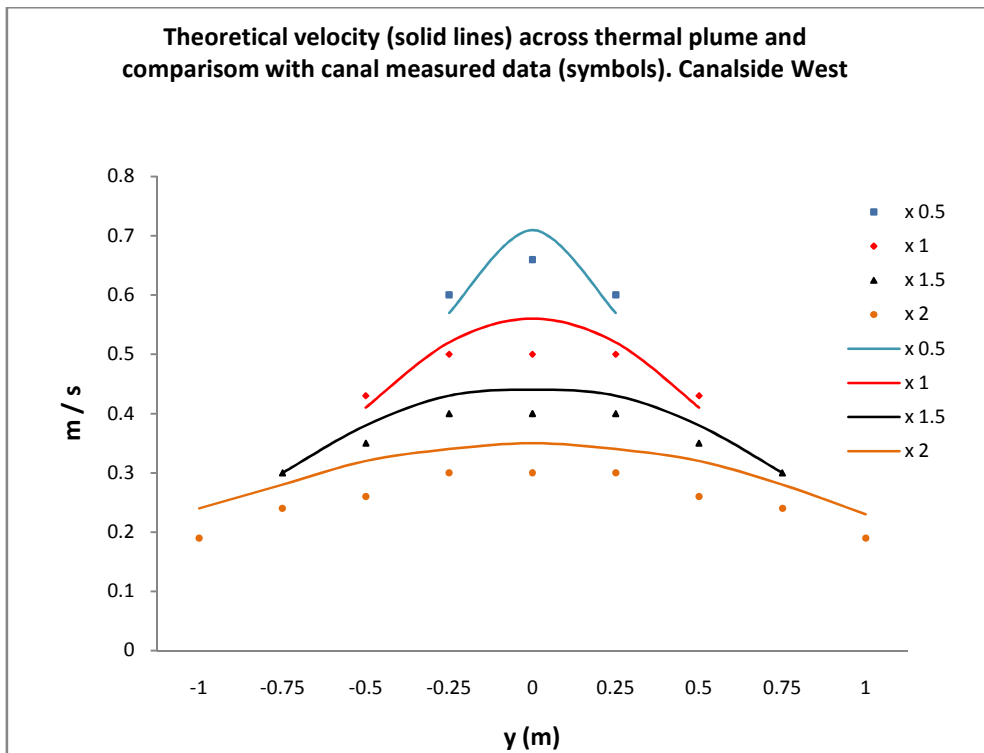


Figure 8.39b: Velocity across path line

Figure 8.39: Theoretical temperature and velocity across plume path line and comparison with canal measured data (Canalside West)

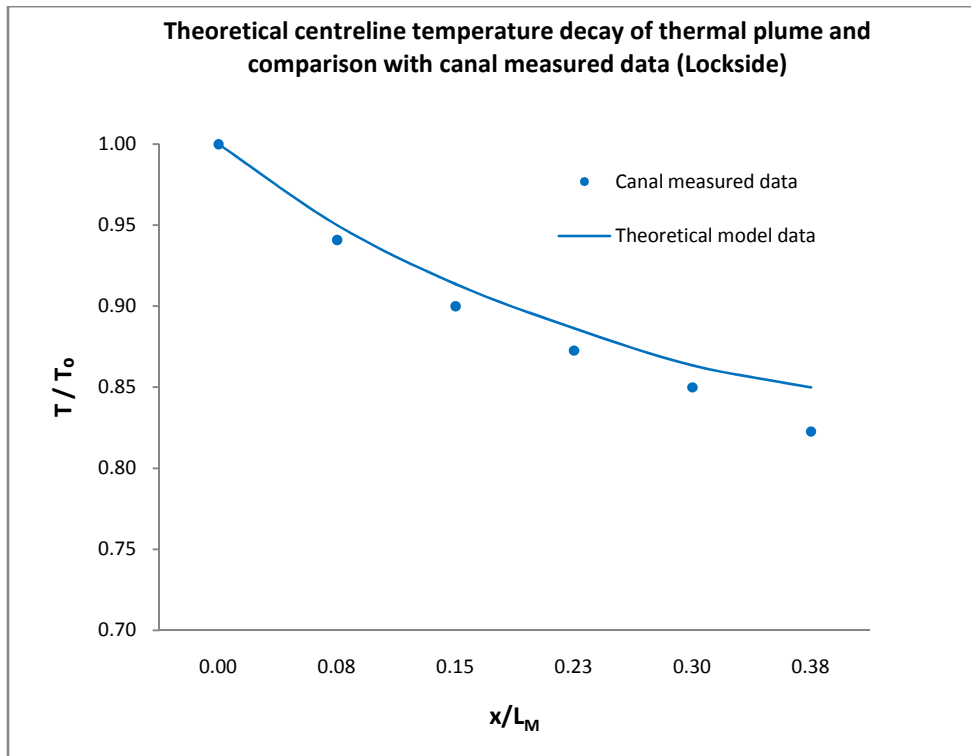


Figure 8.40a: Temperature along path line

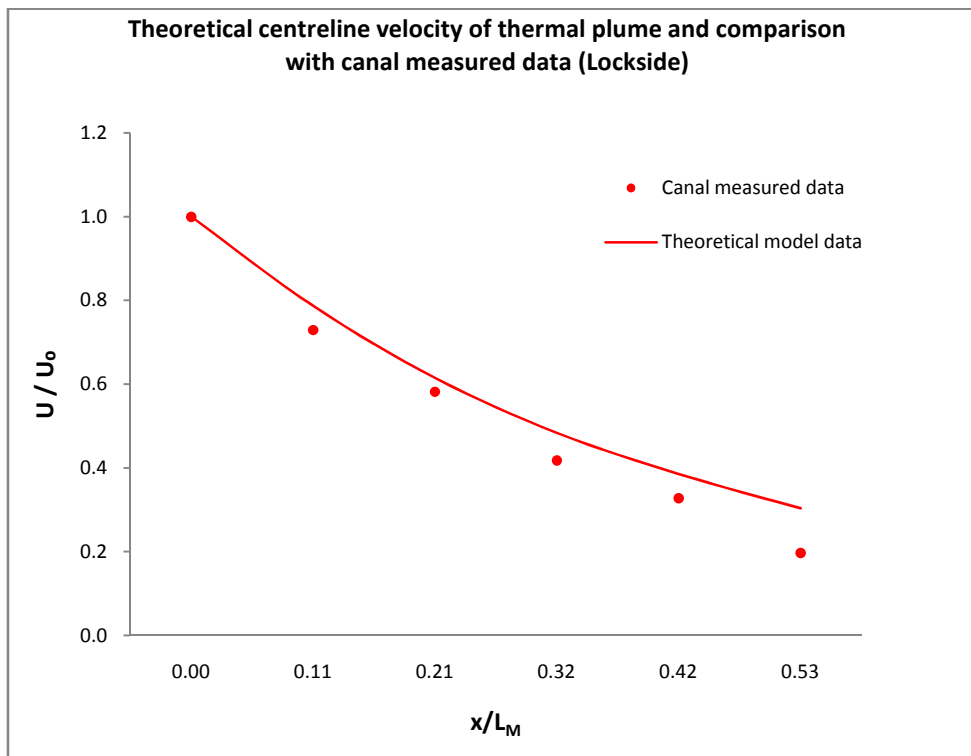


Figure 8.40b: Velocity along path line

Figure 8.40: Theoretical temperature and velocity along plume path line and comparison with canal measured data (Lockside)

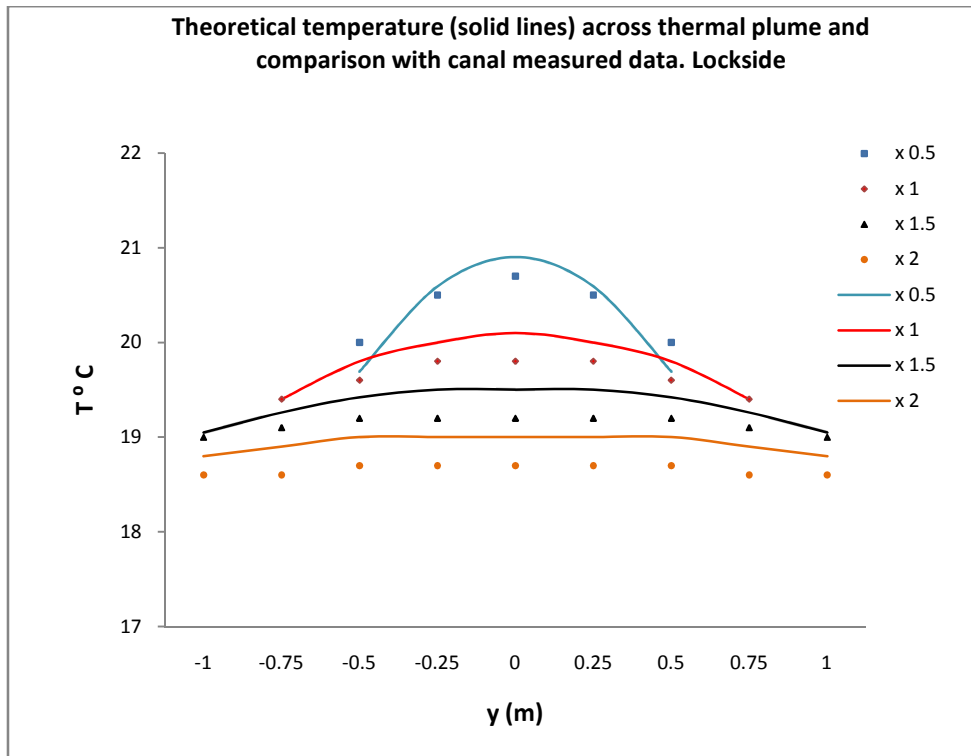


Figure 8.41a: Temperature across path line

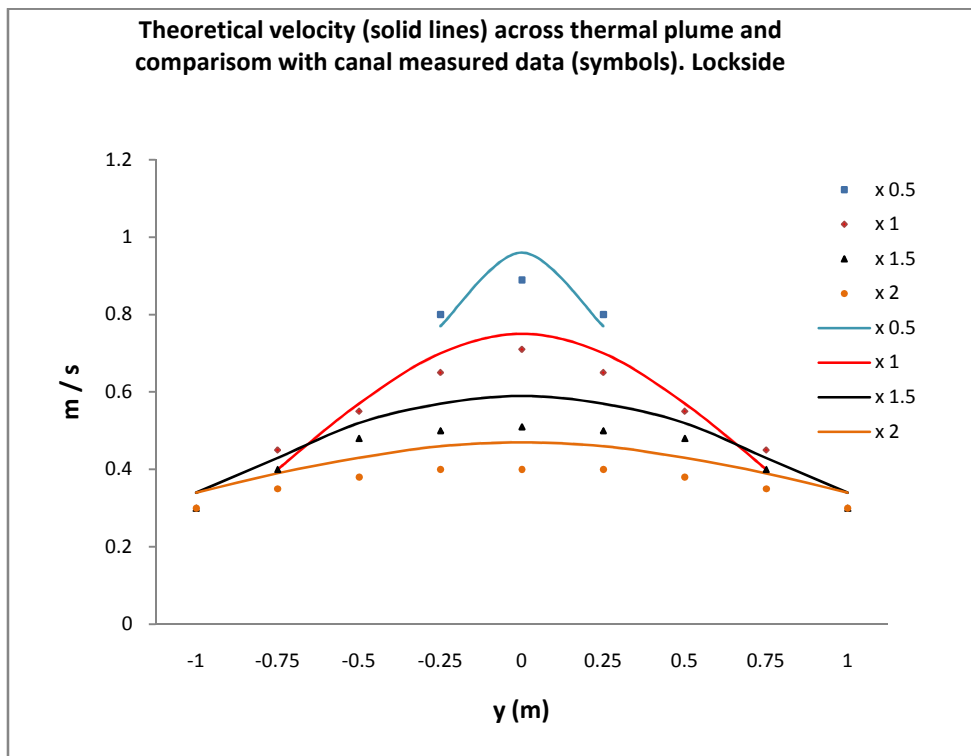


Figure 8.41b: Velocity across path line

Figure 8.41: Theoretical temperature and velocity across plume path line and comparison with canal measured data (Lockside)

The survey carried out at the BBC Mailbox canal site was undertaken during a single day. The measured data includes the temperature for the mixing zone at three different layers, the surface, a layer close to canal bed and the discharge layer, whilst the velocity is measured only on the discharge layer. Due to the limited experimental measured velocity along the plume path line trajectory for this canal site the theoretical model was applied and compared with the plume measured straight centreline velocity.

Figure 8.42a shows the temperature profiles along the plume path line for the Mailbox site. In this instance there is a marginal of difference between the measured data and the prediction according to the model. The measured data indicates a lower temperature and velocity but then stabilises before falling again at a rate predicted by the model. The reason for this is that the plume temperature will be affected by the air ambient temperature after reaches the surface of canal. Thus the plume temperature at the surface will be higher than the predicted temperature during the hotter weather. This can be corrected by undertaking more climatically variable on-site recordings. To undertake this effectively it would be necessary to install a continuous measuring system on a variable range of sites. Figure 8.42b show the temperature across the plume path line.

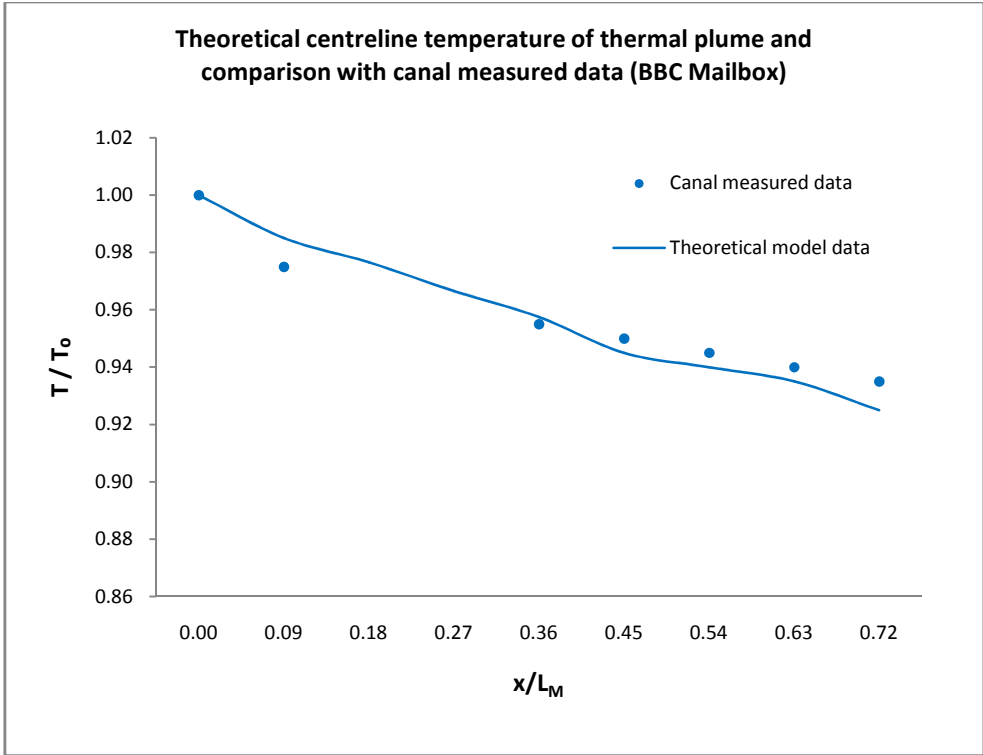


Figure 8.42a: Temperature along path line

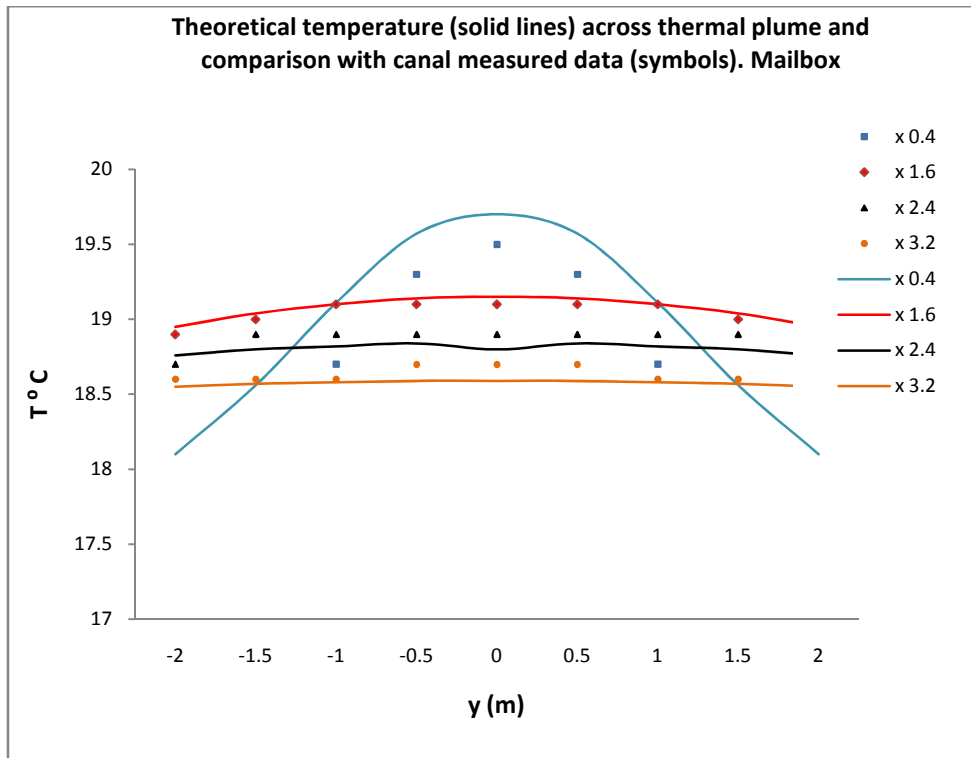


Figure 8.42b: Temperature across path line

Figure 8.42: Theoretical temperature along and across plume path line and comparison with canal measured data (Mailbox)

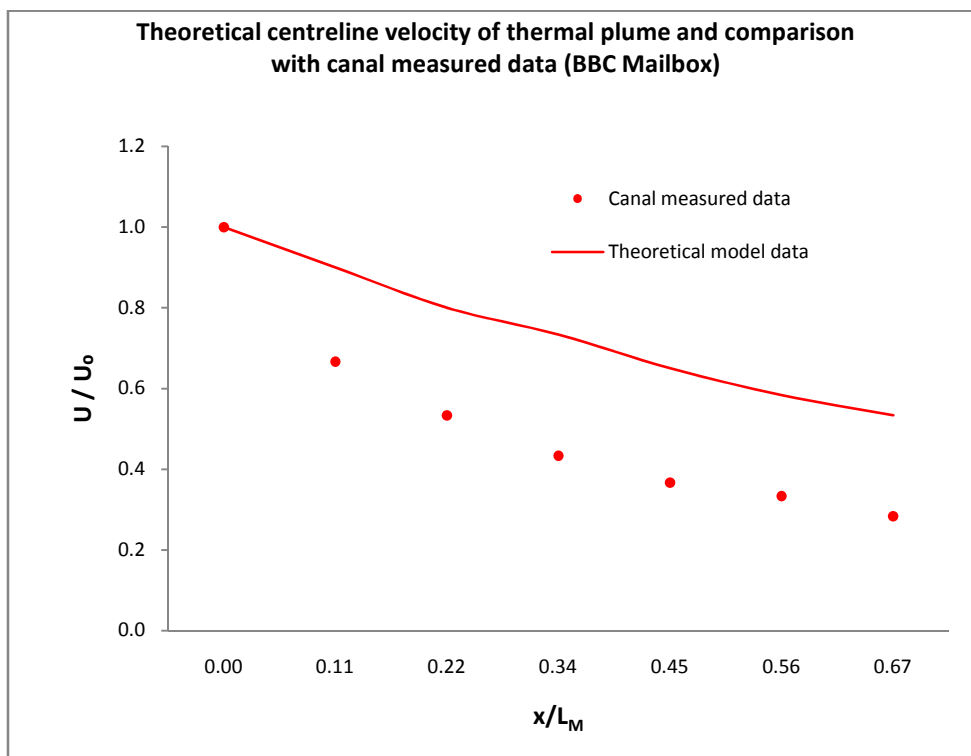


Figure 8.43a: Theoretical velocity along plume path line and comparison with plume straight centreline measured velocity.

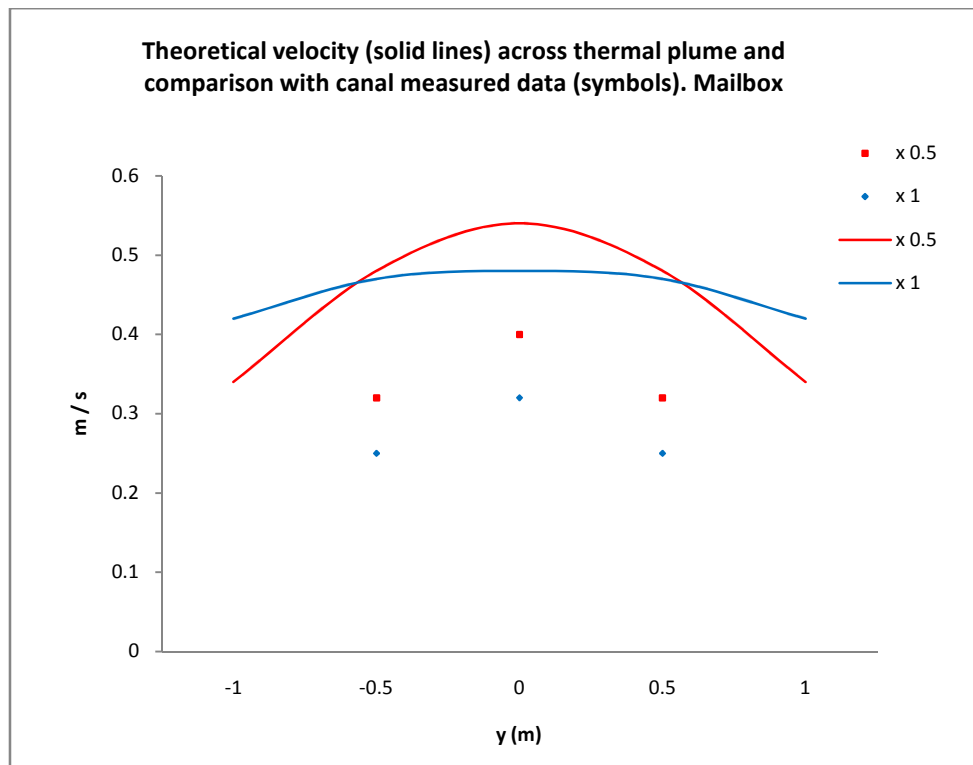


Figure 8.43b: Theoretical velocity across plume path line and comparison with plume straight centreline measured velocity.

Figure 8.43: Theoretical velocity along and across plume (Mailbox)

Figure 8.43a show theoretical velocity along the plume path line predicted by the model and compared with the straight centreline plume measured velocity. The measured velocities are smaller than the predicted velocity. The principal reason was the effectiveness of the recording instrumentation – it not being sufficiently sensitive to measure the low velocities in this instance. In addition another reason for the difference is the path line velocity is bigger than the velocity of the straight centreline as the plume moves to surface due to the buoyancy. Figure 8.43b show the velocity profiles across the plume. Again the figure is a comparison of the theoretical model data against the canal measured data. The experimental measured data along with the theoretical obtained data of the Mailbox site are tabulated in Appendix 11.

8.3.7 Size of Plume – 3D Representation

The results presented earlier give the velocity and temperature profiles along, across and below the surface of the water. These results combined allow a 3D image of the discharge plume to be generated and it is the purpose of this section to discuss the merging of this data and the associated mathematical models. The three dimensional model derived to determine

the size of plume involves a number of equations; therefore the compilation of them to present the 3D image required a computer program to perform that task, in this case MATLAB was used. From the model the size of plume below the free surface of the receiving water can be determined. Its able to produce the isometric view of the plume as well as the plan and side view. The parameters involved in the model are the densimetric Froude Number, depth of the receiving water and the depth of the discharge pipe.

In the following figures the experimental results for the five runs discussed earlier and the canal sites examined will be presented. Figures 8.44 – 8.48 show the isometric 3D view for the laboratory experimental results for all the five runs.

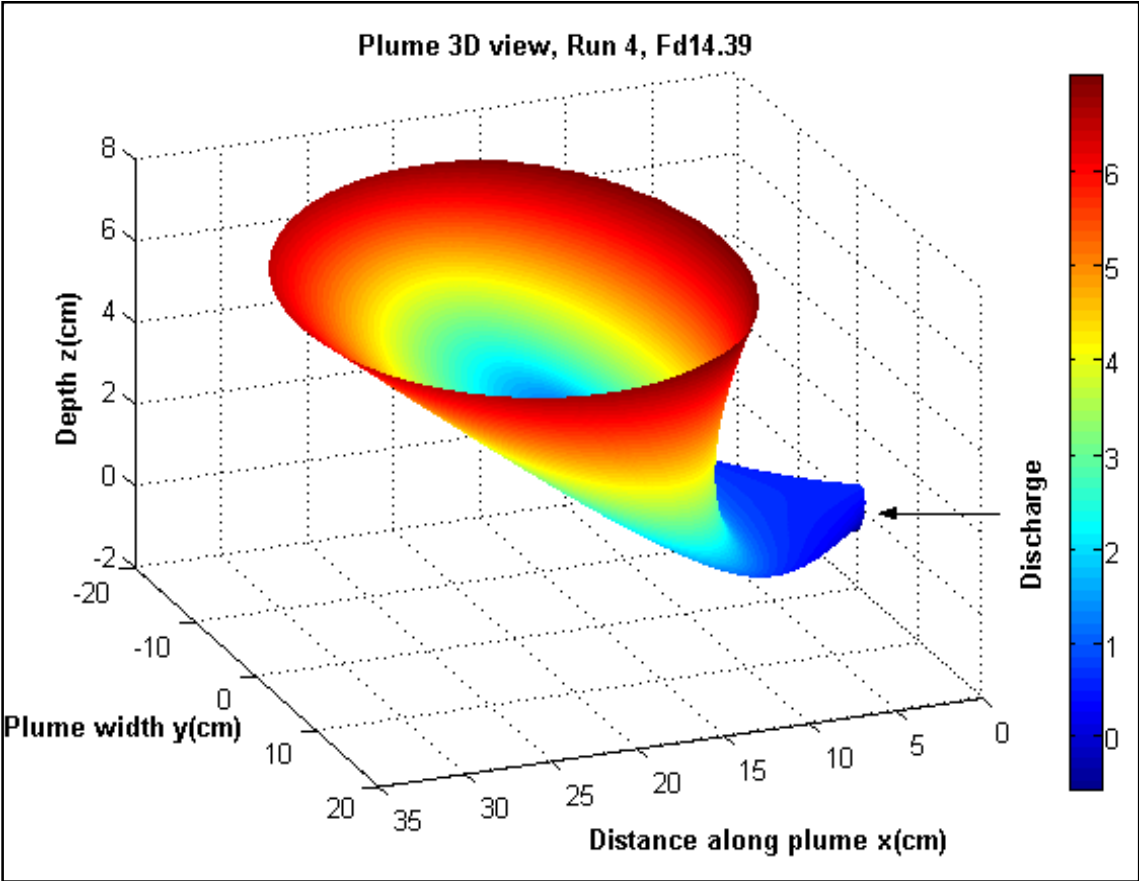


Figure 8.44: Size of thermal plume for experimental run 4, Fd14.39

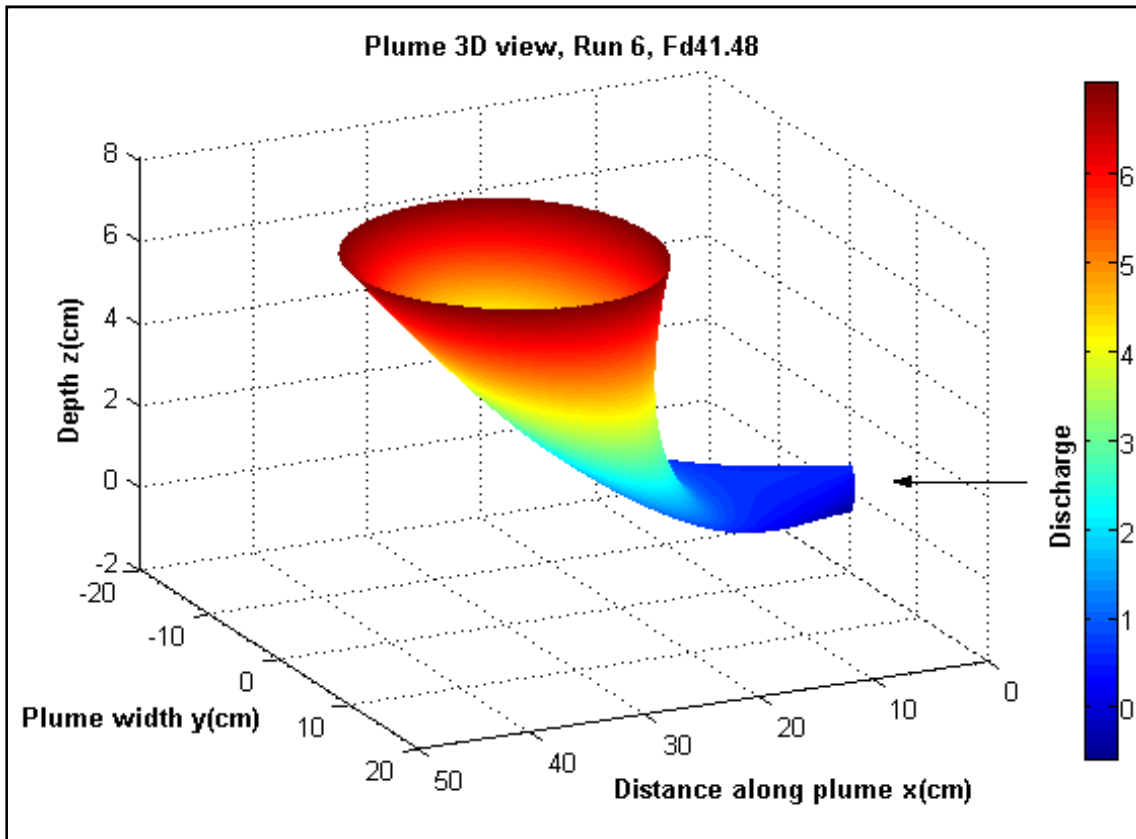


Figure 8.45: Size of thermal plume for experimental run 6, Fd41.48

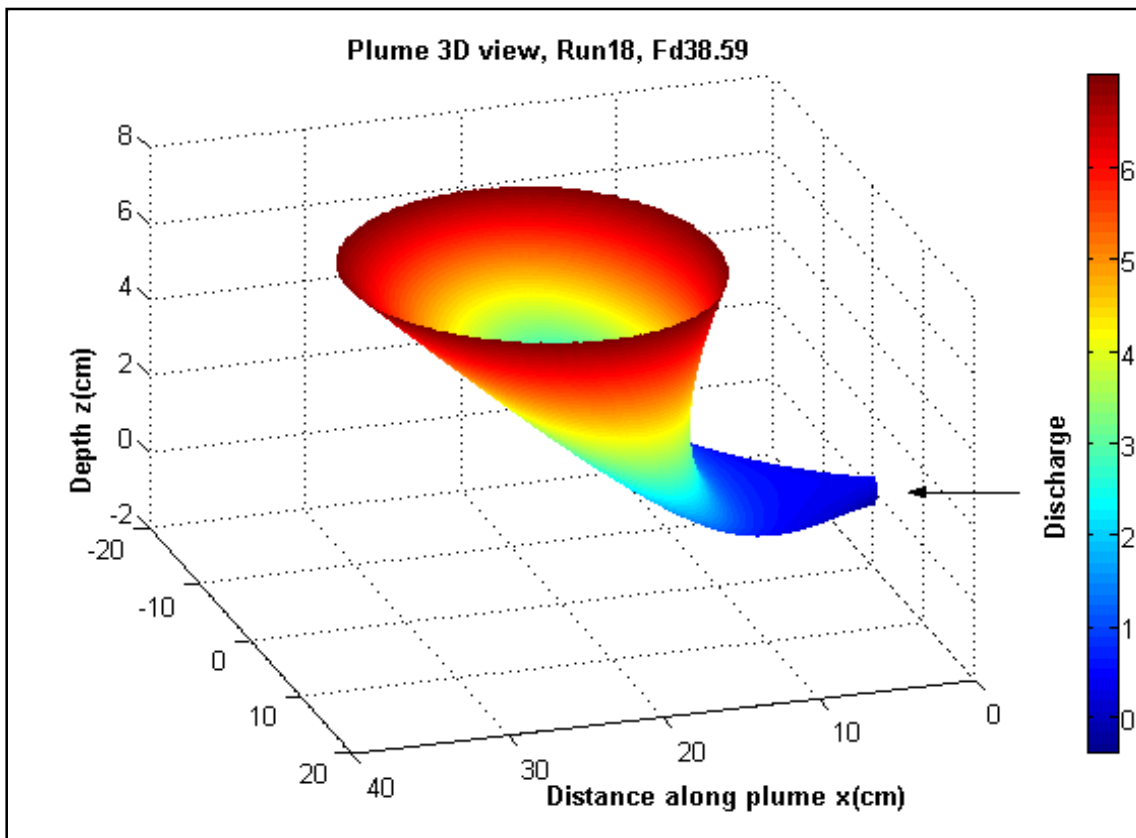


Figure 8.46: Size of thermal plume for experimental run 18, Fd38.59

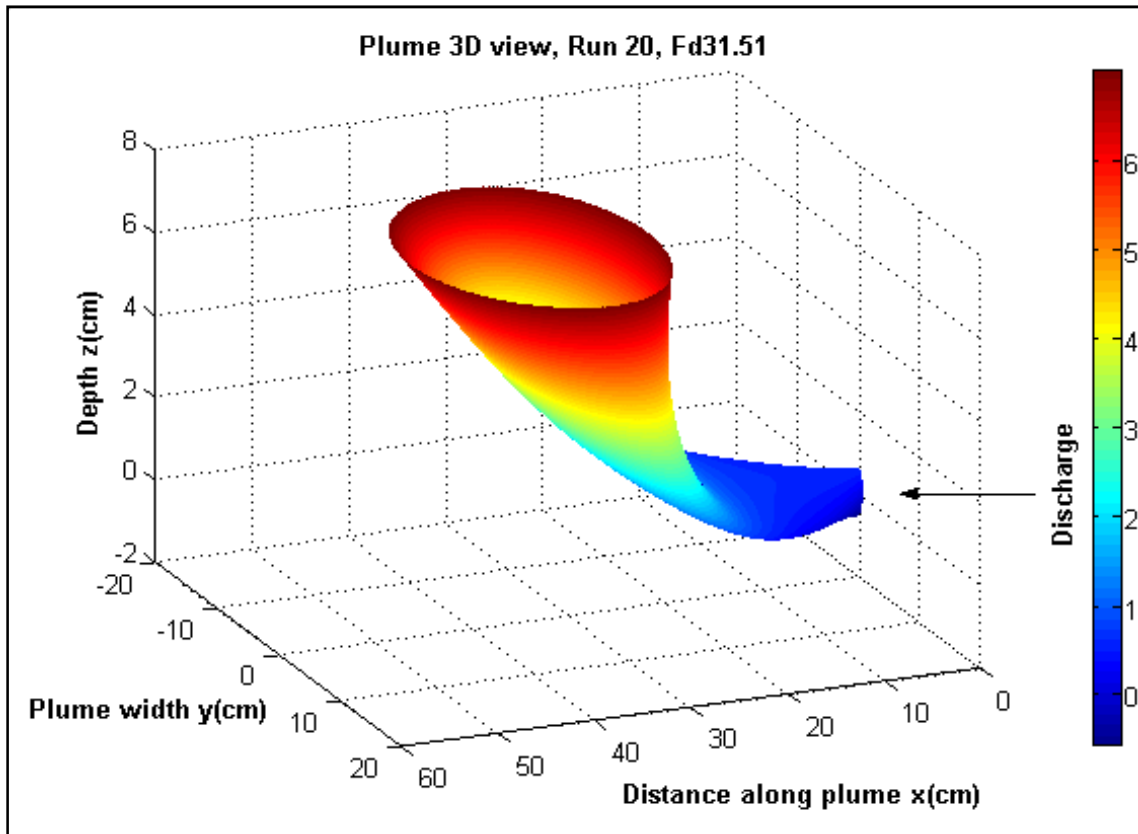


Figure 8.47: Size of thermal plume for experimental run 20, Fd31.51

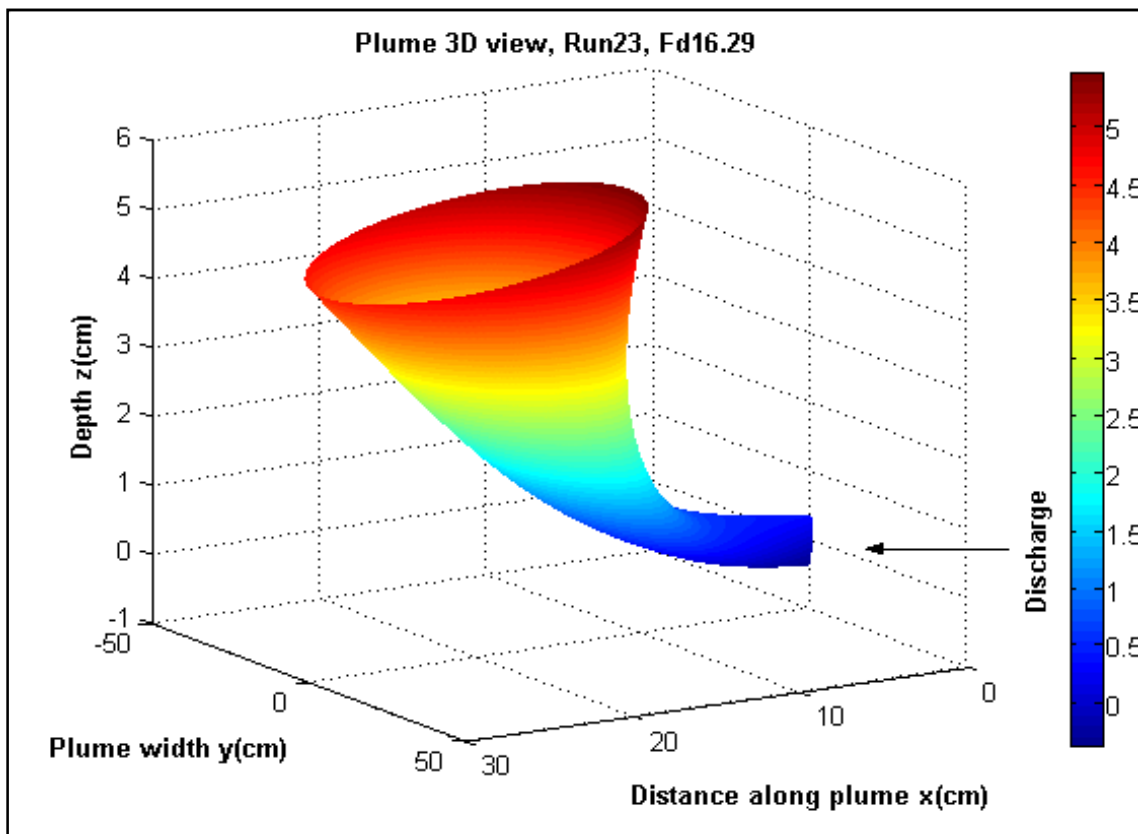


Figure 8.48: Size of thermal plume for experimental run 23, Fd16.29

Figures 8.49 – 8.51 illustrate the plan and sectional view of the thermal plume below the surface for the canal sites, starting with the Canalside West, Lockside and Mailbox. To make the figures more understandable the embankment wall and a section of discharge pipe are added to the right hand side of the figures. The elliptical form in plan views (the “a” referenced figures) and the top flat part in the sectional views (the “b” referenced figures) is the free surface of canal. It must be mentioned that the discharge pipe is located at the right hand side of the figures; and although the outlet size in the z and y directions may appear slightly different they are the same at $x=0$. The reason for that in the plan view as shown in (“a” Figures) is that the plume gets wider very quickly when only a small distance from the outfall. The effect is different to that of an orifice which has a reduced diameter and is caused by fluid attachment to the pipe outlet rim. Because this is an unknown and mainly irrelevant observation, the model does not show the plume within that small distance. The same occurs in the sectional view where the plume within that small distance is not modelled. The small distance that the plume is not modelled is approximately 5cm for the Mailbox site, see Figure 8.51. This distance will be less than that for smaller discharge pipe as in the Canalside West and Lockside sites, Figures 8.49 and 8.50. It is not felt this omission is relevant to the results of the main plume profile. Figure 8.51c show the isometric view of the plume for the Mailbox site.

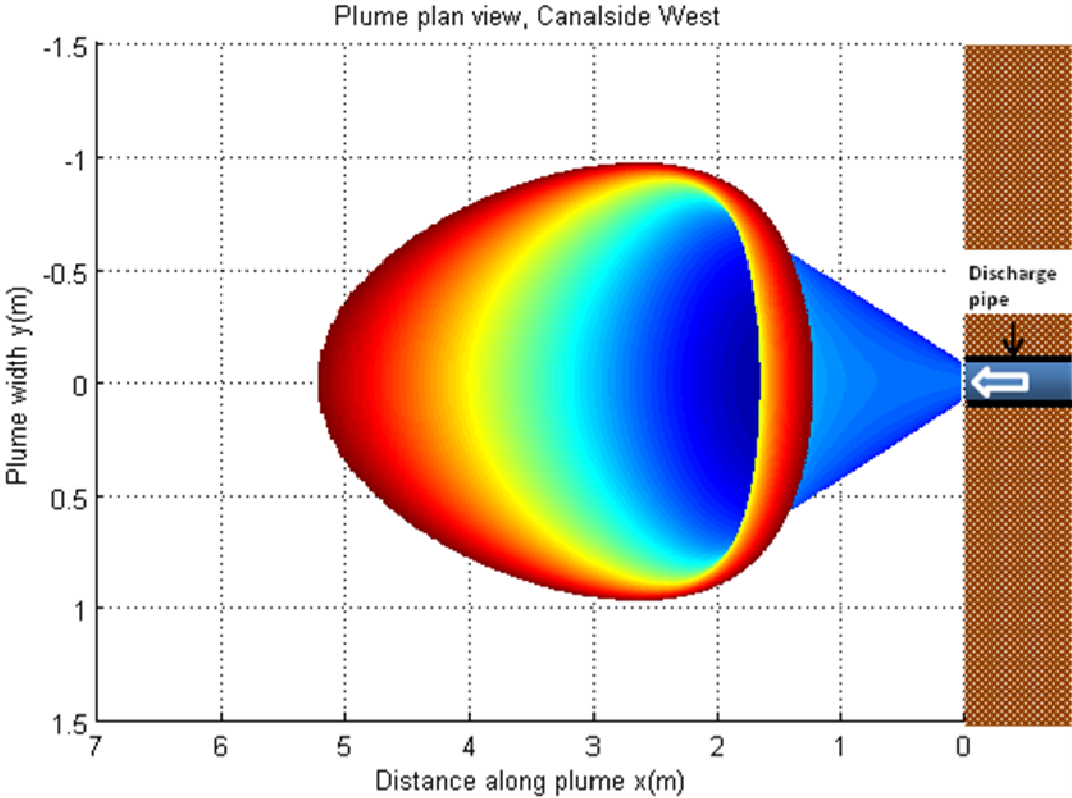


Figure 8.49a: Plan view

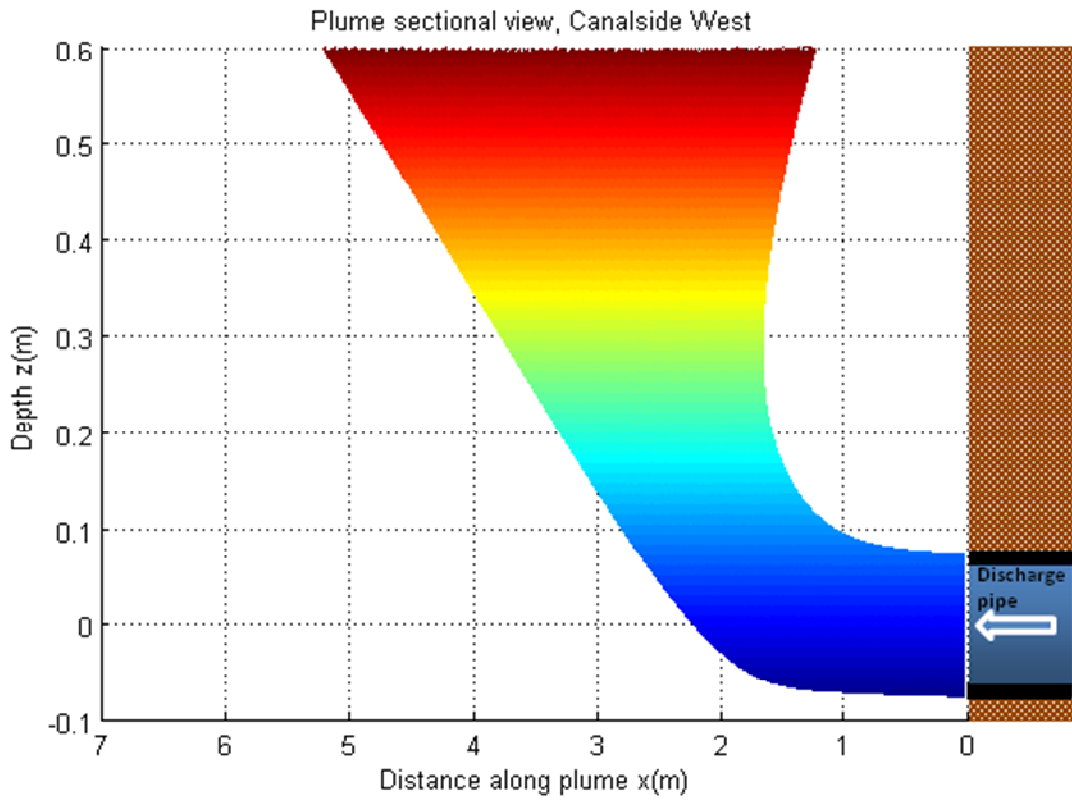


Figure 8.49b: Sectional view

Figure 8.49: Plan and sectional view of thermal plume below the surface at Canalside West

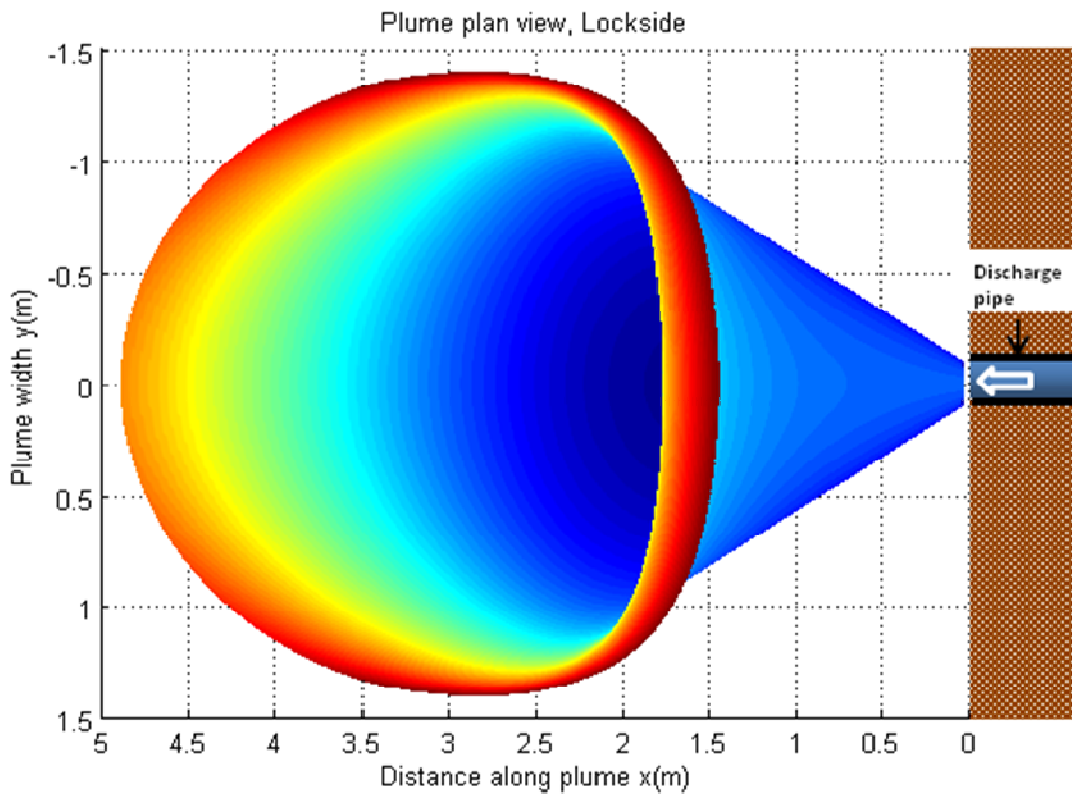


Figure 8.50a: Plan view

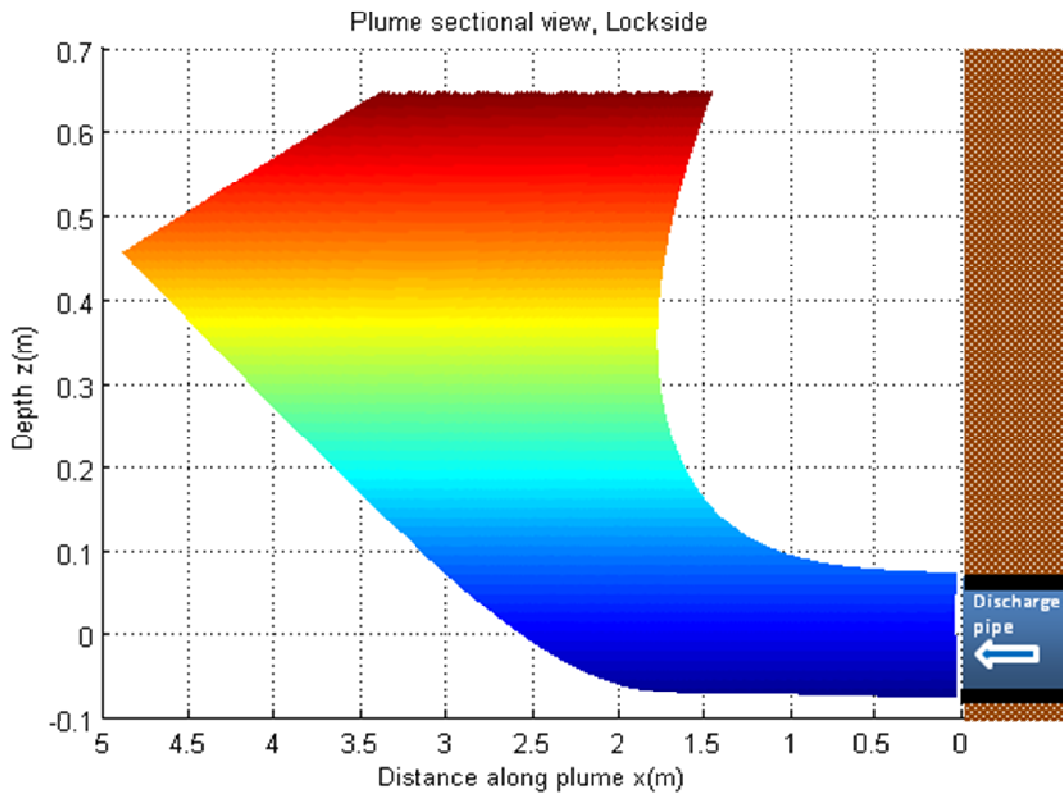


Figure 8.50b: Sectional view

Figure 8.50: Plan and sectional view of thermal plume below the surface at Lockside

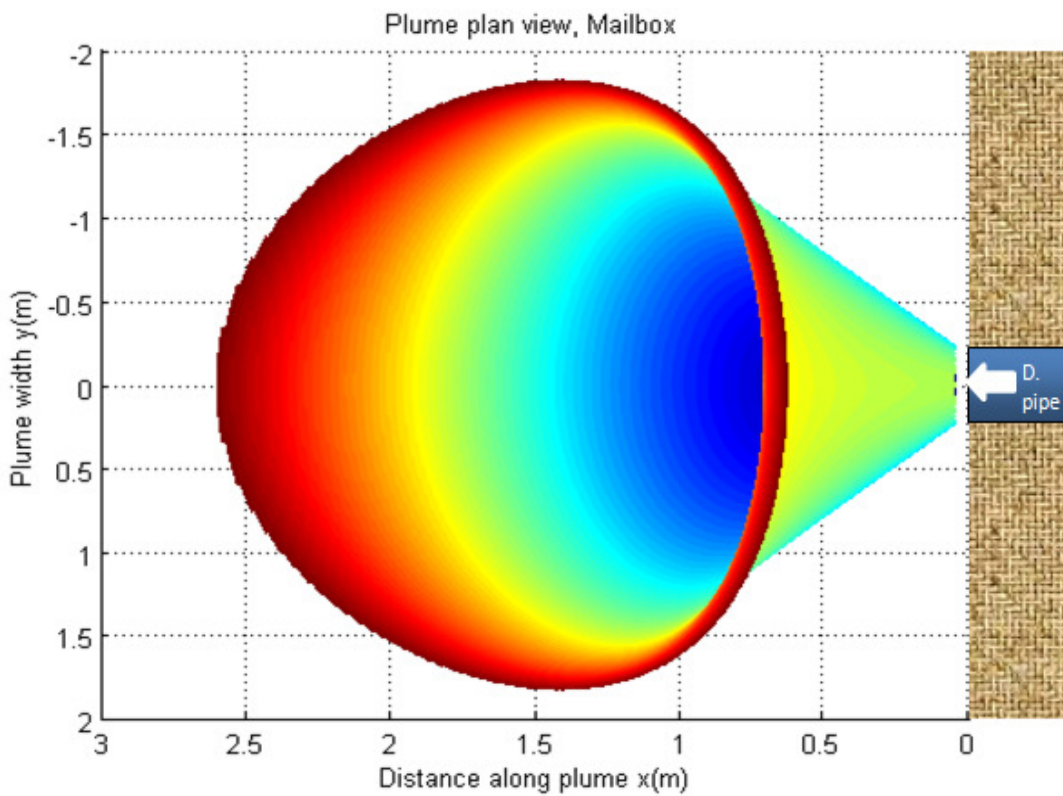


Figure 8.51a: Plan view

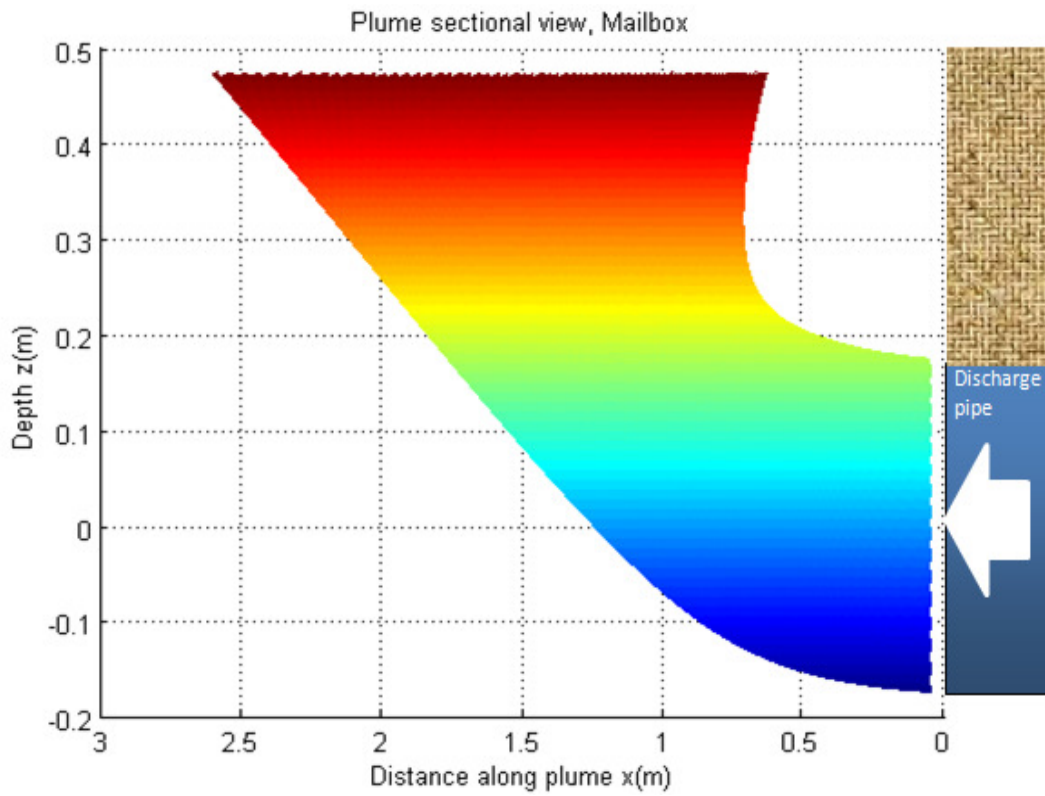


Figure 8.51b: Sectional view

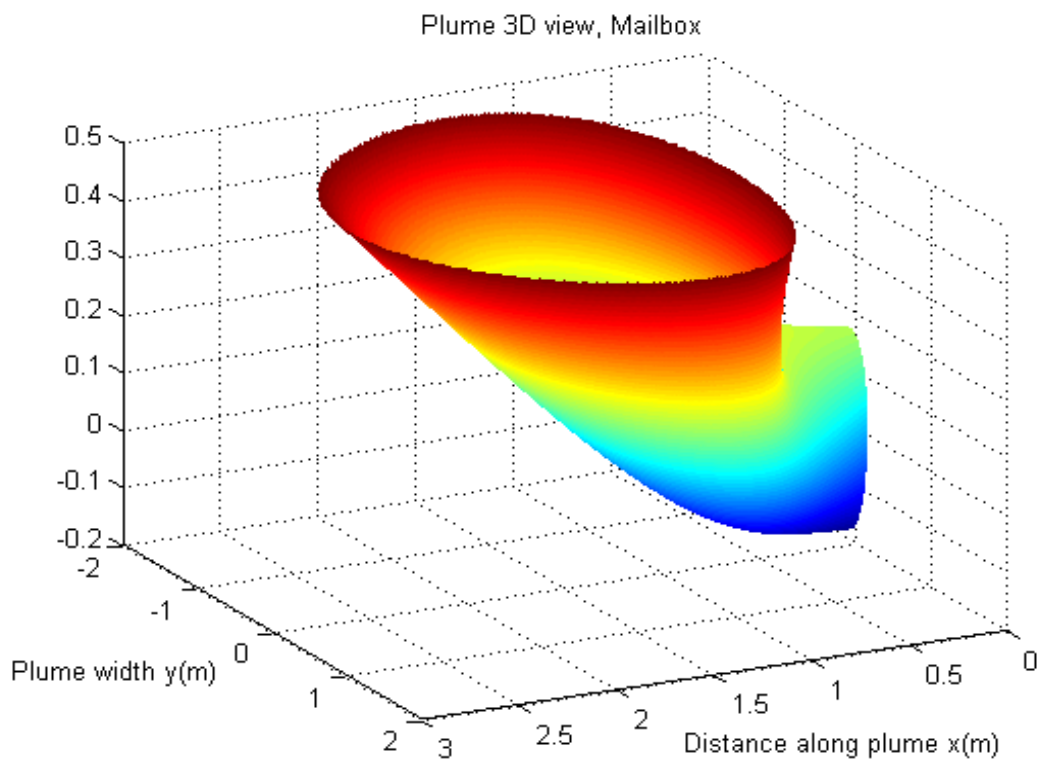


Figure 8.51c: Isometric view

Figure 8.51: Plan, sectional and isometric view of thermal plume below the surface at Mailbox site

9. Summary and Conclusions

9.1 Overview

The discussions regarding global warming are ongoing but the need for more energy needs is not in doubt as the World population expands. In addition the use of existing energy must be used more efficiently and as necessary every advantage needs to be taken to reduce such demands for energy. This research attempts to allow the current process of using canal water for cooling to be used more extensively but still not harm the environment or the eco-balance of the canal system. It concentrates on a study of the thermal plume from heated condensers of a cooling system and then discharged into a body of still water. The British Waterways canal system is one of the sources of water cooling that has the potential to be exploited; its water currently being used to cool buildings adjacent to the canal. Water is normally abstracted from the canal, pumped to the condensers where it absorbs heat and is then returned back to the canal where the heat is dissipated into the body water without affecting aquatic life. This process necessitates the prediction of induced heat diffusion in the receiving water if environmental regulations are not to be infringed. Because the thermal discharge may increase the bulk temperature of the canal water then the recirculation of water back to the intake may also be heated. In addition it is known that an excessive rise of the canal ambient temperature can directly affect the chemical and physical properties of the canal water. This effect can be a reduction of the water's ability to dissolve oxygen and so jeopardise the aquatic life. Because of the known effects and Environment Agency regulations the temperature distribution in the receiving water must be predicted in order to satisfy such criteria. This research presents a novel and holistic technique for investigating warm water discharge into a body of still and shallow receiving water. It uses thermal imaging, on-site testing, scale modelling tank using dyed heated water, computational and mathematical modelling in the studies of thermal discharge and heat diffusion profile prediction. The technique makes use of a thermal camera to observe the heat distribution on the surface of receiving water and the extent of the mixing zone and as such the heated areas can be clearly identified by analysing the thermal images. Mathematical model have been developed to predict temperature distribution of thermal surface discharge into canal and variable values of turbulent diffusivity have been used. The effects of heat turbulent diffusivity on the width of plume has been identified – that is a larger plume is observed for high diffusivity discharge. Mathematical models have been derived to predict the behaviour of thermal submerged and surface discharges into a canal, these models including detail such as plume path line,

temperature and velocity along and across the path line and the size of plume and depth characteristics. In all cases the theoretical results compare very favourably with the site and laboratory results. Of interest is the dependence of the thermal plume temperature distribution within the canal on the discharge temperature, discharge velocity, discharge pipe diameter and its discharge depth and the depth of the receiving water.

9.2 Summary

Most of thermal discharge studies predicted to date cover the cases of thermal plume discharge into large body of deep water such as seas and oceans or discharge into shallow rivers. Such studies have been applied to estimate the temperature distribution in a deep still or shallow flowing receiving water but these have been of a one dimensional nature. They were over conservative in their predictions and as such have rejected what were considered by British Waterways to be viable proposals. The models were not suitable to meet the needs of energy reduction. In the current study an experimental and analytical investigation of heat diffusion of thermal plume discharge into still and shallow receiving water has been carried out. Thermal plume discharge into surface and submerged discharge are described. Laboratory model tank and on-site field trial experiments were used in the experimental investigations. For surface discharge experiments carried out in one canal site and simulated in a laboratory model tank, whereas the submerged discharge performed at three different canal sites and laboratory. For surface discharge temperature and velocity measured along the centreline of plume, whilst in submerged discharge the measurements carried out along the path line of plume. In addition the temperature and velocity profiles across the plume are measured.

In the case of submerged discharge the size of plume and the plume path line are determined by using two discharge pipe diameters, five discharge temperature, three discharge velocity and three different depths for discharge pipe and receiving water. Also the heated water dyed before discharge into the model tank. Thermal camera technology is used to measure the temperature distribution on the surface of mixing zone.

Analytical work has been carried out by using computational CFD package and by producing mathematical equations. FLUENT software is used to determine the temperature and velocity distribution within the mixing zone at different layers and along the centreline of the plume for both surface and submerged discharge. A mathematical model based on heat diffusion

equation has been developed to predict temperature distribution of the thermal plume discharge into and to the surface of the receiving water. The temperature profile determined by the equation is for the discharge layer just below the surface of receiving water. Turbulent diffusivity dividing by discharge velocity is the main parameter involved in the equation.

For submerged discharge equations have been derived from the empirical data to determine the path line of plume when it is deflecting to the surface, temperature and velocity along and across the path line. All the affected parameters such as length scale, densimetric Froude Number, depth of discharge pipe and receiving water are represented in the equations. The number of equations developed was brought together within MATLAB software to produce a three-dimensional model to predict the size of thermal plume below the free surface of the receiving water. In all cases the mathematical models have been compared and validated with the experimental measured data.

9.3 Concluding Remarks

The developed model has been accepted for use by British Waterways and is currently being reviewed by the Environment Agency. It has been applied locally to evaluate a new college build programme and the results have been accepted by the build energy consultants.

It is considered that the general principles used during the study gives an insight into the behaviour of the discharge of warm water into still and shallow receiving canals and the temperature dispersal throughout the plume and may be used to predict future proposals to use canals for cooling purposes.

Experiments

The area of the discharge plume and temperature distribution within the surface of the plume can be clearly defined by the use of the thermal camera. It must be noted that the thermal distribution throughout the depth cannot be obtained using the thermal image camera technique because of the surface reflectivity and its inability to differentiate between distances. The temperature dispersal indicated by the thermal images is corroborated by the temperatures measured within the area of the grid that is around the visible turbulent discharge plume.

Submerged discharge would achieve a greater temperature loss within the submerged plume with the residual heat dissipating across the surface, creating a larger area in which final

balance temperature is achieved. This would leave a sub-surface volume for fishlife to bypass the plume.

The three sites at the University of Huddersfield and BBC Mailbox site all comply with the necessary requirements of British Waterways and the Environment Agency in that the maximum temperatures recorded were within stated acceptable limits.

The geometry of the layout of the sites used for the study varies considerably, impacting on the behaviour of the discharge and temperature dispersal. The aquatic plant growth around the mixing zone in the surface discharge can have an effect on the thermal dispersal by restricting free flow of the discharge plume. There was no evidence of aquatic plant growth within the other three submerged discharge sites that may have affected the results.

Using the discharge temperature measurement as recorded within the plant room gives an overestimation of actual discharge temperature to the canal as there is a significant cooling effect from the underground pipes leading back to the canal. There is some heat loss taking place between plant room, pump house, embankment and the discharge point.

From the field trials and laboratory experiments it can be said that the peak discharge temperature of the plume does not extend below the pipe therefore the maximum temperature need only be considered within the local plume area. In a surface discharge design the heat is being dissipated over a larger surface area which does not constitute a threat to fishlife, whereas in a submerged discharge design the majority of heat dissipates within the body of the canal water.

The discharge plume dissipates the maximum heat loss within a plume size of 1m long x 400mm wide whilst the area of the maximum mixing zone required to achieve full temperature balance is depended on the involved parameters as specified in the equations.

At the CSB site the relative positioning of the inlet some 4.5m downstream from the discharge pipe outlet does not cause any recirculation problems. Any increase in inlet temperature is more influenced by the effect on flow created by the proximity of the embankment to the inlet, the weed growth and the timber posts that were close to the inlet in this case. Within a distance of 4.0m from the discharge point a temperature balance is achieved throughout the canal depth on the centreline of discharge.

The Canalside West less effects on the canal environment is minimal as the temperature balance is achieved within a short distance from the discharge point. At the Lockside site

adequate space is available for fishlife allowing them plenty of room to keep away. The surface temperature of the mixing zone at the Mailbox is relatively constant.

The temperature distribution obtained by thermocouple measurements appears to corroborate the temperature distribution of the discharge plume obtained using the thermal imaging camera.

Theoretical

The presented theoretical models have been shown to closely represent a number of varied real systems. As such it is felt they are applicable for most standard systems that may be required to be evaluated by British Waterways. Indeed it is felt they are applicable for application towards any heated water discharge into a still water environment.

In submerged discharge the proximity of the discharge pipe to the bed z_0/L_M and to free surface $(H - z_0)/L_M$ has considerable effects on the flow pattern, see Figure 9.1. Whereas the length scale, temperature difference and discharge velocity have a significant influences on the plume profiles.

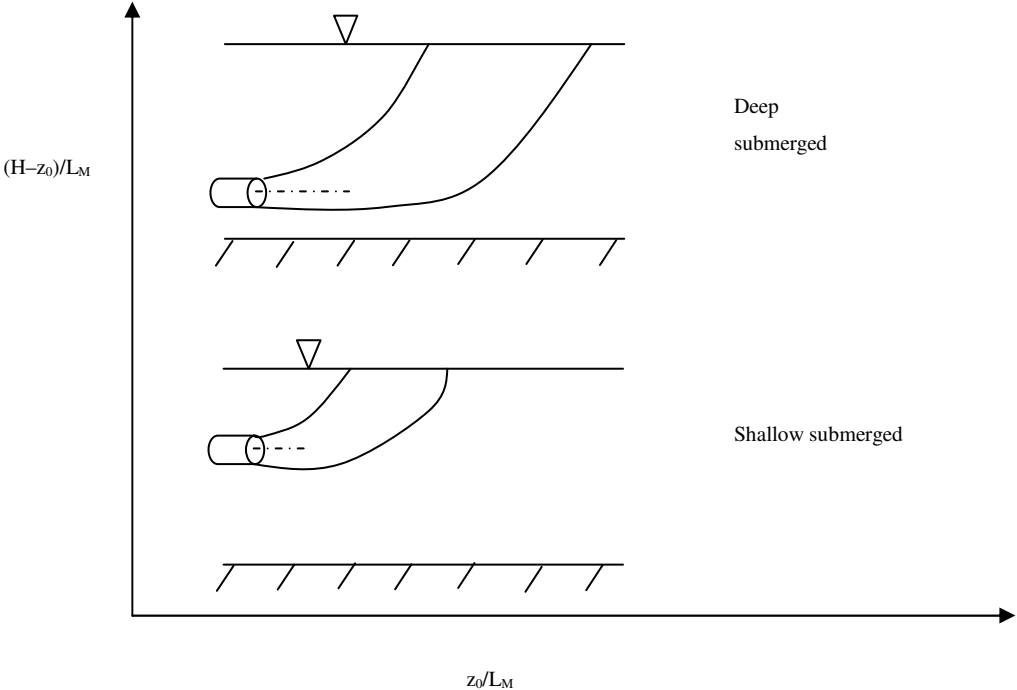


Figure 9.1: Flow pattern regimes

In deep submerged discharge the plume horizontal flow increased and there will be a deflection towards the bed, then the buoyancy is prevailed and the plume rises to free surface.

In shallow discharge the entrainment is reduced between the surface and discharge pipe, therefore the deflection of plume towards the surface will be faster. The dilution along the path line of plume in shallow submerged discharge grows less rapidly than that in deep submerged discharge. In general the bed parameter has limited effects on the dilution along the path line of plume as well as on the lateral diffusion.

The following is a summary of major results and conclusions

- Equations developed to predict the path line of thermal submerged plume, the temperature and the velocity along and across the path line.
- 3-D model of the size of the thermal submerged plume below the surface developed
- 2-D model developed to predict the temperature profile for surface thermal plume
- The equations have been validated against all measured data for all sites with accuracy 95% for temperature and 90% for velocity.
- The beneficial effects of surface and submerged discharge have been investigated and it has been shown that submerged discharge has a better effect regarding heat dissipation.
- Regarding the position of the inlet and outlet pipe it is recommended that the inlet should be located outside the mixing zone.
- For high flow rates, high velocities and high temperature discharges into a still water environment it is better that the direction of discharge should be longitudinal along the length of the canal (in the case of a canal site) and not across the canal. In addition it is recommended that the withdrawal (inlet) pipe be positioned the opposite direction to the discharge line.
- An appropriate value for turbulent diffusivity into a still water environment canal has been derived and confirmed.
- Three-dimensional temperature and velocity profiles have been created using FLUENT CFD modelling software.
- Considering the variations in the effect of surface and submerged discharge regarding discharge velocity, discharge temperature, pipe diameter, determine length and profile of plume and temperature gradient; it has been shown that the surface discharge plume

will be longer than the submerged discharge plume which will be wider when they have the same initial parameters.

- Regarding the effect of the relative position and depth of inlet/outlet pipes and cross sectional shape of the canal on recirculation; for 7°C temperature difference and 4.5m between both pipes then no recirculation occurred.
- The flow pattern, discharge plume size and temperature gradients through the discharge plume are determined by considering the effects of various length scales and depth of receiving water.

9.4 Future Work

The author is planning to expand the current work to consider the total energy balance of the discharged warm water into any body of still water.

In the current study the heat diffusion of thermal discharge into British Waterways canal is investigated. It is shown the size of plume and the length that plume reach to achieve temperature balance. The study does not discuss the way that heat dissipates and where the heat loss goes. There is a need to consider surface water evaporation that can be 1mm per day, heat lost to the canal floor, heat loss to backing and heat loss during underground pipe flows. It is therefore necessary to know the proportion of heat dissipation to all sections and the temperature balance achieved to avoid any potential environmental impact. Based on the theory of (the heat gain = heat loss + losses) the author could produce a model to predict the energy balance in any still water environment.

It is also necessary to analyse the variation in the building loads and canal temperatures and the impact that these variables have on changing plume patterns throughout an operating summer cooling season.

10. References and Bibliography

Abramovich, G. N. (1936), "Theory of the Free Jet and its Applications", Trudy Tsentr. Aerogidrodinam. Inst. 293. 48.

Abramovich, G. N. (1963), "The Theory of Turbulent Jet", *The Massachusetts Institute of Technology*, Massachusetts.

- Anwar, O. H. (1987), "Flow of Surface Buoyant Jet in Cross Flow", *Journal of Hydraulic Engineering*, Vol. 113, (7), pp. 892-904.
- Ari, S., Nagao, M., Sakyo, H., Iwasaki, T. and Suizu, S. (1998), "Spreading of Negatively Buoyant Jet on the Bed Floor", *Parallel Session(Parallel 22)*, Flow Experiment and basics
- Avramenko, A. and Basok, B. (2006), Vortex effect as a consequence negative turbulent diffusivity and viscosity, *Journal of Engineering Physics and Thermophysics*, 79, (5), pp. 957-962.
- Bowley, W. and Sucec, J. (1969), "Trajectory and Spreading of Turbulent Jet in the Presence of Cross Flow Arbitrary Velocity Distribution" ASME No.69-GT-33.
- Campbell, J. F. and Schetz, J. A. (1971), "Penetration and Mixing of Heated Jets in a Waterway and Application to the Thermal Pollution Problem", *AIAA Urban Technology Conference*, May 24-26, New York, USA.
- Campbell, J. F. and Schetz, J. A. (1972), "Flow Properties of Submerged Heated Effluents in a Waterway", *AIAA 10th Aerospace Science Meeting*, January 17-19, Sandiego, USA.
- Cederwall, K. and Brooks, N. (1971), "Buoyant Slot Jets into Stagnant or Flowing Environments", *Keck Lab. Of Hydraulics and Water Resources*, Rep. No. KH-R-25, California Institute of Technology.
- Chapman, S.J. (2004), "Matlab Programming for Engineers", *Thomson*.
- Chadwick, A., Morfett, J. and Borthwick, M.(2004), "Hydraulic in Civil and Environmental Engineering", *Taylor & Francis Group*, London.
- Coulson, J.M. & Richardson, J.F. (2003), "Chemical Engineering", *Butterworth Heinemann*, ISBN 0 7506 4444 3
- Crank, J. (1970), "The Mathematics of Diffusion", Oxford.19 853307 1
- Demissie, M. (1980), "Diffusion of Three Dimensional Slot Jets with Deep and Shallow Submergence", University of Illinois at Urbana-Champaign. Illinois.
- El-Baz, A., Zaghoul, A., Martinuzzi, R. and Baddour, R. (1996), "Plan Surface Jet in a Current, Measurements and Turbulence Modelling", *6th Int. Symp. On Flow Modelling and Turbulence Measurements*, Sept. 8-10, 1996, Tallahasee, Florida, USA.
- Environment Agency (1997), "The Surface Water (Fishlife) (Classification) Regulations", No. 1331, London.
- Erduran, K. S., Kutija, V. (2003), "Quasi-three-dimensional numerical model for flow through flexible, rigid, submerged and non submerged vegetation", *Journal of Hydroinformatics*, 5, (3) pp. 189-202
- Hoar, C. (2005), "Fish response to discharge events from a power plant cooling reservoir in a river affected by acid mine drainage and thermal influences", M.Sc. Dissertation, West Virginia University, USA.
- Horikawa, K., Lin, M. and Sasaki, T. (1979), "Mixing of Heated Water Discharged in the Surface Zone", *Proceeding of the Coastal Engineering*, 3, pp. 2563-2583.
- Jirka, G. H. (2004), "Integral Model for Turbulent Buoyant Jets in Unbounded Stratified Flows", *Environmental Fluid Mechanics*, 4, pp.1-56.

- Kannberg, L. and Davis, L. (1974), "Experimental Investigation of Deep Submerged Multiple Buoyant Jets into Stagnant and Co-moving Ambient", *J. Progress in Astronautics and Aeronautics*, Vol. 36, pp. 153-163.
- Kim, D. G., Seo, W. (2001), "Modelling of the mixing of heated water discharged from a submerged multiport diffuser", *Journal of Hydraulic Research*, 38, (4), pp. 259-269
- Lardicci, C., Rossi, F., Maltagliati, F. (1999), "Detection of Thermal Pollution: Variability of Benthic Communities at Two Different Spatial Scales in an Area Influenced by a Coastal Power Station", *Marine Pollution Bulletin*. April, 38,(4), pp. 296-303 [online] Available from: Science Direct< <http://www.sciencedirect.com/science>>
- Launder, B. and Spalding, D. (1974), "The Numerical Computation of Turbulent Flows", *Computer Methods in Applied Mechanics and Engineering*, Vol. 3, pp. 269-289.
- Launder, B. E., Reece, G. J. and Rodi, W. (1975), "Progress in the Development of Reynolds Stress Turbulence Closure" *J. Fluid Mech.*, Vol. 68, part 3, p 537-566.
- Launder, B. (1975), "On the Effects of a Gravitational Field on the Turbulent Transport of Heat and Momentum", *J. Fluid Mech.*, Vol. 67, pp. 569-581.
- Launder, B. E. and Samaraweera, D. S. (1979), "Application of Second- Moment Turbulence Closure to Heat and Mass Transport in Thin Shear Flows-1, Two Dimensional Transport", *Int. J. Heat Mass Transfer*, Vol. 22, p. 1631.
- Lee, J. H. (1980), "Stability and Mixing of a Round Buoyant Discharge in Shallow Water" *Second International Symposium on stratified Flows*, 2, pp.881-897
- Lee, W. and Huai, W. (1995), "Calculation of whole field for vertical round buoyant jets in static linearly stratified environment", *Journal of Hydraulic Research*, 33, (6), pp. 865-876.
- Massey, B. S. (1989), "Mechanics of Fluids", *Chapman and Hall*, ISBN 0-412-34280-4
- McGuirk, J. J. and Rodi, W. (1978), "Mathematical modelling of three-dimensional heated surface jets", *Journal of Fluid Mechanics*, 95, (4), pp. 609-633.
- Metcalf & Eddy, (1972), "Wastewater Engineering, collection, treatment, disposal", *McGraw-Hill Inc.*, ISBN 07-041675-3
- Moawad, A. K., Rajaratnam, N., Stanley, S. J. (2001), "Mixing with multiple circular turbulent jets", *Journal of Hydraulic Research*, 39, (2) pp. 163-168
- Nakashiki, N. (1996), "Development of a 3-D Model for the Predicting Warm Water Discharge Diffusion", *Abiko Research Laboratory, CRIEPI, Denken*
- Ozturk, H. Z., Sarikaya, A. F., Demir, I. (1995), "A Simplified Model for Thermal Discharges", *Water and Science Technology* 32,(2), pp. 183-191
- Parr, A. D. and Sayre, W. W. (1979), "Multiple Jets in Shallow Flowing Receiving Waters" *Journal of Hydraulic Division*, 105, pp.1357-1374.
- Patankar, S. and Spalding, D. (1972), "A Calculation Procedure for Heat, Mass and Momentum Transfer in Three Dimensional Parabolic Flows", *J. Heat and Mass Transfer*, Vol. 15, pp. 1787-1806.
- Pinheiro, A. and Ortiz, J. 'Comparative Analysis of Heated Water Dispersion in Still Water Body Using Software CORMIX 1, PHOENICS and PLUMAC 2.2' School of Engineering, Mackenzie University, Brazil.

- Qi, M., Chen, Z. and Fu, R. (2001), "Flow structure of the plane turbulent impinging jet in cross flow", *Journal of Hydraulic Research*, 39, (2) pp.155-161
- Robert, P. J. W. and Webster, D. R. (2002), "Turbulent Diffusion", *Environmental fluid mechanics: theories and applications*. New York, ASCE. ISBN 0-7844-0629-4.
- Rodney, J. S., Archie, J. J. and Richard, D. K. (1998), "Horizontal Round Buoyant Jet in Shallow Water", *Journal of Hydraulic Engineering*, 114, (8) pp.910-929.
- Seo, W., Yu, D., Kim, H. S. (2001), "Near Field Mixing of Submerged Multiport Diffusers in Shallow Water with Strong Currents", Seoul National University, Gwanak-Ku, Seoul, Korea
- Seo, W., Yu, D., Kim, H. S. "The Mechanics of Tee Diffuser for Thermal Discharges in Crossflow", Seoul National University, Gwanak-Ku, Seoul, Korea. (Undated)
- Seo, W., Kim, D. G., Shim, M. P. (1998), "Velocity Structure of Wall Jet Discharging from Circular Orifices", *Water Quality in Rivers and Lakes*, Parallel Session (Parallel 42)
- Sherif, A. (1985), "Measurements of the Flow and Thermal Characteristics of Turbulent Jets in Cross Flow", Ph.D. thesis, Iowa State University, USA.
- Sherwin, K., Horsley, M., (1996), "Thermofluids", Chapman & Hall, ISBN 0 -412 59800 0
- Sojisuporn, P. "Application of Numerical Model to Thermal Plume Dispersion from Power Plant at Kanon", *The seventh OMISAR workshop on ocean models Faculty of Science*, Chulalongkorn University, Bangkok (10300) Thailand (undated).
- Stanoyevitch, A. (2005), "Introduction to Matlab with Numerical Preliminaries", John Wiley & Sons.
- Stolzenbach, K. and Harleman, D. (1973), "Three Dimensional Heated Surface Jets", *Water Resources Research*, Vol. 9, pp. 129-137.
- Taylor, G. I. (1921), "Diffusion by continuous movements", *Proceedings of London Mathematical Society*, series 2, 20, pp. 196-212.
- Tennessee Valley Authority. Waste Heat Utilization for Agriculture, State of the Art. Muscle Shoals, Alabama: Tennessee Valley Authority and Electric Power Research Institute, 1978. (EPRI EA-922)
- Tsubono, T. et al. (2002), "Improvement on the Computational Efficiency of the 3-Dimensional Warm Water Diffusion Model", *CRIEPI Rep.* U01040
- Ungate, D., Harleman, R. F. and Jirka, G. H. (1975), "Stability and Mixing of Submerged Turbulent Jets at Low Reynolds Number" *Energy Laboratory Report*. No. MIT-EL 75-014
- Wallis, S. G. and Manson, J. R. (2004), "Methods for predicting dispersion coefficients in rivers", *Water Management*, 157 issue WM3
- Williams, G. P., "Heat Transfer Coefficients for Natural Water Surfaces", *Division of Building Research*, National Research Council. Ottawa, Canada (undated)
- Xin, H. Wen (2000), "Three Dimensional Numerical Simulation of Multiple Jets in Shallow Flowing Receiving Water" *Journal of Hydrodynamics*, 12, (3) pp. 19-28
- Yu-hung, Z. and Xin, H. W. (2005), "Numerical study on the stability and mixing of vertical round buoyant jet in shallow water", *Applied Mathematics and Mechanics*, English Edition, Vol. 26, (1), pp. 92-100
- Zaghloul, A. (1996), "Turbulence Structure of Plane Surface Jets in a Current", Ph.D. thesis, University of Western Ontario, Canada.

Zaric, Z. (1978), "Thermal Effluent Disposal from Power Generation", *Series in Thermal and Fluid Engineering Hemisphere Publishing Corporation*. Washington.

Zeng, P., Chen, H., Ao, B., Ji, P., Wang, X. and Ou, Z. (2002), "Transport of waste heat from a nuclear power plant into coastal water" *Coastal Engineering*, 44, pp. 301-319

Appendices

APPENDIX 1: MEASUREMENTS PROCEDURE

Site 1: Canal basin – wharf

Site 2: Canal Side West

Site 3: Lock side

Re: Onsite data collection

Site 1: Canal basin – wharf

Agree time/date of data collection with Adrian Lee,

All readings to be taken on same day.

Ensure pump set to manual over ride for duration of trial,

Ensure no lockage occurs within 2 hours of data collection,

If lockage occurs during trial, abort, wait 2 hours and restart trial,

Start of trial - Data collection:

Record date and time of start of trial, may be better to record time individual readings/photographs are taken.

Lock 1E:

Photograph gate leakage,

Photograph weir to record flow, if any,

Measure flow over weir

Measure breadth of weir

Measure gate leakage – time to fill bucket

Wharf:

Set-up suitable 2D matrix,

Relate matrix to footbridge for datum for temperature measurement,

Measure wind speed, record direction,

Ambient air temp, in shade,

Measure depth of water

Measure depth to top of inlet pipe

Measure/photograph height of outlet pipe/water surface

Use thermocouple to measure canal ambient water temperature, record in two positions, record position used,

Record water temp adjacent to inlet,

Thermal image of flow

Photograph flow – digital camera

Goyte:

Photograph flow into canal

Pump house:

At start of trial:

Record inlet temperature of all pumps using:-

Pump house gauges

Laser sensor

Record outlet temperature of all pumps using:-

Pump house gauges

Laser sensor

Record pump flow rate of all pumps

Record/calculate heat load/demand

Wharf:

Use thermo-couple:

Record AIR temperature over 2D matrix, 25mm above canal water surface,

Record WATER temperature over 3D matrix, depth of matrix to be advised,

Record VELOCITY thro' plume???HOW-read display from bank???

At end of trial

Record time at end of trial

Recheck initial AIR temperature reading only

Recheck initial WATER temperature reading only

Recheck initial FLOW rate reading only
Recheck canal ambient WATER temperature
Re-measure wind speed/direction

Pump house:

Recheck pump flow rate
Reset pumps back to auto-cycle

Lock 1E

Re-photograph Lock 1E leakage
Measure flow over weir
Measure gate leakage

Equipment required:

Thermal image camera
Digital camera
15m tape measure
Water flow meter
Anemometer – wind speed
Thermocouple – air
Thermocouple – water
Laser temperature instrument
Bucket and stop watch
15m rope
Ball of string
Tent pegs (2)
Chalk
Roll insulating/duck tape
Cable ties
Surveyor's staff/fishing rod????
Staff – water depth
Dinghy,
Lifebelts (2)

Site 1: Canal basin – wharf

Date of Trial:

Time readings taken:

Lock 1E:

Lock Gate:

Photograph leakage rate: tick

Leakage	Bucket capacity	Fill time (sec.)	Time of day
L.H.side			
R.H.side			

L.H./R.H. – Upstream gate looking up stream

Comments:

Weir:

Photograph weir: tick

Measure breadth of weir: mm

Measure depth of flow over weir: mm

OR

Measure height from weir to water level: mm

Comments:

Date of Trial:

Wharf:

Time readings taken:

Thermal image: tick

Digital photograph of flow: tick

Measure wind speed: m/s

Direction:

Ambient air temp t1: °C

Ambient air temp t2: °C

Ambient canal WATER temperature:

Ambient canal WATER temperature:

N.B.

Mark on map/diagram position used for measurements

Inlet:

Ambient INLET WATER temperature:

Height below surface (mm)	Inlet water temp: °C

Depth of water to TOP OF INLET pipe: mm

Depth of water to Adjacent to pipe: mm mm

Goyte:

Digital photograph of flow: tick

Date of Trial:

Time readings taken:

Wharf:

Measured canal AIR temperature:

	Y16									
	Y15									
	Y14									
	Y13									
	Y12									
	Y11									
	Y10									
	Y9									
	Y8									
	Y7									
	Y6									
	Y5									
	Y4									
	Y3									
	Y2									
	Y1									
	Y0									
Distance from outlet (m)		-x4	-x3	-x2	-x1	x0	+x1	+x2	+x3	+x4
		Distance from centre of pipe (mm)								

Pipe
Outlet

Temperatures measured 25-50mm above canal surface.

Date of Trial:

Time readings taken:

Wharf:

Measured canal WATER temperature:

	Y16									
	Y15									
	Y14									
	Y13									
	Y12									
	Y11									
	Y10									
	Y9									
	Y8									
	Y7									
	Y6									
	Y5									
	Y4									
	Y3									
	Y2									
	Y1									
	Y0									
Distance from outlet (m)		-x4	-x3	-x2	-x1	xo	+x1	+x2	+x3	+x4
		Distance from centre of pipe (mm)								

Pipe
Outlet

Temperatures measured mm below canal surface.

Depth of water to TOP OF OUTLET pipe at point of discharge: mm

Date of Trial:

Time readings taken:

Wharf:

Measured canal VELOCITY ()units

	Y16									
	Y15									
	Y14									
	Y13									
	Y12									
	Y11									
	Y10									
	Y9									
	Y8									
	Y7									
	Y6									
	Y5									
	Y4									
	Y3									
	Y2									
	Y1									
	Y0									
Distance from outlet (m)		-x4	-x3	-x2	-x1	x0	+x1	+x2	+x3	+x4
		Distance from centre of pipe (mm)								

Pipe
Outlet

Flow rate: measured mm below canal surface.

Date of Trial:

Time readings taken:

Wharf Pump House:

Pump	Inlet temp. Gauge	Inlet temp. Laser	Outlet temp. Gauge	Outlet temp. Laser	Measured Flow rate	Flow rate units	Time of reading	Rated Pump flow rate – name plate
Pump 1								
Pump 2								
Pump 3								

END OF TRIAL:

Time readings taken:

Recheck initial AMBIENT AIR temperature reading:

Recheck initial WATER temperature reading:

Recheck initial FLOW rate reading

Recheck initial canal WATER temperature reading:

Re-measure wind speed/direction:

Recheck pump flow rate:

Reset pumps back to auto-cycle

Date of Trial:

Time readings taken:

Re-photograph Lock 1E leakage rate:

Re-measure flow over weir:

Re-measure gate leakage:

APPENDIX 2: EQUIPMENT USED

Equipment used throughout the data collection:-

1. Thermal image camera:



Thermal Camera

FLIR Systems S60 thermal imaging camera

Thermal camera setup:

Field of view/min focus distance	24° x 18° / 0.3 m
Spatial resolution (IFOV)	1.3 mrad
Image frequency	50 Hz
Thermal sensitivity @ 50/60Hz	0.06 °C at 30 °C
Electronic zoom function	2,4,8, interpolating
Focus	Automatic or manual
Digital image enhancement	Normal and enhanced
Detector type	Focal plane array (FPA) uncooled microbolometer 320 x 240 pixels
Spectral range	7.5 to 13 µm

Built-in digital video	640 x 480 pixels, full color
Temperature ranges	-40 °C to +120 °C (-40 °F to +248 °F), Range 1 0 °C to +500 °C (+32 °F to 932 °F), Range 2 +350 °C to +1500 °C (+662 to +2732 °F), Range 3
Accuracy (% of reading)	± 2 °C or ± 2%
Measurement modes	Spot/manual (up to 10 movable), Spot/automatic placement at max, min, Area (up to 5 movable), isotherm (2), line profile, Delta T
Emissivity correction pre-	Variable from 0.1 to 1.0 or select from listings in defined material list
Measurement features for	Automatic corrections based on user input reflected ambient temperature, distance, relative humidity, atmospheric transmission, and external optics.
Optics transmission correction sensors	Automatic, based on signals from internal sensors

General data used for test:

Ambient air temperature	17-17.5°C
Relative Humidity	50% (estimated)
Water emissivity	0.96
Viewing distance	3.8m (vertical)

2. Thermocouples

- i) 'K' type thermocouple with 5m lead for water temperature
- ii) 'K' type thermocouple with 5m lead for air temperature.



Digital Thermocouples Meter

3. Flow meter



Turbine Flow Meter

Equipment Calibration:

Various methods of equipment calibration were considered as follows:

Thermocouples

Use boiling water, i.e. 100 degree Celsius,

- a) Use crushed ice, i.e. 0 degree Celsius,
- b) Compare meter readings using two thermocouples and laboratory/calibrated meter.
- c) Compare at 38 degree C against medical thermometer.

The method selected was to compare readings of existing laboratory thermocouple meter with that used for the site measurements.

Thermal Image

The thermocouples were as a comparator for the thermal image.

Use boiling water, compare thermocouple with thermal image.

Use crushed ice, i.e. 0 degree Celsius, compare thermocouple with thermal image.

Flow Meter

No calibration of flow meter was undertaken.

APPENDIX 3: PRELIMINARY CASE STUDY

Preliminary Field Measured Data (Temperature, Velocity and Depth)

Central Services Building – CSB

50mm below surface											
Breadth	Temperature °C										
	5.0	4.5	4.0	3.5	3.0	2.5	2.0	1.5	1.0	0.5	0.0
1m	17.5	17.7	18.3	18.3	18.2	18.1	17.4	17.5	18.5	18.0	18.0
0.8m	17.6	17.8	18.4	18.4	18.2	18.1	17.6	17.7	18.6	18.0	18.1
0.6m	17.7	17.8	18.4	18.4	18.3	18.3	17.8	17.9	18.6	18.1	18.1
0.4m	17.7	17.6	18.4	18.5	18.3	18.7	18.3	18.8	19.1	18.2	18.1
0.2m	18.0	18.1	18.5	18.5	18.9	18.8	18.6	19.2	19.1	18.4	18.1
0m	18.0	18.4	18.6	18.7	19.0	19.1	19.2	19.8	20.5	21.2	24
-0.2m	18.0	18.4	18.1	19.1	19.0	18.7	19.2	19.9	19.6	20.0	18.4
-0.4m	17.8	18.6	18.1	19.0	18.9	18.6	19.2	18.8	18.6	18.9	18.4
-0.6m	17.9	18.7	18.2	18.8	18.6	18.6	19.2	18.7	18.5	18.8	18.4
-0.8m	17.9	19.0	18.4	18.8	18.6	18.5	19.1	18.8	18.5	18.5	18.4
-1m	18.0	19.3	19.0	18.7	18.6	18.7	19.1	18.8	18.5	18.5	18.4

Mid-depth											
Breadth	Temperature °C										
	5.0	4.5	4.0	3.5	3.0	2.5	2.0	1.5	1.0	0.5	0.0
1	18.0	18.1	17.5	17.3	17.7	18.2	18.0	18.0	17.7	18.1	17.7
0.8	18.0	18.3	17.6	17.4	17.8	18.3	18.1	18.0	17.7	18.2	17.7
0.6	17.6	17.6	17.6	17.5	17.5	17.4	18.1	18.2	17.6	18.2	17.8
0.4	17.8	17.6	17.7	17.4	17.3	17.3	17.8	18.2	17.7	18.2	17.6
0.2	17.5	18.3	17.8	17.5	17.3	17.3	17.5	17.8	17.7	18.2	17.6
0.0	18.0	18.2	17.9	17.4	17.4	17.5	17.6	17.8	18.2	18.3	17.9
-0.2	18.3	18.3	18.5	18.7	17.4	17.3	17.7	17.8	18.3	18.3	18.0
-0.4	18.9	18.9	18.5	18.9	18.7	19.0	18.8	17.8	18.3	18.3	18.0
-0.6	18.9	18.9	18.8	18.9	19.0	19.0	18.8	17.9	18.4	18.2	18.1
-0.8	19.4	19.0	18.9	19.2	19.2	18.9	18.7	18.3	18.4	18.3	18.1
-1.0	19.5	19.0	19.1	19.2	19.2	18.9	18.6	18.5	18.4	18.3	18.1

50mm above bed											
Breadth	Temperature °C										
	5.0	4.5	4.0	3.5	3.0	2.5	2.0	1.5	1.0	0.5	0.0
1	17.6	17.8	17.7	17.5	17.4	17.4	17.4	17.6	17.3	17.5	17.5
0.8	17.6	17.8	17.7	17.5	17.4	17.4	17.4	17.6	17.3	17.5	17.5
0.6	17.9	17.6	17.7	17.4	17.4	17.2	17.4	17.4	17.4	17.5	17.5
0.4	17.9	17.6	17.7	17.4	17.4	17.2	17.4	17.4	17.4	17.5	17.4
0.2	17.9	17.6	17.7	17.5	17.5	17.3	17.4	17.3	17.5	17.6	17.4
0.0	18.1	17.9	18.2	17.5	17.9	17.4	17.6	17.4	17.7	18.2	17.5
-0.2	18.7	17.9	19.1	17.5	18.1	17.5	17.7	17.4	18.0	18.2	17.5
-0.4	19.3	17.8	19.1	17.8	19.0	17.4	17.8	17.5	18.1	18.3	17.6
-0.6	19.3	17.8	19.2	18.4	19.1	17.4	18.0	17.5	18.1	18.3	17.7
-0.8	19.4	19.3	19.2	19.2	19.1	17.5	18.7	17.6	18.2	18.3	18.0
-1.0	19.3	19.3	19.3	19.2	19.1	17.5	18.7	18.5	18.2	18.2	18.2

Canalside West Temperature

CSW - Temperature

50mm below surface										
Distance along plume	Temperature °C									
	1.00	0.75	0.50	0.25	0.00	0.25	0.50	0.75	1.00	
2.50	17.6				17.6				17.5	
2.00	17.6	17.6	17.6	17.6	17.7	17.5	17.5	17.5	17.5	
1.50	17.6	17.6	17.7	17.7	18.0	17.6	17.6	17.5	17.5	
1.00	17.7	17.7	17.8	17.8	18.1	17.5	17.7	17.6	17.6	
0.50	17.7	17.7	17.8	17.8	17.9	17.7	17.7	17.6	17.6	
0.00	18.0	18.0	18.1	18.1	18.1	18.1	18.1	18.0	18.0	

Mid-depth										
Distance along plume	Temperature °C									
	1.00	0.75	0.50	0.25	0.00	0.25	0.50	0.75	1.00	
2.50	17.6				17.6				17.6	
2.00	17.7	17.7	17.7	17.7	17.7	17.7	17.7	17.7	17.7	
1.50	17.7	17.8	17.8	17.8	17.8	17.8	17.8	17.7	17.7	
1.00	17.7	17.7	17.8	17.9	17.9	17.9	17.8	17.7	17.7	
0.50	17.7	17.8	17.8	18.0	18.0	18.0	17.8	17.8	17.6	
0.00	17.6	17.6	17.6	17.9	18.6	17.9	17.6	17.6	17.6	

50mm above bed										
Distance along plume	Temperature °C									
	1.00	0.75	0.50	0.25	0.00	0.25	0.50	0.75	1.00	
2.50	18.0				17.6				17.7	
2.00	17.6	17.6	17.6	17.7	17.7	17.7	17.6	17.6	17.6	
1.50	17.6	17.6	17.6	17.7	17.7	17.7	17.6	17.6	17.6	
1.00	17.6	17.6	17.6	17.6	17.6	17.6	17.6	17.6	17.6	
0.50	17.6	17.6	17.6	17.6	17.6	17.6	17.6	17.6	17.6	
0.00	17.6	17.6	17.6	17.6	17.6	17.6	17.6	17.6	17.6	

Lockside - Temperature

Temperature °C - 50mm below surface					
Distance along Plume (m)	Distance across plume (m)				
	-1.00	-0.50	0.00	0.50	1.00
2.00	19.0	19.0	19.0	19.0	19.0
1.50	18.8	19.6	19.9	19.6	18.9
1.00	19.0	19.6	20.0	19.8	19.0
0.50	19.3	20.1	22.5	21.0	20
0.00	19.2	21.0	21.7	21	20.7

Temperature °C - mid-depth					
Distance along Plume (m)	Distance across plume (m)				
	-1.00	-0.50	0.00	0.50	1.00
2.00	18.9	18.8	18.8	18.9	18.9
1.50	18.9	18.9	19	18.9	18.8
1.00	18.9	18.9	19.6	19.0	18.8
0.50	18.9	18.9	20.6	19.1	18.6
0.00	18.9	19.0	24	19.2	18.6

Temperature °C - 50mm above bed					
Distance along Plume (m)	Distance across plume (m)				
	-1.00	-0.50	0.00	0.50	1.00
2.00	18.1	18.6	18.6	18.8	18.5
1.50	18.1	18.4	18.7	18.5	18.5
1.00	18.3	18.3	18.5	18.4	18.4
0.50	18.3	18.3	18.4	18.4	18.3
0.00	18.3	18.3	18.3	18.4	18.3

CSB – Velocity

Canal Flow - at grid points

Coordinate	Velocity (m/s)				
	4.0	3.0	2.0	1.0	0.0
0.4	0.136	0.253	0.172	0.124	0.000
0.2	0.268	0.339	0.368	0.279	0.000
0.0	0.263	0.391	0.669	0.931	1.229
-0.2	0.358	0.391	0.602	0.201	0.000
-0.4	0.100	0.368	0.314	0.120	0.000

Canalside West – Velocity

Flow measured 50mm below surface

Canal Width (m)	Flow rate (m/s)				
	Distance From Dishcharge Pipe (m)				
	-1.00	-0.50	0.00	0.50	1.00
2.50					
2.00	0.050		0.31		0.050
1.50					
1.00	0.100		0.49		0.100
0.50					
0.00	0.000		0.08		0.000

Lockside – Velocity

50mm below surface

Canal Width (m)	Flow Rate m/s				
	Distance From Discharge Pipe (m)				
	-1.00	-0.50	0.00	0.50	1.00
2.00	0.0		0.31		0.0
1.50					
1.00	0.0		0.62		0.0
0.50					
0.00	0.0		0.1		0.0

CSB – Depth

Canal depth at grid points (m)											
Width (m)											
	5.0	4.5	4.0	3.5	3.0	2.5	2.0	1.5	1.0	0.5	0.0
0.8	1.05	1.13	1.03	1.15	1.04	1.09	1.13	1.15	1.13	1.10	1.10
0.6	0.86	1.03	1.08	0.94	0.98	1.05	1.02	1.05	1.00	1.00	1.08
0.4	0.84	1.00	0.95	0.88	0.81	0.94	1.01	1.00	1.01	1.03	1.04
0.2	0.76	0.75	0.75	0.88	0.88	0.98	0.95	0.95	1.01	0.95	0.90
0.0	0.76	0.65	0.79	0.86	0.89	0.90	0.82	0.98	0.93	0.95	0.90
-0.2	0.82	0.75	0.91	0.80	0.73	0.80	0.80	0.90	0.85	0.85	0.85
-0.4	0.74	0.98	0.83	0.76	0.67	0.68	0.74	0.79	0.82	0.90	0.78
-0.6	0.74	0.98	0.80	0.75	0.60	0.77	0.76	0.75	0.75	0.79	0.76
-0.8	0.75	0.5inle		0.64	0.60	0.65	0.76	0.74	0.70	0.76	0.75
-1.0	0.75	0.61			0.56	0.70	0.75	0.75	0.75	0.76	0.75

Canalside West – Depth

Coordinate	Depth m				
	-1.00	-0.50	0.00	0.50	1.00
2.50	1.10	1.20	1.23	1.15	1.15
2.00	1.00	0.99	1.20	1.16	1.05
1.50	1.08	1.06	1.15	1.13	1.08
1.00	1.00	1.06	1.10	1.05	1.00
0.50	0.84	0.95	0.95	1.05	0.80
0.00	0.55	1.06	1.01	1.05	0.67

Lockside – Depth

Coordinates from centre line of outlet pipe

Canal Width (m)	Canal depth at grid points (m)				
	Distance From Discharge Pipe (m)				
	-1.00	-0.50	0.00	0.50	1.00
2.00	1.35	1.34	1.49	1.47	1.60
1.50	1.20	1.26	1.20	1.25	1.40
1.00	1.06	1.10	1.06	1.16	1.15
0.50	1.04	1.06	1.04	1.06	1.04
0.00	0.96	0.80	0.66	0.80	0.95

APPENDIX 4: REFINE CASE STUDY

Refine Field Measured Data (Temperature, Velocity and Depth)

CSB - Temperature

Measured canal at discharge layer temperature: at ($z = 0.075\text{m}$)

Distance from centre of pipe (across canal) perpendicular to plume(m)											
	1	0.8	0.6	0.4	0.2	y = 0	-0.2	-0.4	-0.6	-0.8	-1
x=0	17.15	17.15	17.15	17.15	17.15	24.00	17.15	17.15	17.15	17.15	17.15
0.5	17.15	17.15	17.15	17.31	18.60	20.12	18.60	17.42	17.15	17.15	17.15
1	17.15	17.15	17.15	17.60	18.30	19.15	18.30	17.60	17.20	17.20	17.20
1.5	17.15	17.15	17.40	17.70	18.23	18.85	18.30	17.70	17.40	17.20	17.20
2	17.15	17.20	17.45	17.70	18.10	18.55	18.10	17.70	17.45	17.20	17.20
2.5	17.15	17.17	17.38	17.74	18.05	18.20	18.05	17.74	17.40	17.24	17.20
3	17.15	17.18	17.45	17.70	18.00	18.15	18.00	17.70	17.42	17.20	17.18
3.5	17.15	17.15	17.40	17.75	18.00	18.1	18.00	17.75	17.41	17.18	17.18
4	17.15	17.15	17.35	17.63	17.90	18.05	17.90	17.63	17.37	17.18	17.18
4.5	17.15	17.15	17.30	17.60	17.90	18	17.90	17.60	17.31	17.18	17.15
5	17.15	17.15	17.24	17.53	17.8	17.95	17.8	17.52	17.23	17.15	17.15

Measured canal temperature at (0.6m) below free surface: ($z = 0.6\text{m}$)

Distance from centre of pipe (across canal) perpendicular to plume(m)											
	1	0.8	0.6	0.4	0.2	0	-0.2	-0.4	-0.6	-0.8	-1
0	17.05	17.05	17.05	17.05	17.05	17.05	17.05	17.05	17.05	17.05	17.18
0.5	17.05	17.05	17.05	17.37	17.37	17.37	17.34	17.32	17.21	17.15	17.18
1	17.05	17.05	17.05	17.49	18.05	18.05	18.08	17.79	17.25	17.15	17.18
1.5	17.05	17.05	17.39	17.75	18.03	18.03	18.01	17.74	17.45	17.15	17.18
2	17.05	17.05	17.61	17.61	18.01	18.02	17.89	17.71	17.68	17.15	17.18
2.5	17.05	17.05	17.43	17.6	18	18.01	17.84	17.62	17.61	17.15	17.18
3	17.05	17.15	17.35	17.6	17.93	17.95	17.81	17.61	17.6	17.15	17.18
3.5	17.05	17.15	17.23	17.6	17.6	17.63	17.62	17.6	17.6	17.15	17.18
4	17.05	17.15	17.2	17.51	17.55	17.6	17.58	17.58	17.54	17.15	17.18
4.5	17.05	17.15	17.2	17.29	17.38	17.4	17.37	17.36	17.25	17.15	17.18
5	17.05	17.15	17.15	17.25	17.27	17.35	17.35	17.29	17.21	17.15	17.15

Measured canal temperature at 0.1m above the bed: (z variable)

Distance from centre of pipe (across canal) perpendicular to plume(m)											
	1	0.8	0.6	0.4	0.2	0	-0.2	-0.4	-0.6	-0.8	-1
0	17.05	17.05	17.05	17.05	17.05	17.05	17.05	17.05	17.05	17.05	17.05
0.5	17.05	17.05	17.15	17.31	17.31	17.31	17.31	17.31	17.15	17.05	17.05
1	17.05	17.05	17.15	17.31	17.35	17.35	17.32	17.31	17.15	17.05	17.05
1.5	17.05	17.05	17.15	17.32	17.36	17.36	17.32	17.31	17.15	17.05	17.05
2	17.05	17.05	17.15	17.32	17.34	17.38	17.32	17.32	17.15	17.05	17.05
2.5	17.05	17.05	17.15	17.41	17.5	17.57	17.56	17.45	17.15	17.05	17.05
3	17.05	17.05	17.15	17.41	17.51	17.57	17.55	17.49	17.15	17.05	17.05
3.5	17.05	17.05	17.15	17.39	17.47	17.54	17.52	17.46	17.15	17.05	17.05
4	17.05	17.05	17.15	17.38	17.42	17.51	17.51	17.49	17.15	17.05	17.05
4.5	17.05	17.05	17.15	17.38	17.37	17.37	17.37	17.35	17.15	17.05	17.05
5	17.05	17.05	17.15	17.2	17.25	17.25	17.24	17.21	17.15	17.05	17.05

CSB - Velocity

Measured canal flow (m/sec) on discharge layer: (z = 0.075m)

Distance from centre of pipe (across canal) perpendicular to plume(m)											
	1	0.8	0.6	0.4	0.2	0	-0.2	-0.4	-0.6	-0.8	-1
0	0.03	0.03	0.03	0.03	0.03	1.23	0.03	0.03	0.03	0.03	0.03
0.5	0.03	0.03	0.03	0.07	0.402	0.596	0.415	0.08	0.03	0.03	0.03
1	0.03	0.03	0.08	0.298	0.377	0.574	0.379	0.301	0.08	0.03	0.03
1.5	0.03	0.08	0.178	0.244	0.351	0.465	0.352	0.286	0.178	0.08	0.03
2	0.08	0.144	0.156	0.222	0.332	0.377	0.332	0.244	0.156	0.222	0.08
2.5	0.124	0.132	0.145	0.211	0.31	0.332	0.31	0.231	0.145	0.178	0.132
3	0.122	0.126	0.138	0.2	0.244	0.31	0.288	0.2	0.137	0.134	0.128
3.5	0.12	0.113	0.134	0.134	0.221	0.3	0.228	0.134	0.13	0.126	0.124
4	0.102	0.108	0.111	0.113	0.178	0.2	0.211	0.178	0.123	0.122	0.111
4.5	0.093	0.098	0.101	0.112	0.154	0.156	0.152	0.142	0.111	0.111	0.102
5	0.093	0.093	0.095	0.098	0.102	0.134	0.134	0.102	0.101	0.093	0.073

CSB - Depths

Distance from centre of pipe (across canal) perpendicular to plume(m)											
	1	0.8	0.6	0.4	0.2	0	-0.2	-0.4	-0.6	-0.8	-1
0	1.25	1.15	0.98	0.84	0.80	0.775	0.775	0.75	0.725	0.70	0.66
0.5	1.25	1.13	0.98	0.95	0.80	0.775	0.775	0.77	0.725	0.70	0.65
1	1.25	1.13	0.98	0.95	0.80	0.80	0.78	0.75	0.725	0.70	0.65
1.5	1.25	1.13	1.01	0.95	0.88	0.85	0.78	0.75	0.74	0.725	0.66
2	1.25	1.13	1.01	0.95	0.88	0.85	0.78	0.75	0.725	0.725	0.66
2.5	1.25	1.13	1.05	1.0	0.90	0.85	0.775	0.75	0.725	0.70	0.66
3	1.25	1.13	1.05	1.0	0.95	0.85	0.78	0.75	0.725	0.70	0.66
3.5	1.25	1.13	1.05	1.0	0.95	0.85	0.78	0.75	0.725	0.70	0.65
4	1.25	1.13	1.05	1.01	1.01	0.85	0.78	0.75	0.725	0.70	0.64
4.5	1.25	1.13	1.05	1.01	0.95	0.85	0.78	0.75	0.75	0.75	0.65
5	1.25	1.13	1.05	1.01	0.90	0.85	0.78	0.75	0.75	0.75	0.65

BBC Mailbox – Temperature

Measured canal SURFACE WATER temperature:										
	3.2	18.6	18.6	18.6	18.7	18.7	18.7	18.6	18.6	18.6
	3.0	18.6	18.65	18.7	18.75	18.75	18.75	18.7	18.65	18.6
	2.8	18.65	18.7	18.75	18.8	18.8	18.8	18.75	18.7	18.65
	2.6	18.7	18.8	18.8	18.85	18.85	18.85	18.8	18.8	18.7
	2.4	18.7	18.9	18.9	18.9	18.9	18.9	18.9	18.9	18.7
	2.2	18.8	18.9	18.95	18.95	18.95	18.95	18.95	18.9	18.8
	2.0	18.85	18.95	19.0	19.0	19.0	19.0	19.0	18.95	18.85
	1.8	18.9	19.0	19.0	19.05	19.05	19.05	19.05	19.0	18.9
	1.6	18.9	19.0	19.1	19.1	19.1	19.1	19.1	19	18.9
	1.4	18.7	18.7	18.7	18.85	18.85	18.85	18.7	18.7	18.7
	1.2	18.7	18.7	18.7	18.8	18.8	18.8	18.7	18.7	18.7
	1.0	18.7	18.7	18.7	18.7	18.7	18.7	18.7	18.7	18.7
	0.8	18.7	18.7	18.7	18.7	18.7	18.7	18.7	18.7	18.7
	0.6	18.7	18.7	18.7	18.7	18.7	18.7	18.7	18.7	18.7
	0.4	18.7	18.7	18.7	18.7	18.7	18.7	18.7	18.7	18.7
	0.2	18.7	18.7	18.7	18.7	18.7	18.7	18.7	18.7	18.7
	X=0	18.7	18.7	18.7	18.7	18.7	18.7	18.7	18.7	18.7
Distance from discharge	Y= -2	1.5	1.0	0.5	0	0.5	1.0	1.5	Y=+2	
	Distance from centre of pipe perpendicular to plume(m)									

Measured canal DISCHARGE LEVEL WATER temperature:										
	3.2	18.0	18.0	18.0	18.0	18.0	18.0	18.0	18.0	18.0
	3	18.0	18.0	18.1	18.1	18.10	18.0	18.0	18.0	18.0
	2.8	18.1	18.1	18.1	18.1	18.15	18.1	18.1	18.1	18.1
	2.6	18.2	18.2	18.2	18.2	18.20	18.2	18.2	18.1	18.1
	2.4	18.2	18.2	18.2	18.2	18.28	18.2	18.2	18.2	18.2
	2.2	18.2	18.3	18.3	18.3	18.35	18.2	18.2	18.2	19.2
	2	18.2	18.3	18.3	18.3	18.37	18.2	18.2	18.2	18.1
	1.8	18.2	18.3	18.3	18.3	18.39	18.3	18.2	18.2	18.2
	1.6	18.2	18.3	18.3	18.3	18.41	18.3	18.3	18.3	18.2
	1.4	18.3	18.4	18.4	18.4	18.5	18.3	18.3	18.3	18.2
	1.2	18.3	18.3	18.4	18.4	18.55	18.4	18.4	18.3	18.3
	1	18.4	18.4	18.5	18.5	18.7	18.4	18.4	18.3	18.3
	0.8	18.4	18.5	18.7	18.8	18.84	18.6	18.6	18.6	18.4
	0.6	18.3	18.4	18.7	18.8	19.1	18.8	18.4	18.3	18.2
	0.4	18.2	18.2	18.7	19.3	19.5	19.3	18.7	18.2	18.2
	0.2	18.0	18.1	18.3	18.3	19.6	18.3	18.3	18.2	18.2
	X=0	18.0	18.0	18.0	18.1	20	18.1	18.0	18.0	18.0
Distance from discharge	Y= -2	1.5	1	0.5	0	0.5	1	1.5	Y=	
	Distance from centre of pipe perpendicular to plume(m)									

Measured canal BED WATER temperature:										
	3.2	17.7	17.9	18.1	18.1	18.2	18.1	18.1	17.7	17.5
	3.0	17.7	17.9	18.1	18.1	18.2	18.1	18.1	17.8	17.8
	2.8	17.7	18.0	18.1	18.2	18.2	18.1	18.1	18.0	17.8
	2.6	18.0	18.0	18.0	18.2	18.3	18.1	18.1	18.0	18.0
	2.4	18.0	18.0	18.0	18.2	18.3	18.0	18.1	18.0	18.0
	2.2	18.0	18.0	18.0	18.2	18.3	18.0	18.1	18.0	18.0
	2.0	18.0	18.0	18.0	18.0	18.3	18.0	18.2	18.0	18.0
	1.8	18.0	18.0	18.0	18.0	18.3	18.0	18.0	18.0	18.0
	1.6	18.1	18.1	18.0	18.0	18.3	18.0	18.0	18.0	18.0
	1.4	18.1	18.1	18.0	18.0	18.3	18.0	18.0	18.0	18.0
	1.2	18.1	18.1	18.0	18.0	18.1	18.0	18.0	18.0	18.0
	1.0	18.1	18.1	18.0	18.0	18.1	18.0	18.0	18.0	18.0
	0.8	18.1	18.1	18.0	18.0	18.0	18.4	18.0	18.0	18.0
	0.6	18.0	18.0	18.0	18.0	18.0	18.0	18.0	18.0	18.0
	0.4	18.0	18.0	18.0	18.0	18.0	18.0	18.0	18.0	18.0
	0.2	18.0	18.0	18.0	18.0	18.0	18.0	18.0	18.0	18.0
	X=0	17.9	18.0	18.0	18.0	18.0	18.0	18.0	18.0	18.0
Distance from discharge	Y=-2	1.5	1.0	0.5	0	0.5	1.0	1.5	Y=+2	
	Distance from centre of pipe perpendicular to plume(m)									

BBC Mailbox – Velocity

Measured canal FLOW RATE (m/sec)										
	3.0			0.11		0.17		0.12		
	2.75									
	2.5			0.13		0.2		0.13		
	2.25									
	2.0			0.14		0.22		0.14		
	1.75									
	1.5			0.18		0.26		0.18		
	1.25									
	1.0			0.25		0.32		0.25		
	0.75									
	0.5			0.32		0.4		0.32		
	0.25									
	X=0					0.6				
Distance from discharge	Y= -2	1.5	1.0	0.5	0	0.5	1.0	1.5	Y=	
	Distance from centre of pipe perpendicular to plume (m)									

Canalside West – Temperature

CSW - Temperature

50mm below surface									
Distance along plume	Temperature °C								
	1.00	0.75	0.50	0.25	0.00	0.25	0.50	0.75	1.00
2.50	17.6	17.6	17.6	17.6	17.6	17.6	17.6	17.6	17.5
2.00	17.6	17.6	17.6	17.6	17.7	17.6	17.6	17.6	17.6
1.50	17.6	17.6	17.7	17.7	17.7	17.7	17.7	17.7	17.7
1.00	17.6	17.6	17.7	17.8	17.8	17.7	17.7	17.7	17.6
0.50	17.7	17.8	17.9	17.9	17.9	17.9	17.9	17.8	17.7
0.00	18.1	18.1	18.4	18.4	18.4	18.4	18.4	18.1	18.0

0.6m below surface, discharge layer									
Distance along plume	Temperature °C								
	1.00	0.75	0.50	0.25	0.00	0.25	0.50	0.75	1.00
2.50	17.5	17.5	17.5	17.5	17.5	17.5	17.5	17.5	17.6
2.00	17.5	17.6	17.6	17.6	17.6	17.6	17.6	17.6	17.6
1.50	17.6	17.7	17.8	17.8	17.8	17.8	17.8	17.7	17.7
1.00	17.7	17.8	17.9	18.0	18.0	18.0	18.0	17.8	17.7
0.50	17.9	17.9	18.2	18.4	18.5	18.4	18.3	18.0	18.0
0.00	18.0	18.0	18.3	18.3	19	18.3	18.3	18.0	18.0

50mm above bed									
Distance along plume	Temperature °C								
	1.00	0.75	0.50	0.25	0.00	0.25	0.50	0.75	1.00
2.50	17.5	17.5	17.6	17.6	17.6	17.6	17.6	17.5	17.5
2.00	17.5	17.5	17.6	17.7	17.7	17.7	17.6	17.6	17.6
1.50	17.5	17.6	17.7	17.7	17.7	17.7	17.7	17.7	17.7
1.00	17.7	17.7	17.8	17.8	17.8	17.8	17.8	17.8	17.7
0.50	17.7	17.7	17.8	17.8	17.9	17.9	17.8	17.8	17.7
0.00	17.5	17.6	17.7	17.7	17.7	17.7	17.6	17.6	17.5

Canalside West – Velocity

Flow measured at discharge layer

Distance along plume (m)	Flow (m/s)				
	Distance From Discharge Pipe (m)				
	-1.00	-0.50	0.00	0.50	1.00
2.50	0.045		0.085		0.045
2.00	0.050		0.110		0.050
1.50	0.08		0.255		0.081
1.00	0.100		0.399		0.100
0.50	0.085		0.54		0.087
0.00	0.000		0.913		0.000

Temperature and velocity along plume path line – Canalside West

	Distance along plume (m)					
	0	0.5	1	1.5	2	2.5
Canal measured data T°C	19.0	18.5	18.3	18.1	18.0	18.0
Canal measured data Um/s	0.91	0.66	0.5	0.4	0.3	0.18

Canalside West – Depth

	Depth mm				
Distance along plume	-1.00	-0.50	0.00	0.50	1.00
2.50	1.10	1.20	1.23	1.15	1.15
2.00	1.00	0.99	1.20	1.16	1.05
1.50	1.08	1.06	1.15	1.13	1.08
1.00	1.00	1.06	1.10	1.05	1.00
0.50	0.84	0.95	0.95	1.05	0.80
0.00	0.55	1.06	1.01	1.05	0.67

Lockside – Temperature

Temperature °C - 50mm below surface					
Distance along Plume (m)	Distance across plume (m)				
	-1.00	-0.50	0.00	0.50	1.00
2.00	18.4	18.5	18.5	18.5	18.4
1.50	18.6	18.7	18.8	18.7	18.6
1.00	18.8	19.5	19.5	19.4	18.8
0.50	19.0	19.3	19.8	19.3	19.1
0.00	20.0	20.1	20.4	20.1	19.9

Temperature °C – 0.65m below surface, discharge layer					
Distance along Plume (m)	Distance across plume (m)				
	-1.00	-0.50	0.00	0.50	1.00
2.00	18.0	18.1	18.1	18.1	18.1
1.50	18.1	18.3	18.5	18.3	18.3
1.00	18.3	18.4	19.4	18.4	18.4
0.50	18.4	18.5	20.5	18.5	18.4
0.00	18.5	19.0	22	19.1	18.7

Temperature °C - 50mm above bed					
Distance along Plume (m)	Distance across plume (m)				
	-1.00	-0.50	0.00	0.50	1.00
2.00	17.7	17.7	17.7	17.7	17.7
1.50	17.8	18.0	18.0	18.0	17.9
1.00	18.2	18.4	18.4	18.4	18.2
0.50	18.4	18.7	19.1	19.0	18.5
0.00	18.7	19.0	19.5	19.0	18.7

Lockside – Velocity

Flow at discharge layer

Canal Width (m)	Flow m/s				
	Distance From Discharge Pipe (m)				
	-1.00	-0.50	0.00	0.50	1.00
2.00	0.085		0.231		0.085
1.50	0.110		0.35		0.110
1.00	0.25		0.542		0.245
0.50	0.072		0.89		0.075
0.00	0.0		1.217		0.0

Temperature and velocity along plume path line – Lockside

Distance along plume (m)						
	0	0.5	1	1.5	2	2.5
Canal measured data T°C	22	20.7	19.8	19.2	18.7	18.1
Canal measured data Um/s	1.22	0.89	0.71	0.51	0.4	0.24

Lockside – Depth

Coordinates from centre line of outlet pipe

Canal Width (m)	Canal depth at grid points (m)				
	Distance From Discharge Pipe (m)				
	-1.00	-0.50	0.00	0.50	1.00
2.00	1.35	1.34	1.49	1.47	1.60
1.50	1.20	1.26	1.20	1.25	1.40
1.00	1.06	1.10	1.06	1.16	1.15
0.50	1.04	1.06	1.04	1.06	1.04
0.00	0.96	0.80	0.66	0.80	0.95

APPENDIX 5: KIRKLEES COLLEGE CASE STUDY

Kirklees College Canal Water Cooling System Heat Rejection

By: Jafar Ali and John Fieldhouse

University of Huddersfield

School of Computing and Engineering

Department of Engineering and Technology

A report submitted to
Kirklees College, July, 2010

Summary

This study is undertaken by the University of Huddersfield to determine the possibility of using British Waterways canal water cooling system by Kirklees College. It is found that the canal will be able to absorb the rejected heat of 3470 kW within 3-4m distance from the outfall. These results are presented for a number of different models developed by the University of Huddersfield to predict the behaviour of thermal plume discharge into shallow and still receiving water.

The maximum temperature of water discharged does not exceed the Environment Agency Regulation limit of 28°C, for limitation of impact to aquatic life.

Introduction

The University of Huddersfield have developed three models to predict the behaviour of cooling water discharge into the British Waterway's canal that runs through Huddersfield, known as Huddersfield Narrow canal. The models are linked together and each investigates different properties from a given thermal discharge; one model predicts temperature decay whereas another predicts velocity and finally a 3-dimensional model of the size of the plume represents the discharge zone. In this study all these models are run to investigate the possibility of using canal to dissipate heat rejected by Kirklees College.

The initial temperature and flow rate data used in this study, and applied to the model, has been provided by Kirklees College contractor Max Fordham consulting engineers and is described in the following sections.

Note: Three studies are described within the main report – two single discharge outlets (each with different pipe diameters), the second multi-point discharge and the third a further single discharge with different initial parameters.

Study 1a – Single discharge but 2 different discharge diameters.

Temperature Prediction

The university has developed a mathematical model that may be used to predict the temperature dilution of cooling water discharge into a still water environment – typically British Waterways canals. The model is applied to determine the temperature profile of the cooling water discharge from Kirklees (Huddersfield Technical) College new building into

the Huddersfield narrow canal using the initial temperature and flow rate data provided by Max Fordham. The following data has been used;

Study 1a - Pipe Diameter 475 mm

- Discharge temperature is 24°C,
- Canal ambient temperature is 19°C,
- Discharge pipe diameter **0.475m**
- Discharge flow rate is **166.32 l/s**.

The discharge velocity will be 0.94m/s, the average depth of canal assumed to be 1.2m and the depth of discharge to the bed 0.55m. *Figure 1* illustrates the temperature dilution along the plume path line.

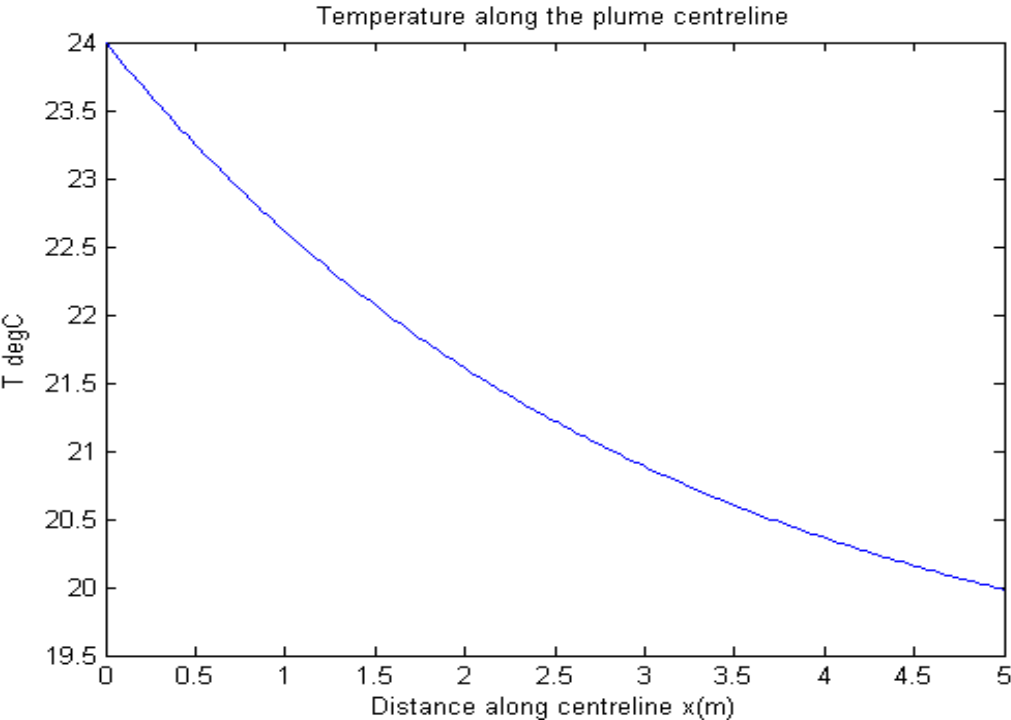


Figure 1: Temperature dilution along the centreline of the plume

For temperature along the lateral axis (y) across the plume path line, the following profiles obtained, see *figure 2*:

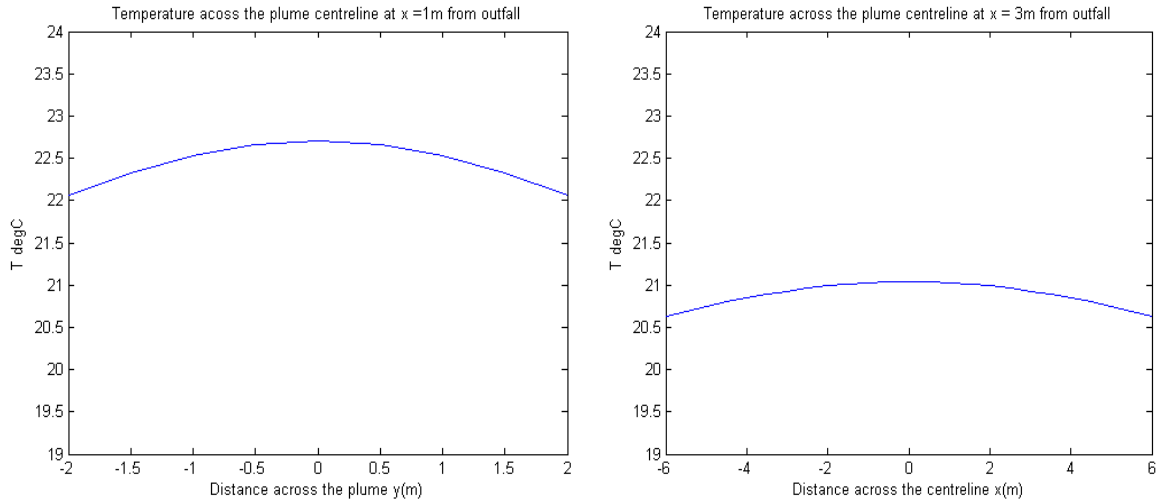


Figure 2: Temperature dilution across the centreline at $x = 1\text{m}$ and $x = 3\text{m}$ from outfall

Velocity Prediction

The parameters used in the previous clause are used in this section to predict the velocity profile along the plume path line using the model developed by the University of Huddersfield. The obtained result is shown in *figure 3*:

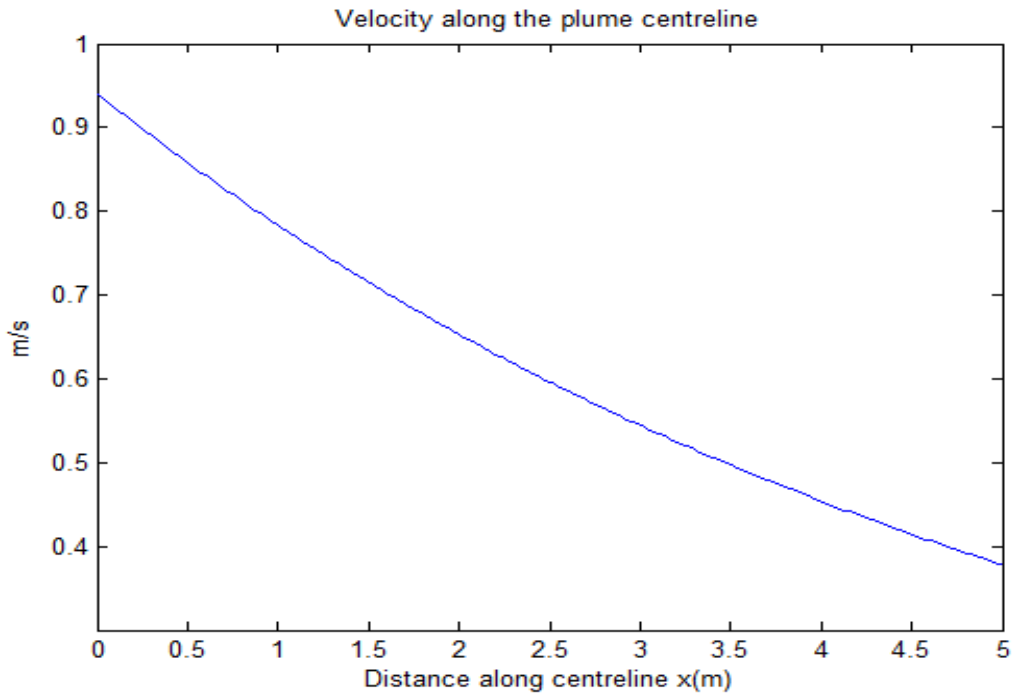


Figure 3: Velocity along the plume centreline

The lateral velocity profile along the y axis across the plume path line is demonstrated in *figure 4*:

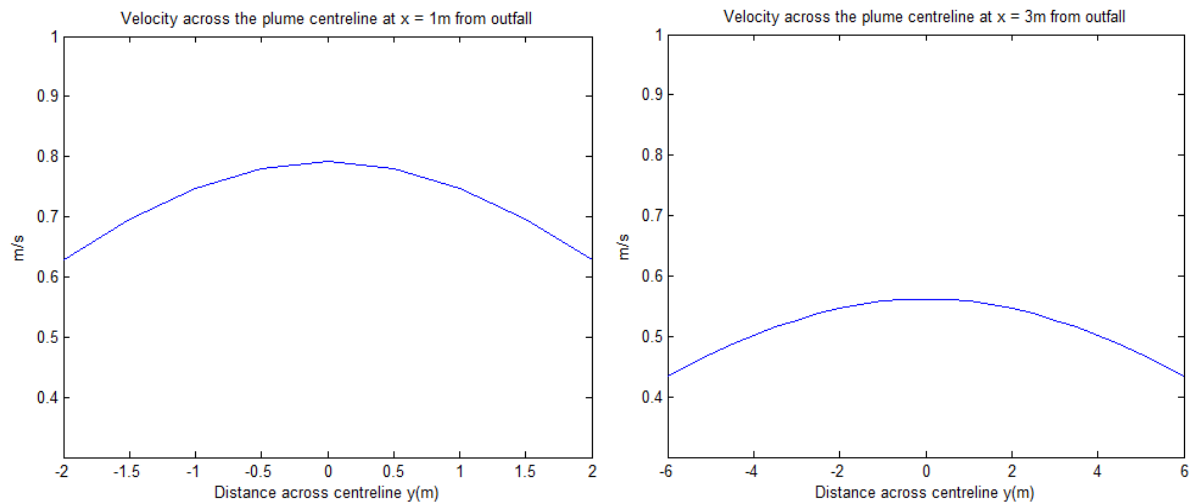


Figure 4: Velocity across the plume centreline at $x = 1\text{ m}$ and $x = 3\text{ m}$

3D Model Plume Size

To observe the behaviour of the thermal plume below the free surface of canal, the university has developed a 3D model to predict the plume size. This model is the most important prediction as it is the characteristics of the mixing zone below the surface which has been difficult to predict in the past. Using the parameters given in the last two clauses the size of the plume discharged by the Kirklees College new site will be as shown in *figure 5*. The figures show the plan and sectional view of the discharge plume below the free surface of canal. Note the colour gradients in the figure indicate to the distance and not temperature or velocity. Flat surface in the sectional view is the free surface of canal and -0.5 is the bed level of canal.

Study 1b – Pipe Diameter 500 mm

General parameters as before but pipe diameter 500mm

- Discharge temperature is 24°C ,
- Canal ambient temperature is 19°C ,
- Discharge pipe diameter **0.500m**
- Discharge flow rate is 166.32 l/s.

The discharge velocity will be **0.848m/s**, the average depth of canal assumed to be 1.2m and the depth of discharge to the bed 0.55m.

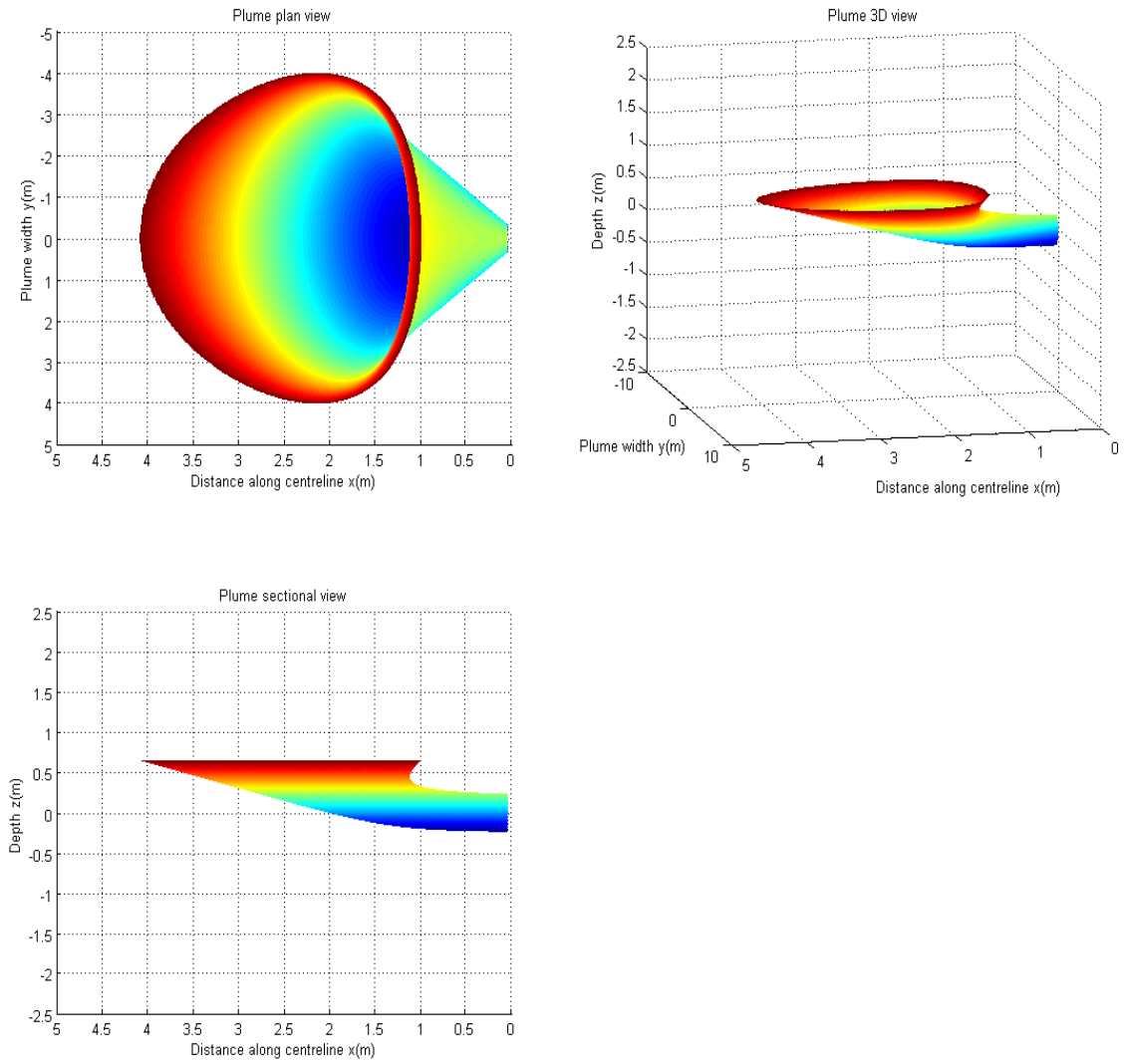


Figure 5: Size of thermal plume below the free surface of canal (plan and sectional view).

Temperature:

The temperature dilution along the centreline of the plume is presented in *figure 6*. *Figure 7* demonstrates the temperature dilution across the centreline of the plume.

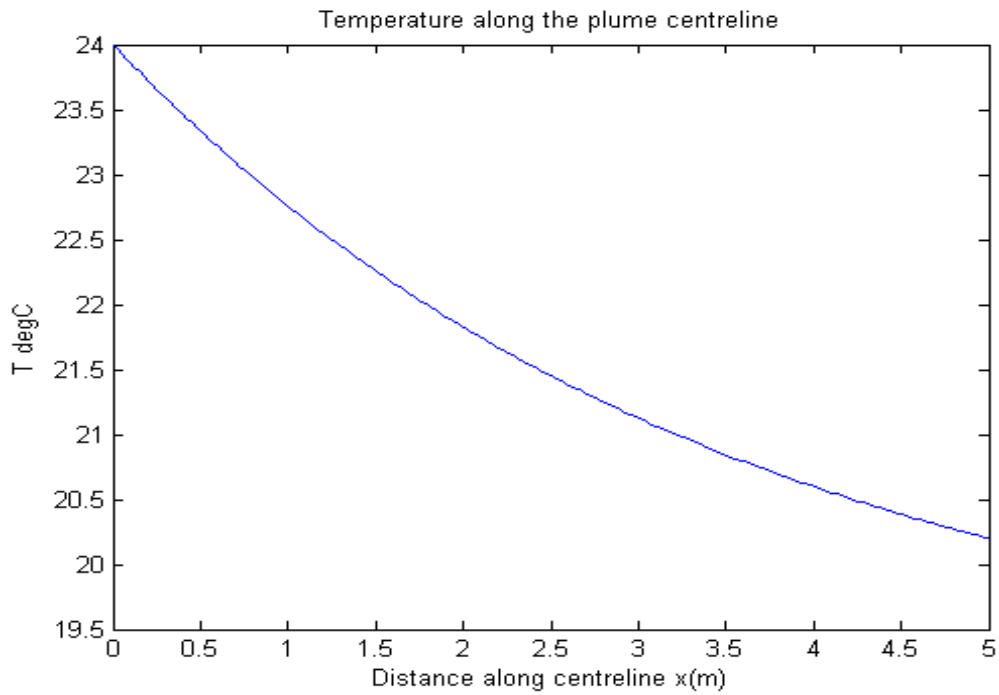


Figure 6: Temperature dilution along the plume centreline

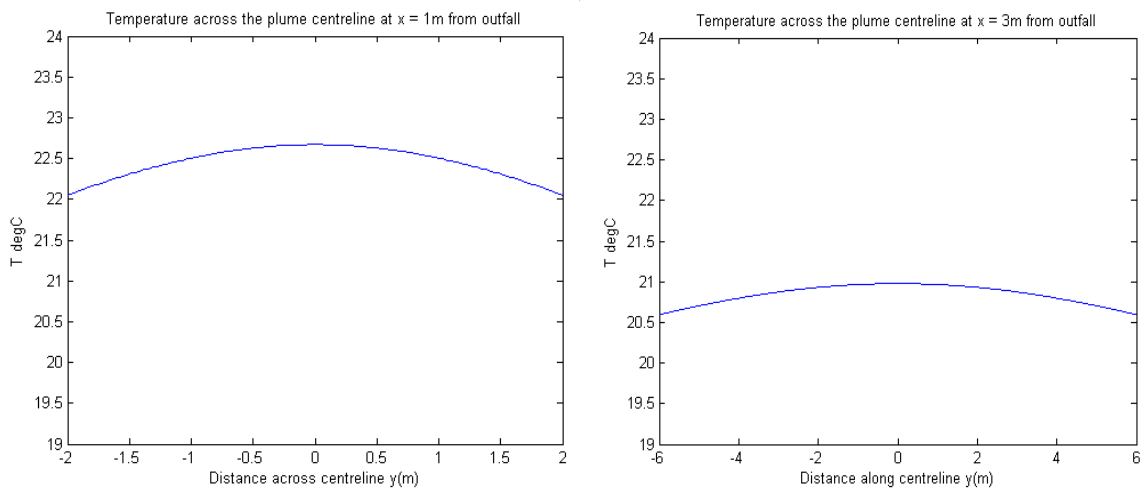


Figure 7: Temperature dilution across the plume path line at x = 1m and x = 3m

Velocity:

Velocity decay along the centreline of the plume illustrates in *figure 8*, the velocity across the centreline of the plume at two locations 1m and 3m from the outfall are shown in *figure 9*.

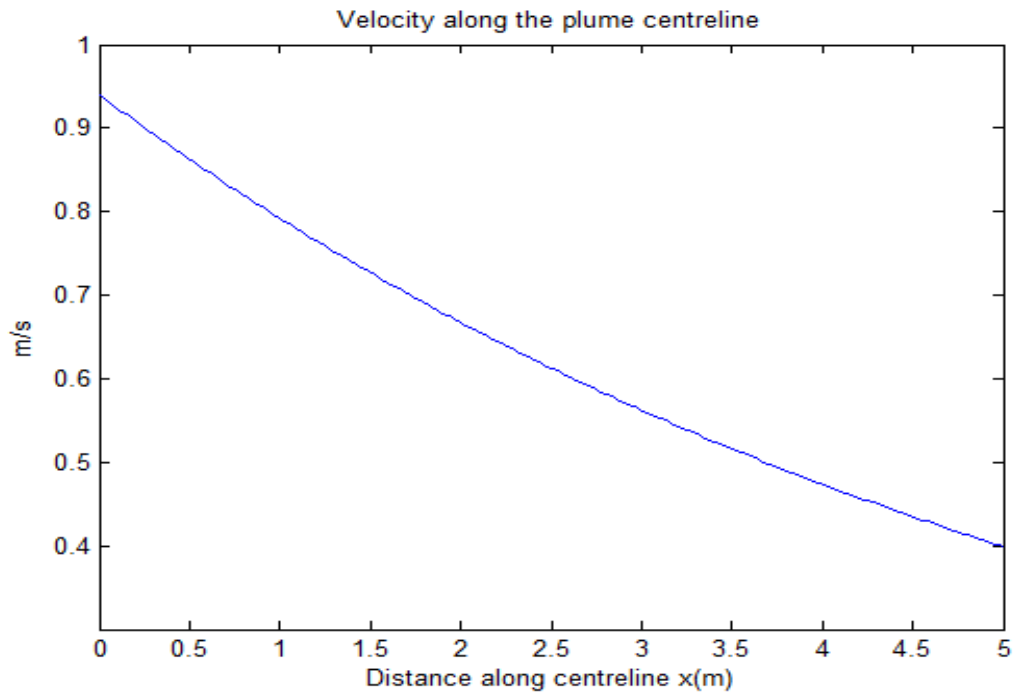


Figure 8: Velocity along the plume centreline

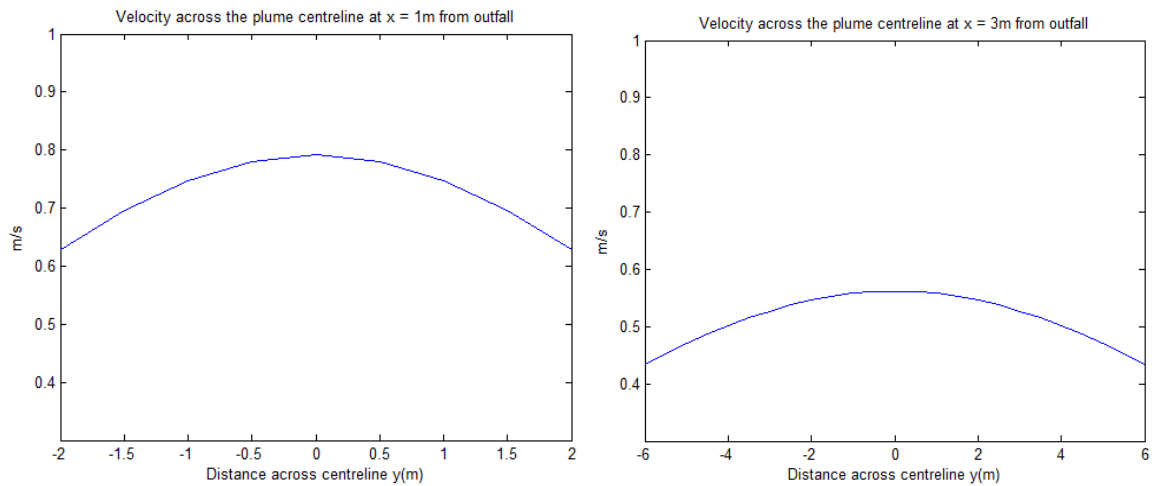


Figure 9: Velocity across the plume centreline at x = 1m and x = 3m

Plume size:

In *figure 10* the size of the plume is presented in different view. The colours in the figure indicate to the distance.

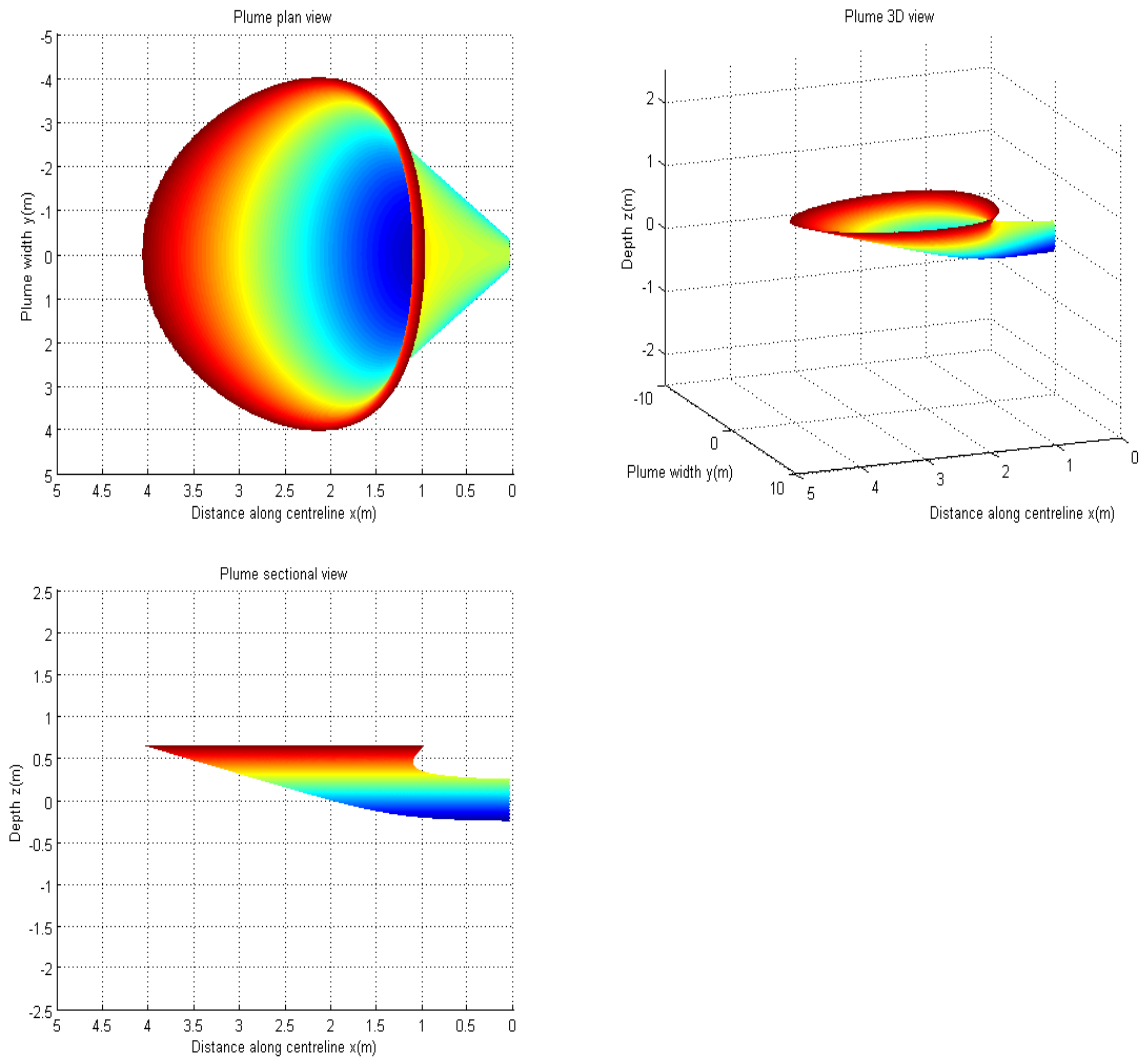


Figure 10: Plume size (colours indicate to distance). Flat surface in the sectional view is the free surface of canal and -0.5 is the bed level of canal.

In case of multiple outlet discharge the plan view of mixing zone will be as shown in *figure 11*. Ten nozzles of 0.1m diameter and 0.5m apart are modelled. The length of the plume illustrate in the figure is 1.2m from the outfalls. Discharge temperature is 24°C and the ambient 19°C; the mixing zone will be as follow.

Study 2 – Multiple point discharge (10 outlets).

Criteria:

General parameters as before but pipe diameter 100mm per outlet

- Discharge temperature is 24°C,
- Canal ambient temperature is 19°C,
- Discharge pipe diameter **0.100m**

- Total discharge flow rate is 166.32 l/s
- Discharge per outlet 16.6 l/s.
- $Fd = 64.77$

The discharge velocity will be **2.1 m/s**, the average depth of canal assumed to be 1.2m and the depth of discharge to the bed 0.55m. *Figure 11* demonstrate the size of plumes for a distance 1.2m from the outfall.

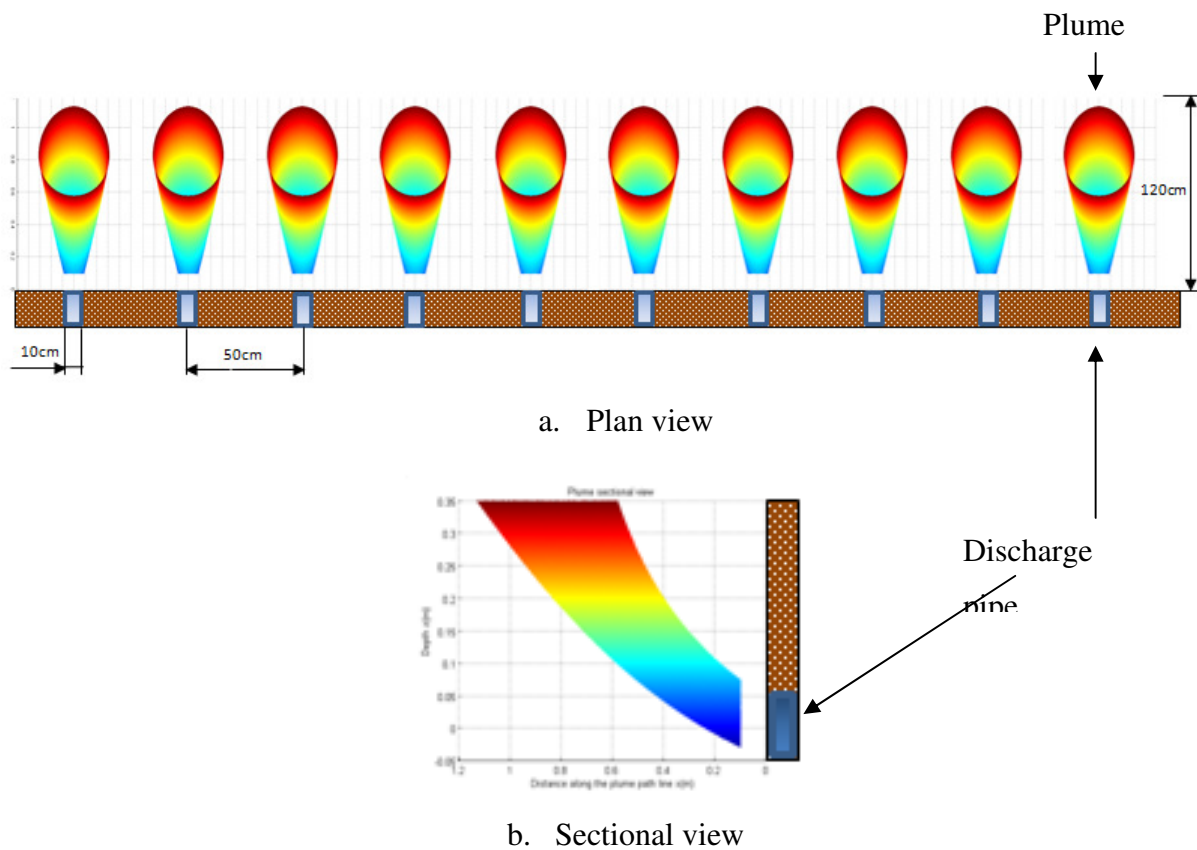


Figure 11: Multi diffusers discharge (colours indicate to distance)

Figure 12 shows the dilution of the temperature along the centreline of a single plume in multi-point discharge, whilst *figure 13* shows the temperature dilution across the centreline at two different locations; $x = 1\text{m}$ and $x = 3\text{m}$ from the outfall.

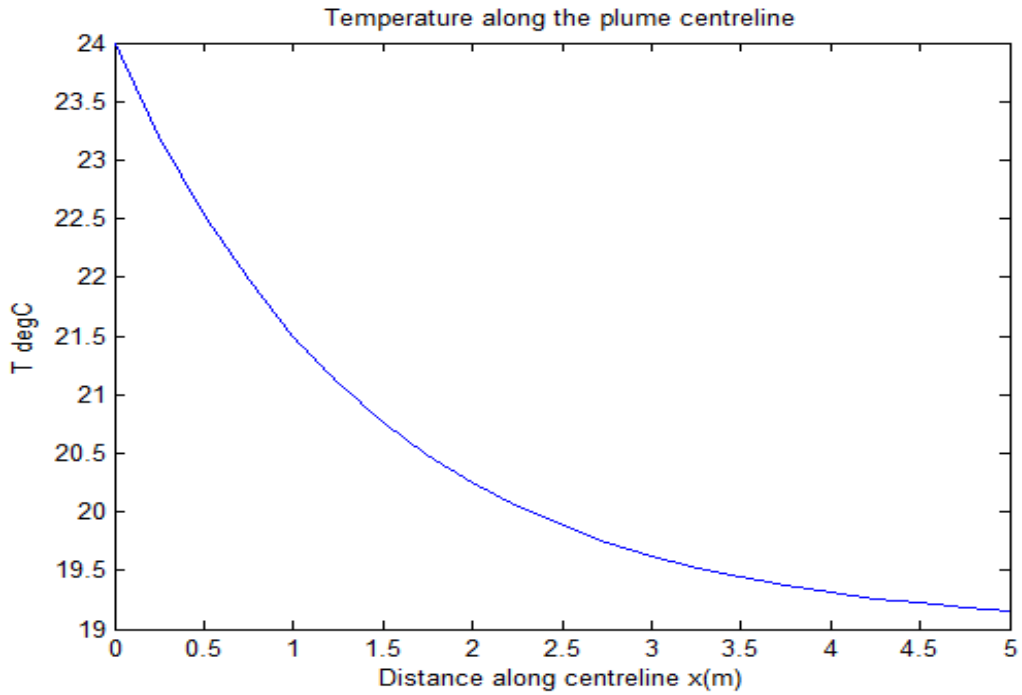


Figure 12: Temperature along the centreline of the plume (multipoint discharge)

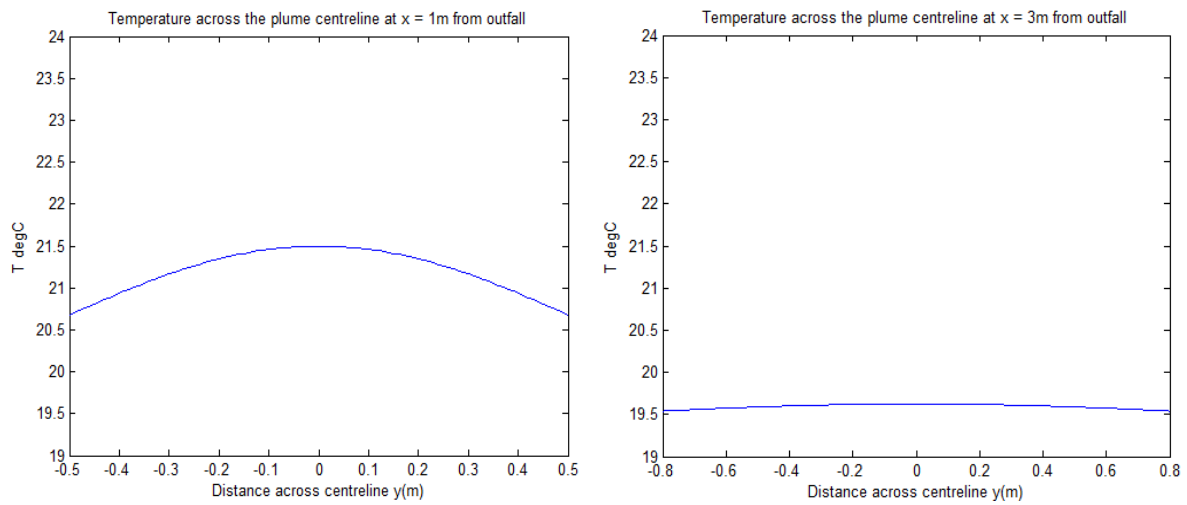


Figure 13: Temperature across the centreline at x = 1m and x = 3m from outfall

In figures 14 and 15 velocity decays along and across the centreline of the plume are presented respectively.

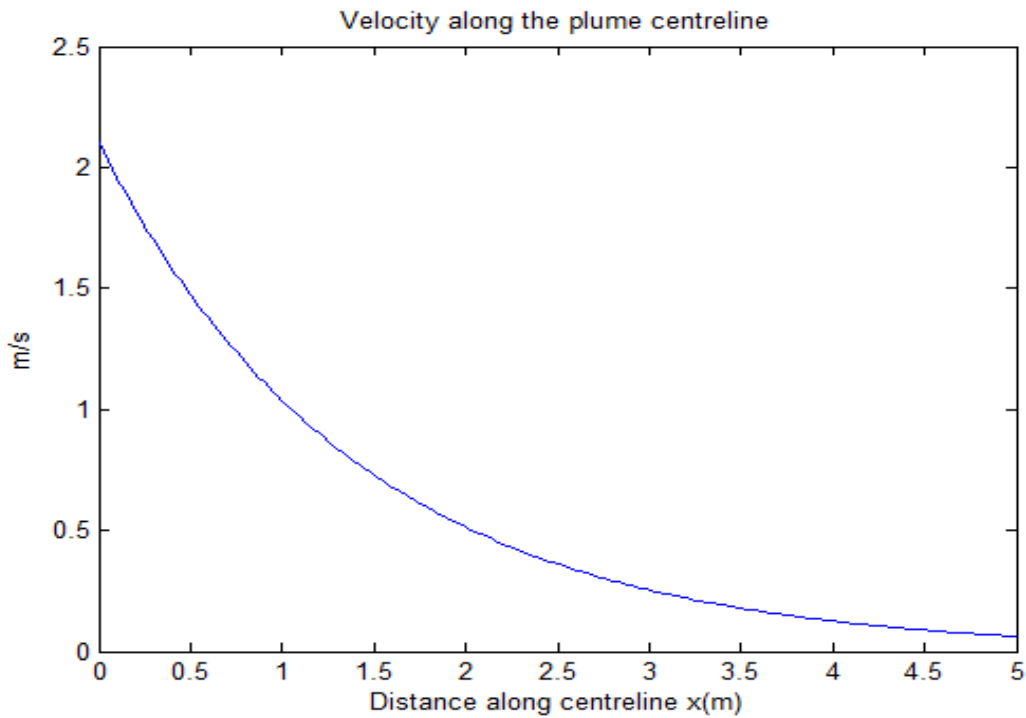


Figure 14: Velocity along the centreline of plume (multipoint discharge)

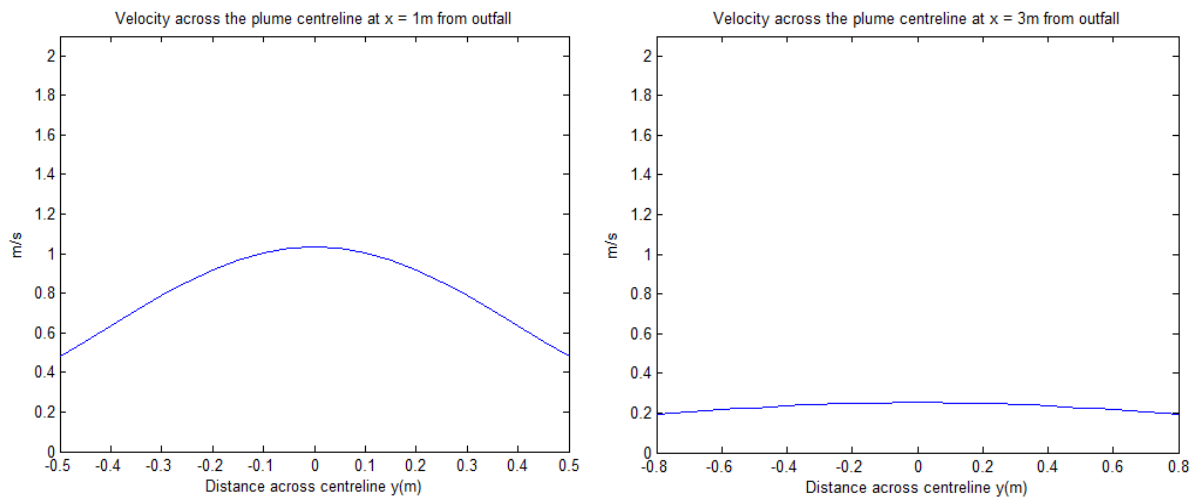


Figure 15: Velocity across the centreline of plume at x = 1m and x = 2m from outfall

Study Results

The studies indicate to the following results:

1. Temperature: the core temperature profile in *figure 1* shows clearly how it is decreased from 24°C at the outfall when $x = 0\text{m}$ to just above the canal ambient temperature 19.5°C when $x = 3\text{m}$. The lateral distribution *figure 2* indicates to temperature around 21.4°C when $x = 1\text{m}$ and around 21.16°C when $x = 2\text{m}$.

2. Velocity: it is reduced from 0.94m/s at the outfall when $x = 0\text{m}$ to 0.18m/s when $x = 3\text{m}$, see *figure 3*. The lateral velocity profiles in *figure 4* show the velocity around 0.54m/s at the centre (path line) and 0.33m/s at $y = 1\text{m}$ and $x = 1\text{m}$. These values reduced to 0.31m/s at the centre and 0.2m/s at $y = 1\text{m}$ and $x = 2\text{m}$.

3. Plume size: 3 dimensional view of the plume size below the free surface is produced in *figure 5*. The edges of the plume and the area when the plume reaches the surface can be seen clearly. A big area between the canal bed and mixing zone is shown in *figure 5* which can be used by the aquatic to pass the region safely if temperature in the mixing zone is not desirable for them.

In study 1a when the discharge pipe diameter is 0.5 and velocity 0.848m/s, slight different will achieve in heat dissipation and velocity reduced, see figures 6 to 10.

Multi point discharged is studied and the profiles of the temperature and velocity are presented. The graphs show the temperature balance within a distance 5m from the outfall in the case of the multi-point discharge, but the impact between the edges of the plume is not considered in this study.

Conclusions

The great decrease in the plume temperature within a distance of 3m from the outfall indicates to the ability of canal to dissipate the amount of heat discarded. The temperature difference of 0.5°C between the plume and the canal ambient water temperature means the majority of heat loaded to the canal is dissipated within the mixing zone. The remaining heat will be lost when the temperature difference becomes zero. Beyond the mixing zone the canal water ambient temperature is not affected. As the biological impact the temperature at any point does not reach the Environment Agency limit 28°C and region is safe for aquatic life-forms. The study concludes that the Kirklees College and their contractors can safely using the canal water cooling system using the parameters provided by the Max Fordham and as applied in this study.

APPENDIX 6: ENVIROENERGY NOTTINGHAM CASE STUDY

MODELLING COOLING WATER DISCHARGE FROM ENVIROENERGY INTO NOTTINGHAM CANAL

By: Jafar Ali and John Fieldhouse

University of Huddersfield

School of Computing and Engineering

Department of Engineering and Technology

A report submitted to
British Waterways, August, 2010

Summary

This report is study the heat diffusion profile of cooling water discharge from Enviroenergy into Nottingham canal. Two different plumes are discussed and the path line of each plume is predicted. Temperature and velocity profiles along and across the plume path line are determined. In addition Three-dimensional model of the size of the plumes are presented.

The study is theoretical application only without comparison with the experimental measured data. It is intended to carry out the theoretical analyses first and then to perform the experiments on the canal site.

1. Introduction

This report should be considered as part of the validation procedure for acceptance of the mathematical model as developed at the University of Huddersfield. The process is to provide this preliminary report and then to compare these predicted results with the on-site measurements.

The parameters used in this report are provided by the British Waterways; however in some cases some approximations are required. It is known that the discharge is multi diffusers; three pipes with diameter 15in (0.381m) and a single pipe with diameter 6in (0.152m). The depth of canal at margins is 0.5m and at the centre is 1m. Temperature difference is 5 °C, therefore it is assumed that the discharge temperature 25 °C and the canal ambient 20 °C.

Discharge velocity is not given, the maximum flow rate been measured is 1619 m³/hr (0.45m³/s). This value is the total flow rate from the pipes (four discharge pipes).

The following flow rates are obtained by assuming the discharge is proportional to the pipe areas, i.e. the discharge velocity is the same:

Flow rate for the big pipes = 0.1425m³/s

Flow rate for the small pipe = 0.02267m³/s

Total flow rate = Flow rate for the big pipes + Flow rate for the small pipe

$$(0.45\text{m}^3/\text{s}) = 3 * (0.1425\text{m}^3/\text{s}) + (0.02267\text{m}^3/\text{s})$$

Discharge velocity of all pipes will be:

$$U = 1.25\text{m/s}$$

Note that the flow rate distribution described above means the bigger pipe will be 6.25 times the smaller pipe as they have a diameter 2.5 times the diameter of the small pipe.

2. Big pipes plume study

Three of the discharge pipes have same diameter and it's bigger than the other pipe. The following parameters are used to model plume discharged from the big pipes:

Average depth of canal within the mixing zone: $H = 0.6\text{m}$

Canal ambient water temperature: $T_a = 20^\circ\text{C}$

Discharge temperature: $T_0 = 25^\circ\text{C}$

Discharge pipe diameter: $D_{01} = 0.381\text{m}$

Discharge velocity: $U = 1.25\text{m/s}$

Discharge pipe depth: $z_0 = 0.31$

Densimetric Froude number $F_{d1} = 18.96$

The path line of plume from the centre of the discharge pipe to the free surface of canal will be as illustrated in figure 2.1

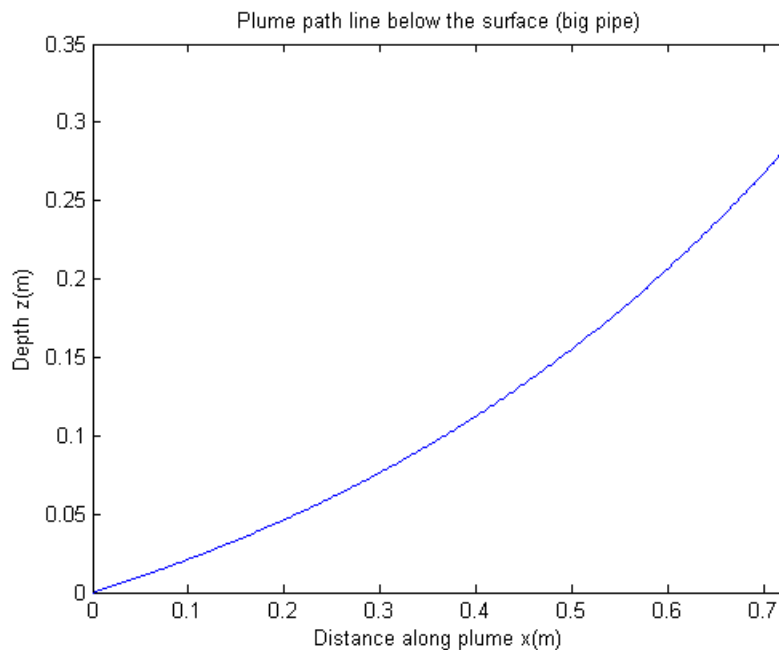
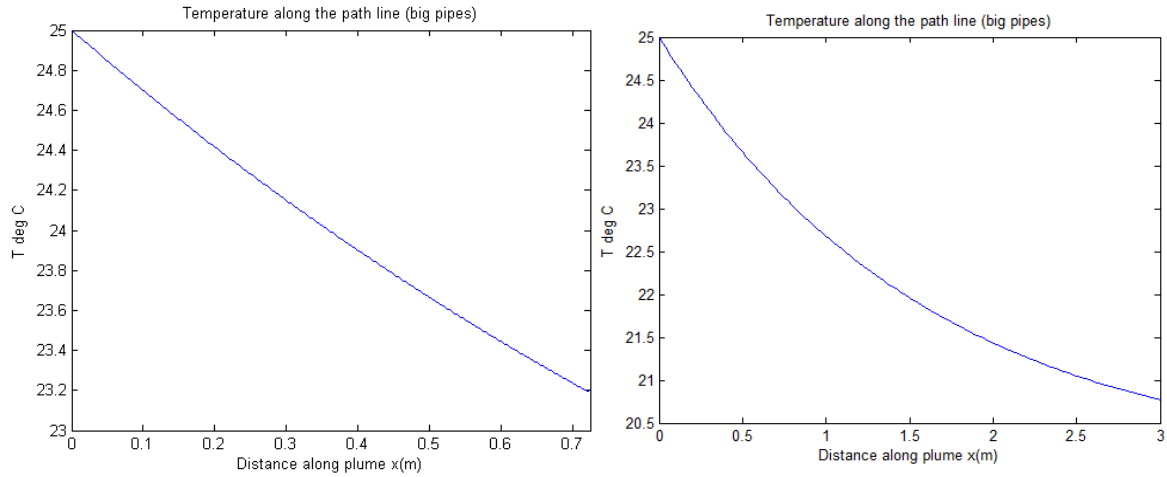


Figure 2.1: Plume path line

2.1 Temperature study

Temperature along the path line of plume is predicted and presented in the figure 2.2a. Whereas the temperature along the path line for longer distance i.e. after the plume reaches the free surface is presented in figure 2.2b.

Note: the developed model by the University of Huddersfield is better evaluating the temperature and velocity for the path line of plume before reaching the surface. Because the plume beyond that point at the surface affected by atmosphere. However the model still able to give a good percentage of accuracy for path line on the surface.



2.2a: Temperature along the path line below the surface 2.2b: Temperature along the path line within 3m

Figure 2.2: Temperature along the path line

The lateral distribution of temperature across the path line of plume are determined at four different distance from the outfall; at $x = 0.5$ m, $x = 1$ m, $x = 2$ m and $x = 3$ m. It is important to know the width of plume to determine the lateral distribution along it. Assume the width as a constant along the plume and equal to 4m. Therefore the temperature distributions across the path line of plume are as in the figure 2.3.

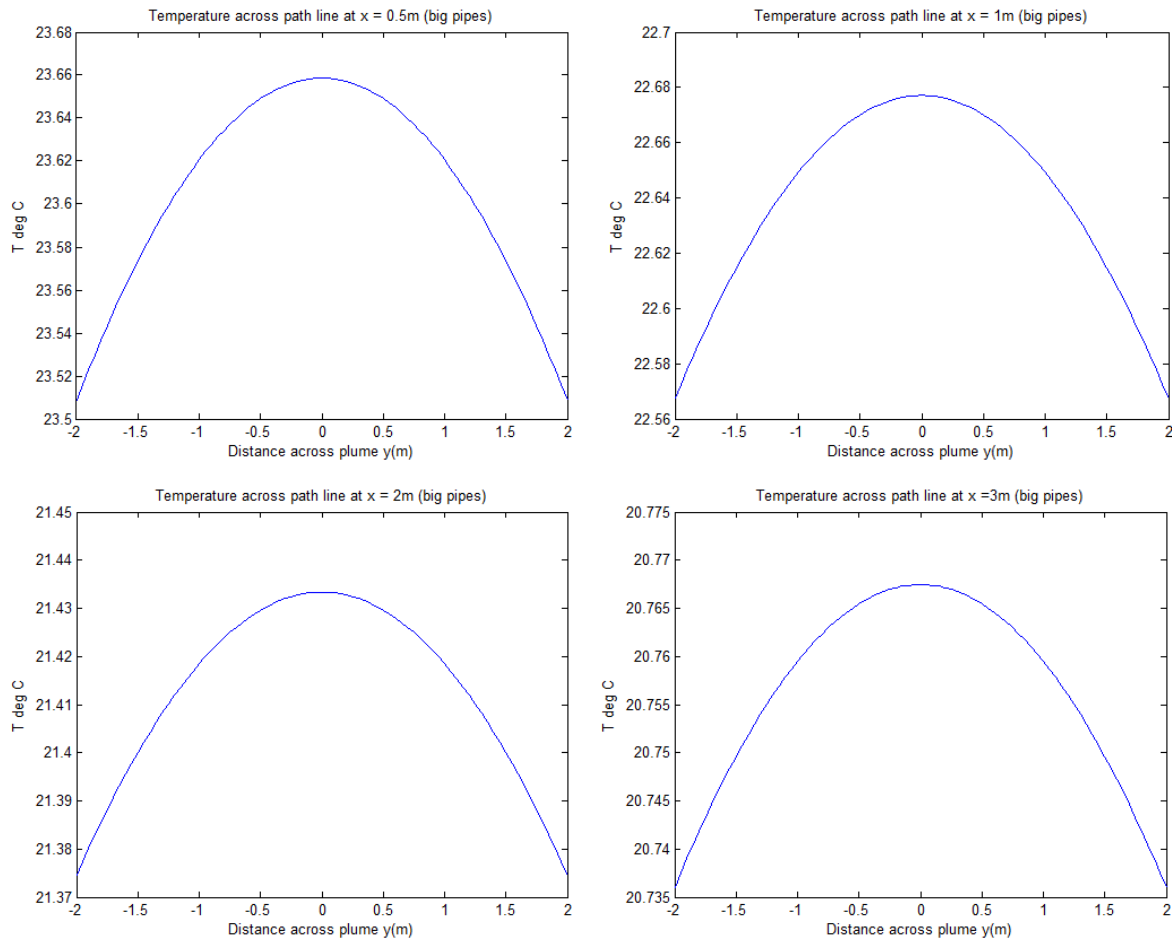
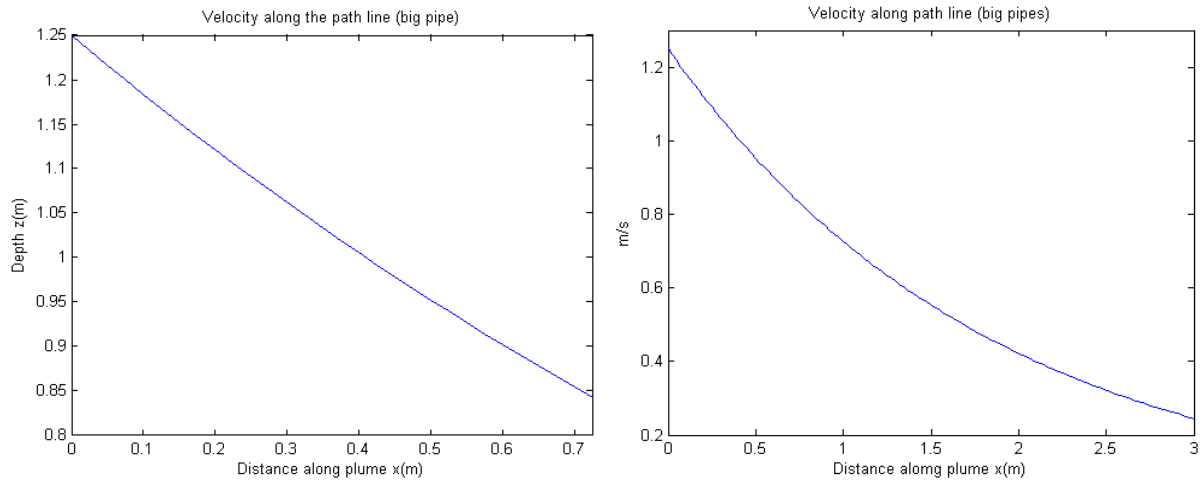


Figure 2.3: Temperature across the path line of plume

2.2 Velocity study

The profiles of temperature and velocity are self similar and the same procedure applied to determine them, figure 2.4 present the velocity along the path line. Figure 2.5 present the velocity across the path line.



2.4a: Velocity along the path line below the surface

2.4b: Velocity along the path line within 3m

Figure 2.4: Velocity along the path line of plume

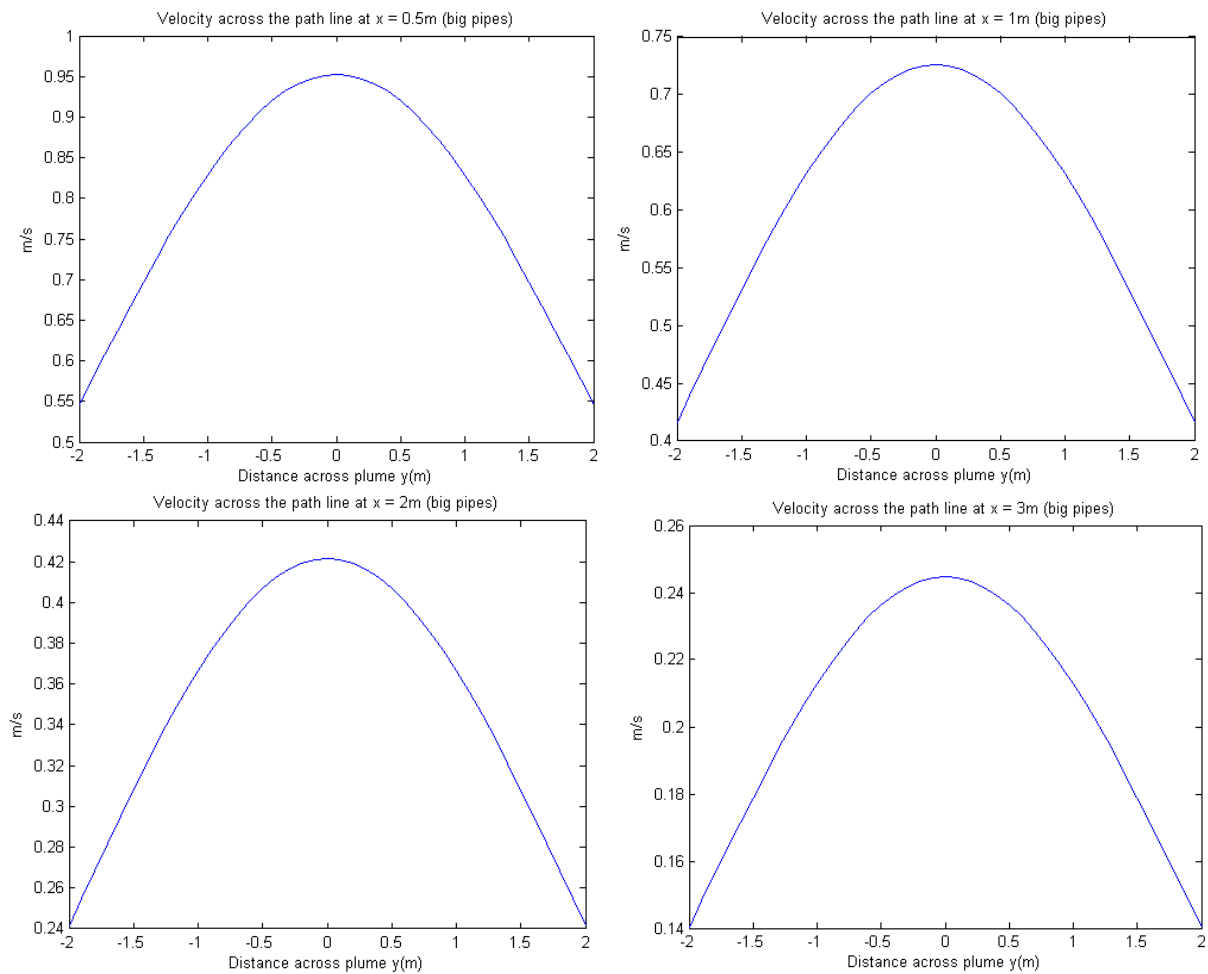


Figure 2.5 Velocity across the path line of plume

2.3 3D Model

The size of plume below the surface is predicted, the isometric view of the plume is presented in figure 2.6, whereas the plan view is presented in figure 2.7.

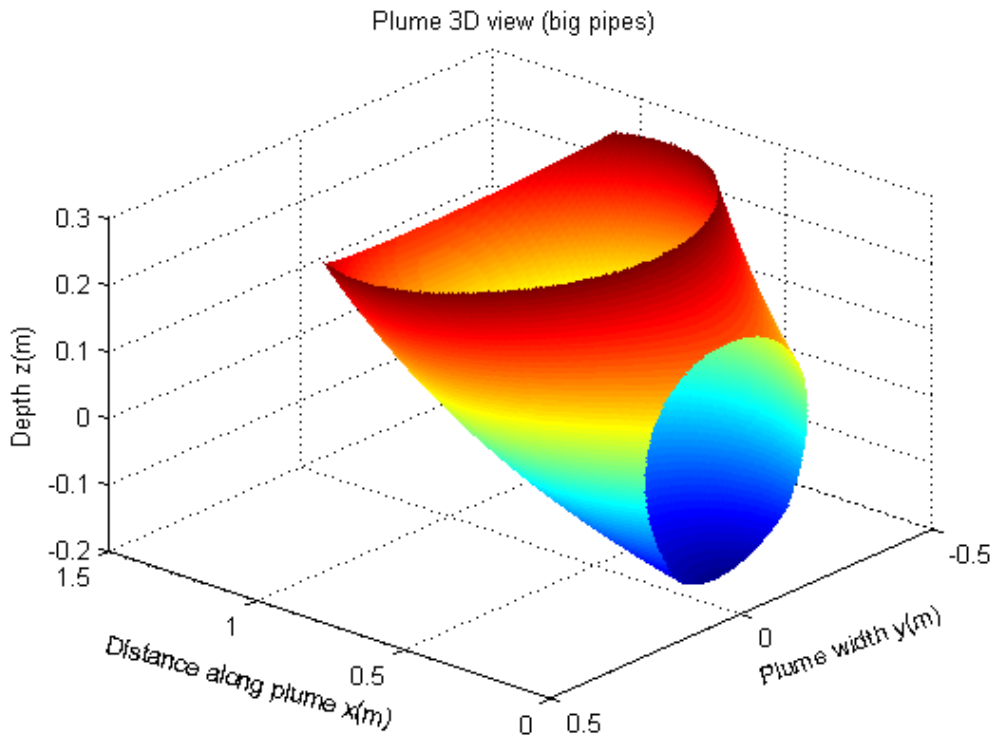


Figure 2.6: Size of plume below the free surface of canal

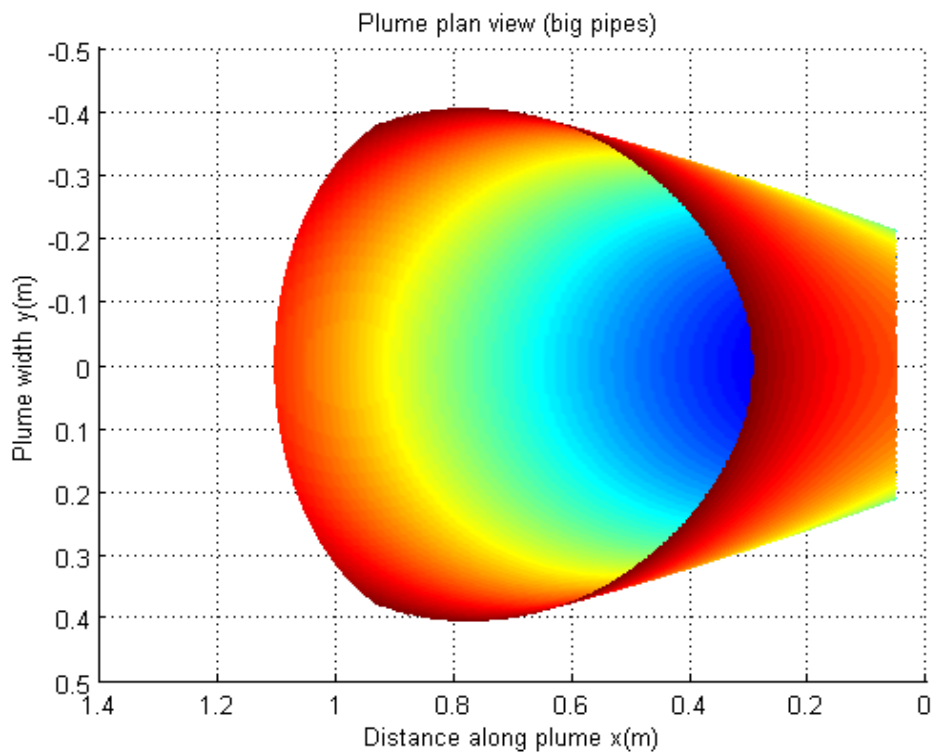


Figure 2.7: Plan view of the plume

From the plan view of the plume it is found that the width of the plume at $x = 0.5\text{m}$ is 0.7m ($y = \pm 3.5$) and not 4m as it is modelled and presented in the figures 2.3 and 2.5. And then the plume get wider, therefore the lateral distribution model for temperature and velocity will be repeated. Determine the lateral profiles at four different distance from the outfall ($x = 0.5, 1, 2$

and 3m) and four different width of ($y = \pm 0.35, \pm 0.5, \pm 1$ and ± 2 m). Figures 2.8 and 2.9 are illustrated temperature and velocity profiles respectively.

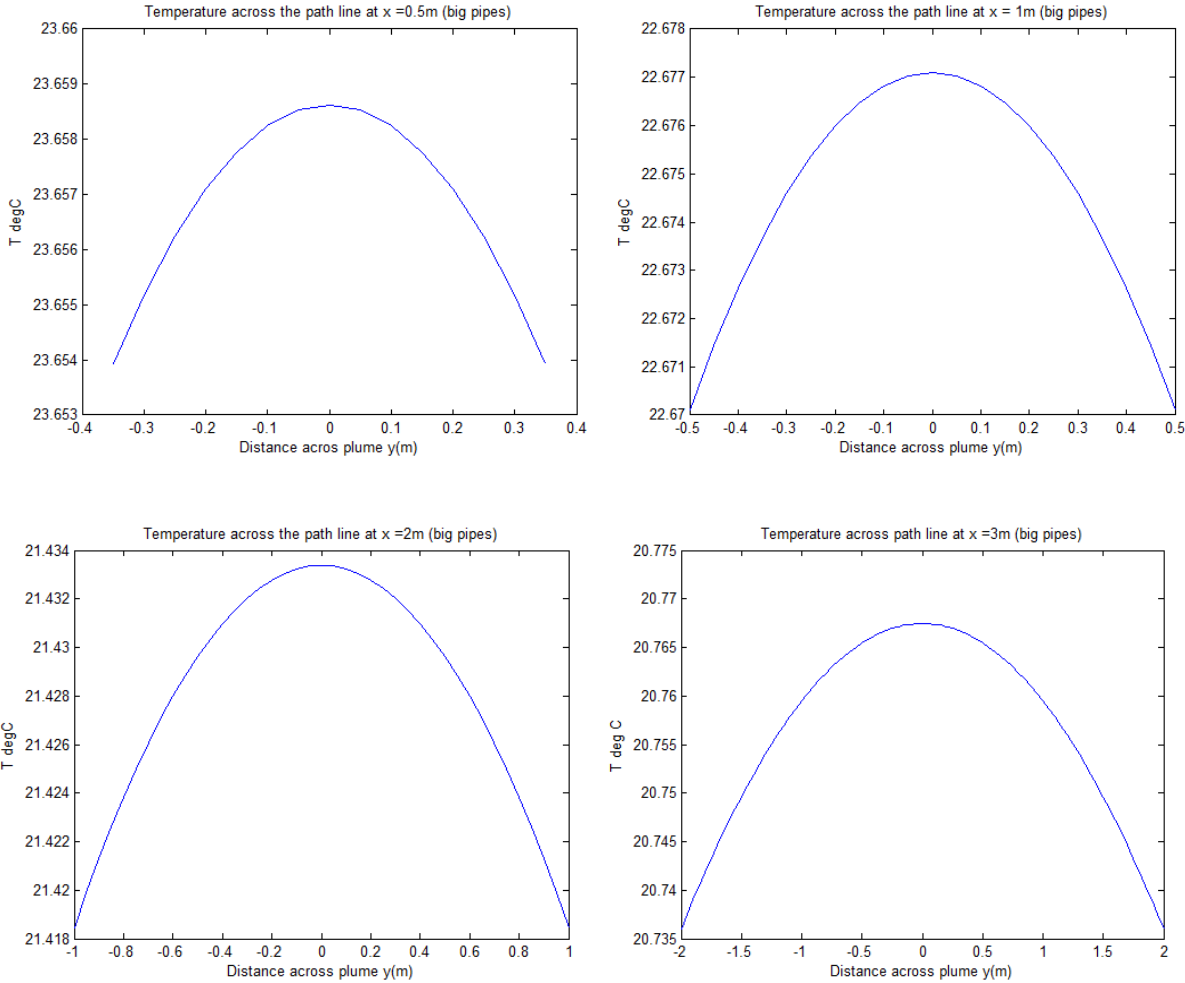
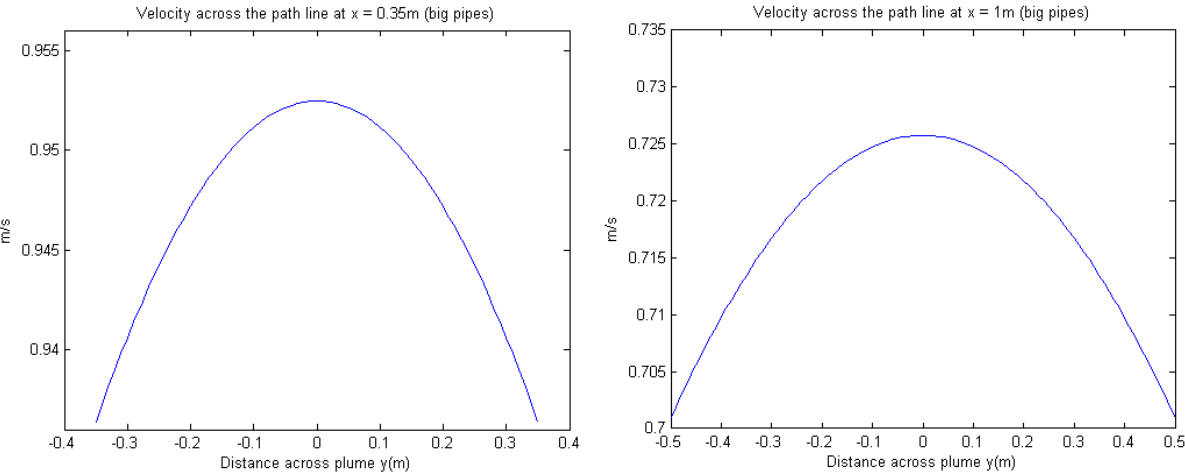


Figure 2.8: Temperature across the path line



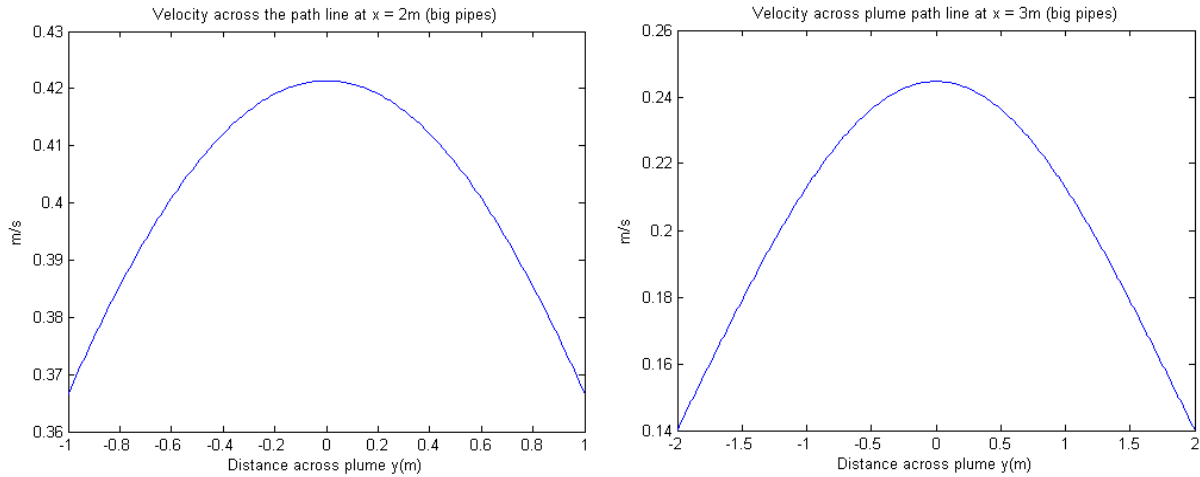


Figure 2.9: Velocity across the path line of plume

3. Small pipe plume study

The number of the big discharge pipes is three, the fourth pipe is the smaller and it will be studied in this section. The following parameters are used for the small pipe that is similar to the big pipes parameters except the pipe diameter:

Average depth of canal within the mixing zone: $H = 0.6\text{m}$

Canal ambient water temperature: $T_a = 20^\circ\text{C}$

Discharge temperature: $T_0 = 25^\circ\text{C}$

Discharge pipe diameter: $D_{02} = 0.152\text{m}$

Discharge velocity: $U = 1.25\text{m/s}$

Discharge pipe depth: $z_0 = 0.31$

Densimetric Froude number $F_{d2} = 30.03$

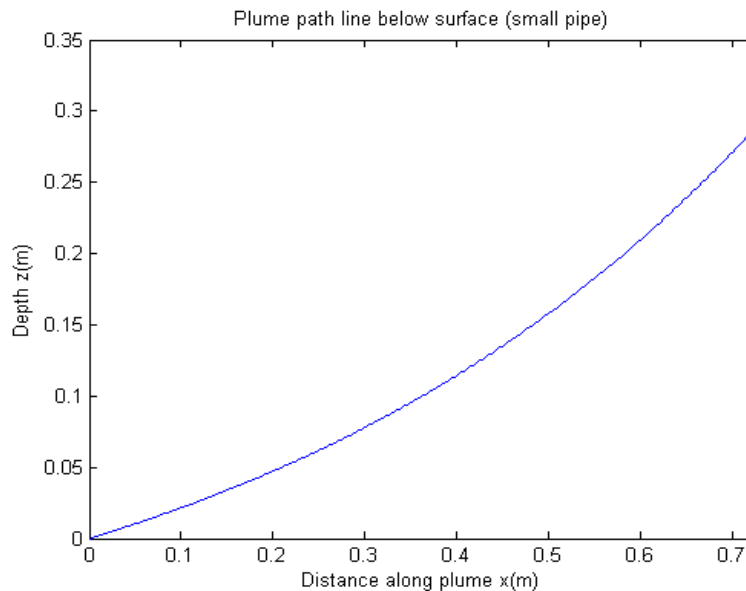


Figure 3.1: Plume path line

Figure 3.1 shows the path line of plume from the centre of the discharge pipe to the free surface of canal.

The analyses start with 3D-model to determine the size of the plume, so the width of the plume will be known. This is help to predict the temperature and velocity profiles across it, across the path line of the plume.

3.1 3D Model

The size of the plume discharged from the small pipe is presented in the figure 3.2 and the plan view of the plume in the figure 3.3:

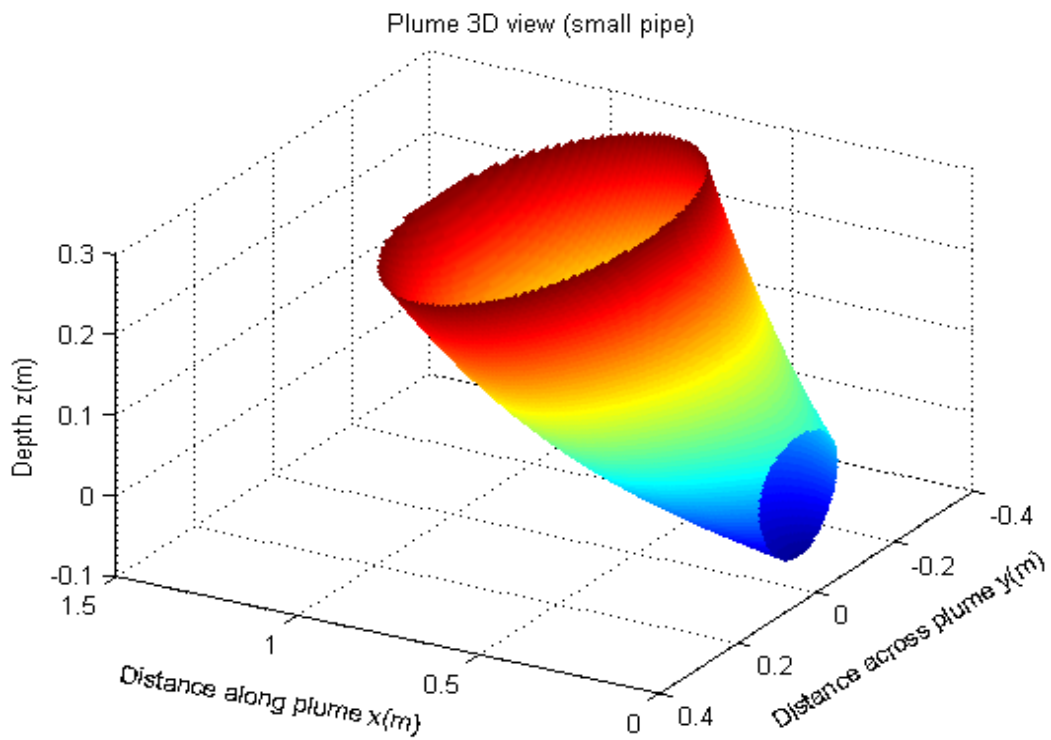


Figure 3.2: Size of the plume below the free surface

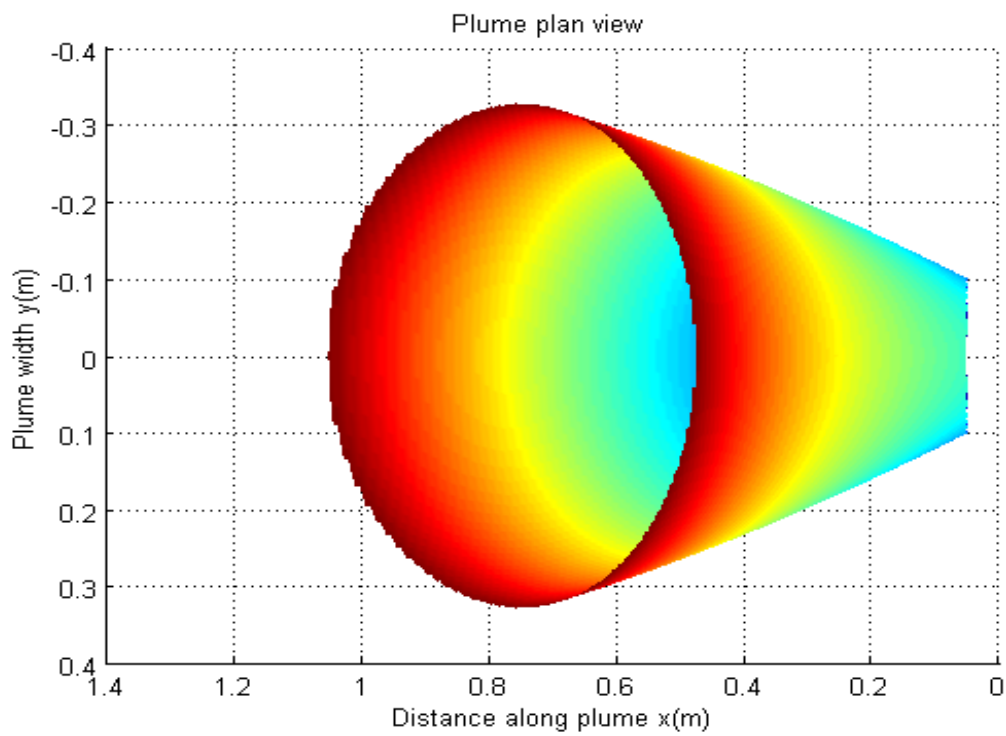
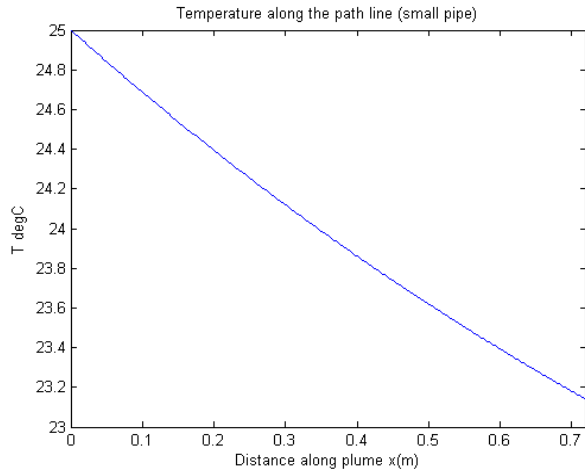


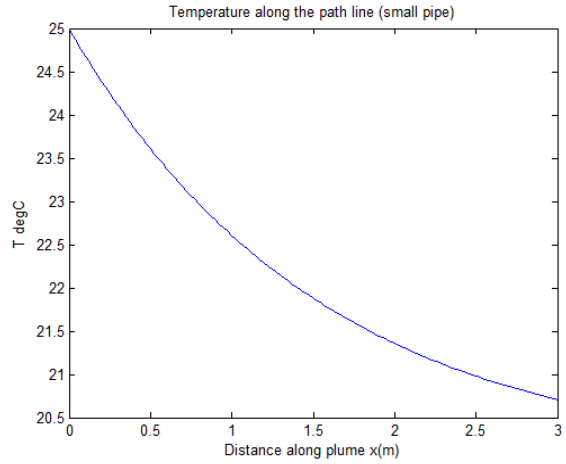
Figure 3.3: Plan view of the plume

3.2 Temperature study

Temperature along the centreline of plume is presented in the figure 3.4. Part (a) of the figure is the temperature profile along the path line below the surface, whilst part (b) is the temperature profile along the path line of the plume to extend to 3m downstream.



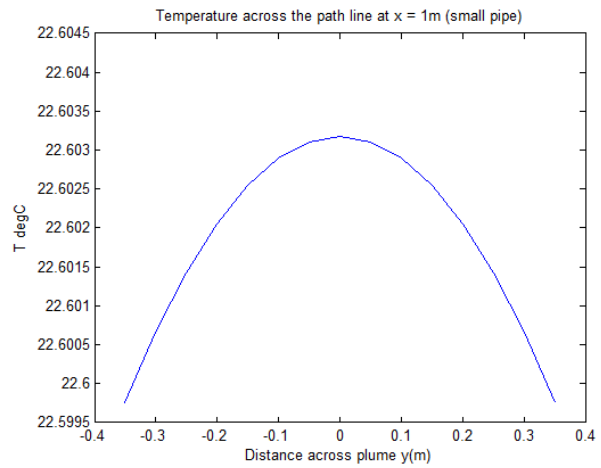
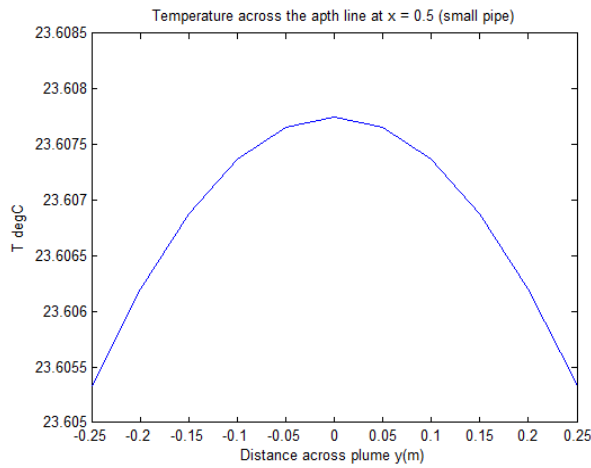
3.4a: Temperature along the path line below the surface



3.4b: Temperature along the path line within 3m

Figure 3.4: Temperature along the path line

Figure 3.5 show the temperature across the path line at four different distance from the discharge ($x = 0.5, 1, 2$ and 3m) and along the width ($y = \pm 0.25, \pm 0.35, \pm 0.75$ and ± 1.5)



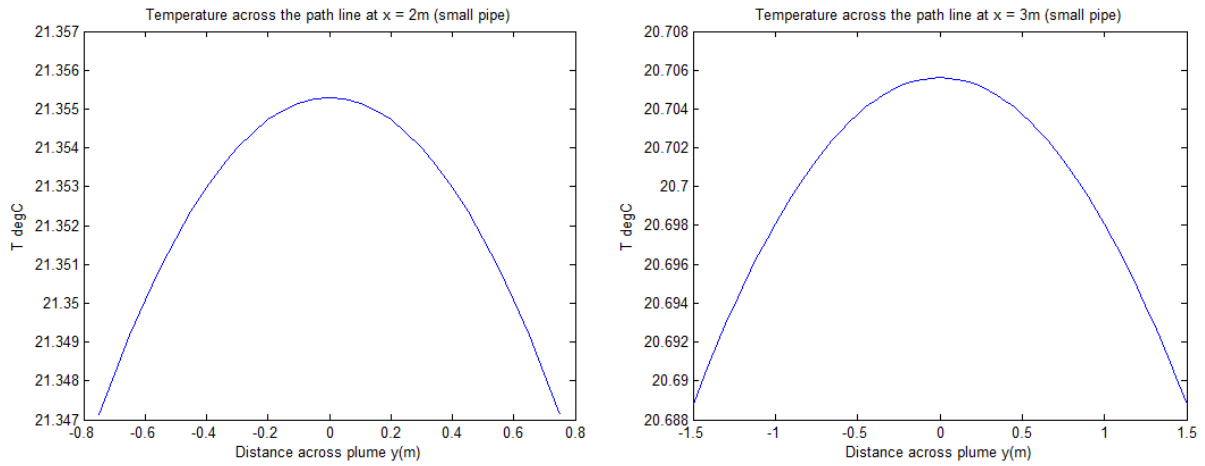
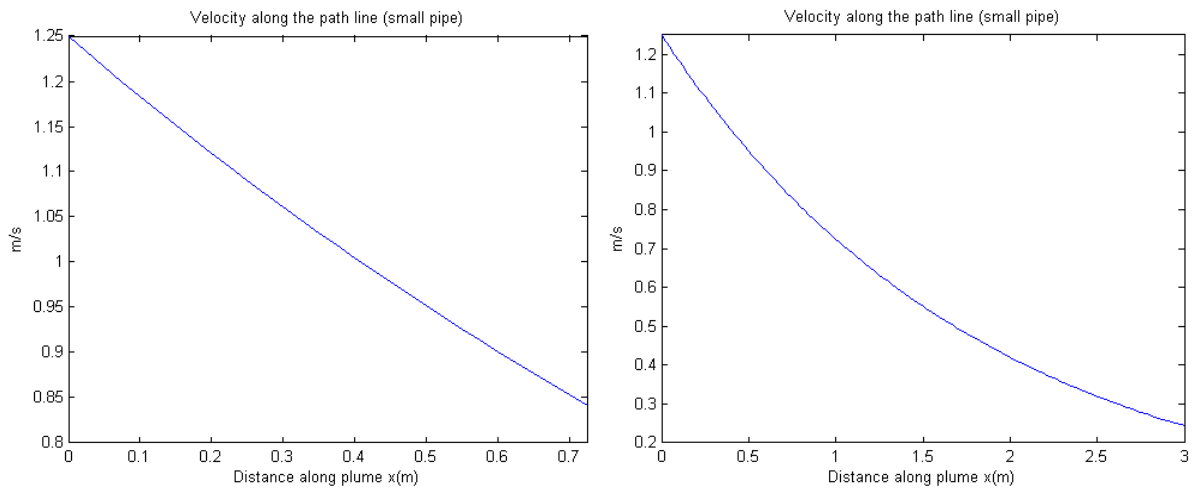


Figure 3.5: Temperature across the path line of plume

3.3 Velocity study

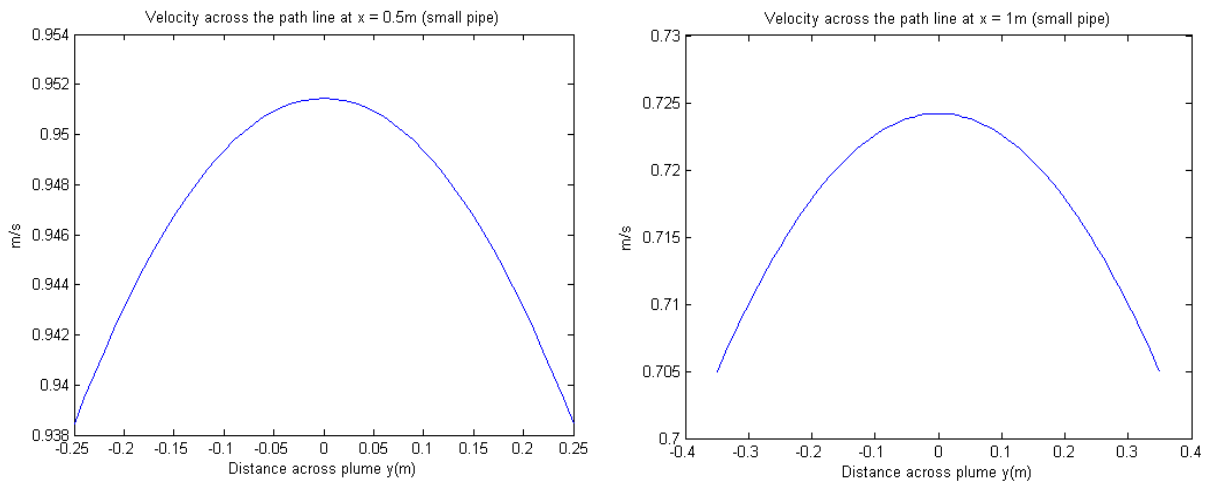
The above procedures are followed to determine velocity profiles along the same axis. Figures 3.6 show the velocity along the path line of plume whilst figures 3.7 show the velocity across the path line.



3.6a: Velocity along the path line below the surface

3.6b: Velocity along the path line within 3m

Figure 3.6: Velocity along the path line of plume



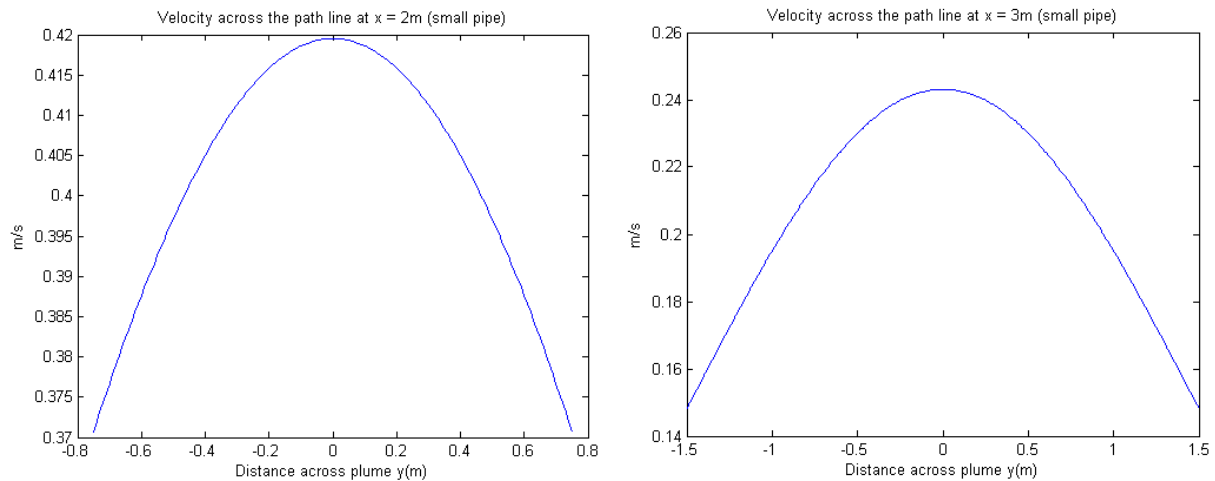


Figure 3.7: Velocity across the path line of plume

4. Conclusion

Two thermal plumes have been studied and treated individually. The path line of the plume is predicted. The temperature and velocity along and across the path line are determined. Temperature balance achieved within three meters from the outfall. Size of the plume below the free surface of canal is predicted, the isometric and plan view for each plume are presented. The theoretical results in this report will be compared with the experiments measured data after the latter are performed. Therefore the comparison of the results is not included in the current study.

Appendix: On-site measurements procedure

The plan may be changed to suite the site application

Average depth of canal within the mixing zone: H

Canal ambient water temperature: T_a

Air ambient temperature:

Thermal image:

Big pipes data

Discharge temperature: T_{01}

Discharge pipe diameter: D_{01}

Discharge velocity: U_1

Discharge pipe depth: z_{01}

Temperature on the surface of canal									
Distance across plume									
Distance along plume	-2	-1.5	-1	-0.5	0	0.5	1	1.5	2
0									
0.8									
1									
2									
3									

Temperature below the surface of canal at various depth										
Distance across plume										
Distance below surface	Distance along plume	-2	-1.5	-1	-0.5	0	0.5	1	1.5	2
0.34	0									
0.32	0.1									
0.27	0.3									
0.19	0.5									
0.07	0.7									

Velocity:

Velocity on the surface of canal									
Distance across plume									
Distance along plume	-2	-1.5	-1	-0.5	0	0.5	1	1.5	2
0									
0.8									
1									
2									
3									

Velocity below the surface of canal at various depth										
Distance across plume										
Distance below surface	Distance along plume	-2	-1.5	-1	-0.5	0	0.5	1	1.5	2
0.34	0									
0.32	0.1									
0.27	0.3									
0.19	0.5									
0.07	0.7									

Small pipe data

Discharge temperature: T_{02}

Discharge pipe diameter: D_{02}

Discharge velocity: U_2

Discharge pipe depth: z_{02}

Temperature on the surface of canal									
Distance across plume									
Distance along plume	-2	-1.5	-1	-0.5	0	0.5	1	1.5	2
0									
0.8									
1									
2									
3									

Temperature below the surface of canal at various depth										
Distance across plume										
Distance below surface	Distance along plume	-2	-1.5	-1	-0.5	0	0.5	1	1.5	2
0.34	0									
0.32	0.1									
0.27	0.3									
0.19	0.5									
0.07	0.7									

Velocity:

Velocity on the surface of canal									
Distance across plume									
Distance along plume	-2	-1.5	-1	-0.5	0	0.5	1	1.5	2
0									
0.8									
1									
2									
3									

Velocity below the surface of canal at various depth										
	Distance across plume									
Distance below surface	Distance along plume	-2	-1.5	-1	-0.5	0	0.5	1	1.5	2
0.34	0									
0.32	0.1									
0.27	0.3									
0.19	0.5									
0.07	0.7									

APPENDIX 7: 3-D PLUME SIZE MATLAB CODE

```
% Finding the size of the discharge plume below the surface
% Insert longitudinal distance
x= %space curve [x y z]
% insert desimetric Froude number
Fd =

%Insert canal depth
H =

%Insert discharge pipe depth
z0 =

%Discharge pipe diameter
D =
Lm =((pi/4)^0.25)*D*Fd;
m = H - z0;
y=zeros(size(x));
% Plume path line equation
z = (0.1*z0/Fd*exp(( (1.4*D*Fd/(H-z0)))*(x./Lm)))-(0.1*z0/Fd);
%ind=find(z>m);
%z(ind)=NaN;

N=length(x);
% Plume edge equation
zu = (D/2)+((0.1*z0/Fd*exp(( (1.7*D*Fd/(H-z0)))*(x./Lm)))-(0.1*z0/Fd));

rz = (zu - z);

% Plume half width equation
ry =(D/2) + ((15.5 * (D)/Lm)) * x - (0.1*(z0)/Lm^2)*x.^2;

x=x'; %rows changed to columns
y=y'; %ditto
z=z'; %ditto

dydx = ((1.4*D*Fd/(H-z0))*0.1*z0/Fd*exp(( (1.4*D*Fd/(H-z0)))*(x./Lm)));
```

```

%dydx=a*alpha*exp(alpha*x);
mag=sqrt(1+dydx.^2);
n=[-dydx./mag zeros(N,1) 1./mag]; %unit normal vector
b=[zeros(N,1) ones(N,1) zeros(N,1)]; %binormal vector

subdivs=500; %number of angular subdivisions

X=zeros(N,subdivs);
Y=zeros(N,subdivs);
Z=zeros(N,subdivs);

theta=0:(2*pi/(subdivs-1)):(2*pi);

for i=1:N
    X(i,:)=x(i) + rz(i)*n(i,1)*cos(theta) + ry(i)*b(i,1)*sin(theta);
    Y(i,:)=y(i) + rz(i)*n(i,2)*cos(theta) + ry(i)*b(i,2)*sin(theta);
    Z(i,:)=z(i) + rz(i)*n(i,3)*cos(theta) + ry(i)*b(i,3)*sin(theta);
end

ind=find(Z>m);
Z(ind)=NaN; % to cut any values above m
ind = find(X<0.05);
X(ind)=NaN;

%index = find (x==5);
surf(X,Y,Z);

shading interp

%view(180,90)
view(180,0)
%view(168,41)
vvv

```

APPENDIX 8: EXPERIMENTAL AND PREDICTED PLUME PATH LINE DATA

Plume centreline path z (cm), experiment															
Fd	0	2.5	5	7.5	10	12.5	15	17.5	20	22.5	25	27.5	30	32.5	35
Fd14.39	0	0.1	0.2	0.4	0.8	1.4	2.4	3.8	7						
Fd41.48	0	0	0	0.1	0.2	0.4	0.7	1.1	1.7	2.4	3.5	5.4	7		
Fd38.59	0	0	0.2	0.4	0.6	1.1	1.7	3	4.9						
Fd31.51	0	0	0	0	0.1	0.2	0.4	0.7	1.1	1.5	2.1	3	4.1	5.8	7
Fd16.29	0	0.1	0.2	0.4	0.7	1.2	2	3.1	7						

Plume centreline path z (cm), model															
Fd	0	2.5	5	7.5	10	12.5	15	17.5	20	22.5	25	27.5	30	32.5	35
Fd14.39	0	0.07	0.19	0.39	0.74	1.33	2.34	4.05	6.96						
Fd41.48	0	0.02	0.05	0.1	0.18	0.3	0.5	0.81	1.31	2.1	3.36	5.37	8.57		
Fd38.59	0	0.03	0.1	0.22	0.44	0.85	1.61	3.03	5.67						
Fd31.51	0	0.01	0.03	0.06	0.1	0.17	0.27	0.42	0.64	0.98	1.5	2.27	3.45	5.23	7.91
Fd16.29	0	0.05	0.15	0.32	0.63	1.16	2.11	3.8	6.8						

APPENDIX 9: EXPERIMENTAL AND PREDICTED TEMPERATURES ALONG AND ACROSS PLUME PATH

(Temperature along plume path line)

Temperature along plume path line □ C, experiment															
Fd	0	2.5	5	7.5	10	12.5	15	17.5	20	22.5	25	27.5	30	32.5	35
Fd14.39	24	22.1	20.3	19.3	18.6	18.1	17.8	17.6	17.4						
Fd41.48	20	19.5	19.1	18.7	18.5	18.2	18	17.85	17.7	17.6	17.5	17.4	17.3		
Fd38.59	25	23	21.5	20.3	19.7	19	18.4	18	17.8						
Fd31.51	25	23.7	22.6	21.8	21.1	20.4	19.8	19.4	19	18.7	18.4	18.2	18	17.8	17.6
Fd16.29	25	22.2	20	18.8	18.1	17.7	17.5	17.4	17.2						

Temperature along plume path line □ C, model															
Fd	0	2.5	5	7.5	10	12.5	15	17.5	20	22.5	25	27.5	30	32.5	35
Fd14.39	24	21.96	20.51	19.49	18.76	18.25	17.88	17.63	17.44						
Fd41.48	20	19.55	19.17	18.85	18.57	18.34	18.14	17.97	17.82	17.7	17.59	17.5	17.43		
Fd38.59	25	23.19	21.79	20.71	19.87	19.22	18.72	18.33	18.03						
Fd31.51	25	23.62	22.48	21.53	20.75	20.1	19.56	19.12	18.75	18.45	18.2	18	17.82	17.68	17.56
Fd16.29	25	21.64	19.69	18.56	17.9	17.53	17.3	17.18	17.1						

(Temperature across plume path line)

Run 4, Fd 14.39															
Temperature across the plume path line □ C, experiment															
	-17.5	-15	-12.5	-10	-7.5	-5	-2.5	0	2.5	5	7.5	10	12.5	15	17.5
x 5						19.2	19.9	20.3	19.9	19.2					
x 10				18.15	18.35	18.45	18.52	18.6	18.52	18.45	18.35	18.15			
x 15		17.62	17.64	17.66	17.67	17.68	17.8	17.8	17.8	17.68	17.67	17.66	17.64	17.62	
x 20			17.26	17.27	17.28	17.3	17.4	17.4	17.4	17.3	17.28	17.27	17.26		
Temperature across the plume path line □ C, model															
x 5						19.38	20.18	20.51	20.18	19.38					
x 10				18.12	18.37	18.57	18.71	18.76	18.71	18.57	18.37	18.12			
x 15		17.54	17.63	17.71	17.78	17.83	17.87	17.88	17.87	17.83	17.78	17.71	17.63	17.54	
x 20	17.3	17.33	17.36	17.39	17.41	17.43	17.44	17.44	17.44	17.43	17.41	17.39	17.36	17.33	17.3

Run 6, Fd 41.48															
Temperature across the plume path line □ C, experiment															
	-17.5	-15	-12.5	-10	-7.5	-5	-2.5	0	2.5	5	7.5	10	12.5	15	17.5
x 5							18.8	19.1	18.8						
x 10							18.4	18.5	18.4						
x 15						17.9	18	18	18	17.9					
x 20					17.6	17.65	17.7	17.7	17.7	17.65	17.6				
Temperature across the plume path line □ C, model															
x 5							18.74	19.17	18.74						
x 10							18.46	18.57	18.46						
x 15						17.98	18.09	18.13	18.09	17.98					
x 20					17.66	17.74	17.8	17.82	17.8	17.74	17.66				

Run 18, Fd 38.59															
Temperature across the plume path line □ C, experiment															
	-17.5	-15	-12.5	-10	-7.5	-5	-2.5	0	2.5	5	7.5	10	12.5	15	17.5
x 5							20.8	21.5	20.8						
x 10						19.2	19.5	19.7	19.5	19.2					
x 15						18.38	18.4	18.4	18.4	18.38					
x 20					17.75	17.78	17.8	17.8	17.8	17.78	17.75				
Temperature across the plume path line □ C, model															
x 5							20.6	21.79	20.6						
x 10						19.02	19.63	19.87	19.63	19.02					
x 15						18.45	18.65	18.72	18.65	18.45					
x 20					17.81	17.93	18	18.03	18	17.93	17.81				

Run 20, Fd 31.51															
Temperature across the plume path line □ C, experiment															
	-17.5	-15	-12.5	-10	-7.5	-5	-2.5	0	2.5	5	7.5	10	12.5	15	17.5
x 5							21.8	22.6	21.8						
x 10						20	20.7	21.1	20.7	20					
x 15					18.9	19.2	19.65	19.8	19.65	19.2	18.9				
x 20				18.15	18.31	18.6	18.9	19	18.9	18.6	18.31	18.15			
Temperature across the plume path line □ C, model															
x 5							21.43	22.48	21.43						
x 10						19.88	20.51	20.74	20.51	19.88					
x 15					18.93	19.26	19.49	19.56	19.49	19.26	18.93				
x 20				18.3	18.48	18.63	18.72	18.76	18.72	18.63	18.48	18.3			

Run 23, Fd 16.29

Temperature across the plume path line □ C, experiment

	-17.5	-15	-12.5	-10	-7.5	-5	-2.5	0	2.5	5	7.5	10	12.5	15	17.5
x 5							19.5	20	19.5						
x 10							17.8	18.1	17.8						
x 15			17.1	17.2	17.3	17.4	17.5	17.5	17.5	17.4	17.3	17.2	17.1		
x 20			17	17.03	17.05	17.1	17.2	17.2	17.2	17.1	17.05	17.03	17		

Temperature across the plume path line □ C, model

x 5						18.39	19.28	19.69	19.28	18.39					
x 10				17.42	17.59	17.75	17.86	17.91	17.86	17.75	17.59	17.42			
x 15			17.17	17.21	17.25	17.28	17.3	17.3	17.3	17.28	17.25	17.21	17.17		
x 20		17.04	17.06	17.07	17.08	17.09	17.1	17.1	17.1	17.09	17.08	17.07	17.06	17.04	

APPENDIX 10: EXPERIMENTAL AND PREDICTED VELOCITY ALONG AND ACROSS PLUME PATH LINE

(Velocity along plume path line)

Velocity along plume path line cm/s, experiment															
Fd	0	2.5	5	7.5	10	12.5	15	17.5	20	22.5	25	27.5	30	32.5	35
Fd14.39	19.00	15.7	13.2	10.8	9.13	7.8	6.9	6	5.5						
Fd41.48	34.00	29	25	21	17.5	15	12.45	11	9.4	8	6.95	6.1	5.55		
Fd38.59	45.00	37	29.25	24	19.05	16	12.45	10.5	8.5						
Fd31.51	45.00	40	34.5	30	26.45	23	20	17	15.15	13	11.45	10	8.85	7.55	6.4
Fd16.29	19.00	15.3	12.1	9.8	7.8	6.3	5	4	3.2						

Velocity along plume path line cm/s, model															
Fd	0	2.5	5	7.5	10	12.5	15	17.5	20	22.5	25	27.5	30	32.5	35
Fd14.39	19	16.14	13.71	11.64	9.89	8.4	7.13	6.06	5.15						
Fd41.48	34	29.31	25.27	21.78	18.78	16.19	13.95	12.03	10.37	8.94	7.71	6.64	5.73		
Fd38.59	45	35.98	28.77	23	18.39	14.7	11.76	9.4	7.52	6					
Fd31.51	45	38.7	33.29	28.64	24.63	21.18	18.22	15.67	13.48	11.59	9.97	8.58	7.38	6.35	5.46
Fd16.29	19	14.84	11.59	9.05	7.07	5.52	4.31	3.37	2.63						

(Velocity across plume path line)

Run 4, Fd 14.39															
Velocity across the plume path line cm/s, experiment															
	-17.5	-15	-12.5	-10	-7.5	-5	-2.5	0	2.5	5	7.5	10	12.5	15	17.5
x 2.5							8.5	15.7	8.5						
x 5							11.25	13.2	11.25						
x 20					4.5	4.75	5	5.5	5	4.75	4.5				
Velocity across the plume path line cm/s, model															
x 2.5							8.84	16.14	8.84						
x 5						6.54	11.39	13.71	11.39	6.54					
x 20		2.94	3.49	4.01	4.47	4.83	5.1	5.15	5.1	4.83	4.47	4.01	3.49	2.94	

Run 6, Fd 41.48															
Velocity across the plume path line cm/s, experiment															
	-17.5	-15	-12.5	-10	-7.5	-5	-2.5	0	2.5	5	7.5	10	12.5	15	17.5
x 5							16.25	25	16.25						
x 10							16.15	17.5	16.15						
x 30					5.15	5.25	5.5	5.55	5.5	5.25	5.15				
Velocity across the plume path line cm/s, model															
x 5							16.53	25.27	16.53						
x 10							16.36	18.78	16.36						
x 30	2.19	2.83	3.51	4.19	4.8	5.3	5.62	5.73	5.62	5.3	4.8	4.19	3.51	2.83	2.19

Run 18, Fd 38.59															
Velocity across the plume path line cm/s, experiment															
	-17.5	-15	-12.5	-10	-7.5	-5	-2.5	0	2.5	5	7.5	10	12.5	15	17.5
x2.5															
x 5							16.5	29.25	16.5						
x 22.5						5	5.5	7.05	5.5	5					
Velocity across the plume path line cm/s, model															
x2.5															
x 5							16.64	28.77	16.64						
x 22.5					4.15	5.1	5.77	6	5.77	5.1	4.15				

Run 20, Fd 31.51															
Velocity across the plume path line cm/s, experiment															
	-17.5	-15	-12.5	-10	-7.5	-5	-2.5	0	2.5	5	7.5	10	12.5	15	17.5
x 5							22.5	34.5	22.5						
x 10						15	22	26.45	22	15					
x 35						5.2	5.5	6.4	5.5	5.2					
Velocity across the plume path line cm/s, model															
x 5							22.19	33.29	22.19						
x 10						14.95	21.74	24.63	21.74	14.95					
x 35	2.94	3.47	3.98	4.46	4.87	5.19	5.39	5.46	5.39	5.19	4.87	4.46	3.98	3.47	2.94

Run 23, Fd 16.29

Velocity across the plume path line cm/s, experiment

	-17.5	-15	-12.5	-10	-7.5	-5	-2.5	0	2.5	5	7.5	10	12.5	15	17.5
x 2.5							5.25	15.3	5.25						
x 5						3.5	8.5	12.1	8.5	3.5					
x 20						2.5	2.7	3.2	2.7	2.5					

Velocity across the plume path line cm/s, model

x 2.5							5.2	14.84	5.2						
x 5						3.3	8.47	11.59	8.47	3.3					
x 20	0.66	0.95	1.3	1.68	2.04	2.35	2.56	2.63	2.56	2.35	2.04	1.68	1.3	0.95	0.66

APPENDIX 11: CANAL SITES AND PREDICTED PATH LINE DATA

(Canalside West data)

Canal depth $H = 1.1\text{m}$

Discharge pipe depth $z_0 = 0.5$

Discharge pipe diameter $D_0 = 0.15\text{m}$

Discharge temperature $T_0 = 19^\circ\text{C}$

Discharge velocity $U_0 = 0.91$

Canal ambient temperature $T_a = 17.5$

Densimetric Froude number $F_d = 46.8$

Length scale $L_M = (\pi/4) D_0^2 F_d = 6.6$

Temperature along the plume path line °C, Canalside West						
	0	0.5	1	1.5	2	2.5
Canal measured data	19.0	18.5	18.3	18.1	18.0	18.0
Theoretical model data	19.0	18.6	18.4	18.2	18.08	17.9

Velocity along the plume path line m/s, Canalside West						
	0	0.5	1	1.5	2	2.5
Canal measured data	0.91	0.66	0.5	0.4	0.3	0.18
Theoretical model data	0.91	0.71	0.56	0.44	0.35	0.28

Temperature across the plume path line °C, experiment									
	-1	-0.75	-0.5	-0.25	0	0.25	0.5	0.75	1
x 0.5			18.3	18.45	18.5	18.45	18.3		
x 1		18.10	18.3	18.3	18.3	18.3	18.3	18.1	
x 1.5		18.1	18.1	18.1	18.1	18.1	18.1	18.1	
x 2	18.0	18.0	18.0	18.0	18.0	18.0	18.0	18.0	18.0
Temperature across the plume path line °C, model									
x 0.5	17.66	17.89	18.22	18.54	18.6	18.54	18.22	17.89	17.66
x 1	17.97	18.14	18.3	18.4	18.4	18.4	18.3	18.14	17.97
x 1.5	18	18.11	18.18	18.2	18.2	18.2	18.18	18.11	18
x 2	17.98	18.02	18.05	18.08	18.08	18.08	18.05	18.02	17.98

Velocity across the plume path line m/s, experiment									
	-1	-0.75	-0.5	-0.25	0	0.25	0.5	0.75	1
x 0.5				0.6	0.66	0.6			
x 1			0.43	0.5	0.5	0.5	0.43		
x 1.5		0.3	0.35	0.4	0.4	0.4	0.35	0.3	
x 2	0.19	0.24	0.26	0.3	0.3	0.3	0.26	0.24	0.19
Velocity across the plume path line m/s, model									
x 0.5				0.57	0.71	0.57			
x 1			0.41	0.52	0.56	0.52	0.41		
x 1.5		0.3	0.38	0.43	0.44	0.43	0.38	0.3	
x 2	0.24	0.28	0.32	0.34	0.35	0.34	0.32	0.28	0.23

(Lockside data)

Canal depth $H = 1.1\text{m}$

Discharge pipe depth $z_{\square} = 0.45$

Discharge pipe diameter $D_{\square} = 0.15\text{m}$

Discharge temperature $T_{\square} = 22^{\circ}\text{C}$

Discharge velocity $U_{\square} = 1.22$

Canal ambient temperature $T_a = 17.5$

Densimetric Froude number $F_d = 33.34$

Length scale $L_M = (\pi/4)\square\square^2\square D_{\square} F_d = 4.71$

Temperature along the plume path line $\square\text{C}$, Lockside						
	0	0.5	1	1.5	2	2.5
Canal measured data	22	20.7	19.8	19.2	18.7	18.1
Theoretical model data	22.0	20.9	20.1	19.5	19	18.7

Velocity along the plume path line m/s, Lockside						
	0	0.5	1	1.5	2	2.5
Canal measured data	1.22	0.89	0.71	0.51	0.4	0.24
Theoretical model data	1.22	0.96	0.75	0.59	0.47	0.37

Temperature across the plume path line ° C, experiment									
	-1	-0.75	-0.5	-0.25	0	0.25	0.5	0.75	1
x 0.5			20	20.5	20.7	20.5	20		
x 1		19.4	19.6	19.8	19.8	19.8	19.6	19.4	
x 1.5	19	19.1	19.2	19.2	19.2	19.2	19.2	19.1	19
x 2	18.6	18.6	18.7	18.7	18.7	18.7	18.7	18.6	18.6
Temperature across the plume path line ° C, model									
x 0.5			19.69	20.59	20.9	20.59	19.69		
x 1		19.4	19.8	20	20.1	20	19.8	19.4	
x 1.5	19.05	19.26	19.42	19.5	19.5	19.5	19.42	19.26	19.05
x 2	18.8	18.9	19	19	19	19	19	18.9	18.8

Velocity across the plume path line m/s, experiment									
	-1	-0.75	-0.5	-0.25	0	0.25	0.5	0.75	1
x 0.5				0.8	0.89	0.8			
x 1		0.45	0.55	0.65	0.71	0.65	0.55	0.45	
x 1.5	0.3	0.4	0.48	0.5	0.51	0.5	0.48	0.4	0.3
x 2	0.3	0.35	0.38	0.4	0.4	0.4	0.38	0.35	0.3
Velocity across the plume path line m/s, model									
x 0.5				0.77	0.96	0.77			
x 1		0.4	0.57	0.7	0.75	0.7	0.57	0.4	
x 1.5	0.34	0.43	0.52	0.57	0.59	0.57	0.52	0.43	0.34
x 2	0.34	0.39	0.43	0.46	0.47	0.46	0.43	0.39	0.34

(Mailbox data)

Canal depth $H = 1.4\text{m}$

Discharge pipe depth $z_{\square} = 0.0.925$

Discharge pipe diameter $D_{\square} = 0.35\text{m}$

Discharge temperature $T_{\square} = 20^{\circ}\text{C}$

Discharge velocity $U_{\square} = 0.6\text{m/s}$

Canal ambient temperature $T_a = 17.5^{\circ}\text{C}$

Densimetric Froude number $F_d = 13.55$

Length scale $L_M = (\pi/4)_{\square}^2_{\square} D_{\square} F_d = 4.46$

Temperature along the plume path line °C, Mailbox									
	0	0.4	0.8	1.2	1.6	2	2.4	2.8	3.2
Canal measured data	20	19.5	Unknown	Unknown	19.1	19	18.9	18.8	18.7
Theoretical model data	20.0	19.7	19.53	19.33	19.15	18.9	18.8	18.7	18.5

Velocity along the plume straight centreline m/s, Mailbox							
	0	0.5	1	1.5	2	2.5	3
Canal measured data	0.6	0.4	0.32	0.26	0.22	0.2	0.17
Theoretical model data	0.6	0.54	0.48	0.44	0.39	0.35	0.32

Temperature across the plume path line °C, experiment									
	-2	-1.5	-1	-0.5	0	0.5	1	1.5	2
x 0.4			18.7	19.3	19.5	19.3	18.7		
x 1.6	18.9	19	19.1	19.1	19.1	19.1	19.1	19	18.9
x 2.4	18.7	18.9	18.9	18.9	18.9	18.9	18.9	18.9	18.7
x 3.2	18.6	18.6	18.6	18.7	18.7	18.7	18.6	18.6	18.6
Temperature across the plume path line °C, model									
x 0.4	18.1	18.56	19.11	19.57	19.7	19.57	19.11	18.56	18.1
x 1.6	18.95	19.04	19.1	19.14	19.15	19.14	19.1	19.04	18.95
x 2.4	18.76	18.8	18.82	18.84	18.8	18.84	18.82	18.8	18.76
x 3.2	18.55	18.57	18.58	18.59	18.59	18.59	18.58	18.57	18.55

Velocity across the plume straight centreline m/s, experiment					
	-1	-0.5	0	0.5	1
x 0.5	0.32		0.4		0.32
x 1	0.25		0.32		0.25
Velocity across the plume straight centreline m/s, model					
x 0.5	0.34	0.48	0.54	0.48	0.34
x 1	0.42	0.47	0.48	0.47	0.42